

NIST GCR 99-769

**MIXING AND RADIATION PROPERTIES OF
BUOYANT LUMINOUS FLAME
ENVIRONMENTS: I. SELF-PRESERVING
PLUMES**

**Z. Dai, R. Sangras, L.-K. Tseng
and G.M. Faeth**

**University of Michigan
Department of Aerospace Engineering
Ann Arbor, MI 48109-2140**

NIST

**United States Department of Commerce
Technology Administration
National Institute of Standards and Technology**

NIST GCR 99-769

**MIXING AND RADIATION PROPERTIES OF
BUOYANT LUMINOUS FLAME
ENVIRONMENTS: I. SELF-PRESERVING
PLUMES**

Prepared for

**U.S. Department of Commerce
Building and Fire Research Laboratory
National Institute of Standards and Technology
Gaithersburg, MD 20899**

By

**Z. Dai, R. Sangras, L.-K. Tseng
and G.M. Faeth**

**University of Michigan
Department of Aerospace Engineering
Ann Arbor, MI 48109-2140**

Final Report

**October 1998
Issued March 1999**



Notice:

This report was prepared for the Laboratory for Building and Fire Research of the National Engineering Laboratory, National Institute of Standards and Technology, under Grant number 60NANB4D1696. The statements and conclusions contained in this report are those of the authors and do not necessarily reflect the views of the National Institute of Standards and Technology or the Laboratory for Building and Fire Research.

**MIXING AND RADIATION
PROPERTIES OF BUOYANT
LUMINOUS FLAME ENVIRONMENTS
I. SELF-PRESERVING PLUMES**

Z. Dai, R. Sangras, L.-K. Tseng and G.M. Faeth
Department of Aerospace Engineering
The University of Michigan
Ann Arbor, Michigan 48109-2140

Prepared for:

U.S. Department of Commerce
National Institute of Standards and Technology
(formerly National Bureau of Standards)
Laboratory for Building and Fire Research
Washington, DC 20234

Final Report
Grant No. 60NANB4D1696
H.R. Baum, NIST Scientific Officer

October 1998

MIXING AND RADIATION PROPERTIES OF BUOYANT LUMINOUS FLAME ENVIRONMENTS: I. SELF-PRESERVING PLUMES

Abstract

An investigation of the structure and mixing properties of buoyant turbulent plumes is described, motivated by the need to resolve effects of buoyancy/turbulence interactions and to provide data required to benchmark models of buoyant turbulent flows for fire environments. The flows considered included round free plumes, plane free plumes and plane adiabatic wall plumes in an attempt to consider various buoyant flow types representative of the environment of unwanted fires. Measurements included laser-induced fluorescence (LIF) to find mixture fraction statistics, laser velocimetry (LV) to find velocity statistics and combined LIF/LV to find combined mixture-fraction/velocity statistics. Present measurements emphasized self-preserving conditions far from the source where effects of source disturbances and momentum have been lost. The results show that earlier measurements in the literature were not carried out far enough from the source to provide self-preserving properties and that actual self-preserving plumes are narrower with larger maximum scaled mean mixture fractions and velocities than previously thought. Mixture fraction fluctuations in buoyant turbulent plumes are also substantially larger than in nonbuoyant turbulent flows due to turbulence production by buoyant instabilities combined with fast rates of streamwise decay of mean mixture fractions in plumes. Free plumes were found to mix much faster than adiabatic wall plumes because the presence of the wall inhibits both access to the flow and the development of large turbulent eddies that dominate turbulent mixing processes in these flows. This induced rate of mixing for turbulent wall flows is a concern in fires because it extends the length of the flame-containing region and reduces effects of dilution on reducing temperature levels and toxic gas concentrations in fire plumes.

Acknowledgments

This research was supported by the U.S. Department of Commerce, National Institute of Standards and Technology (formerly National Bureau of Standards), Grant No. 60NANB4D1696, with H. R. Baum of the Laboratory for Building and Fire Research serving as Scientific Officer.

Table of Contents

	<u>Page</u>
Abstract.....	iv
Acknowledgments.....	v
List of Tables	vii
List of Figures	viii
Nomenclature	ix
1. Introduction	1
2. Turbulent Round Free Plumes	3
2.1 Introduction.....	3
2.2 Experimental Methods.....	4
2.3 Self-Preserving Scaling	5
2.4 Results and Discussion.....	6
2.5 Conclusions.....	14
3. Turbulent Plane Free Plumes.....	15
3.1 Introduction.....	15
3.2 Experimental Methods.....	15
3.3 Self-Preserving Scaling	16
3.4 Results and Discussion.....	17
3.5 Conclusions.....	21
4. Turbulent Adiabatic Wall Plumes.....	23
4.1 Introduction.....	23
4.2 Experimental Methods.....	23
4.3 Self-Preserving Scaling	24
4.4 Results and Discussion.....	24
4.5 Conclusions.....	27
References.....	30
Appendix A: Dai et al. (1994).....	33
Appendix B: Dai et al. (1995a)	43
Appendix C: Dai et al. (1995b).....	52
Appendix D: Dai and Faeth (1996).....	62
Appendix E: Sangras et al. (1998a).....	66
Appendix F: Sangras et al. (1998a).....	103

List of Tables

<u>Table</u>		<u>Page</u>
1	Summary of Publications.....	1
2	Development of Plane Buoyant Turbulent Plumes	19
3	Development of Plane Turbulent Adiabatic Wall Plumes.....	26

List of Figures

<u>Figure</u>	<u>Caption</u>	<u>Page</u>
1	Development of radial profiles of mean mixture fractions for round turbulent plumes.....	7
2	Development of radial profiles of rms mixture fraction fluctuations for round turbulent plumes.....	8
3	Radial profiles of mean streamwise velocities for self-preserving round turbulent plumes.....	9
4	Radial profiles of mean radial velocities for self-preserving round turbulent plumes.....	11
5	Radial profiles of rms velocity fluctuations for self-preserving round turbulent plumes.....	12
6	Radial distributions of turbulent mass fluxes for self-preserving round turbulent plumes.....	13
7	Cross stream profiles of mean mixture fractions in self-preserving round turbulent plumes.....	18
8	Cross stream profiles of rms mixture fraction fluctuations in self-preserving round turbulent plumes.....	20
9	Typical temporal power spectral densities of mixture fraction fluctuations in self-preserving plane turbulent plumes.	22
10	Cross stream profiles of mean mixture fractions in self-preserving plane turbulent wall and free plumes.....	25
11	Cross stream profiles of rms mixture fraction fluctuations in self-preserving plane turbulent wall and free plumes.....	28
12	Typical temporal power spectral densities of mixture fraction fluctuations in self-preserving plane turbulent adiabatic wall plumes.	29

Nomenclature

b	=	source width
B_o	=	source buoyancy flux
d	=	source diameter
f	=	mixture fraction
E_o	=	entrainment coefficient, Eq. (9)
$E_f(n)$	=	temporal power spectral density of f
$F(r \text{ or } y/(x-x_o))$	=	scaled cross stream distribution of \bar{f} in self-preserving region
Fr_o	=	source Froude number
g	=	acceleration of gravity
ℓ_f	=	characteristic plume radii based on \bar{f}
ℓ_M	=	Morton length scale
ℓ_u	=	characteristic plane radii based on \bar{u}
$\ell_{1/2}$	=	characteristic plume halfwidth where $\bar{f} = \bar{f}/2$
M_o	=	source specific momentum flux
n	=	frequency
Q	=	plume volume flux
r	=	radial distance
Re_o	=	source Reynolds number, $u_o d/v_o$ or $u_o b/v_o$
u	=	streamwise velocity
$U(r \text{ or } y/(x-x_o))$	=	scaled cross stream distribution of \bar{u} in self-preserving region
x	=	streamwise distance
y	=	cross stream distance
z	=	distance along slot from its midpoint
Z'	=	slot length
ν	=	kinematic viscosity
ρ	=	density
τ_f	=	temporal integral scale of mixture fraction fluctuations
Subscripts		
c	=	centerline value
o	=	initial value or virtual origin location
∞	=	ambient value

Superscripts

$(\bar{\quad})$ = time-averaged mean value

$(\bar{\quad})'$ = root-mean-squared fluctuating value

1. Introduction

An investigation of the structure and mixing properties of buoyant turbulent flows, typical of those found in the environment of unwanted fires, is described. The findings of the research have applications to modeling unwanted fires, to controlling the emission of radiant energy, toxic materials and soot from fires, to developing materials test codes for fire properties, and to developing fire detectors.

The properties of buoyant turbulent flows are a central feature of unwanted fires and are needed to understand effects of turbulence/radiation interactions. In particular, past studies have demonstrated the importance of turbulence/radiation interactions with actual radiant fluxes from turbulent flames being 2-3 times larger than estimates based on mean properties in the flames, see Faeth et al. (1989) and references cited therein. In addition, stochastic simulation techniques have been developed to estimate effects of turbulence/radiation interactions in flames, based on laminar flamelet concepts and a knowledge of mixture fraction statistics, see Kounalakis et al. (1991) and references cited therein. In spite of extensive past studies, however, available information about the properties of buoyant turbulent flows was too limited to allow use of the stochastic simulation methodology to estimate effects of turbulence/radiation interactions. Furthermore, earlier work, see Dai et al. (1994) and references cited therein, suggested that past measurements of buoyant turbulent plumes had not been completed far enough from the source to observe fully-developed (self-preserving) buoyant turbulent plume behavior, see Dai et al. (1994) and references cited therein. This shortcoming is problematical due to uncertain effects of source disturbances and incomplete flow development on measurements used to assess models of buoyant turbulent flows that are needed to address problems of practical fire environments. Thus, the objective of the present investigation was to experimentally determine the mean and turbulent properties of self-preserving buoyant turbulent plumes in order to help fill this gap in the literature.

The present investigation considered the following three flows, in turn: turbulent round free plumes, turbulent plane free plumes and turbulent adiabatic wall plumes. The present discussion of the three phases of the research is brief, more details about the investigation can be found in the articles, papers, reports and theses describing aspects of the investigation that are summarized in Table 1 and cited in the list of references. Finally, key references are included in the appendices to this report, e.g., Dai et al. (1994,1995a,b), Dai and Faeth (1996) and Sangras et al. (1998a,b) in Appendices A-F, respectively.

Table 1. Summary of Publications

Archival Publications (articles and book chapters):

Sangras, R., Dai, Z. and Faeth, G.M. (1998) Mixture fraction statistics of plane self-preserving buoyant turbulent adiabatic wall plumes. J. Heat Trans., submitted.

Sangras, R., Dai, Z. and Faeth, G.M. (1998) Mixing structure of plane self-preserving buoyant turbulent plumes, J. Heat Transfer, in press.

Faeth, G. M. (1997) Combustion fluid dynamics (tools and methods), Proceedings of the Workshop on Fuels with Improved Fire Safety, National Academy Press, Washington, DC, pp. 81-96.

Dai, Z., and Faeth, G.M. (1996) Measurements of the structure of self-preserving round buoyant turbulent plumes. J. Heat Trans. 118, 493-495.

Dai, Z., Tseng, L.-K. and Faeth, G.M. (1995) Velocity/mixture-fraction statistics of round, self-preserving buoyant turbulent plumes. J. Heat Trans. 117, 918-926.

Dai, Z., Tseng, L.-K. and Faeth, G.M. (1995) Velocity statistics of round, fully-developed buoyant turbulent plumes, J. Heat Trans. 117, 138-145.

Dai, Z., Tseng, L.-K., and Faeth, G.M. (1994) Structure of round, fully-developed, buoyant turbulent plumes, J. Heat Trans. 116, 409-417.

Papers:

Sangras, R., Dai, Z. and Faeth, G.M. (1998) Structure of self-preserving turbulent adiabatic wall plumes, Proceedings of Annual Conference on Fire Research, NIST, Gaithersburg, MD, in press.

Sangras, R., Dai, Z. and Faeth, G.M. (1998) Mixture fraction statistics of plane self-preserving buoyant turbulent adiabatic wall plumes, Proceedings of the 5th ASME/JSME Joint Thermal Engineering Conference, San Diego, California, in press.

Sangras, R., Dai, Z. and Faeth, G.M. (1998) Mixing structure of plane self-preserving buoyant turbulent plumes, Proceedings of the 7th AIAA/ASME Joint Thermodynamics and Heat Transfer Conference, ASME, New York, HTD-357-1, 197-206.

Faeth, G.M. (1996) Self-preserving buoyant turbulent plumes, Proceedings: Fluid Mechanics of Fires — A Symposium in Honor of Professor Edward Edon Zukoski, 13th Joint Meeting of UJNR Panel in Fire Research and Safety, Gaithersburg, MD, 38-45.

Dai, Z. and Faeth, G.M. (1995) Evaluation of approximate models of buoyant turbulent flows, Proceedings Intl. Conf. Fire Res. and Engr., Soc. Fire Protection Engrs., Boston, 141-146.

Dai, Z., Tseng, L.-K. and Faeth, G.M. (1995) Velocity/mixture-fraction statistics of round, self-preserving buoyant turbulent plumes. Proc. 30th National Heat Trans. Conf. (R.I. Peterson et al., eds.), ASME, New York, HTD-Vol. 304 (Vol. 2), 19-38.

Dai, Z. Tseng, L.-K. and Faeth, G.M., (1994) Properties of self-preserving, round buoyant turbulent plumes, Bull. Amer. Phys. Soc. 39, 1469 (abstract only).

Z. Dai, Tseng, L.-K. and Faeth, G.M. (1994) Velocity statistics of round, fully-developed buoyant turbulent plumes, ASME Winter Annual Meeting, Chicago.

Reports and Theses:

Dai, Z., Krishnan, S.S., Lin, K.-C., Sangras, R., Wu, J.-S., and Faeth, G.M. (1996) Mixing and radiation properties of buoyant luminous flame environments. Report No. GDL/GMF-96-01, The University of Michigan, Ann Arbor.

Dai, Z., Krishnan, S.S., Lin, K.-C., Sangras, R., Wu, J.-S., and Faeth, G.M. (1995) Mixing and radiation properties of buoyant luminous flame environments. Report No. GDL/GMF-95-02, The University of Michigan, Ann Arbor.

Dai, Z. (1995) Structure of self-preserving round buoyant turbulent plumes. Ph.D. Thesis, The University of Michigan, Ann Arbor.

2. Turbulent Round Free Plumes

2.1 Introduction

Scalar mixing of round buoyant turbulent plumes in still environments is an important fundamental problem that has attracted significant attention since the classical study of Rouse et al. (1952). Recent work, however, suggests that more information about the turbulence properties of scalar quantities within buoyant turbulent flows is needed to address turbulence/radiation interactions in fire environments (Kounalakis et al., 1991). Thus, the objective of the present investigation was to measure mixture fraction statistics in round buoyant turbulent plumes in still environments, noting that mixture fraction statistics provide information needed to find fluctuations of all scalar properties using conventional laminar flamelet concepts of turbulent diffusion flames (Faeth et al., 1989). Associated measurements of mean and fluctuating velocity statistics, as well as combined velocity/mixture-fraction statistics, were also completed in order to provide insight about the turbulence properties of these flows. In order to simplify interpretation of the results, the experiments emphasized fully-developed buoyant turbulent plumes, where effects of the source have been lost and both mean and fluctuating properties become self-preserving (Tennekes and Lumley, 1972).

Extensive reviews of earlier studies of round buoyant turbulent plumes can be found in Kotsovinos (1985), List (1982), Papanicolaou and List (1987,1988), Pivovarov et al. (1992) and Ramaprian and Chandrasekhara (1985,1989). The earliest work concentrates on scaling within self-preserving plumes (Rouse et al., 1952; Morton, 1959; Morton et al., 1956). Subsequent measurements (Abraham, 1960; George et al., 1977; Kotsovinos, 1985; Nakagome and Hirata, 1977; Ogino et al., 1980; Peterson and Bayazitoglu, 1992; Shabbir 1987; Shabbir and George, 1992; Zimin and Frik, 1977) exhibited significant differences when plotted in terms of self-preserving scaling. List (1982) and Papanicolaou and List (1987,1988) attribute these differences to problems of reaching self-preserving plume conditions with experimental uncertainties being a contributing factor.

Two parameters must be considered when evaluating whether a turbulent plume is self-preserving: (1) the distance from the virtual origin normalized by the source diameter, $(x-x_0)/d$, as a measure of conditions where source disturbances have been lost; and, the distance from the virtual origin normalized by the Morton length scale, $(x-x_0)/\ell_M$ as a measure of conditions where buoyancy-induced momentum becomes large compared to source momentum. The Morton length scale is defined as follows for a round plume having uniform properties at the source (Morton, 1959; List, 1982):

$$\ell_M = (\pi/4)^{1/4}(\rho_\infty d u_0^2 / (g|\rho_0 - \rho_\infty|))^{1/2} \quad (1)$$

where an absolute value has been used for the density difference to allow for both rising and falling plumes. By these measures, there is good reason to suspect that self-preserving conditions were not reached due to inadequate distances of past measurements from the source. In particular, the early measurements all involved $(x-x_0)/d \leq 62$ which is relatively small compared to values of $(x-x_0)/d > 100$ required to reach self-preserving nonbuoyant round turbulent jets (Tennekes and Lumley, 1972).

The preceding discussion suggests that existing measurements of the properties of buoyant turbulent plumes probably involve transitional plumes rather than self-preserving plumes because the measurements were not carried out far enough from the source. Thus, the objective of the present investigation was to establish conditions where self-preserving behavior could be observed, and to complete measurements of mixture fraction, velocity and combined mixture-fraction/velocity statistics for these conditions.

In the following, experimental methods and self-preserving scaling are described first. The results are then discussed before summarizing conclusions. The following description of the study is brief, more details can be found in Dai and Faeth (1996) and Dai et al. (1994,1995a,b) which appear in Appendixes A-D.

2.2 Experimental Methods

The experiments involved source flows of carbon dioxide and sulfur hexafluoride in still air at atmospheric pressure and normal temperature in order to provide a straightforward specification of the buoyancy flux within the test plumes. This approach yielded downward-flowing, negatively buoyant plumes. Measurements of mixture fraction, velocity and combined mixture-fraction/velocity statistics were carried out using laser-induced iodine fluorescence (LIF), laser velocimetry (LV) and combined LIF/LV, respectively.

The plumes were observed in a double enclosure contained in a large, high-bay test area. The outer enclosure was $3000 \times 3000 \times 3400$ mm high and had plastic side walls and a screen ceiling to provide air entrained by the plumes. The plume itself was in a $1100 \times 1100 \times 3200$ mm high screened enclosure. The plume sources were rigid round tubes (inside diameters of 6.4 and 9.7 mm) with flow straighteners and length-to-diameter ratios of 50:1. The plume flow was removed through 300 mm diameter ducts mounted on the floor at the four corners of the outer enclosure. The plume and the inner enclosure could be traversed to accommodate rigidly mounted optical instrumentation.

The source flow was seeded with iodine vapor for LIF by passing a portion of it through a bed of iodine crystals; the source flow was monitored to account for changes of iodine concentrations. The ambient air in the enclosure was seeded with oil drops (roughly 1 μm nominal diameter) for LV using several multiple jet spray generators located above the screened ceiling.

The LIF signal was produced by the unfocussed beam at 514 nm wavelength of an argon-ion laser. This wavelength causes iodine to fluoresce at longer (yellow) wavelengths which were observed using a detector having a long-pass optical filter with a cut-off wavelength of 520 nm. The LIF signal was calibrated by measurements of progressively diluted air/source mixtures at the source exit. Effects of differential diffusion and gradient broadening were small for present conditions yielding experimental uncertainties (95% confidence) less than 5 and 10% for mean and fluctuating mixture fractions (except near the edge of the flow where uncertainties are larger).

Dual-beam frequency-shifted LV was used for the velocity measurements based on the 514.5 nm line of an argon-ion laser. Various orientations of the plane of the laser beams were used to find the three components of mean and fluctuating velocities, and the Reynolds stress. The low-pass filtered output of the signal processor was sampled at equal

time intervals to avoid velocity bias while frequency shifting avoided directional bias and ambiguity. Experimental uncertainties (95% confidence) were estimated to be less than 5 and 13% for mean and fluctuating velocities, respectively (except near the edge of the flow where uncertainties are larger). Combined LIF/LV measurements are straightforward with the present approach. Given all these results conservation checks could be completed and were satisfactory within experimental uncertainties. Buoyancy fluxes were conserved within 5% and the balance between plume momentum and buoyancy terms was satisfied with 18%, which also is comparable to the experimental uncertainties of these properties.

2.3 Self-Preserving Scaling

The state relationship for density as a function of mixture fraction, assuming an ideal gas mixture, is as follows:

$$\rho = \rho_{\infty} / (1 - f(1 - \rho_{\infty} / \rho_0)) \quad (2)$$

Far from the source in the self-preserving region, $f \ll 1$, and Eq. (2) can be linearized as follows:

$$\rho = \rho_{\infty} + f \rho_{\infty} (1 - \rho_{\infty} / \rho_0), \quad f \ll 1 \quad (3)$$

The measurements of mean mixture fractions and streamwise mean velocities then take the following forms (List, 1982):

$$F(r/(x-x_0)) = \bar{f} g B_0^{2/3} (x-x_0)^{5/3} |\rho_{\infty} - \rho_0| / \rho_0 \quad (4)$$

$$U(r/(x-x_0)) = \bar{u} ((x-x_0) / B_0)^{1/3} \quad (5)$$

where $F(r/(x-x_0))$ and $U(r/(x-x_0))$ are appropriately scaled universal functions of mean mixture fraction and streamwise velocity in the self-preserving portion of the flow. Other mean and fluctuating properties of the flow also yield universal functions in terms of $r/(x-x_0)$ when appropriately normalized by \bar{f} and \bar{u} in the self-preserving region.

Assuming uniform properties at the source exit, the source momentum and buoyancy fluxes can be found as follows (List, 1982):

$$M_0 = (\pi/4) d^2 u_0^2 \quad (6)$$

$$B_0 = (\pi/4) d^2 u_0 g |\rho_0 - \rho_{\infty}| / \rho_{\infty} \quad (7)$$

In terms of these parameters, the Morton length scale becomes (List):

$$\ell_M = M_0^{3/4} / B_0^{1/2} \quad (8)$$

which properly retrieves Eq. (1) for ℓ_M . Other properties such as characteristic Reynolds numbers, characteristic plume diameters, etc., can be found in Dai et al. (1994, 1995a,b).

2.4 Results and Discussion

The development of round buoyant turbulent plumes toward self-preserving conditions can be seen from the radial profiles of mean mixture fractions for the two plume sources (CO_2 and SF_6) illustrated in Fig. 1. The scaling parameters used in this figure are such that the ordinate is $F(r/(x-x_0))$. The profiles exhibit progressive narrowing as streamwise distances increase, however, self-preserving conditions are observed when $(x-x_0)/d > 87$ which corresponds to $(x-x_0)/\ell_M \geq 12$ and extend to the largest distance from the source that was accessible, i.e., $(x-x_0)/d = 151$ and $(x-x_0)/\ell_M = 43$. This range of conditions corresponds to characteristic plume Reynolds numbers of 2500–4200 which are large for unconfined turbulent flows.

Present profiles of mean mixture fractions are compared extensively with other measurements in the literature in Dai and Faeth (1994), e.g., with George et al. (1977), Shabbir and George (1992), Papanicolaou and List (1987,1988) and Papantoniou and List (1989). In general, present results for self-preserving conditions had a characteristic plume radii up to 30% smaller and scaled mean mixture fractions at the axis up to 30% larger, than earlier results in the literature. In keeping with the trends seen in Fig. 1, this behavior follows because the earlier results were not obtained far enough from the source to reach the self-preserving regime.

Radial profiles of mixture fraction fluctuations are plotted in terms of self-preserving variables in Fig. 2 as a function of distance from the source. Near the source, the profiles are broad and exhibit a dip near the axis similar to the behavior of nonbuoyant jets, see Papanicolaou and List (1987,1988). The profiles evolve with increasing streamwise distance, however, with both the width and the magnitude of the dip decreasing. Eventually, self-preserving behavior is reached when $(x-x_0)/d \geq 87$ and $(x-x_0)/\ell_M > 12$. This is not surprising because self-preserving conditions for both mean and fluctuating properties should be observed at the same time. Similar to mean mixture fractions, the mixture fraction fluctuation profiles of Papanicolaou and List (1987,1988), Shabbir and George (1992) and George et al. (1977) are similar to transitional plumes and are broader in terms of $r/(x-x_0)$ than the present measurements.

The gradual disappearance of the dip in mixture fraction fluctuations near the axis is an interesting feature of the results illustrated in Fig. 2. This behavior is expected near the jet exit where the flow is similar to a nonbuoyant turbulent jet and has reduced mixture fraction fluctuations near the axis because turbulence production is small in this region due to symmetry requirements. In contrast, effects of buoyancy provide turbulence production near the axis of plumes in spite of symmetry due to buoyant instability in the streamwise direction. This added production accounts for much larger values of \bar{f}'/\bar{f} near the axis of plumes, 0.45, compared to nonbuoyant jets, ca. 0.25, which also implies much stronger effects of turbulence/radiation interactions for buoyant turbulent plumes than for nonbuoyant turbulent jets.

Measurements of velocities were limited to the self-preserving portion of the flow in order to avoid concentration bias because only the ambient air was seeded. Mean streamwise velocity distributions are illustrated in Fig. 3 for the two sources. In this figure, the velocities have been scaled so that the ordinate of the plot is $U(r/(x-x_0))$. It is evident that the mean streamwise velocities satisfy the requirements for self-preserving behavior quite well for $99 \leq (x-x_0)/d \leq 151$, which essentially corresponds to the self-preserving region based on mean mixture fraction distributions.

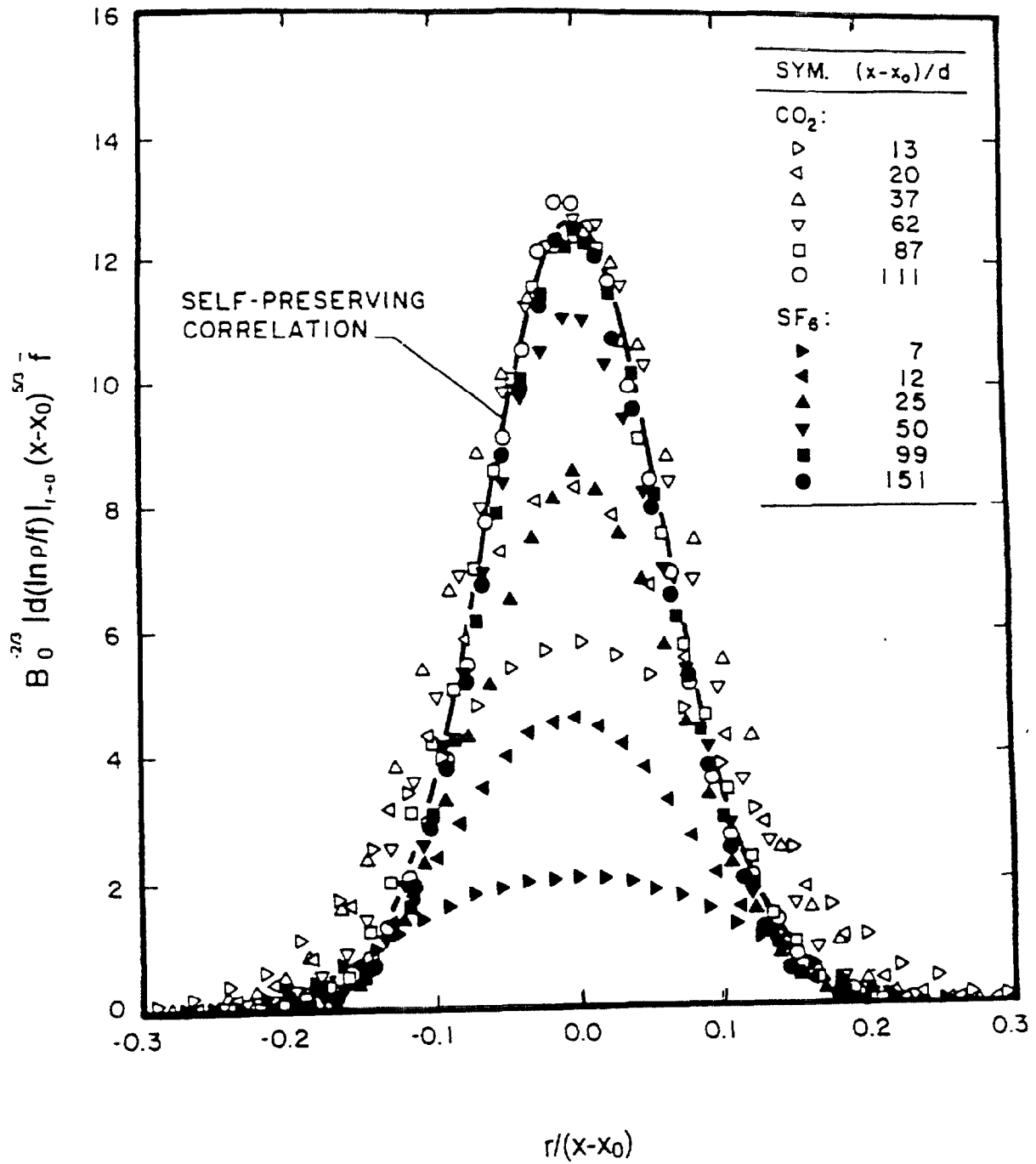


Fig. 1 Development of radial profiles of mean mixture fractions for round turbulent plumes.

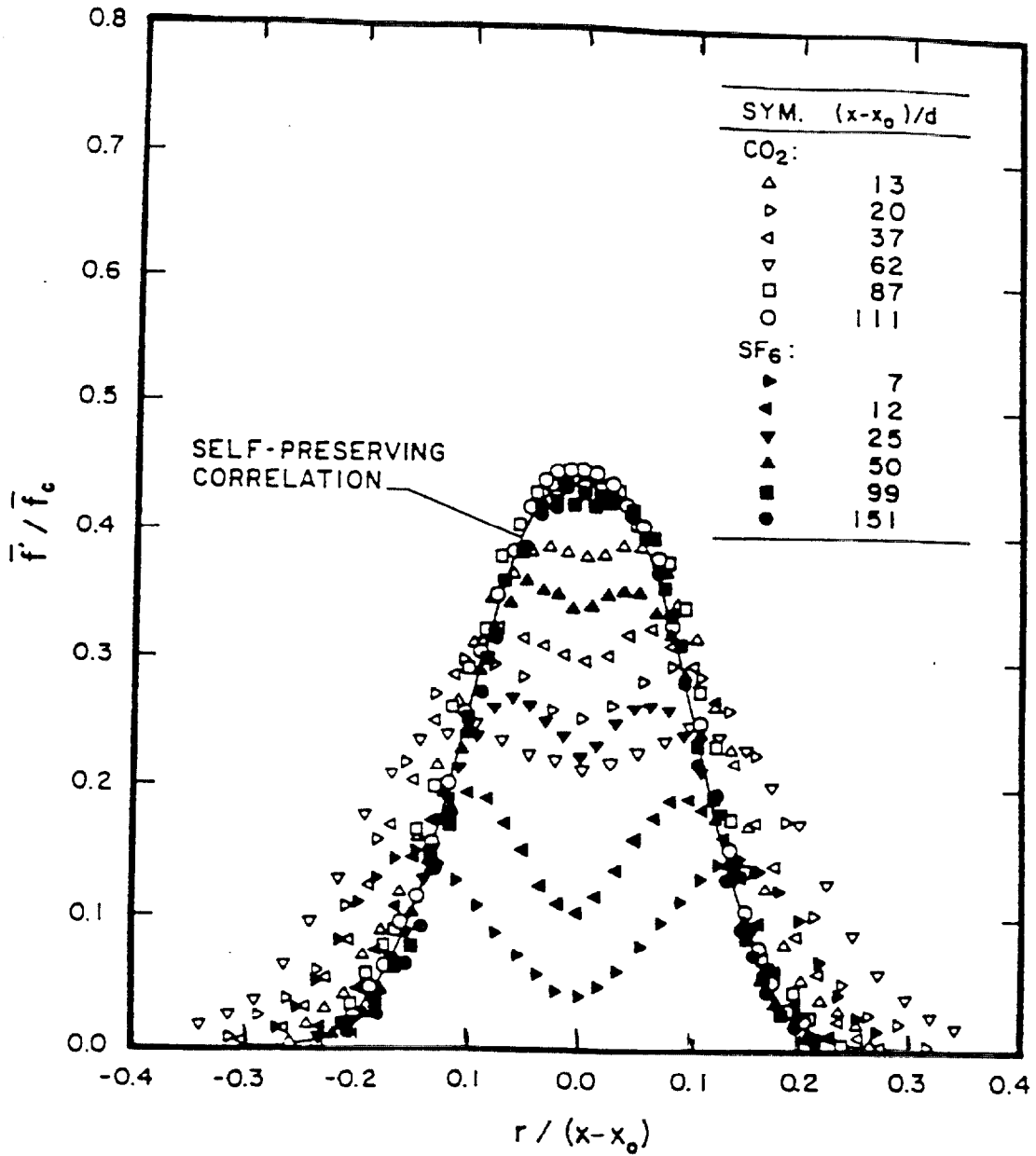


Fig. 2 Development of radial profiles of rms mixture fraction fluctuations for round turbulent plumes.

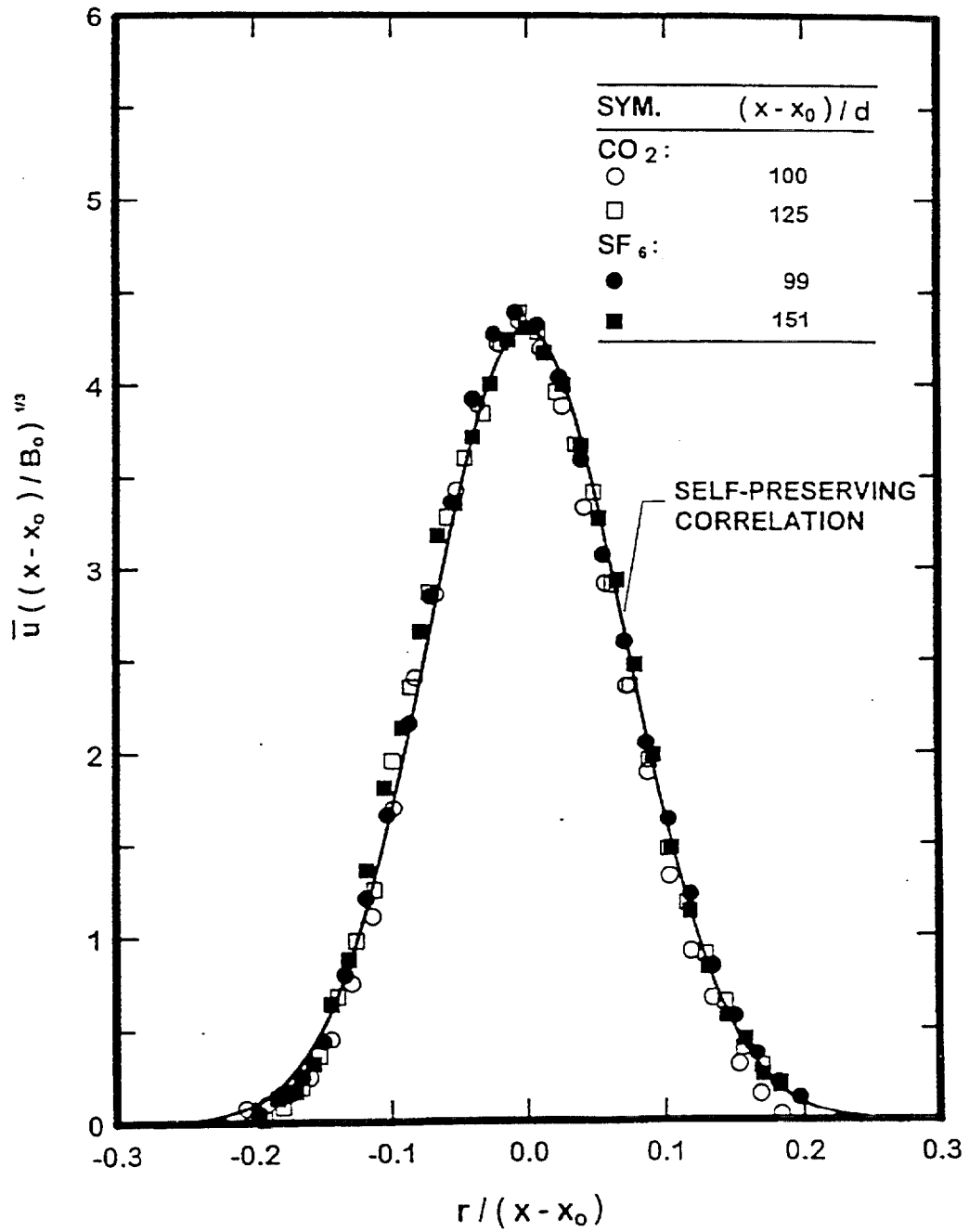


Fig. 3 Radial profiles of mean streamwise velocities for self-preserving round turbulent plumes.

Present measurements of $U(r/(x-x_0))$ were compared with several earlier measurements in the literature, e.g., Nakagone and Hirata (1977), Ogino et al. (1980), George et al. (1977), Shabbir and George (1992) and Papanicolaou and List (1988). Present characteristic flow radii were up to 40% smaller and present values of $U(r/(x-x_0))$ near the axis were up to 25% larger than these earlier values in the literature.

Measurements of cross stream mean velocities are plotted according to self-preserving variables in Fig. 4. These results properly exhibit self-preserving behavior and are also consistent with present measurements of \bar{u} through the continuity equation. These results can also be used to find the entrainment constant of the flow, defined as follows (Dai et al., 1995a):

$$dQ/dx = E_0 \ell_v \bar{u}_c \quad (9)$$

Present measurements of E_0 yielded a value of 0.086, which is up to 40% smaller than earlier results for transitional plumes (based on the same sources as before).

Radial profiles of rms velocity fluctuations within self-preserving round buoyant turbulent plumes are illustrated in Fig. 5. These profiles are universal within experimental uncertainties over the present test range. The presence of a dip near the axis is similar to nonbuoyant jets and is expected because turbulence production is reduced near the axis due to symmetry (Panchapakesan and Lumley, 1993). Nevertheless, this behavior differs from the mixture fraction fluctuations illustrated in Fig. 2 which is another unusual feature of buoyant turbulent plumes. Finally, while the velocity fluctuations are nearly isotropic near the edge of the flow, streamwise velocity fluctuations are roughly 25% larger than the rest near the axis, which is not unusual for a turbulent shear flow.

Present measurements of turbulent mass fluxes are illustrated in Fig. 6 for self-preserving conditions as an example of combined mixture-fraction/velocity measurements. The tangential turbulent mass flux is properly negligible for an axisymmetric flow, the remaining components adequately satisfy the requirements for self-preserving flow. The consistency of present measurements was evaluated as described by Dai et al. (1995b) and yield excellent results as illustrated in Fig. 6. These results, and corresponding results for velocity fluctuations, indicate countergradient diffusion in the streamwise direction which is problematical for simple turbulence models. The results also show that the streamwise turbulent mass flux is appreciable for self-preserving conditions, comprising roughly 15% of the total buoyancy flux of the plume. Finally, the turbulent Prandtl/Schmidt number, which often is assumed to be a constant for simple turbulence models, was found to vary appreciably for the present classical self-preserving flow (although the value near the axis is roughly 0.8 which is the value used in most turbulence models).

The final stage of these measurements is reported in Dai and Faeth (1996) which established that the findings of Dai and Faeth (1994,1995a,b) were not affected by coflow or by confinement. It should also be noted that results considered here are only a small sample of the findings of Dai et al. (1994,1995a,b) which should be consulted for full details.

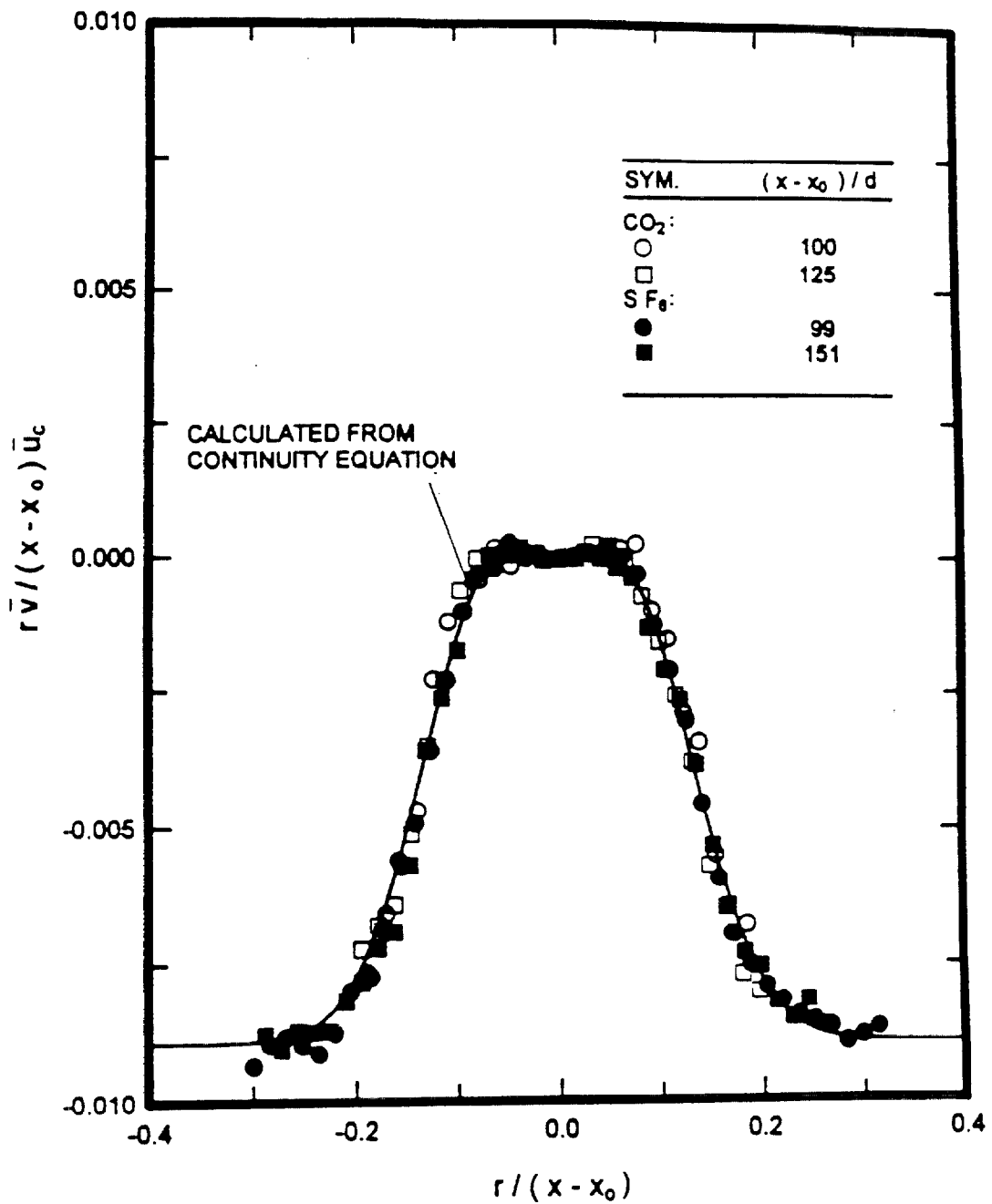


Fig. 4 Radial profiles of mean radial velocities for self-preserving round turbulent plumes.

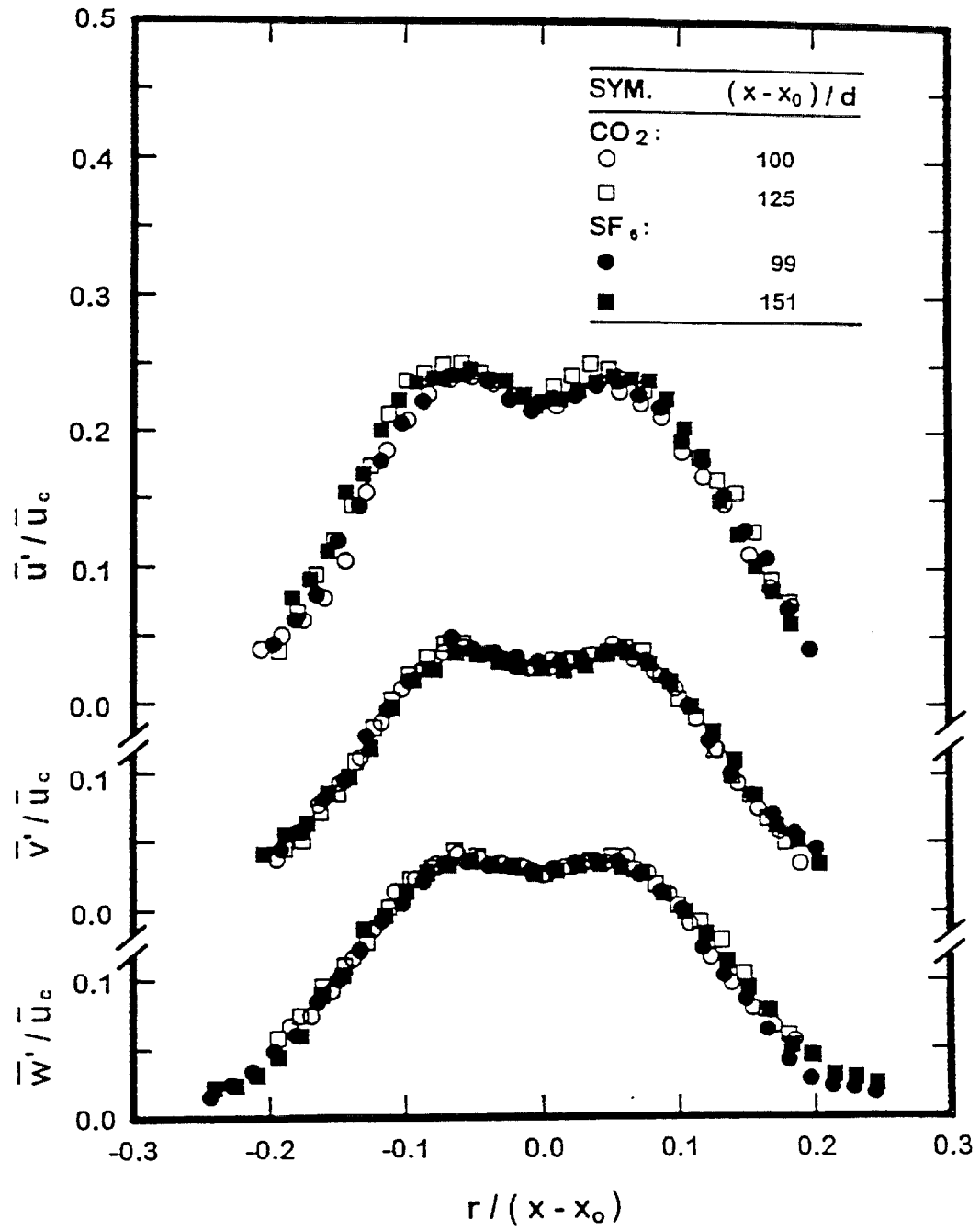


Fig. 5 Radial profiles of rms velocity fluctuations for self-preserving round turbulent plumes.

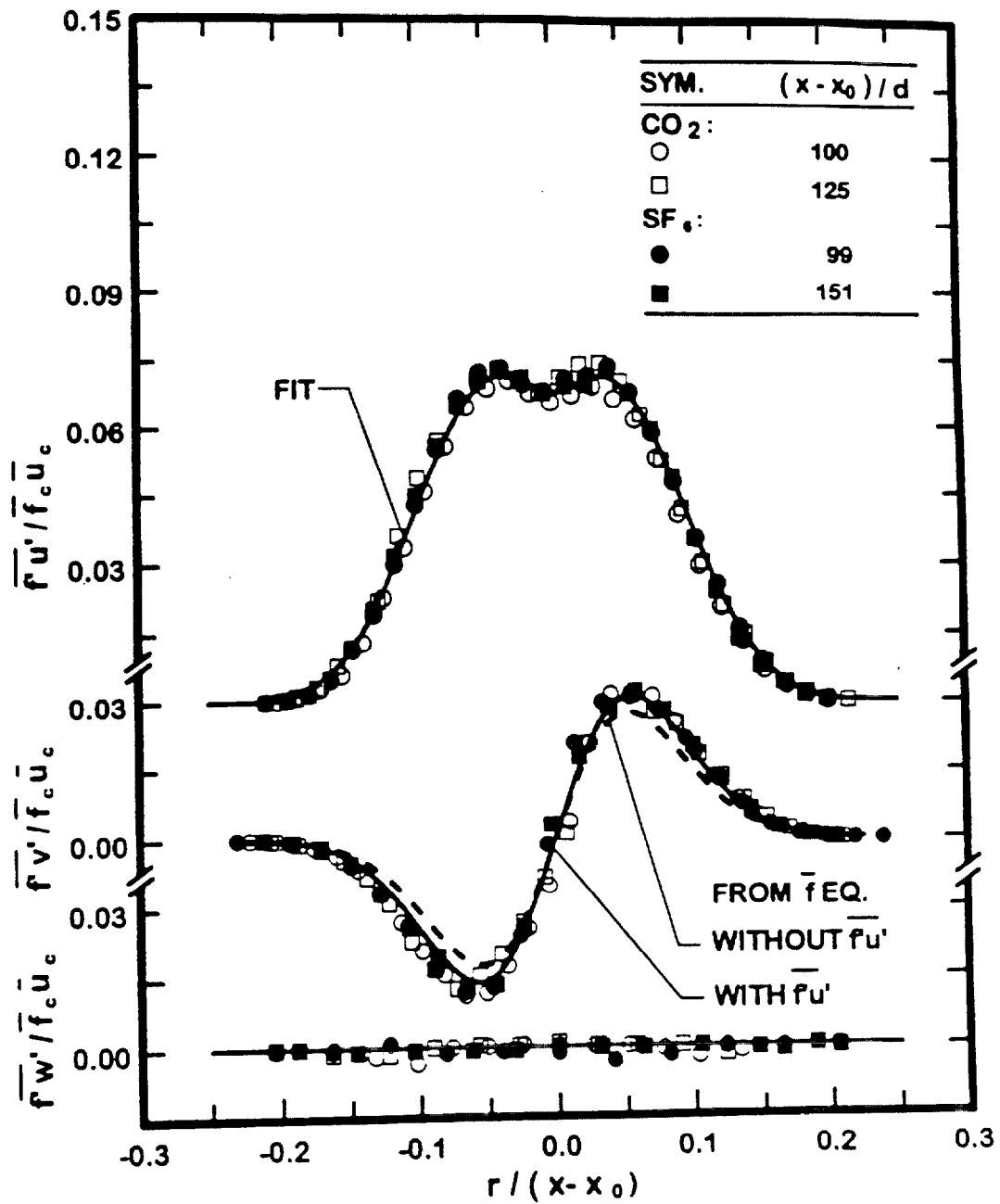


Fig. 6 Radial distributions of turbulent mass fluxes for self-preserving round turbulent plumes.

2.5 Conclusions

The statistics of mixture fraction, velocity and combined mixture-fraction/velocity properties were measured for round buoyant turbulent plumes in still air. The test conditions involved buoyant jet sources of carbon dioxide and sulfur hexafluoride with measurements extending to $(x-x_0)/d = 151$ and $(x-x_0)/\ell_M = 43$, and emphasizing self-preserving properties. The major conclusions of the study are as follows:

1. Present measurements indicated self-preserving behavior for $(x-x_0)/d \geq 87$ and $(x-x_0)/\ell_M \geq 12$ which is farther from the source than earlier studies where $(x-x_0)/d \leq 62$ and which are probably still in the transitional plume region. As a result of further development of self-preserving behavior, present plumes were up to 40% narrower, scaled mean properties near the axis were up to 30% larger, and entrainment coefficients were up to 40% smaller than earlier measurements in the literature.

2. Radial profiles of mixture fraction fluctuations for self-preserving buoyant turbulent plumes do not exhibit a dip near the axis similar to nonbuoyant jets due to additional turbulence production from streamwise instability of the flow. Surprisingly, this trend does not extend to velocity fluctuations, however, where both preserving buoyant turbulent plumes and nonbuoyant turbulent jets exhibit a dip in velocity fluctuations near the axis.

3. Streamwise turbulent fluxes of mass and momentum exhibited countergradient diffusion near the edge of the flow although the larger radial turbulent fluxes satisfied gradient diffusion approximations. This observation raises concerns about the use of simple gradient diffusion hypotheses for the complex buoyant turbulent flows of interest in practical fire environments.

4. Several other approximations used in simple turbulence models were not satisfied by the present relatively simple and classical buoyant turbulent flow: the turbulent Prandtl/Schmidt number was not constant, the ratio of characteristic velocity to mixture fraction time scales was not constant, and the coefficient of the radial gradient diffusion approximation for the Reynolds stress is not constant. These difficulties also raise concerns about the use of simple turbulence models for complex buoyant flame environments.

5. Streamwise turbulent mass fluxes are quite large near the axis of buoyant turbulent plumes, where corresponding correlation coefficients are unusually large (roughly 0.7). This behavior, combined with the rapid decay of mean mixture fractions in the streamwise direction is a strong source of production of scalar fluctuations, which probably is responsible for the large values of mixture fraction fluctuation intensities, roughly 0.45, near the axis of round buoyant turbulent plumes. Corresponding quantities concerning velocity fluctuations are more typical of nonbuoyant turbulent flows which probably is responsible for the much smaller velocity intensities near the axis of round buoyant turbulent plumes, roughly 0.18-0.25. These differences probably are also responsible for the absence and presence of the dip near the axis of mixture fraction and velocity fluctuation profiles, respectively, mentioned earlier for round buoyant turbulent plumes.

3. Turbulent Plane Free Plumes

3.1 Introduction

Given results for round buoyant turbulent plumes, other flows were addressed that are more directly relevant to flows encountered during unwanted fires within structures. The first flow that was considered was the turbulent plane free plume because it is the simplest configuration similar to plane turbulent flows along surfaces but without the complication of the actual presence of a surface. This flow is also of great fundamental importance as the classical buoyant turbulent plane or line plume, analogous to the classical nonbuoyant turbulent plane or line jet. Similar to the round buoyant turbulent plume study, fully-developed (self-preserving) flows far from the source were emphasized in order to avoid the complexities of transitional plumes, even though few practical buoyant turbulent plumes ever reach the self-preserving region.

In view of the increased generality of the findings, past studies of plane buoyant turbulent free plumes generally emphasized the properties of the self-preserving region of the flow. These studies included Rouse et al. (1952), Lee and Emmons (1961), Harris (1967), Anwar (1967), Kounalakis et al. (1977,1985) and Ramaprian and Chandrasekhara (1985,1989). These studies are in reasonably good agreement; for example, appropriately scaled flow widths and mean mixture fractions near the plane of symmetry agree within 13%, which is comparable to estimated experimental uncertainties. Whether these results still represent self-preserving behavior is questionable, however, because the measurements generally were limited to the region relatively close to the source, $(x-x_0)/b \leq 60$, with values of $(x-x_0)/\ell_M$ as small as 5-6 and with source aspect ratios, as small as 13:1 in some instances. In contrast, Dai and Faeth (1994,1995a,b) only observe self-preserving behavior for round buoyant turbulent plumes farther from the source, $(x-x_0)/d > 80$ and $(x-x_0)/\ell_M$ as small as 5-6. Another limitation of past studies of plane buoyant turbulent plumes is that the measurements of turbulence properties are very limited, and are nonexistent for the gaseous plumes typical of many practical applications.

In view of these observations, the objective of the present investigation was to measure mean and fluctuating mixture fraction properties of plane free turbulent plumes in still gases, emphasizing conditions in the self-preserving portion of the flow.

In the following experimental methods and self-preserving scaling are described first. Results are then considered before summarizing conclusions. The following description of the study is brief, more details can be found in Sangras et al. (1998a) which appears in Appendix E.

3.2 Experimental Methods

The experiments involved source flows of helium/air mixtures in still air at atmospheric pressure and normal temperature in order to provide straightforward specification of the buoyancy flux of the test plumes. This approach yielded upward flowing, positively buoyant plumes. Measurements of mixture fraction statistics were carried out using LIF.

The plumes were observed in a double enclosure contained in a large, high-bay test area. The outer enclosure was $3400 \times 2000 \times 3600$ mm high and had porous walls parallel to the source and a porous ceiling both made of filter material. The filter material controlled room disturbances and light leakage into the test area while allowing free inflow of air and outflow of the plume (doubling the filter thickness had no effect on flow properties). After

leaving the test enclosure, the plume gases were captured in a hood near the ceiling of the laboratory and subsequently exhausted using a blower.

The test plume was located at the plane of symmetry of the inner enclosure. The source slot was 9.4 mm wide and 876 mm long and was mounted at the center of a flat floor 876 mm long and 1220 mm wide. The flow/slot assembly was mounted normal to 1220 × 2440 mm high end walls. The inner enclosure was completed by installing a pair of screen arrays across the openings between the outer extremities of the two end walls, similar to the use of screens by Dai et al. (1994,1995a,b) for round plumes and by Gutmark and Wygnowski (1976) for plane free turbulent jets. Horizontal traversing was carried out by mounting the floor/wall assembly on linear bearings so that it could be moved by a stepping motor having 5 μm positioning accuracy. Vertical traversing was carried out by shifting the floor on the end walls. Optical access was provided by windows in the end walls.

The helium and air flows were mixed, passed through iodine beds and then through long lines (length-to-diameter ratios of 1200) to insure uniform mixing. This flow then entered a source manifold, passed through a bed of beads, a section of filter and a contraction to the final slot exit.

Mixture fractions were measured using iodine LIF based on the 514 nm line of an argon-ion laser. The same arrangement as Dai et al. (1994) was used except that the laser was focused at the measuring volume. The LIF signal was calibrated at the source exit by diverting a portion of the source flow to the LIF measuring volume through a plastic tube. Effects of preferential diffusion and extinction of the laser and fluorescence signals were negligible. Experimental uncertainties (95% confidence) were smaller than 6 and 12% for mean and rms fluctuating mixture fractions (except near the edge of the flow where uncertainties were larger).

3.3 Self-Preserving Scaling

The state relationships for plume density as a function of mixture fraction are unchanged from before, e.g., Eq. (2) for general conditions and the approximation of Eq. (3) for self-preserving conditions where $f \ll 1$. Mean mixture fraction and mean streamwise velocity distributions then take the following forms (List, 1982):

$$F(y/(x-x_0)) = \bar{f} g B_0^{2/3} (x-x_0) |\rho_0 - \rho_\infty| / \rho_0 \quad (10)$$

$$U(y/(x-x_0)) = \bar{u} / B_0^{1/3} \quad (11)$$

where $F(y/(x-x_0))$ and $U(y/(x-x_0))$ are appropriately scaled universal fractions of mean mixture fraction and streamwise velocity in the self-preserving portion of the flow. Other mean and fluctuating properties of the flow also yield universal functions in terms of $y/(x-x_0)$ when appropriately normalized by \bar{f} and \bar{u} in the self-preserving region.

Assuming uniform properties at the source exit, the source momentum and buoyancy fluxes can be found as follows (List, 1982):

$$M_0 = b u_0^2 \quad (12)$$

$$B_0 = b u_0 g |\rho_0 - \rho_\infty| / \rho_\infty \quad (13)$$

In terms of these parameters, the Morton length scale becomes (List, 1982):

$$\ell_M = M_0/B_0^{2/3} \quad (14)$$

Other parameters such as characteristic Reynolds numbers, characteristic plume widths, etc., can be found in Sangras et al. (1998a).

3.4 Results and Discussion

Two source flows were used, having initial density ratios $\rho_0/\rho_\infty = 0.770$ and 0.500 . The self-preserving regions were relatively far from the source, $(x-x_0)/b \geq 76$; therefore, the locations of virtual origins could not be distinguished from $x_0/b = 0$.

Present measurements of cross stream distributions of mean mixture fractions for the two sources are illustrated in Fig. 7. The scaling parameters of Eq. (10) have been used when plotting the figure so that the ordinate of the plot is $F(y/(x-x_0))$. Results for $z/Z = 0$ and $1/4$ are the same, confirming that the flow is reasonably two dimensional. The measurements indicate self-preserving behavior for $76 \leq (x-x_0)/b \leq 155$ and $9 \leq (x-x_0)/\ell_M \leq 21$ with the larger dimensional limited to avoid small flow aspect ratios. The range of conditions corresponded to characteristic plane Reynolds numbers of 3700-7500, which are large for unconfined turbulent flows.

Measurements of mean mixture fractions due to Rouse et al. (1952). Kounalakis et al. (1977) and Ramaprian and Chandrasekhara (1989) are also plotted in Fig. 7 for comparison with the present measurements (results from other past studies will be considered later). These distributions are up to 30% broader at the e^{-1} points and up to 30% larger at the plane of symmetry than the present measurements; reasons for these differences will be discussed next.

The larger scaled widths of the earlier mean mixture fraction distributions are typical of developing plumes. This behavior is not surprising because the earlier studies involved averages of measurements for $6 \leq (x-x_0)/b \leq 60$ (Rouse et al. (1952) may be an exception but the range of $(x-x_0)/b$ cannot be specified in this case because the source was a linear array of combusting jets so that b is not known) whereas Dai et al. (1994) only observed self-preserving behavior for mean mixture fraction distributions for round plumes at larger distances from the source. Corresponding flow development behavior for plane buoyant turbulent plumes can be seen from Table 2 where characteristic plume widths are summarized as a function of $(x-x_0)/b$. It is evident that $\ell_{1/2}/(x-x_0)$ tend to decrease with increasing $(x-x_0)/b$ with present findings serving as a reasonable limit for the rest.

The second issue concerning the distributions of mean mixture fractions seen in Fig. 7 is that present scaled values are smaller than the rest. It is felt that these differences are caused by problems of finding B_0 during the earlier studies. In particular, B_0 was known accurately for the present study but had to be found from measurements of velocity and mixture fraction distributions for the other studies which involves attendant problems of finding streamwise turbulent transport of B_0 , see Sangras et al. (1998a) for a discussion of this difficulty.

Comparison of present measurements of mean mixture fraction distributions with earlier work generally suggests that the earlier results were not found far enough from the

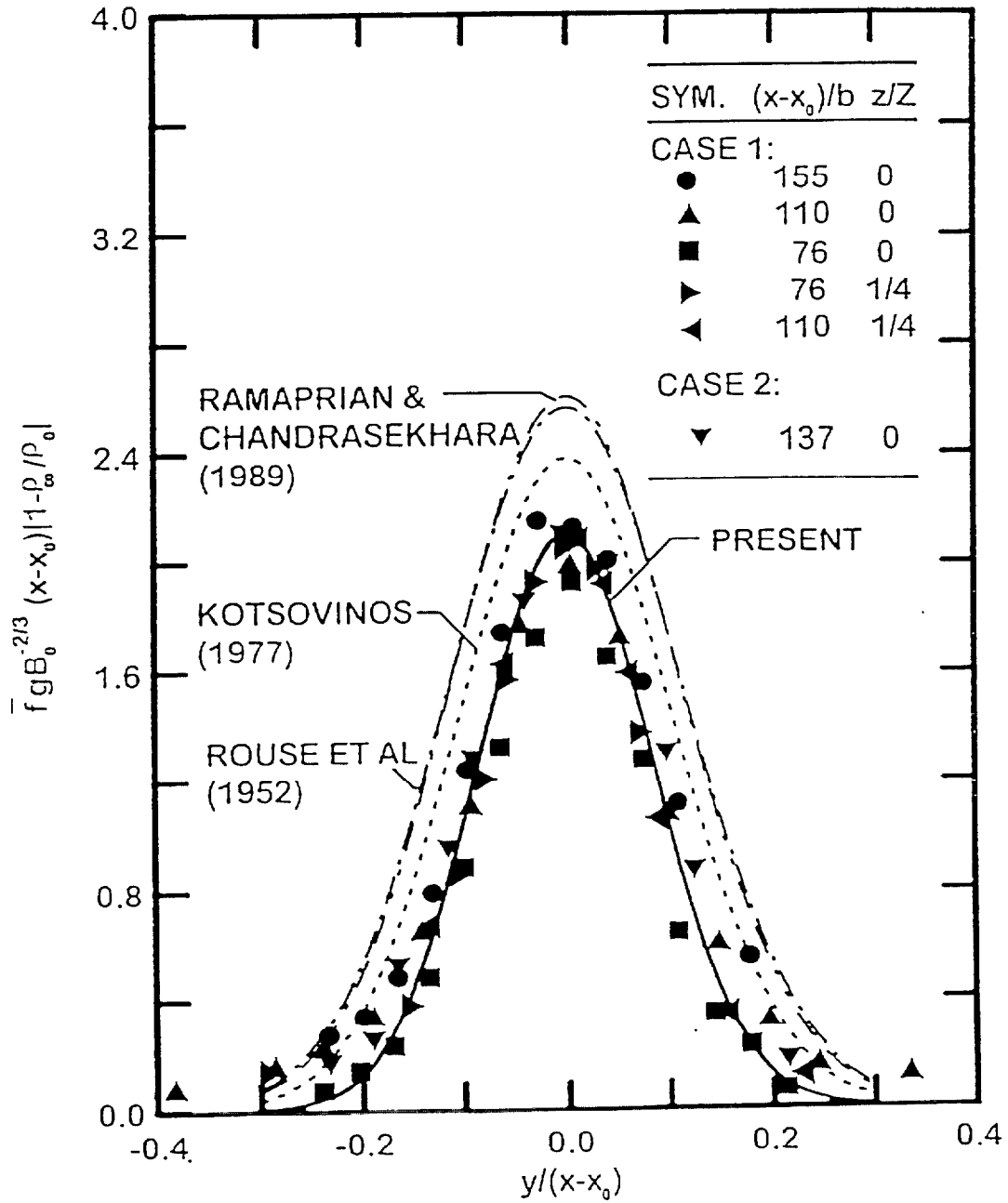


Fig. 7 Cross stream profiles of mean mixture fractions in self-preserving round turbulent plumes.

Table 2. Development of Plane Buoyant Turbulent Plumes^a

Source	$(x-x_0)/b$	$\ell_{1/2}/(x-x_0)$
Present (developing region)	13	0.15
	50 ^b	0.08
Present (self-preserving region)	76-155	0.08
Ramaprian and Chandrasekhara (1989)	20	0.14
	50	0.13
	60	0.13
Kotsovinos (1977)	14	0.15
	36	0.13

^aPlane buoyant turbulent plumes in still and unstratified environments. Entries are ordered chronologically.

^bNot judged to be in the self-preserving region because the mixture fraction fluctuation intensity at the plane of symmetry was not equal to the self-preserving value of 47%.

source to achieve self-preserving behavior, with excessively small flow aspect ratios being a contributing factor in some instances. Earlier studies of Lee and Emmons (1961) and to some extent Harris (1967) and Anwar (1968) were obtained at relatively large distances from the source where self-preserving behavior should have been approached. In these cases, broader distributions of \bar{f} probably resulted from disturbances that tend to increase flow widths and are difficult to avoid far from the source. Thus, over the measurements reported by Rouse et al. (1952), Lee and Emmons (1961), Harris (1967), Anwar (1969), Kotsovinos (1977) and Ramaprian and Chandrasekhara (1989) it is found that characteristic flow widths (based on e^{-1} points) are up to 36% larger and scaled mean mixture fractions near the plane of symmetry up to 24% larger than the present measurements.

Measurements of cross stream distributions of rms mixture fraction fluctuations are plotted in Fig. 8. The measurements of Kotsovinos (1977) and Ramaprian and Chandrasekhara (1989) are shown on this plot along with the present measurements. The distributions of Kotsovinos (1977) and Ramaprian and Chandrasekhara (1989) are broad and exhibit a dip near the plane of symmetry much like developing round plumes seen in Fig. 2. In contrast, present results reach a maximum near the plane of symmetry, similar to the self-preserving round plumes seen in Fig. 2. The present value of $(\bar{f}'/\bar{f})_c$ near the plane of symmetry, 47%, is also larger than the results of the other studies, 42%. As discussed earlier, this absence of the dip in the scaled \bar{f}' distribution and the unusually large values of $(\bar{f}'/\bar{f})_c$ for buoyant turbulent plumes probably is caused by the streamwise buoyant instability combined with the relatively rapid decay of mean mixture fractions with streamwise distance for these flows. Thus, the contribution of buoyancy to turbulence for both round and plane buoyant turbulent plumes is seen to be appreciable.

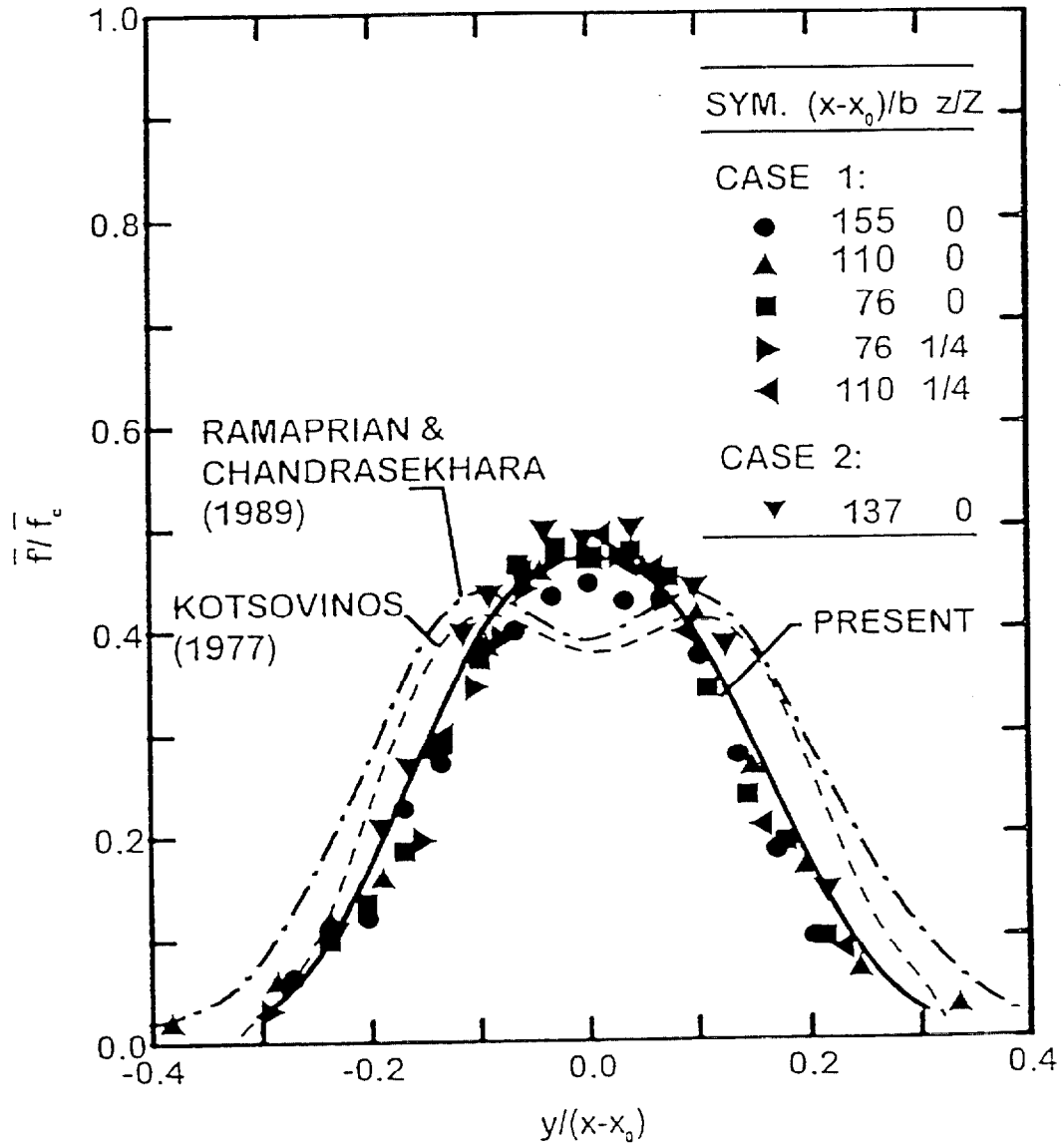


Fig. 8 Cross stream profiles of rms mixture fraction fluctuations in self-preserving round turbulent plumes.

Some typical temporal power spectral densities of mixture fraction fluctuations for plane free turbulent plumes are illustrated in Fig. 9. These results are for the case 1 plume with $76 \leq (x-x_0)/b \leq 155$ with the spectra normalized as described by Hinze (1975). These results are similar to earlier observations for round plumes due to Dai et al. (1994) and Papanicolaou and List (1987,1988). The normalized spectra are relatively independent of cross stream position and the low frequency region is also relatively independent of streamwise position when plotted in the manner of Fig. 9.

The spectra of Fig. 9 initially decay according to the $-5/3$ power of frequency, which is the well known inertial range of the turbulence spectrum which has been called the inertial-convective region for scalar property fluctuations where effects of molecular diffusion are small (Tennekes and Lumley, 1972). This is followed by a prominent region where the spectra decay according to the -3 power of frequency, which has been termed the inertial-diffusive subrange by Papanicolaou and List (1987). This region is not observed for nonbuoyant flows and is thought to be caused by variations of the local rate of dissipation of mixture fraction fluctuations due to buoyancy-generated forces.

3.5 Conclusions

Mixture fraction statistics were measured in plane buoyant turbulent plumes in still air emphasizing fully-developed (self-preserving) conditions. The test conditions involved buoyant jet sources of helium and air to give ρ_0/ρ_∞ of 0.500 and 0.770 with measurements extending to $(x-x_0)/b = 155$ and $(x-x_0)/\ell_M = 21$. The major conclusions of the study are as follows:

1. Present measurements indicated self-preserving behavior for $(x-x_0)/b \geq 76$ and $(x-x_0)/\ell_M \geq 9$. In this region, distributions of mean mixture fractions were up to 36% narrower with scaled values at the plane of symmetry up to 24% smaller than earlier results in the literature. Several reasons can be advanced for these differences: many measurements were not completed far enough from the source to achieve self-preserving behavior, in some instances there were problems of accurately finding the plume buoyancy flux, in some instances flow aspect ratios were questionably small, and in some instances control of flow instabilities (flapping) may be a factor.

2. Cross stream distributions of mixture fraction fluctuations in the self-preserving region of plane buoyant turbulent plumes do not dip near the plane of symmetry similar to plane nonbuoyant jets. Instead, effects of buoyancy cause mixture fraction fluctuations to reach a maximum at the plane of symmetry which is unusually large, 47%. This behavior is similar to findings for self-preserving round buoyant turbulent plumes, and provides strong evidence of significant effects of buoyancy/turbulence interactions in both these flows.

3. The low frequency portion of the temporal spectra of mixture fraction fluctuations scale in a relatively universal manner. The spectra exhibit the well known $-5/3$ power inertial decay region but this is followed by a prominent -3 power inertial-diffusive decay region, which is generally observed in buoyant turbulent flows but is not observed in nonbuoyant turbulent flows.

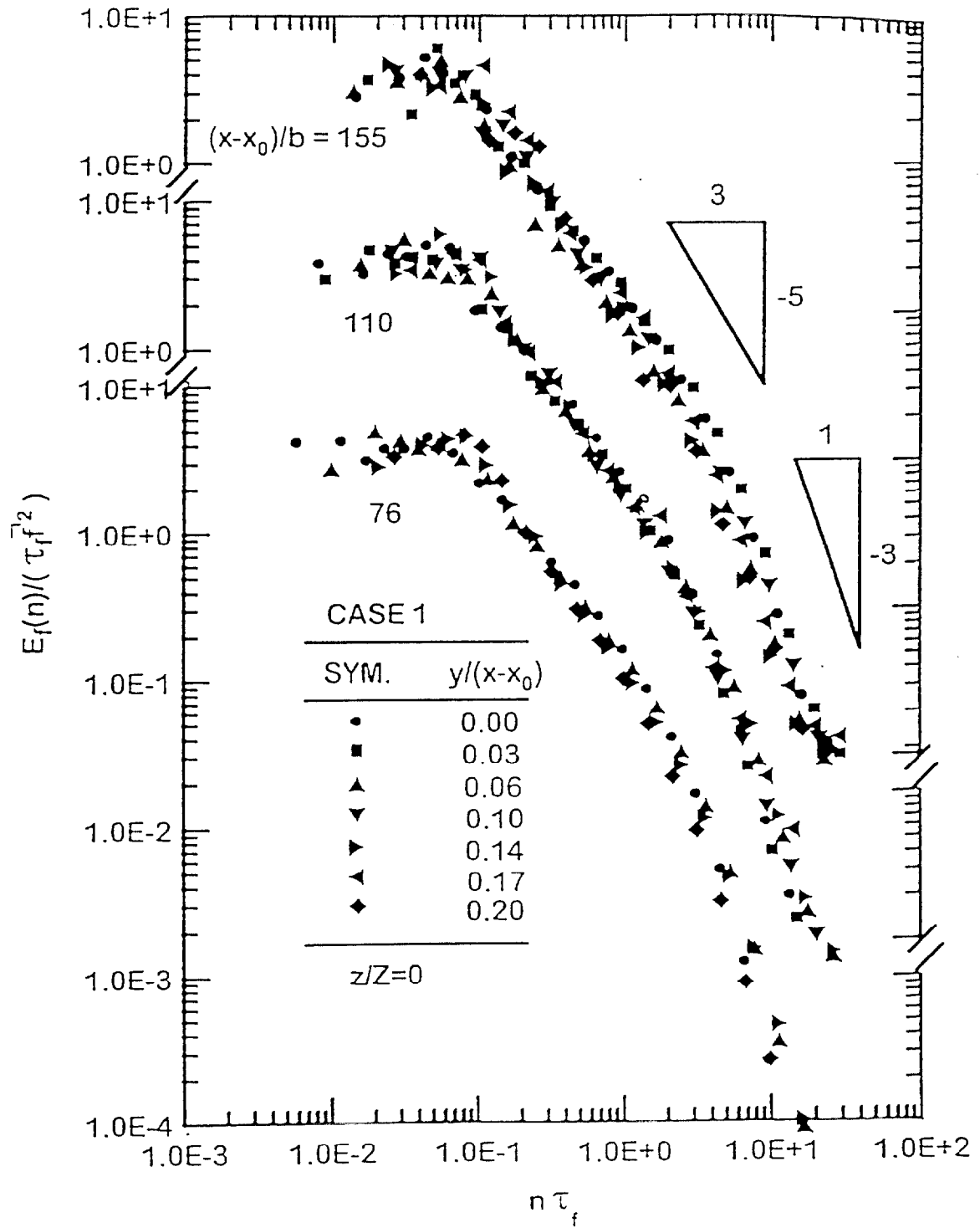


Fig. 9 Typical temporal power spectral densities of mixture fraction fluctuations in self-preserving plane turbulent plumes

4. Turbulent Adiabatic Wall Plumes

4.1 Introduction

Plane turbulent wall plumes are caused by sources of buoyancy along the base of flat walls. These flows are of interest because they are classical buoyant turbulent flows with numerous applications for confined natural convection processes and unwanted fires. Thus, the objective of this phase of the investigation was to extend the measurements of round buoyant turbulent plumes of Dai et al. (1994,1995a,b) and plane free buoyant turbulent plumes of Sangras et al. (1998a) to consider plane turbulent wall plumes using similar methods. Present considerations were limited to turbulent plumes along smooth plane vertical surfaces for conditions where the streamwise buoyancy flux is conserved; this implies flow along an adiabatic wall for a thermal plume.

Present measurements emphasize fully-developed conditions far from the source where effects of source disturbances and momentum have been lost. Free line plumes become self-preserving at such conditions but adiabatic wall plumes never formally reach self-preserving behavior because the growth rate of the near-wall boundary layer and the outer plume-like region are not the same. Nevertheless, the outer plume-like region grows more rapidly than the near-wall boundary layer and eventually dominates wall plumes far from the source, where wall plumes approximate self-preserving behavior with scaling similar to free line plumes (Grella and Faeth, 1975; Liburdy and Faeth, 1978). Thus, self-preserving behavior of adiabatic wall plumes was sought in this approximate sense during the present investigation.

Past studies of turbulent adiabatic wall plumes include Grella and Faeth (1975), Lai et al. (1986), Lai and Faeth (1997) and references cited therein. Grella and Faeth (1975) used an array of small flames at the base of a smooth vertical insulated wall for their experiments and completed hot wire probe measurements of temperatures and velocities. Lai et al. (1986) and Lai and Faeth (1987) reported LIF and LV measurements of adiabatic wall plumes created by gas mixtures. In both sets of experiments, however, there were questions about whether self-preserving behavior was actually achieved.

In view of these observations, the objective of the present investigation was to measure mean and fluctuating scalar properties of adiabatic wall plumes, emphasizing conditions in the approximate self-preserving region far from the source.

In the following, experimental methods and self-preserving scaling are described first. Results are then considered before summarizing conclusions. The following description of the study is brief, more details can be found in Sangras et al. (1998b) which appears in Appendix F.

4.2 Experimental Methods

The experiments involved source flows of helium/air mixtures in still air along a smooth vertical wall. This approach provides a straightforward specification of the plume buoyancy flux and avoids problems of parasitic heat losses associated with thermal plumes. Measurements of mixture fraction statistics were carried out using LIF.

The experimental arrangement was the same as for the free line plume study of Sangras et al. (1998a) except for installation of the smooth vertical wall located at the side of the source slot. The arrangement of the LIF system was also the same as for the free line plume study except that optical traps were used to intercept the laser beam at the wall in order to avoid laser beam reflections. Experimental uncertainties were also the same as before. Two sources were used involving helium/air mixtures with initial density ratios,

$\rho_0/\rho_\infty = 0.750$ and 0.550 , which are slightly different from the sources used by Sangras et al. (1998a).

4.3 Self-Preserving Scaling

The state relationships for density are unchanged from before, Eqs. (1) and (2). In addition, assuming approximate self-preserving behavior for adiabatic wall plumes in the sense discussed earlier, mean and fluctuating mixture fractions can be scaled in terms of self-preserving variables in the same manner as for free line plumes, Eqs. (10) and (11). The main difference, however, is that the resulting universal functions, $F(y/(x-x_0))$ and $U(y/(x-x_0))$, are not the same for wall plumes and for free line plumes. In addition these functions never reach universal behavior near the wall due to the different growth rate of the wall boundary layer and the outer plume-like region. Nevertheless, the wall layer grows more slowly than the plume and it is the latter that dominates flow properties far from the source. Thus, the self-preserving properties of the outer plume-like region is the main interest in the following.

4.4 Results and Discussion

Present measurements of cross stream distributions of mean mixture fractions for the test sources are illustrated in Fig. 10. The scaling parameters of Eq. (10) are used on the plot so that the value of the ordinate is $F(y/(x-x_0))$. Results for $z/Z = 0$ and $1/4$ are the same, confirming that the flow is reasonably two dimensional. Present measurements yield universal distributions for $97 \leq (x-x_0)/b \leq 155$ and $12 \leq (x-x_0)/\ell_M \leq 21$ which implies self-preserving flow. These conditions correspond to characteristic Reynolds numbers of 3800-6700, which are large for unconfined turbulent flow.

Measurements of $F(y/(x-x_0))$ for a variety of plane buoyant turbulent plumes have been plotted in Fig. 10 for comparison with the present measurements, as follows: results for adiabatic wall plumes from Grella and Faeth (1975) and Lai and Faeth (1987), results for isothermal wall plumes from Liburdy and Faeth (1978) and results for free line plumes from Sangras et al. (1998a). The measurements of Grella and Faeth (1975), Lai and Faeth, 1987) and Liburdy and Faeth (1978) all exhibit streamwise variations of mean mixture fractions scaled for approximate self-preserving behavior; therefore, results plotted for these sources in Fig. 10 are for conditions farthest from the source. The results for free line plumes from Sangras et al. (1998a), however, are best-fit averages over the self-preserving region.

Considering the three adiabatic wall plume results in Fig. 10, it is evident that the measurements of Lai and Faeth (1987) are broader than the present results and that the values of F for both Grella and Faeth (1975) and Lai and Faeth (1987) are considerably larger than present results near the wall. The larger scaled widths of mean mixture fraction distributions of the earlier measurements of adiabatic wall plumes are typical of transitional plumes. This behavior is illustrated by values of $\ell_f/(x-x_0)$ summarized in Table 3 for the measurements of Lai et al. (1986) and the present investigation. The progressive reduction of $\ell_f/(x-x_0)$ with increasing distance from the source, tending toward the value observed during the present investigation, is evident. The results of Grella and Faeth (1975) cannot be treated the same way because a source width cannot be defined for these measurements, however, it is encouraging that their measurements farthest from the source tend to approach the present measurements for self-preserving conditions. Differences between the magnitudes of F for Grella and Faeth (1975) and the present study follow because B_0 had to be found from measurements for the results of Grella and Faeth (1975) but was known

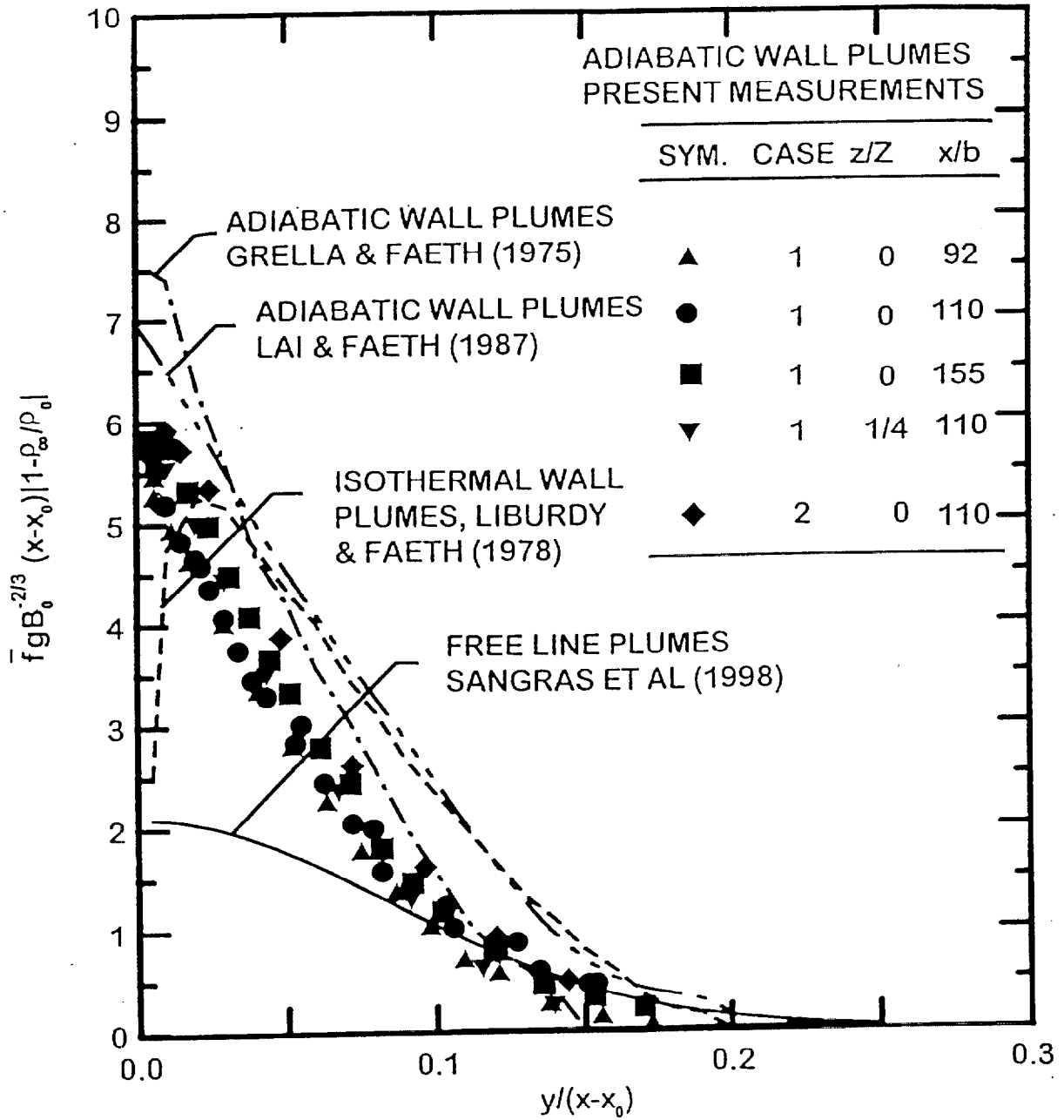


Fig. 10 Cross stream profiles of mean mixture fractions in self-preserving plane turbulent wall and free plumes.

directly from the source mixture for the present flows, see Sangras et al. (1998B) for more discussion of this point.

Table 3. Development of Plane Turbulent Adiabatic Wall Plumes*

Source	$(x-x_0)/b$	$\ell_f/(x-x_0)$
Lai et al. (1986)	10.0	0.173
	20.0	0.118
	37.5	0.093
Present (self-preserving region)	92-155	0.076

*Plane turbulent adiabatic wall plumes along a smooth vertical wall in still and unstratified environments.

The comparison between $F(y/(x-x_0))$ for adiabatic wall plumes and free line plumes, plotted in Fig. 10, is also of interest. Both results represent self-preserving behavior and have the same buoyancy flux but it is evident that the adiabatic wall plumes spread much slower than the free line plumes, e.g. ℓ_f is 53% larger for the free line plumes and $F(0)$ is 2.7 times larger for the adiabatic wall plumes. This behavior has undesirable implications for unwanted fires because the reduced mixing rates of wall plumes compared to free line plumes imply that fire plumes along surfaces spread much farther from the source than would be the case for an unconfined fire. This behavior enhances fire spread rates and also reduces the rate of dilution of toxic substances within fire-caused buoyant flows.

The reduced rates of mixing of adiabatic wall plumes compared to free line plumes can be attributed to reduced access to the ambient environment, direct effects of wall friction and inhibition of turbulent mixing due to the presence of the wall. Reduced access to mixing comes about because adiabatic wall plumes only mix on one side while free line plumes mix on both sides. This effect might be expected to increase $F(0)$ by a factor of 2; instead, $F(0)$ increases even more, by a factor of 2.7, which suggests other effects are influencing the mixing rate. Direct effects of wall friction are small, however, as reported by Grella and Faeth (1975). Thus, the presence of the wall must reduce mixing rates in its own right, by inhibiting cross stream motion at the largest scales that significantly contribute to mixing. The isothermal wall plume results of Liburdy and Faeth (1978) also support this mechanism, as discussed by Sangras et al. (1998b).

Measurements of cross stream distributions of mixture fraction fluctuations are plotted in Fig. 11. Results plotted on this figure include findings for adiabatic wall plumes from Lai and Faeth (1987), for isothermal walls from Liburdy and Faeth (1978) and results for free line plumes from Sangras et al. (1998a). As before, results for Lai and Faeth (1987) and Grella and Faeth (1975) do not extend to self-preserving conditions and only findings farthest from the source are shown while results from the present investigation represent self-preserving behavior.

Mixture fraction fluctuations for adiabatic wall plumes in Fig. 11 become small as the wall and free stream are approached and reach a maximum near $y/(x-x_0) = 0.02$. Values of \bar{f}' for adiabatic wall plumes are larger than for free line plumes in this region, mainly

because values of \bar{f} are larger. In contrast, mixture fraction fluctuation intensities are larger for free line plumes than for wall plumes, 42% compared to 37%, which is consistent with the wall stabilizing turbulent motion.

Typical power spectral densities of mixture fraction fluctuations are illustrated in Fig. 12. The properties of these results are generally similar to observations made for free line plumes in connection with the discussion of Fig. 9.

4.5 Conclusions

Mixture fraction statistics were measured in plane turbulent adiabatic wall plumes rising along flat smooth vertical walls in still air, emphasizing fully-developed (self-preserving) conditions. The test conditions consisted of buoyant jet sources of helium and air to give ρ_0/ρ_∞ of 0.750 and 0.550 with measurements extending to $(x-x_0)/b = 155$ and $(x-x_0)/\ell_M = 21$. The major conclusions of the study are as follows:

1. Present measurements yielded distributions of mean mixture fractions that approximated self-preserving behavior in the outer plume-like region of the flow for $(x-x_0)/b \geq 92$ and $(x-x_0)/\ell_M \geq 12$. In this region, distributions of mean mixture fractions were up to 22% narrower with scaled values at the wall up to 31% smaller than earlier results in the literature. These differences were caused by past problems of completing measurements far enough from the source to reach self-preserving conditions and accurately finding the plume buoyancy flux.

2. Self-preserving turbulent adiabatic wall plumes mix much slower than comparable free line plumes, e.g., characteristic widths are 58% larger and scaled maximum mean mixture fractions are 2.7 times smaller for free line plumes than for comparable adiabatic wall plumes. These differences came about because the wall limits mixing to one side and inhibits the large-scale turbulent motion that dominates the mixing process.

3. The stabilizing effect of the wall reduces maximum mean mixture fraction fluctuation intensities in adiabatic wall plumes compared to free line plumes, e.g., the maximum intensities for the two flows are 37 and 47%, respectively. Nevertheless, turbulence/radiation interactions are much larger for adiabatic wall plumes than for free line plumes because mean mixture fractions are larger for the wall plumes for otherwise comparable conditions.

4. Temporal power spectra of mixture fraction fluctuations for adiabatic wall plumes are qualitatively similar to spectra in round and plane free turbulent plumes. Thus, prominent $-5/3$ power inertial-convective and -3 power inertial-diffusive decay regions are seen with the latter region being a characteristic of buoyant flows that is not seen in nonbuoyant flows.

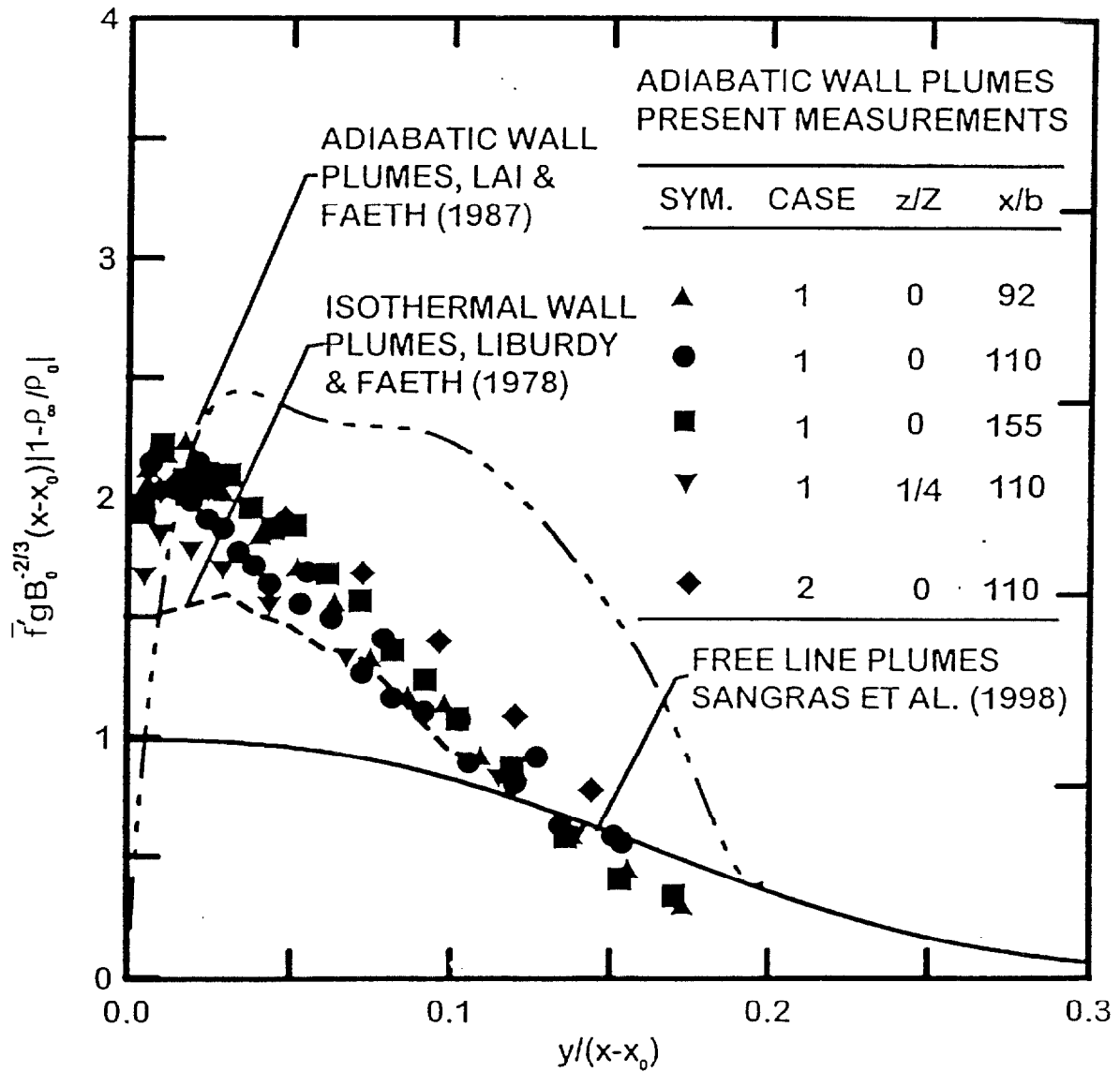


Fig. 11 Cross stream profiles of rms mixture fraction fluctuations in self-preserving plane turbulent wall and free plumes.

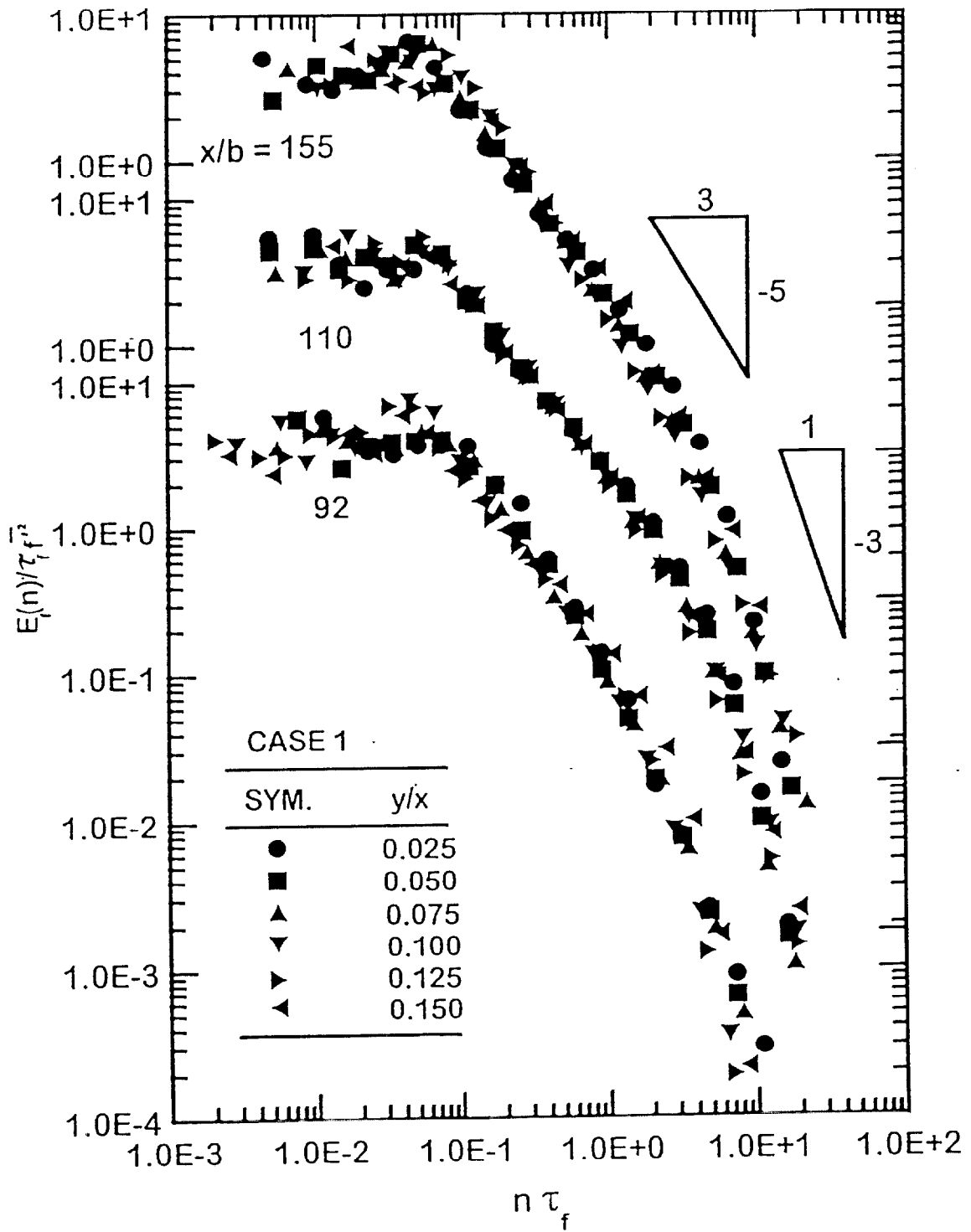


Fig. 12 Typical temporal power spectral densities of mixture fraction fluctuations in self-preserving plane turbulent adiabatic wall plumes.

References

- Abraham, G. (1960) "Jet Diffusion in Liquid of Greater Density," ASCE J. Hyd. Div., Vol. 86, pp. 1-13.
- Anwar, H.O. (1969) "Experiment on an Effluent Discharging from a Slot in Stationary or Slow Moving Fluid of Greater Density," J. Hydr. Res., Vol. 7, pp. 411-430.
- Dai, Z., and Faeth, G.M. (1996) "Measurements of the Structure of Self-Preserving Round Buoyant Turbulent Plumes," J. Heat Trans., Vol. 118, pp. 493-495.
- Dai, Z., Tseng, L.-K., and Faeth, G.M. (1994) "Structure of Round, Fully-Developed, Buoyant Turbulent Plumes," J. Heat Trans., Vol. 116, pp. 409-417.
- Dai, Z., Tseng, L.-K., and Faeth, G.M. (1995a) "Velocity Statistics of Round, Fully-Developed Buoyant Turbulent Plumes," J. Heat Transfer, Vol. 117, pp. 138-145.
- Dai, Z., Tseng, L.-K. and Faeth, G.M. (1995b) "Velocity/Mixture-Fraction Statistics of Round, Self-Preserving Buoyant Turbulent Plumes," J. Heat Trans., Vol. 117, pp. 918-926.
- Faeth, G.M., Gore, J.P., Chuech, S.G., and Jeng, S.-M. (1989) "Radiation from Turbulent Diffusion Flames," Ann. Rev. Num. Fluid Mech. and Heat Trans., Vol. 2, Hemisphere Publishing Corp., Washington, D.C., 1-38.
- George, W.K., Jr., Alpert, R.L., and Tamanini, F. (1977) "Turbulence Measurements in an Axisymmetric Buoyant Plume," Int. J. Heat Mass Trans., Vol. 20, pp. 1145-1154.
- Grella, J.J., and Faeth, G.M. (1975) "Measurements in a Two-Dimensional Thermal Plume Along a Vertical Adiabatic Wall," J. Fluid Mech., Vol. 71, pp. 701-710.
- Gutmark, E., and Wygnanski, I. (1976) "The Plane Turbulent Jet," J. Fluid Mech., Vol. 73, pp. 465-495.
- Harris, P.R. (1967) "The Densimetric Flows caused by the Discharge of Heated Two-Dimensional Jets Beneath a Free Surface," Ph.D. Thesis, University of Bristol, Bristol, UK.
- Hinze, J.O. (1975) *Turbulence*, 2nd Ed., McGraw-Hill, New York, pp. 175-319.
- Kotsovinos, N.E. (1977) "Plane Turbulent Buoyant Jets. Part 2. Turbulence Structure," J. Fluid Mech., Vol. 81, pp. 45-62.
- Kotsovinos, N.E. (1985) "Temperature Measurements in a Turbulent Round Plume," Int. J. Heat Mass Trans., Vol. 28, pp. 771-777.
- Kotsovinos, N.E., and List, E.J. (1977) "Turbulent Buoyant Jets. Part 1. Integral Properties," J. Fluid Mech., Vol. 81, pp. 25-44.
- Kounalakis, M.E., Sivathanu, Y.R., and Faeth, G.M. (1991) "Infrared Radiation Statistics of Nonluminous Turbulent Diffusion Flames," J. Heat Trans., Vol. 113, pp. 437-445.
- Lai, M.-C., and Faeth, G.M. (1987) "Turbulence Structure of Vertical Adiabatic Wall Plumes," J. Heat Trans., Vol. 109, pp. 663-670.

- Lai, M.-C., Jeng, S.-M., and Faeth, G.M. (1986) "Structure of Turbulent Adiabatic Wall Plumes," J. Heat Trans., Vol. 108, pp. 827-834.
- Lee, S.L. and Emmons, H.W. (1961) "A Study of Natural Convection Above a Line Fire," J. Fluid Mech., Vol. 11, pp. 353-368.
- Liburdy, J.A., and Faeth, G.M. (1978) "Heat Transfer and Mean Structure of a Turbulent Thermal Plume Along Vertical Isothermal Walls," J. Heat Trans., Vol. 100, pp. 177-183.
- Liburdy, J.A., Groff, E.G., and Faeth, G.M. (1979) "Structure of a Turbulent Thermal Plume Rising Along an Isothermal Wall," J. Heat Trans., Vol. 101, pp. 299-355.
- List, E.J. (1982) "Turbulent Jets and Plumes," Ann. Rev. Fluid Mech. Vol. 14, pp. 189-212.
- Mizushima, T., Ogino, F., Veda, H., and Komori, S. (1979) "Application of Laser-Doppler Velocimetry to Turbulence Measurements in Non-Isothermal Flow," Proc. Roy. Soc. London, Vol. A366, pp. 63-79.
- Morton, B.R. (1959) "Forced Plumes," J. Fluid Mech., Vol. 5, pp. 151-163.
- Morton, B.R., Taylor, G.I., and Turner, J.S. (1956) "Turbulent Gravitational Convection from Maintained and Instantaneous Sources," Proc. Roy. Soc. London, Vol. A234, pp. 1-23.
- Nakagome, H., and Hirata, M. (1977) "The Structure of Turbulent Diffusion in an Axisymmetrical Thermal Plume," *Heat Transfer and Turbulent Buoyant Convection* (D.B. Spalding and N. Afgan, eds.), McGraw-Hill, New York, pp. 367-372.
- Ogino, F., Takeuchi, H., Kudo, I., and Mizushima, T. (1980) "Heated Jet Discharged Vertically in Ambients of Uniform and Linear Temperature Profiles," Int. J. Heat Mass Trans., Vol. 23, pp. 1581-1588.
- Panchapakesan, N.R., and Lumley, J.L. (1993) "Turbulence Measurements in Axisymmetric Jets of Air and Helium. Part 2. Helium Jet," J. Fluid Mech., Vol. 246, pp. 225-247.
- Papanicolaou, P.N., and List, E.J. (1987) "Statistical and Spectral Properties of Tracer Concentration in Round Buoyant Jets," Int. J. Heat Mass Trans., Vol. 30, pp. 2059-2071.
- Papanicolaou, P.N., and List, E.J. (1988) "Investigation of Round Vertical Turbulent Buoyant Jets," J. Fluid Mech., Vol. 195, pp. 341-391.
- Papantoniou, D., and List, E.J. (1989) "Large Scale Structure in the Far Field of Buoyant Jets," J. Fluid Mech., Vol. 209, pp. 151-190.
- Peterson, J., and Bayazitoglu, Y. (1992) "Measurements of Velocity and Turbulence in Vertical Axisymmetric Isothermal and Buoyant Plumes," J. Heat Trans., Vol. 114, pp. 135-142.
- Pivovarov, M.A., Zhang, H., Ramaker, D.E., Tatem, P.A., and Williams, F.W. (1992) "Similarity Solutions in Buoyancy-Controlled Diffusion Flame Modelling," Combust. Flame, Vol. 92, pp. 308-319.

- Ramaprian, B.R., and Chandrasekhara, M.S. (1985) "LDA Measurements in Plane Turbulent Jets," J. Fluids Engr., Vol. 107, pp. 264-271.
- Ramaprian, B.R., and Chandrasekhara, M.S. (1989) "Measurements in Vertical Plane Turbulent Plumes," J. Fluids Engr., Vol. 111, pp. 69-77.
- Rouse, H., Yih, C.S., and Humphreys, H.W. (1952) "Gravitational Convection from a Boundary Source," Tellus, Vol. 4, pp. 201-210.
- Sangras, R., Dai, Z., and Faeth, G.M. (1998a) "Mixing Structure of Plane Self-Preserving Buoyant Turbulent Plumes," J. Heat Transfer, in press.
- Sangras, R., Dai, Z. and Faeth, G.M. (1998b) "Mixture Fraction Statistics of Plane Self-Preserving Buoyant Turbulent Adiabatic Wall Plumes," J. Heat Trans., submitted.
- Seban, R.A., and Behnia, M.M. (1976) "Turbulent Buoyant Jets in Unstratified Surroundings," Int. J. Heat Mass Trans., Vol. 19, pp. 1197-1204.
- Shabbir, A. (1987) "An Experimental Study of an Axisymmetric Turbulent Buoyant Plume and Evaluation of Closure Hypotheses," Ph.D. Thesis, State University of New York at Buffalo.
- Shabbir, A., and George, W.K. (1992) "Experiments on a Round Turbulent Buoyant Plume," NASA Technical Memorandum 105955.
- Tennekes, H., and Lumley, J.L. (1972) *A First Course in Turbulence*, MIT Press, Cambridge, Massachusetts, pp. 113-124.
- Zimin, V.D., and Frik, P.G. (1977) "Averaged Temperature Fields in Asymmetrical Turbulent Streams over Localized Heat Sources," Izv. Akad. Nauk. SSSR, Mckhanika Zhidkosti Gaza, Vol. 2, pp. 199-203.

Appendix A: Dai et al. (1994)

Structure of Round, Fully Developed, Buoyant Turbulent Plumes

Z. Dai
Graduate Student Research Assistant.

L.-K. Tseng
Research Fellow.

G. M. Faeth
Professor.
Fellow ASME

Department of Aerospace Engineering,
The University of Michigan,
Ann Arbor, MI 48109-2118

An experimental study of the structure of round buoyant turbulent plumes was carried out, emphasizing conditions in the fully developed (self-preserving) portion of the flow. Plume conditions were simulated using dense gas sources (carbon dioxide and sulfur hexafluoride) in a still air environment. Mean and fluctuating mixture fraction properties were measured using single- and two-point laser-induced iodine fluorescence. The present measurements extended farther from the source (up to 151 source diameters) than most earlier measurements (up to 62 source diameters) and indicated that self-preserving turbulent plumes are narrower, with larger mean and fluctuating mixture fractions (when appropriately scaled) near the axis, than previously thought. Other mixture fraction measurements reported include probability density functions, temporal power spectra, radial spatial correlations and temporal and spatial integral scales.

Introduction

Scalar mixing of round buoyant turbulent plumes in a still environment is an important fundamental problem that has attracted significant attention since the classical study of Rouse et al. (1952). However, recent work suggests that more information about the turbulence properties of scalar quantities within buoyant turbulent flows is needed to address turbulence/radiation interactions in fire environments (Kounalakis et al., 1991). In particular, the response of radiation to turbulent fluctuations is affected by the moments, probability density functions, and temporal and spatial correlations of scalar property fluctuations. In turn, scalar property fluctuations can be represented by mixture fraction (defined as the mass fraction of source fluid) fluctuations, using state relationships found from conserved-scalar concepts for both non-reactive and flame environments (Bilger, 1976; Sivathanu and Faeth, 1990). Thus, the objective of the present investigation was to measure mixture fraction statistics in round buoyant turbulent plumes in still environments. In order to simplify interpretation of the results, the experiments emphasized fully developed buoyant turbulent plumes, where effects of the source have been lost and both mean and fluctuating properties become self-preserving (Tennekes and Lumley, 1972).

The discussion of previous studies will be brief because several reviews of turbulent plumes have appeared recently (Kotsovinos, 1985; List, 1982; Papanicolaou and List, 1987, 1988). The earliest work concentrated on the scaling of flow properties within fully developed turbulent plumes (Rouse et al., 1952; Morton, 1959; Morton et al., 1956). Measurements of mean properties within plumes generally have satisfied the resulting scaling relationships; however, there are considerable differences among various determinations of centerline values, radial profiles, and flow widths (Abraham, 1960; George et al., 1977; Kotsovinos, 1985; List, 1982; Ogino et al., 1980; Peterson and Bayazitoglu, 1992; Shabbir and George, 1992; Rouse et al., 1952; Zimin and Frik, 1977). Aside from problems of experimental methods in some instances, List (1982) and Papanicolaou and List (1987, 1988) attribute these differences to problems of reaching fully developed plume conditions.

Two parameters are helpful for estimating when turbulent plumes become self-preserving. The first of these is the distance

from the virtual origin normalized by the source diameter, $(x-x_0)/d$. Based on results for nonbuoyant round turbulent jets, values of $(x-x_0)/d$ greater than ca. 40 and 100 should be required for self-preserving profiles of mean and fluctuating properties, respectively (Tennekes and Lumley, 1972). By these measures, all past measurements over the cross section of plumes, which invariably used buoyant jets for the plume source, probably involve transitional plumes, e.g., they generally are limited to $(x-x_0)/d \leq 62$, aside from some limited measurements in liquids by Papanicolaou and List (1989). The main reason for not reaching large values of $(x-x_0)/d$ for plumes, similar to jets, is that scalar properties decay much faster for plumes, e.g., proportional to $(x-x_0)^{-3/3}$ for plumes rather than $(x-x_0)^{-1}$ for jets. Thus, it is difficult to maintain reasonable experimental accuracy far from the source within the plumes. A contributing factor is that plume velocities are relatively small in comparison to jets so that controlling room disturbances far from the source is more difficult for plumes.

The second parameter useful for assessing conditions for self-preserving buoyant turbulent plumes is the distance from the virtual origin normalized by the Morton length scale, $(x-x_0)/l_M$. The Morton length scale is defined as follows for a round plume having uniform properties at the source (Morton, 1959; List, 1982):

$$l_M = (\pi/4)^{1/4} (\rho_m u_0^2 / (g |\rho_o - \rho_m|))^{1/2} \quad (1)$$

where an absolute value has been used for the density difference in order to account for both rising and falling plumes. Large values of $(x-x_0)/l_M$ are required for buoyancy-induced momentum to become large in comparison to the source momentum so that the buoyant features of the flow are dominant. The ratio of l_M to d is proportional to the source Froude number, defined as follows (List, 1982):

$$Fr_o = (4/\pi)^{1/4} l_M/d = (\rho_m u_0^2 / (g |\rho_o - \rho_m| d))^{1/2} \quad (2)$$

The source Froude number quantifies the initial degree of buoyant behavior of the source, e.g., $Fr_o = 0$ for a purely buoyant source. Papanicolaou and List (1987, 1988) suggest that buoyancy-dominated conditions for mean and fluctuating quantities are reached for $(x-x_0)/l_M$ greater than ca. 6 and 14, respectively. A greater proportion of existing data for mean properties exceed this criterion; however, the effect of transitional plume behavior (in terms of $(x-x_0)/d$) on these observations raises questions about the adequacy of this criterion.

Naturally, in instances where reaching self-preserving con-

Contributed by the Heat Transfer Division and presented at the National Heat Transfer Conference, Georgia, August 8-11, 1993. Manuscript received by the Heat Transfer Division March 1993; revision received July 1993. Keywords: Fire/Flames, Natural Convection, Turbulence. Associate Technical Editor: Y. Jaluria.

ditions for mean properties is questionable, it is likely that turbulent properties are transitional. Thus, the turbulence measurements of George et al. (1977) and Shabbir and George (1992) for x/d in the range 8–25, normally would not be thought to represent self-preserving conditions. The turbulence measurements of Papanicolaou and List (1987, 1988) for x/d in the range 12–62 probably represent transitional plumes as well with results at larger distances, x/d , of 20–62, subject to additional uncertainties due to systematic instrument errors (Papanicolaou and List, 1988). In contrast, the measurements of Papantoniou and List (1989) were carried out at $x/d = 105$, which should be within the self-preserving region; however, unusually large concentration fluctuations were observed, which they attribute to the large Schmidt numbers of the liquid plumes used in these tests, i.e., molecular mixing was inhibited at small scales that still could be resolved by their instrument system. Thus, the relevance of the Papantoniou and List (1988) turbulence measurements to gaseous plumes of interest for radiation processes in flame environments is questionable.

The preceding discussion suggests that existing measurements of mean and fluctuating properties within plumes probably involve either transitional plumes or liquid plumes exhibiting large Schmidt number effects that are not typical of gases. Thus, the objective of the present investigation was to complete measurements of the mean and fluctuating mixture fraction properties of buoyant turbulent plumes in gases, emphasizing conditions within the self-preserving turbulent plume region where the specific features of the source have been lost. The mixture fraction properties considered included mean and fluctuating values, probability density functions, temporal power spectra, radial spatial correlations, and temporal and spatial integral scales. The experiments involved source flows of carbon dioxide and sulfur hexafluoride in still air at atmospheric pressure and temperature, in order to provide a straightforward specification of the buoyancy flux within the test plumes. This approach yielded downward-flowing, negatively buoyant plumes. Measurements of mixture fraction properties were undertaken using laser-induced iodine fluorescence (LIF).

Experimental Methods

Test Apparatus. A sketch of the experimental apparatus is shown in Fig. 1. In order to minimize room disturbances and contamination of adjacent areas by iodine vapor, the plumes were observed in a double enclosure contained within a large, high-bay test area. The outer enclosure (3000 × 3000 × 3400 mm high) had plastic side walls with a

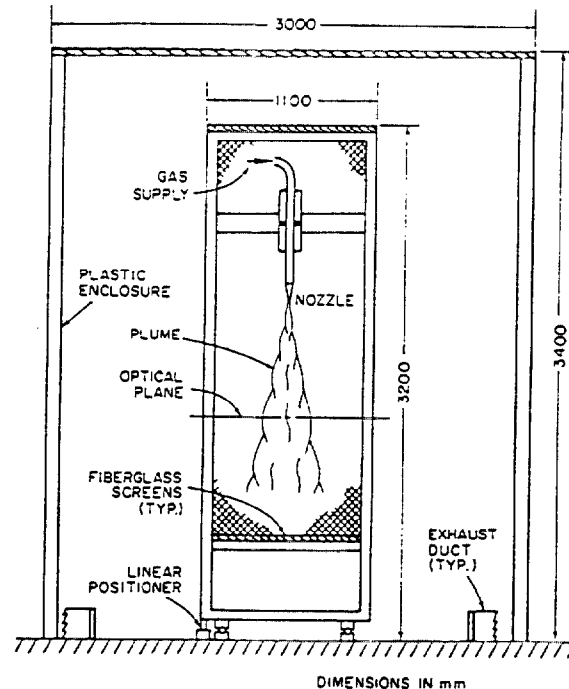


Fig. 1 Sketch of the buoyant turbulent plume apparatus

screen across the top for air inflow in order to compensate for removal of air entrained by the plume. The plume itself was within a smaller enclosure (1100 × 1100 × 3200 mm high) with plastic screen walls (square pattern, 630 wires/m with a wire diameter of 0.25 mm). The small enclosure was mounted on linear bearings and could be traversed in one direction using a stepping motor driven linear positioner (5 μ m positioning accuracy) in order to accommodate rigidly mounted instrumentation. The plume flow was removed through 300-mm-dia ducts that were mounted on the floor at the four corners of the outer enclosure. The exhaust flow was controlled by a bypass/damper system in order to match plume entrainment rates and to minimize flow disturbances. All components that might contact iodine vapor were plastic, painted, or sealed in plastic wrap, in order to prevent corrosion.

The plume sources consisted of rigid plastic tubes having inside diameters of 6.4 and 9.7 mm with flow straighteners at

Nomenclature

a, b = parameters in the Frenkiel function
 d = source diameter
 $E_f(n)$ = temporal power spectral density of f
 f = mixture fraction
 $F(r/(x-x_0))$ = scaled radial distribution of \bar{f} in self-preserving region
 Fr_0 = source Froude number, Eq. (2)
 g = acceleration of gravity
 k_f = plume width coefficient, Eq. (8)
 l_c = characteristic plume radius
 l_f = characteristic plume radius based on mean mixture fraction
 l_M = Morton length scale, Eq. (1)
 n = frequency
 $PDF(f)$ = probability density function of mixture fraction
 r = radial distance
 Re_c = characteristic plume Reynolds number
 $= \bar{u}_c l_c / \nu_\infty$

Re_0 = source Reynolds number = $u_0 d / \nu_0$
 u = streamwise velocity
 x = streamwise distance
 Δr = radial distance increment
 Λ_{fr} = radial spatial integral scale of mixture fraction fluctuations
 ν = kinematic viscosity
 ρ = density
 τ_f = temporal integral scale of mixture fraction fluctuations

Subscripts

c = centerline value
 o = initial value or virtual origin location
 ∞ = ambient value

Superscripts

$(\bar{\quad})$ = time-averaged mean value
 $(\overline{\quad})$ = root-mean-squared fluctuating value

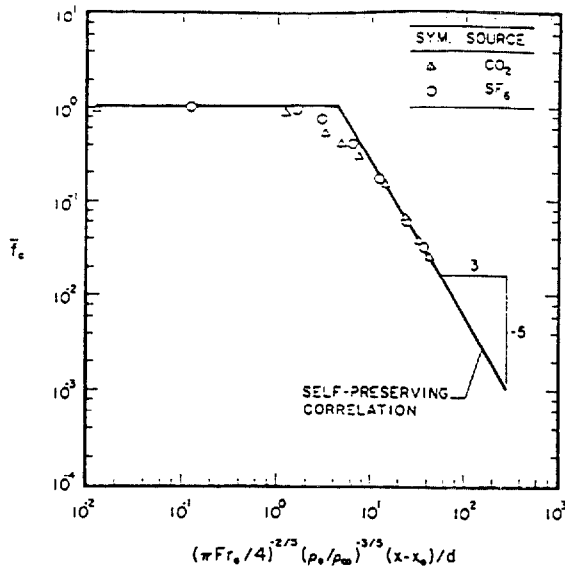


Fig. 2 Mean mixture fractions along the axis

sufficient to resolve the smallest scales of the turbulence within the self-preserving region of the plumes.

Self-Preserving Scaling

The state relationship for density as a function of mixture fraction is needed to relate the present measurements to properties in the self-preserving region. Assuming an ideal gas mixture, the exact state relationship for density becomes:

$$\rho = \rho_\infty / (1 - f(1 - \rho_o/\rho_\infty)) \tag{3}$$

Additionally, far from the source in the self-preserving region, $f \ll 1$, and Eq. (3) can be linearized as follows:

$$\rho = \rho_\infty + f\rho_\infty(1 - \rho_o/\rho_\infty), \quad f \ll 1 \tag{4}$$

The measurements involved mean and fluctuating mixture fraction properties at various streamwise positions. Mean properties were then scaled in terms of the self-preserving variables of fully developed turbulent plumes, as follows (List, 1982):

$$\bar{f} = (\pi Fr_o/4)^{2/3} (\rho_o/\rho_\infty) ((x-x_o)/d)^{-5/3} F(r/(x-x_o)) \tag{5}$$

$F(r/(x-x_o))$ represents the appropriately scaled radial profile function of mean mixture fraction, which becomes a universal function in the self-preserving region far from the source where Eq. (4) applies. Equation (5) was used to extrapolate measurements of mean mixture fractions along the axis in order to identify the virtual origin that yielded the best fit of the data. As noted earlier, the location of the virtual origin is controlled by source properties like turbulence levels, ρ_o/ρ_∞ , and the initial Froude numbers; however, it was beyond the scope of the present investigation to quantitatively study these relationships.

Finally, although velocity measurements were not made during the present study, it was of interest to find characteristic plume Reynolds numbers, $Re_c = \bar{u}_c d / \nu_\infty$. This was done by adopting the expressions of Rouse et al. (1952) for \bar{u}_c and l_c at self-preserving conditions to yield:

$$Re_c = 0.43((x-x_o)/(d Fr_o))^{2/3} u_o d / \nu_\infty \tag{6}$$

Results and Discussion

Mean Properties. The variation of mean mixture fractions along the axis of the two test plumes is illustrated in Fig. 2.

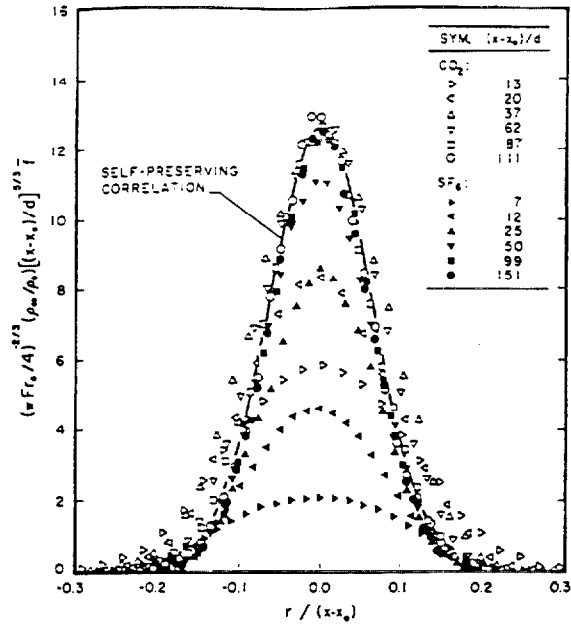


Fig. 3 Development of radial profiles of mean mixture fractions

The measurements are plotted in terms of the variables of Eq. (5). In addition, lines showing the asymptotic behavior of the present measurements at small and at large distances from the source are shown on the plot. The limiting behavior at small distances, $(x-x_o)/d \ll 1$, is $\bar{f}_c = 1$ which the measurements satisfy by definition. The limit at large distances follows from Eq. (5) for conditions where $\bar{f}_c \ll 1$ and Eq. (4) applies. Then $F(0) = 12.6$ independent of source flow properties, based on the best fit of present measurements, and $\bar{f}_c \sim ((x-x_o)/d)^{-5/3}$. This latter condition is reached for values of the abscissa of Fig. 2 greater than 10, which implies $(x-x_o)/d$ and $(x-x_o)/l_M$ on the order of 100 and 10, respectively. Within the intermediate region, where the abscissa of Fig. 2 is in the range 0.1-10, results depend on source properties like Re_o , Fr_o , and ρ_o/ρ_∞ so that the differences in this region seen in Fig. 2 for the two sources are anticipated. Naturally, this implies that conditions required to reach self-preserving plume behavior depend on these variables as well.

A more complete picture of the development of transitional plumes toward self-preserving conditions can be obtained from the radial profiles of mean mixture fractions for the two sources illustrated in Fig. 3. In this case, the scaling parameters of Eq. (5) are used so that the ordinate is equal to $F(r/(x-x_o))$. The measurements are plotted for various streamwise distances with $(x-x_o)/d \geq 7$. The radial mean mixture fraction profiles show progressive narrowing, with scaled values at the axis progressively increasing, as the streamwise distance increases. However, self-preserving conditions are observed for the present measurements when $(x-x_o)/d \geq 87$, which also corresponds to $(x-x_o)/l_M \geq 12$. The subsequent variation of the profiles with streamwise distance is well within experimental uncertainties over the range that was achieved during the present experiments: $87 \leq (x-x_o)/d \leq 151$ and $12 \leq (x-x_o)/l_M \leq 43$. This regime corresponds to characteristic plume Reynolds numbers of 2500-4200, which are reasonably high for unconfined turbulent flows. For example, this range is comparable to the highest characteristic wake Reynolds numbers where measurements of turbulent wake properties have been reported, while turbulent wakes exhibit self-preserving turbulence properties at characteristic wake Reynolds numbers as low as 70 (Wu and Faeth, 1993). The actual streamwise distance required

Table 2 Summary of self-preserving turbulent plume properties^a

Source	Medium	$(x-x_0)/d$	$(x-x_0)/l_M$	k_f^2	$2l_f/(x-x_0)$	$F(0)$	(\bar{f}'/\bar{f}_c)
Present study	gaseous	87-151	12-43	125	0.09	12.6	0.45
Papantoniou and List (1989)	liquid	105	24.33	—	0.08-0.09	—	0.64
Papanicolaou and List (1988)	liquid	22-62	9-62	80	0.11	14.3	0.40
Papanicolaou and List (1987)	liquid	12-20	> 5	80	0.11	11.1	0.40
Shabbir and George (1992)	gaseous	10-25	6-15	68	0.12	9.4	0.40
George et al. (1977)	gaseous	8-16	6-12	65	0.12	9.1	0.40

^aRound turbulent plumes in still, unstratified environments. Range of streamwise distances are for conditions where quoted self-preserving properties were found from measurements over the cross section of the plumes. Entries are ordered in terms of decreasing k_f .

to reach self-preserving conditions for mean mixture fractions, however, is likely to vary with source properties. For example, larger values of ρ_0/ρ_∞ and lower source Reynolds numbers tend to retard development toward self-preserving conditions, based on present findings during preliminary tests, while larger source Froude numbers require larger values of $(x-x_0)/d$ in order to achieve values of $(x-x_0)/l_M$ where buoyancy dominates flow properties.

Within the self-preserving region, present radial profiles of mean mixture fractions are reasonably approximated by a Gaussian fit, similar to past work (Rouse et al., 1952; George et al., 1977; List, 1982; Papanicolaou and List, 1987, 1988; Shabbir and George, 1992) as follows:

$$F(r/(x-x_0)) = F(0)\exp\{-k_f^2(r/(x-x_0))^2\} \quad (7)$$

where

$$k_f = (x-x_0)/l_f \quad (8)$$

Thus, l_f represents the characteristic plume radius where $\bar{f}'/\bar{f}_c = e^{-1}$. The best fit of the present data in the self-preserving region yielded $F(0) = 12.6$ and $k_f^2 = 125$. This yielded the correlation illustrated in Fig. 3, which is seen to be a good representation of the measurements in the self-preserving region, i.e., $(x-x_0)/d \geq 87$ and $(x-x_0)/l_M \geq 12$. This yields a value of $l_f/(x-x_0)$ of roughly 0.09, which is in good agreement with the values of 0.08-0.09 found by Papantoniou and List (1989) for measurements at large distances from the source, $(x-x_0)/d = 105$ and $(x-x_0)/l_M$ of 24 and 33.

The present values of normalized streamwise distance required to reach self-preserving conditions within round buoyant turbulent plumes are similar to past observations for round turbulent jets (Hinze, 1975; Tennekes and Lumley, 1972); however, they are substantially larger than streamwise distances reached during past measurements of the self-preserving properties of turbulent plumes using buoyant jet sources, aside from the study of Papantoniou and List (1989). This behavior is quantified in Table 2, where the range of streamwise distances considered for measurements of radial profiles of self-preserving plume properties, and the corresponding reported values of k_f^2 , $l_f/(x-x_0)$, and $F(0)$ are summarized for representative recent studies and associated earlier work from the same laboratories. Past measurements generally satisfy the criterion for buoyancy-dominated flow, i.e., $(x-x_0)/l_M > 6$ (Papanicolaou and List, 1987, 1988). Aside from the measurements of Papantoniou and List (1989) and the present study, however, the other results were obtained at values of $(x-x_0)/d$ that normally are not associated with self-preserving conditions for jetlike sources. Somewhat like the tendency for transitional plume conditions to have broader profiles than the self-preserving regime in Fig. 3, the values of k_f^2 tend to increase progressively as the maximum streamwise position is increased—almost doubling over the range of conditions given in Table 2. This yields a corresponding reduction of charac-

teristic plume radius of 30 percent, and an increase of the scaled mean mixture fraction at the axis of 30 percent, when approaching self-preserving conditions over the range considered in Table 2 (ignoring the unusually large value of $F(0)$ reported by Papanicolaou and List (1988), which is thought to be due to a systematic instrument error, as noted earlier). Discrepancies between transitional and self-preserving plumes of this magnitude have a considerable impact on the empirical parameters obtained by fitting turbulence models to measurements. For example, Pivovarov et al. (1992) suggest that the standard set of constants used in empirical turbulence models is inadequate based on the assumption of self-preserving plumes in conjunction with past measurements for transitional plumes; however, their predictions using standard constants are in fair agreement with the present measurements of self-preserving plume properties under the same assumptions.

Root-Mean-Square Fluctuations. Radial profiles of mixture fraction fluctuations at various streamwise distances are plotted in Fig. 4 for the two sources. Near the source, the profiles are rather broad and exhibit a dip at the axis as approached, much like the behavior of nonbuoyant jets (Becker et al., 1967; Papanicolaou and List, 1987, 1988). The profiles evolve, however, with both the width and the magnitude of the dip near the axis gradually decreasing as the streamwise distance is increased. Eventually, self-preserving behavior is reached at conditions similar to the self-preserving conditions for mean mixture fractions in Fig. 3, e.g., $(x-x_0)/d \geq 87$ and $(x-x_0)/l_M \geq 12$. This behavior is not surprising because self-preserving conditions for mean properties are a generally necessary condition for self-preserving conditions for turbulence properties (Tennekes and Lumley, 1972). Within the self-preserving region, present measurements can be correlated reasonably well by the following empirical relationship:

$$\bar{f}'/\bar{f}_c = 0.45 \exp(-40(r/(x-x_0))^{2.5}) \quad (9)$$

Analogous to mean mixture fractions, the measurements of rms mixture fraction fluctuations of Papanicolaou and List (1987, 1988), Shabbir and George (1992), and George et al. (1977) are similar to transitional plumes in the latter stages of development. Thus, although these profiles do not exhibit a dip near the axis, they are broader in terms of $r/(x-x_0)$ than the present measurements in the self-preserving region. Additionally, Papanicolaou and List (1987, 1988), Shabbir and George (1992), and George et al. (1977) find $(\bar{f}'/\bar{f}_c) = 0.40$, rather than 0.45 for the present measurements, as summarized in Table 2. On the other hand, Papantoniou and List (1989) measure (\bar{f}'/\bar{f}_c) of roughly 0.64 at conditions that should be within the self-preserving region; however, as discussed earlier, this large value probably is caused by the large Schmidt number of their liquid plumes, which inhibits small-scale mixing in comparison to plumes in gases.

The gradual disappearance of the dip in mixture fraction fluctuations is an interesting feature of the results illustrated

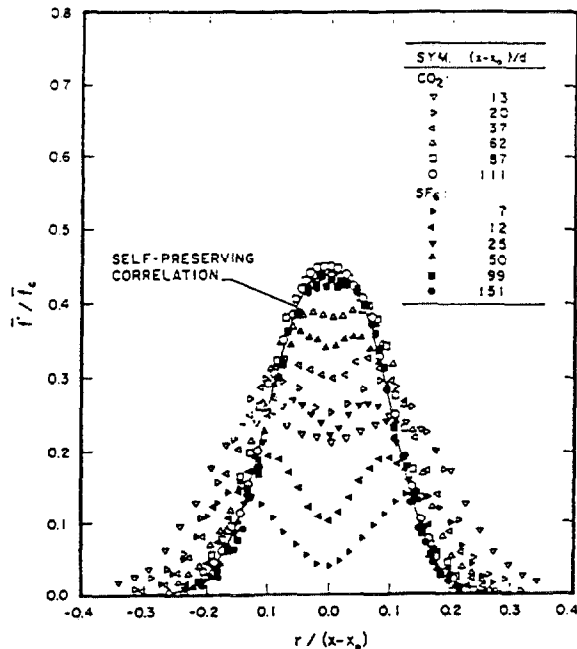


Fig. 4 Development of radial profiles of rms mixture fraction fluctuations

in Fig. 4. The development of the flow from source conditions, where mixture fraction fluctuations are less than 1 percent, is certainly a factor in this behavior. However, the gradual disappearance of nonbuoyant dynamics as $(x-x_0)/l_M$ becomes large also is a factor. In particular, nonbuoyant jets have reduced mixture fraction fluctuations near the axis because turbulence production is small in this region in view of symmetry requirements (Becker et al., 1967; Papanicolaou and List, 1987, 1988). In contrast, effects of buoyancy provide turbulence production near the axis for plumes in spite of symmetry due to buoyant instability in the streamwise direction, i.e., the density approaches the ambient density in the streamwise direction. This added turbulence production accounts for increased mixture fraction fluctuation levels near the axis of plumes in comparison to jets in the self-preserving region, i.e., $(\bar{f}'/\bar{f})_c$ ca. 0.45 for plumes in comparison to 0.15-0.18 for jets (Papanicolaou and List, 1987). Even maximum values of \bar{f}'/\bar{f}_c in jets, ca. 0.25 at an $r/(x-x_0)$ of roughly 0.1, are substantially less than the maximum plume values (Papanicolaou and List, 1987). Thus, the contribution of buoyancy to turbulence is appreciable, with the large mixture fraction fluctuations of turbulent self-preserving plumes helping to explain the large radiation fluctuation levels observed in the plumes above buoyant turbulent diffusion flames (Kounalakis et al., 1991).

Probability Density Functions. Mean and fluctuating velocities are reasonably descriptive because the probability density functions of velocities in turbulent flows generally are well represented by a Gaussian distribution function that only has two moments. This is not the case for the probability density functions of mixture fraction, however, because the mixture fraction is limited to the finite range 0-1 by definition, so that finite range distribution functions must be used, e.g., the clipped-Gaussian function or the algebraically more convenient beta function; see Lockwood and Naguib (1975) for the properties of these two distributions. Thus, some typical probability density functions from present measurements are plotted along with these distribution in Fig. 5. Both distributions are defined by two moments; thus, the predicated distributions are based on the measured values of \bar{f} and \bar{f}' at each location considered.

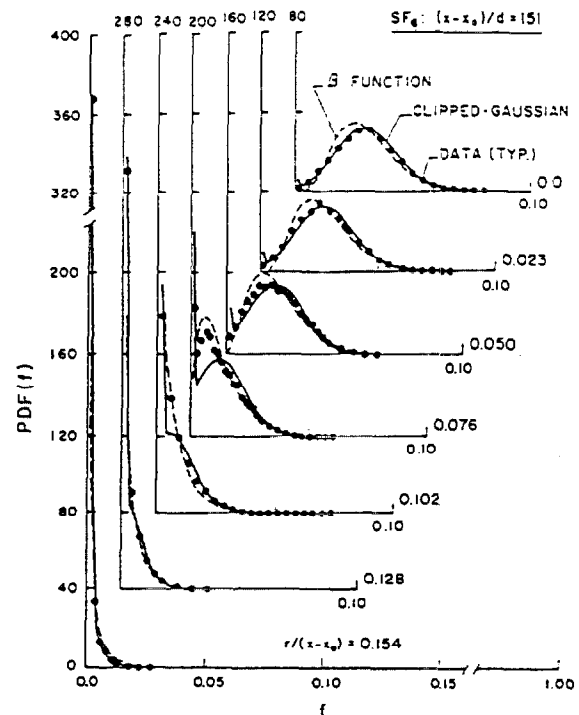


Fig. 5 Typical probability density functions of mixture fractions at self-preserving conditions: SF₆ source at $(x-x_0)/d = 151$

The measured probability density functions illustrated in Fig. 5 are qualitatively similar to earlier measurements for flames, plumes, and jets (Kounalakis et al., 1991; Papanicolaou and List, 1987, 1988; Becker et al., 1967). At the axis, the probability density function is nearly Gaussian, although it still has a small spike at $f = 0$ representing some period when unmixed ambient fluid reaches the axis. With increasing radial distance, the spike at $f = 0$ increases and eventually dominates the distribution as the edge of the plume is approached. There is little to choose between representing the probability density functions by either clipped-Gaussian or beta functions although the ease of use of the beta function is helpful for reducing computation times during simulations (Lockwood and Naguib, 1975).

Temporal Power Spectral Densities. Temporal correlations, or temporal power spectral densities, which are their Fourier transform (Hinze, 1975; Tennekes and Lumley, 1972), must be known in order to simulate the temporal aspects of radiation fluctuations (Kounalakis et al., 1991). Some typical measurements of temporal power spectra for the sulfur hexafluoride plumes are illustrated in Fig. 6; results for the carbon dioxide plumes were similar. Spectra are plotted for $(x-x_0)/d$ in the range 25-151, considering radial positions over the full width of the flow at each streamwise position. The temporal spectra are relatively independent of radial position at particular streamwise location. Similarly, the low-frequency portion of the spectra is relatively independent of streamwise distance when normalized in the manner of Fig. 6. However, there are systematic variations in the decaying portion of the spectra with streamwise distance that will be discussed next. Spectra of transitional plumes reported by Papanicolaou and List (1987, 1988) are qualitatively quite similar to the results illustrated in Fig. 6.

The decay of the spectra with increasing frequency is an interesting feature of the results illustrated in Fig. 6. The spectra initially decay according to the $-5/3$ power of frequency,

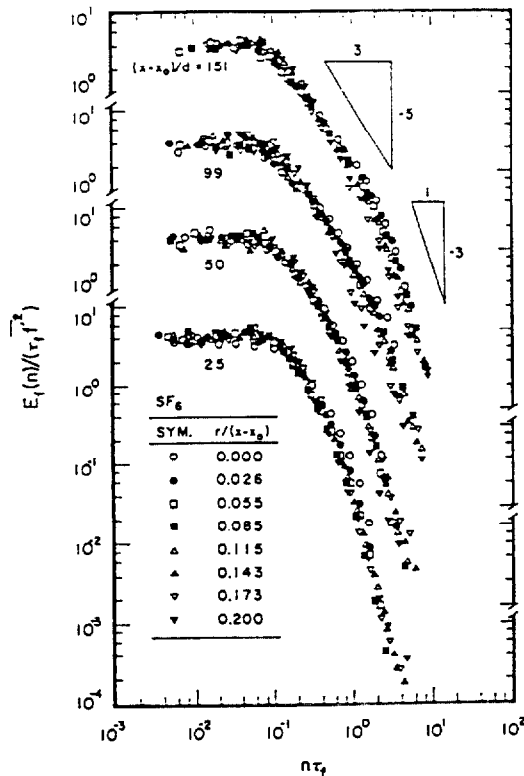


Fig. 6 Typical temporal power spectral densities of mixture fraction fluctuations: SF₆ source

analogous to the well-known inertial region of the turbulence spectrum of velocity fluctuations which has been called the inertial-convective region for scalar property fluctuations (Tennekes and Lumley, 1972). Within this region, mixture fraction fluctuations simply are convected and effects of molecular diffusivities are small. This is followed by a region where the spectrum decays more rapidly, yielding a slope of roughly -3 , that has been observed during several investigations of highly buoyant flows with molecular Prandtl/Schmidt numbers in the range $0.7-7$, but not in nonbuoyant flows (Mizushima et al, 1979; Papanicolaou and List, 1987, 1988). Papanicolaou and List (1987) argue that this portion of the spectrum agrees with the behavior expected for the inertial-diffusive subrange, where the variation of the local rate of dissipation of mixture fraction fluctuations in buoyant flows is due to buoyancy-generated inertial forces rather than viscous forces. An effect of this type is plausible due to the progressive increase of the span of the inertial range as $(x-x_0)/d$ increases, e.g., the intersections of the $-5/3$ and -3 regions of the spectra occur at roughly $n\tau_f = 0.4, 0.8, 1.5,$ and 2.0 for $(x-x_0)/d = 25, 50, 99,$ and 151 , respectively. This behavior is analogous to the anticipated reductions of microscales with increasing streamwise distance, which suggests a diffusive effect. However, understanding of the behavior of the spectra of buoyant turbulent flows in this region is very limited and clearly merits additional study. At higher frequencies, the mixture fraction microscale should be approached where the spectrum becomes small; unfortunately, existing measurements have had neither the spatial nor the temporal resolution needed to resolve this region.

Radial Spatial Correlations. Spatial correlations also must be known in order to simulate aspects of radiation fluctuations, due to effects of optical path lengths on radiation intensities (Kounalakis et al., 1991). Spatial correlations also are impor-

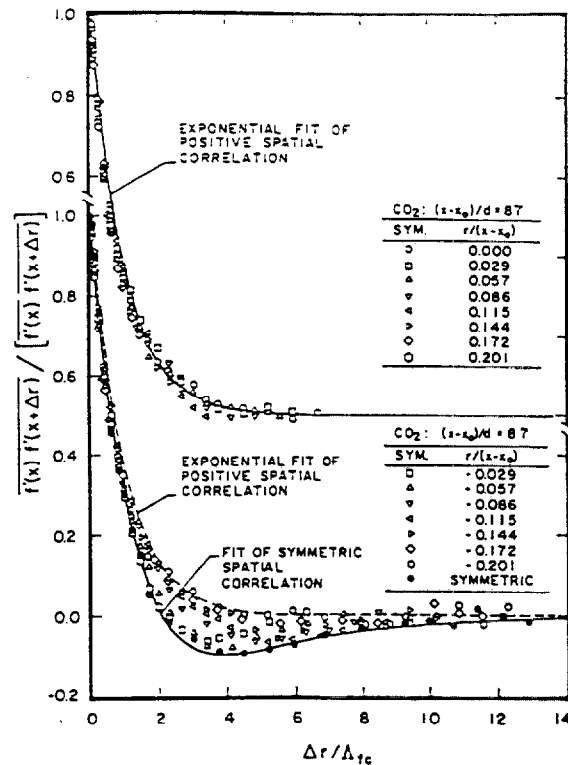


Fig. 7 Typical radial spatial correlations of mixture fraction fluctuations: CO₂ source

tant fundamental properties of turbulence that have received significant attention in the past (Hinze, 1975; Tennekes and Lumley, 1972). Study of these properties was begun during the present investigation by measuring radial spatial correlations, which largely control radiation fluctuations in boundary layer flows, like plumes (Kounalakis et al., 1991).

The general properties of spatial correlations in turbulent shear flows vary depending on whether the two points considered are on the same or on opposite sides of planes or lines of symmetry. This orientation will be indicated for the present radial correlations by a coordinate system along the radial direction extending from $-\infty$ to ∞ with Δr always greater than zero and the left-most position denoting the position of the correlation. Thus, $r < 0$ implies that both points are on the same side of the axis for $\Delta r < |r|$ and on the opposite side thereafter. If $r > 0$, then both points are always on the same side of the axis. Finally, Corrsin and Uberoi (1950) introduced symmetric lateral spatial correlations for jets, where the two points are spaced equally on either side of the axis (at $-\Delta r/2$ and $\Delta r/2$), thus, there is only one correlation of this type at each streamwise position.

The present measurements of two-point radial and symmetric correlations are illustrated in Fig. 7. These results are for carbon dioxide plumes at $(x-x_0)/d = 87$, which is within the self-preserving region. Other measurements within the self-preserving region were similar. The measurements are presented in two groups, with results for $r > 0$ at the top, and results for $r < 0$ and symmetric correlations at the bottom. The distance increment is normalized by Λ_{frc} ; however, Λ_{fr} is relatively constant over the range of the measurements. The results for $r > 0$ in Fig. 7 exhibit an exponential decay; however, this is an artifact of experimental limitations, e.g., the region near $\Delta r = 0$ should have a nonexponential (quadratic) behavior in terms of Δr as the microscale limit is approached (Becker et al., 1967; Hinze, 1975; Tennekes and Lumley, 1972). This

is not seen in Fig. 7 because the present spatial resolution was not adequate to resolve the smallest scales. In terms of $\Delta r/\Lambda_{frc}$ the exponential fit of the radial spatial resolution was not adequate to resolve the smallest scales. In terms of $\Delta r/\Lambda_{frc}$ the exponential fit of the radial spatial correction is quite simple:

$$\overline{f'(r)f'(r+\Delta r)} / \overline{f'(r)f'(r+\Delta r)} = \exp(-\Delta r/\Lambda_{frc}) \quad (10)$$

where it should be understood that $\Delta r > 0$ as defined earlier. The results in Fig. 7 show that Eq. (10) provides a good fit of the measurements whenever both points of the correlation are on the same side of the axis, e.g., $r > 0$ or $\Delta r < |r|$ when $r < 0$. This approximation is effective because Λ_{frc} is relatively constant over the range of the measurements, as noted earlier. Notably, a radial spatial correlation at the plume axis in the self-preserving region, reported by Papantoniou and List (1989), has essentially the same shape as Eq. (10).

The symmetric spatial correlation provides the other limiting behavior of the radial spatial correlations seen in Fig. 7. These correlations exhibit a Frenkiel function shape as follows: similar to the exponential fit at small Δr ; crossing to a region of negative correlations at $\Delta r/\Lambda_{frc} = 2.1$, which corresponds to $\Delta r/(x-x_0) = 0.07$; reaching a maximum negative value of -0.1 near $\Delta r/\Lambda_{frc} = 4$, which corresponds to $\Delta r/(x-x_0) = 0.13$; and finally decaying from the negative side toward zero as $\Delta r/\Lambda_{frc}$ becomes large. This behavior can be represented by the following empirical fit:

$$\overline{f'(\Delta r/2)f'(-\Delta r/2)} / \overline{f'(\Delta r/2)^2} = (1 - 0.11(\Delta r/\Lambda_{frc})^3)\exp(-\Delta r/\Lambda_{frc}) \quad (11)$$

The present behavior is qualitatively similar to symmetric correlations observed in nonbuoyant jets, except that the negative correlation region is reached sooner in jets. $\Delta r/(x-x_0)$ in the range 0.04-0.06, and the maximum negative correlation is larger in jets, in the range -0.10 to -0.18 (Corrsin and Uberoi, 1950; Becker et al., 1967).

The Frenkiel function behavior of the symmetric correlation is probably caused by the requirement for conservation of scalar flux. In particular, fluctuations of one sign must be compensated by fluctuations of the other sign on opposite sides

of the axis so that the mixture fraction flux is preserved as a whole. Similar behavior is well known for the lateral spatial correlations of velocity fluctuations in isotropic turbulence due to conservation of mass requirement (Hinze, 1975). The rather slow final decay of the negative portion of the symmetric correlation, in comparison to the exponential decay for $r > 0$, also tends to support a large-scale requirement of this type. Unfortunately, interpreting the Frenkiel function shape of the symmetric correlation will require information about velocities (or scalar fluxes) that currently is not available.

The measured spatial correlations for negative r in Fig. 7 generally are intermediate between the exponential and Frenkiel function limits. Naturally, the exponential correlation is retrieved exactly when $\Delta r < |r|$ and both points are on the same side of the axis. On the other hand, when $\Delta r \approx 2|r|$ for $r < 0$, the symmetric correlation is retrieved. Not surprisingly, other values of Δr generally represent an interpolation between these two limits. Most of the complexities of radial spatial correlations however, involve relatively small values of the correlations, which should not have a large effect on radiation fluctuations.

Integral Scales. The properties of the temporal power spectra and radial spatial correlations are completed by the corresponding temporal and spatial integral scales. Present measurements of the integral scales are plotted as a function of radial distance in Fig. 8 for both sources. The measurements extend into the self-preserving region, $25 \leq (x-x_0)/d \leq 151$; however, effects of streamwise distance are relatively small when plotted in the manner of Fig. 8.

The temporal integral scales at the top of Fig. 8 have been plotted by adopting Taylor's hypothesis for the relationship between spatial and temporal integral scales. Then the temporal integral scales have been normalized using self-preserving turbulent plume scaling relationships, i.e., length scales are proportional to $(x-x_0)$ and the velocity scales of the self-preserving region (Rouse et al., 1952; List, 1982). This approach seems robust and provides a good correlation of the temporal integral scales over the range of the present measurements. The results show a progressive increase of τ_t with radial distance. This follows from Taylor's hypothesis because spatial integral scales are relatively independent of radial position (see the lower part of Fig. 8) while streamwise mean velocities decrease as the edges of the plumes are approached.

The radial spatial integral scales for the plumes in the present self-preserving region, $(x-x_0)/d \geq 87$, are plotted in the lower part of Fig. 8. These integral scales were found from the correlations for positive values of r , as discussed previously. They have been normalized by $(x-x_0)$ to indicate scaling in the self-preserving region, similar to the temporal integral scales. The results indicate relatively little variation of Λ_{fr} for $r/(x-x_0) < 0.15$, followed by a reduction toward zero at large radial distances. This behavior follows from the intermittency of the flow at larger radial distances where the dimensions of turbulent fluid having mixture fractions greater than zero must decrease progressively. Present measurements yield $\Lambda_{fr}/(x-x_0) = 0.033$ near the axis ($r/(x-x_0) < 0.09$) within the self-preserving region ($(x-x_0)/d \geq 87$). In contrast, Papantoniou and List (1989) report somewhat scattered and consistently lower values of $\Lambda_{fr}/(x-x_0)$ at comparable streamwise distances, in the range 0.011-0.022 for $r/(x-x_0) \leq 0.044$. The large Schmidt numbers of the liquid plumes considered by Papantoniou and List (1989) may be responsible for the differences between the two studies because this allows larger amounts of unmixed fluid to penetrate the flow than in gaseous plumes. Thus, large Schmidt numbers would tend to reduce spatial correlations, while increasing concentration fluctuations as discussed earlier.

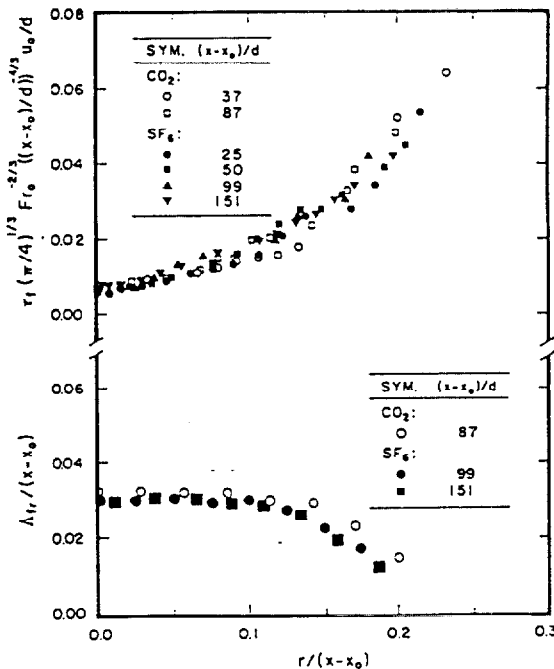


Fig. 8 Radial distributions of temporal and radial spatial integral scales

Conclusions

Mixture fraction statistics were measured in round buoyant

turbulent plumes in still air. The test conditions involved buoyant jet sources of carbon dioxide and sulfur hexafluoride to give ρ_0/ρ_∞ of 1.51 and 5.06 and source Froude numbers of 7.80 and 3.75, respectively, with $(x-x_0)/d$ in the range 0-151 and $(x-x_0)/L_s$ in the range 0-43. The major conclusions are as follows:

1 The present measurements, supported by earlier findings of Papanicolaou and List (1989) for similar conditions, yielded distributions of mean mixture fractions in self-preserving plumes that were up to 30 percent narrower, with scaled values at the axis up to 30 percent larger, than other results found using buoyant jet sources in the literature, e.g., Papanicolaou and List (1987, 1988), Shabbir and George (1992), George et al. (1977), and Rouse et al. (1952), among others. Based on the observation that the earlier results were similar to behavior within the transitional plume region during the present study, it appears that the earlier results were not obtained at sufficient distances from the source to reach self-preserving conditions. In particular, self-preserving conditions were reached for $(x-x_0)/d \geq 87$ during the present measurements and those of Papanicolaou and List (1989), while the earlier measurements, for comparable source Froude numbers, involved $(x-x_0)/d \leq 62$. Naturally, distances from the source to reach self-preserving conditions depend on source properties like Re_0 , Fr_0 , and ρ_0/ρ_∞ , and may be much shorter for purely buoyant sources (Kotsovinos, 1985); quantifying these effects merits additional study.

2 Radial profiles of mixture fraction fluctuations in the self-preserving region for plumes do not exhibit reduced values near the axis similar to jets. Instead, effects of buoyancy cause mixture fraction fluctuations to be maximum at the axis with intensities of roughly 45 percent. These large intensities probably are responsible for the large radiation fluctuation levels observed in the near-overfire region of fires.

3 Probability density functions of mixture fractions can be approximated reasonably well by either clipped-Gaussian or beta functions. Unlike nonbuoyant turbulent jets, finite levels of intermittency are observed at the axis within the self-preserving region of turbulent plumes.

4 The low-frequency portion of the temporal spectra of mixture fraction fluctuations is a robust property of plumes, which scale in a relatively universal manner even in the transitional plume region. The spectra exhibit the well-known $-5/3$ power inertial decay region followed by a -3 power inertial-diffusive region. The latter region has been observed by others in buoyant flows but is not observed in nonbuoyant flows; thus, it is an interesting buoyancy/turbulence interaction that merits further study.

5 Radial spatial correlations were limited by correlations where both points were on the same side of the axis, which exhibited an exponential decay, and symmetric correlations, which approximated a Frenkiel function. This behavior probably follows from conservation of scalar flux considerations, but more measurements and study are required to understand the phenomena controlling spatial correlations. Behavior near microscales was not addressed during the present study due to the limited spatial resolution of the measurements.

6 Integral scales behaved as anticipated and provisional scaling relationships have been proposed that merit additional study. Temporal integral scales were smallest at the axis, which follows from Taylor's hypothesis noting that mean velocities are largest in this region. Radial spatial integral scales were largest at the axis, which follows from the topography of the flow, i.e., the streamwise extent of particular sections of partially mixed turbulent fluid must decrease as the intermittency increases toward the edge of the flow.

Acknowledgments

This research was supported by the United States Department of Commerce, National Institute of Standards and Technology, Grant No. 60NANB1D1175, with H. R. Baum of the Building and Fire Research Laboratory serving as Scientific Officer.

References

- Abraham, G., 1960, "Jet Diffusion in Liquid of Greater Density," *ASCE J. Hyd. Div.*, Vol. 86, pp. 1-13.
- Becker, H. A., Hottel, H. C., and Williams, G. C., 1967, "The Nozzle-Fluid Concentration Field of the Round, Turbulent, Free Jet," *J. Fluid Mech.*, Vol. 30, pp. 285-303.
- Bilger, R. W., 1976, "Turbulent Jet Diffusion Flames," *Prog. Energy Combust. Sci.*, Vol. 1, pp. 87-109.
- Bird, R. B., Stewart, W. E., and Lightfoot, E. N., 1960, *Transport Phenomena*, Wiley, New York, pp. 502-513.
- Corrsin, H. Y., and Uberoi, M. S., 1950, "Further Experiments on the Flow and Heat Transfer in a Heated Turbulent Jet," NACA Rept. No. 998.
- George, W. K., Jr., Alpert, R. L., and Tamanini, F., 1977, "Turbulence Measurements in an Axisymmetric Buoyant Plume," *Int. J. Heat Mass Trans.*, Vol. 20, pp. 1145-1154.
- Hiller, B., and Hanson, R. K., 1990, "Properties of the Iodine Molecule Relevant to Laser-Induced Fluorescence Experiments in Gas Flows," *Expts. Fluids*, Vol. 10, pp. 1-11.
- Hinze, J. O., 1975, *Turbulence*, 2nd ed., McGraw-Hill, New York, pp. 175-319.
- Kotsovinos, N. E., 1985, "Temperature Measurements in a Turbulent Round Plume," *Int. J. Heat Mass Trans.*, Vol. 28, pp. 771-777.
- Kounalakis, M. E., Sivathanu, Y. R., and Faeth, G. M., 1991, "Infrared Radiation Statistics of Nonluminous Turbulent Diffusion Flames," *ASME JOURNAL OF HEAT TRANSFER*, Vol. 113, pp. 437-445.
- Lai, M.-C., and Faeth, G. M., 1987, "A Combined Laser-Doppler Anemometer/Laser-Induced Fluorescence System for Turbulent Transport Measurements," *ASME JOURNAL OF HEAT TRANSFER*, Vol. 109, pp. 254-256.
- List, E. J., 1982, "Turbulent Jets and Plumes," *Ann. Rev. Fluid Mech.*, Vol. 14, pp. 189-212.
- Lockwood, F. C., and Naguib, A. S., 1975, "The Prediction of Fluctuations in the Properties of Free, Round-Jet Turbulent Diffusion Flames," *Combust. Flame*, Vol. 24, pp. 109-124.
- Mizushima, T., Ogino, F., Veda, H., and Komori, S., 1979, "Application of Laser-Doppler Velocimetry to Turbulence Measurements in Non-isothermal Flow," *Proc. Roy. Soc. London*, Vol. A366, pp. 63-79.
- Morton, B. R., Taylor, G. I., and Turner, J. S., 1956, "Turbulent Gravitational Convection From Maintained and Instantaneous Sources," *Proc. Roy. Soc. London*, Vol. A234, pp. 1-23.
- Morton, B. R., 1959, "Forced Plumes," *J. Fluid Mech.*, Vol. 5, pp. 151-163.
- Ogino, F., Takeuchi, H., Kudo, I., and Mizushima, T., 1980, "Heated Jet Discharged Vertically in Ambients of Uniform and Linear Temperature Profiles," *Int. J. Heat Mass Transfer*, Vol. 23, pp. 1531-1538.
- Papanicolaou, P. N., and List, E. J., 1987, "Statistical and Spectral Properties of Tracer Concentration in Round Buoyant Jets," *Int. J. Heat Mass Transfer*, Vol. 30, pp. 2059-2071.
- Papanicolaou, P. N., and List, E. J., 1988, "Investigation of Round Vertical Turbulent Buoyant Jets," *J. Fluid Mech.*, Vol. 195, pp. 341-391.
- Papanicolaou, D., and List, E. J., 1989, "Large Scale Structure in the Far Field of Buoyant Jets," *J. Fluid Mech.*, Vol. 209, pp. 151-190.
- Peterson, J., and Bayazitoglu, Y., 1992, "Measurements of Velocity and Turbulence in Vertical Axisymmetric Isothermal and Buoyant Plumes," *ASME JOURNAL OF HEAT TRANSFER*, Vol. 114, pp. 135-142.
- Pivovarov, M. A., Zhang, H., Ramaker, D. E., Tatem, P. A., and Williams, F. W., 1992, "Similarity Solutions in Buoyancy-Controlled Diffusion Flame Modelling," *Combust. Flame*, Vol. 92, pp. 308-319.
- Rouse, H., Yih, C. S., and Humphreys, H. W., 1952, "Gravitational Convection From a Boundary Source," *Tellus*, Vol. 4, pp. 201-210.
- Shabbir, A., and George, W. K., 1992, "Experiments on a Round Turbulent Buoyant Plume," NASA Technical Memorandum 105955.
- Sivathanu, Y. R., and Faeth, G. M., 1990, "Generalized State Relationships for Scalar Properties in Nonpremixed Hydrocarbon/Air Flames," *Combust. Flame*, Vol. 82, pp. 211-230.
- Stårner, S. H., and Bilger, R. W., 1983, "Differential Diffusion Effects on Measurements in Turbulent Diffusion Flames by the Mie Scattering Technique," *Prog. Astro. and Aero.*, Vol. 88, pp. 81-104.
- Tennekes, H., and Lumley, J. L., 1972, *A First Course in Turbulence*, MIT Press, Cambridge, MA.
- Wu, J.-S., and Faeth, G. M., 1993, "Sphere Wakes in Still Surroundings at Intermediate Reynolds Numbers," *AIAA J.*, Vol. 31, pp. 1448-1455.
- Zimin, V. D., and Frik, P. G., 1977, "Averaged Temperature Fields in Asymmetrical Turbulent Streams Over Localized Heat Sources," *Izv. Akad. Nauk. SSSR, Mekhanika Zhidkosti Gaza*, Vol. 2, pp. 199-203.

Appendix B: Dai et al. (1995a)

Velocity Statistics of Round, Fully Developed, Buoyant Turbulent Plumes

Z. Dai

Graduate Student Research Assistant.

L. K. Tseng¹

Research Fellow.

G. M. Faeth

Professor,
Fellow ASME

Department of Aerospace Engineering,
The University of Michigan,
Ann Arbor, MI 48109-2118

An experimental study of the structure of round buoyant turbulent plumes was carried out, limited to conditions within the fully developed (self-preserving) portion of the flow. Plume conditions were simulated using dense gas sources (carbon dioxide and sulfur hexafluoride) in a still air environment. Velocity statistics were measured using laser velocimetry in order to supplement earlier measurements of mixture fraction statistics using laser-induced iodine fluorescence. Similar to the earlier observations of mixture fraction statistics, self-preserving behavior was observed for velocity statistics over the present test range (87–151) source diameters and 12–43 Morton length scales from the source), which was farther from the source than most earlier measurements. Additionally, the new measurements indicated that self-preserving plumes are narrower, with larger mean streamwise velocities near the axis (when appropriately scaled) and with smaller entrainment rates, than previously thought. Velocity statistics reported include mean and fluctuating velocities, temporal power spectra, temporal and spatial integral scales, and Reynolds stresses.

Introduction

The structure of round buoyant turbulent plumes in still and unstratified environments is an important fundamental problem that has attracted significant attention since the classical study of Rouse et al. (1952). However, recent work has highlighted the need for more information about buoyant turbulent plumes in order to address effects of turbulence/radiation interactions (Kounalakis et al., 1991), and to help benchmark models of buoyant turbulent flows (Dai et al., 1994). Thus, the objective of the present investigation was to measure mean and fluctuating velocity properties in round buoyant turbulent plumes in order to supplement earlier measurements of mean and fluctuating scalar properties (mixture fractions) in these flows, due to Dai et al. (1994). The fully developed region, where effects of the source have been lost and the properties of the flow become self-preserving, was emphasized due to its fundamental importance for simplifying both theoretical considerations and the interpretation of the measurements (Tennekes and Lumley, 1972), even though few practical plumes reach these conditions.

Several reviews of turbulent plumes have appeared (Chen and Rodi, 1980; Kotsovinos, 1985; List, 1982; Papanicolaou and List, 1987, 1988); therefore, the discussion of past studies will be brief. The earliest work emphasized the development of similarity relationships for flow properties within fully developed (self-preserving) buoyant turbulent plumes (Rouse et al., 1952; Morton et al., 1956; Morton, 1959). Subsequently, many workers reported observations of mean properties at self-preserving conditions; however, the various determinations of centerline values and flow widths generally were not in good agreement (Abraham, 1960; Chen and Rodi, 1980; Dai et al., 1994; George et al., 1977; Kotsovinos, 1985; Kotsovinos and List, 1987; Mizushima et al., 1979; Nakagome and Hirata, 1977; Ogino et al., 1980; Papanicolaou and List, 1987, 1988; Papantoniou and List, 1989; Peterson and Bayazitoglu, 1992; Seban and Behnia, 1976; Shabir and George, 1992; Zimin and Frik, 1977). Papanicolaou and List (1987, 1988), Papantoniou and List (1989), and Dai et al.

(1994) attribute these discrepancies mainly to problems of fully reaching self-preserving conditions, with conventional experimental uncertainties serving as a contributing factor.

Self-preserving round buoyant plume conditions are reached when streamwise distances from the plume source are large in comparison to two characteristic length scales, as follows: (1) the source diameter, as a measure of conditions where effects of source disturbances have been lost; and (2) the Morton length scale, as a measure of conditions when the buoyant features of the flow are dominant. For general buoyant jet sources, the Morton length scale is defined as follows (Morton, 1959; List, 1982; Papanicolaou and List, 1988):

$$l_w = M_0^{1/4} / B_0^{1/2} \quad (1)$$

For round plumes with uniform properties defined at the source (similar to the present experiments), the source specific momentum flux, M_0 , and the source buoyancy flux, B_0 , are defined as follows (List, 1982; Dai et al., 1994):

$$M_0 = (\pi/4) d^2 u_0^2 \quad (2)$$

$$B_0 = (\pi/4) d^2 u_0 g |\rho_0 - \rho_\infty| / \rho_\infty \quad (3)$$

where an absolute value of the density difference has been used in Eq. (3) to account for both rising and falling plumes. Substituting Eqs. (2) and (3) into Eq. (1) then yields the following expression for l_w for round plumes that have uniform properties at the source:

$$l_w = (\pi/4)^{1/4} (\rho_\infty u_0^2 / (g |\rho_0 - \rho_\infty|))^{1/2} \quad (4)$$

The ratio, l_w/d , is proportional to the source Froude number, defined as follows for conditions analogous to those of Eq. (4) (List, 1982):

$$Fr_0 = (4/\pi)^{1/4} l_w/d = (\rho_\infty u_0^2 / (g |\rho_0 - \rho_\infty| d))^{1/2} \quad (5)$$

The source Froude number is a convenient measure of the dominance of buoyancy at the source, e.g., $Fr_0 = 0$ and ∞ for purely buoyant and for purely nonbuoyant sources, respectively.

Papanicolaou and List (1987, 1988) suggest that buoyancy-dominated conditions for mean and fluctuating quantities are reached for $(x - x_0)/l_w$ greater than roughly 6 and 14, respectively, which has been satisfied by most past measurements seeking results at self-preserving conditions (Dai et al., 1994). However, aside from the measurements of Papantoniou and List (1989) and Dai et al. (1994), to be discussed subsequently, ex-

¹ Current address: School of Mechanical Engineering, Purdue University, West Lafayette, IN.

Contributed by the Heat Transfer Division for publication in the JOURNAL OF HEAT TRANSFER. Manuscript received by the Heat Transfer Division November 1993, revision received April 1994. Keywords: Natural Convection, Plumes, Turbulence. Associate Technical Editor: Y. Jaluria.

isting measurements of radial profiles of mean and fluctuating properties in buoyant turbulent plumes have been limited to $(x - x_0)/d$ in the range 6–62, with most measurements emphasizing the lower end of this range, see Papanicolaou and List (1987, 1988), Shabbir and George (1992), George et al. (1977), Ogino et al. (1980), Nakagome and Hirata (1977), and Peterson and Bayazitoglu (1992), among others. This range of normalized streamwise distances is rather small to achieve self-preserving conditions, based on findings for nonbuoyant round turbulent jets where values of $(x - x_0)/d$ greater than roughly 40 and 100 are required to achieve self-preserving profiles of mean and fluctuating properties, respectively (Hinze, 1975; Tennekes and Lumley, 1972). Similar behavior for round buoyant turbulent plumes recently has been established by Papantoniou and List (1989) and Dai et al. (1994). These measurements were limited to scalar properties and found that self-preserving mean and fluctuating mixture fractions (i.e., the mass fraction of source material in a sample) only were achieved at $(x - x_0)/d$ and $(x - x_0)/l_w$ greater than roughly 100 and 10, respectively. These results also showed that self-preserving buoyant turbulent plumes were narrower, with larger mean and fluctuating scalar properties at the axis (when appropriately scaled), than earlier reported measurements of self-preserving scalar properties made closer to the source. Finally, it seems likely that self-preserving behavior for other properties only is achieved at comparable conditions.

The preceding discussion suggests that existing measurements of mean and fluctuating velocities within round buoyant turbulent plumes probably involve transitional plumes. Thus, the objective of the present investigation was to extend the scalar property measurements of Papantoniou and List (1989) and Dai et al. (1994) to consider mean and fluctuating velocity properties within the self-preserving region of round buoyant turbulent plumes. Present test conditions were identical to those of Dai et al. (1994), and involved source flows of carbon dioxide and sulfur hexafluoride in still air at room temperature and atmospheric pressure. This approach yields downwardly flowing negatively buoyant plumes in still and unstratified environments, and allows straightforward specification of the buoyancy flux within the test plumes.

Experimental Methods

Test Apparatus. Description of the experimental apparatus will be brief; see Dai et al. (1994) for more details. The test plumes were within a screened enclosure (which could be traversed to accommodate rigidly mounted instrumentation) that was mounted within an outer enclosure. The plume sources were

long round tubes that could be traversed in the vertical direction within the inner enclosure for measurements at various streamwise distances from the source. The ambient air within the enclosure was seeded with oil drops (roughly 1 μm nominal diameter) for laser velocimetry (LV) measurements of velocities, using several multiple jet spray generators (TSI, model 9306) that discharged above the screened top of the outer enclosure. In the self-preserving region where present measurements were made, maximum mixture fractions were less than 6 percent; therefore, effects of concentration bias (because only the ambient air was seeded) were negligible.

Instrumentation. Dual-beam, frequency-shifted LV was used for the velocity measurements, based on the 514.5 nm line of an argon-ion laser. The optical axis of the LV passed horizontally through the flow with signal collection at right angles to the optical axis to yield a measuring volume having a diameter of 400 μm and a length of 260 μm . A darkened enclosure as well as a laser line filter in front of the detector were used to minimize effects of background light. Various orientations of the plane of the laser beams were used to find the three components of mean and fluctuating velocities, as well as the Reynolds stress, as described by Lai and Faeth (1987).

The detector output was amplified and processed using a burst counter signal processor (TSI, model 1980B). The low-pass filtered analog output of the signal processor was sampled at equal time intervals in order to avoid problems of velocity bias, while directional ambiguity and bias were controlled by frequency shifting. The detector output was sampled at rates more than twice the break frequency of the low-pass filter in order to control alias signals. Seeding levels were controlled so that effects of step noise contributed less than 3 percent to determinations of velocity fluctuations, based on measurements of temporal spectra to be discussed later. Experimental uncertainties (95 percent confidence) were mainly governed by finite sampling time limitations and are estimated to be less than 5 and 13 percent for mean and fluctuating velocities, respectively; the corresponding uncertainties for Reynolds stresses are estimated to be less than 16 percent.

Test Conditions. The experiments involved carbon dioxide and sulfur hexafluoride plumes as summarized in Table 1. For $(x - x_0)/d \geq 87$, where self-preserving conditions were observed, the Kolmogorov microscales of velocity fluctuations were less than 350 μm ; therefore, the spatial resolution of present measurements was not sufficient to resolve the smallest scales of turbulence. Present source conditions were identical to those of Dai et al. (1994), however, the locations of the virtual origins of

Nomenclature

B_0 = source buoyancy flux, Eq. (3)	l_f, l_s = characteristic plume radii based on \bar{f} and \bar{u}	x = streamwise distance
d = source diameter	l_M = Morton length scale, Eqs. (1) and (4)	η = dimensionless radial distance, Eq. (15)
$E_i(n)$ = temporal power spectral density of velocity component i	M_0 = source-specific momentum flux, Eq. (2)	ν = kinematic viscosity
E_n = entrainment constant, Eq. (19)	n = frequency	ρ = density
f = mixture fraction	Q = plume volumetric flow rate	τ_f, τ_u = temporal integral scales of f' and u'
$F(r/(x - x_0))$ = scaled radial distribution of \bar{f} in self-preserving region	r = radial distance	Subscripts
Fr_0 = source Froude number, Eq. (5)	Re_0 = source Reynolds number = $u_0 d / \nu_0$	c = centerline value
g = acceleration of gravity	u = streamwise velocity	0 = initial value or virtual origin location
k_f, k_u = plume width coefficients based on \bar{f} and \bar{u}	$U(r/(x - x_0))$ = scaled radial distribution of \bar{u} in self-preserving region	∞ = ambient value
	v = radial velocity	Superscripts
	w = tangential velocity	$(\bar{\quad})$ = time-averaged mean value
		$(\quad)'$ = root-mean-squared fluctuating value

Table 1 Summary of test conditions*

Source Properties	CO ₂	SF ₆
Density (kg/m ³)	1.75	5.37
Kinematic viscosity (cm ² /s)	3.5	2.6
Diameter (mm)	9.7	6.4
Average velocity (m/s)	1.74	1.39
Reynolds number, Re ₀	2000	4600
Froude number, Fr ₀	7.80	3.75
Morton length scale, $l_0 \sqrt{d}$	7.34	3.53
Virtual origin, based on \bar{f}_{x_0}/d^3	12.7	0.0
Virtual origin, based on \bar{u}_{x_0}/d	0.0	0.0

*Flow directed vertically downward in still air with an ambient pressure, temperature, density and kinematic viscosity of 99 ± 0.5 kPa, 297 ± 0.5 K, 1.16 kg/m³ and 14.8 mm²/s. Source passage length-to-diameter ratios of 50:1.

^bBased on the measurements of Dai et al. (1994).

the carbon dioxide plume, based on \bar{f} from Dai et al. (1994) and based on \bar{u} for the present measurements, were not identical. It was beyond the scope of the present investigation to study the reasons for different locations of these virtual origins; however, such behavior is not surprising because the initial conditions and Prandtl/Schmidt numbers are not the same for mixture fractions and velocities.

Self-Preserving Scaling

The general state relationship for density as a function of mixture fraction, assuming ideal gas behavior, is given as follows for the present plume flows (Dai et al., 1994):

$$\rho = \rho_a / (1 - f(1 - \rho_a/\rho_0)) \tag{6}$$

Then, noting that $f \ll 1$ in the self-preserving region, Eq. (6) can be linearized as follows:

$$\rho = \rho_a + f\rho_a(1 - \rho_a/\rho_0), f \ll 1 \tag{7}$$

Under present assumptions, conservation principles and the state relationship for density imply that the buoyancy flux is conserved for buoyant turbulent plumes. Then mean streamwise velocities and mixture fractions can be scaled as follows in the self-preserving region, where flow properties are independent of source properties like d and u_0 (List, 1982):

$$\bar{u}((x - x_0)/B_0)^{1/3} = U(r/(x - x_0)) \tag{8}$$

$$\bar{f}gB_0^{2/3}(x - x_0)^{2/3} |d \ln \rho/df|_{r=0} = F(r/(x - x_0)) \tag{9}$$

For present conditions, it can be seen from Eq. (7) that

$$|d \ln \rho/df|_{r=0} = |\rho_0 - \rho_a|/\rho_0 \tag{10}$$

is a measure of the buoyancy potential with the extent of mixing. As before, an absolute value has been used in Eq. (10) to account for both rising and falling plumes. The x_0 in Eqs. (8) and (9) are the virtual origins for \bar{u} and \bar{f} , respectively, as noted in Table 1. The $U(r/(x - x_0))$ and $F(r/(x - x_0))$ are appropriately scaled radial profile functions of mean streamwise velocities and mixture fractions, which become universal functions in the self-preserving region far from the source where Eq. (7) applies. Equations (8) and (9) were used to extrapolate present measurements of mean mixture fractions and velocities along the axis to find the corresponding values of the virtual origins, as discussed earlier.

Results and Discussion

Mean Velocities. The evolution of mean and fluctuating mixture fractions from source to self-preserving conditions has been

considered by Dai et al. (1994). Present measurements of velocity properties were limited to the region where self-preserving behavior was observed for mean and fluctuating mixture fractions: namely, $(x - x_0)/d \geq 87$ and $(x - x_0)/l_0 \geq 12$. Within this region, velocity properties also were observed to be self-preserving. Present measurements of mean streamwise velocities for the self-preserving region are illustrated in Fig. 1. The scaling parameters of Eq. (8) are used in the figure so that the ordinate is equal to $U(r/(x - x_0))$. The variation of $U(r/(x - x_0))$ is seen to be universal within experimental uncertainties over the range of the measurements, as anticipated for self-preserving flow. In contrast, results at smaller values of $(x - x_0)/d$, not shown in Fig. 1, exhibited broader profiles and smaller values of $U(0)$, analogous to the behavior of \bar{f} observed by Dai et al. (1994) in the transitional region of buoyant turbulent plumes.

Within the self-preserving region, present radial profiles of mean streamwise velocities are reasonably approximated by a Gaussian fit, similar to past work (Rouse et al., 1952; Papanicolaou and List, 1988; Ogino et al., 1980; Nakagome and Hirata, 1977; Shabbir and George, 1992; George et al., 1977) as follows:

$$U(r/(x - x_0)) = U(0) \exp\{-k_s^2(r/(x - x_0))^2\} \tag{11}$$

where

$$k_s = (x - x_0)/l_s \tag{12}$$

and l_s is a characteristic plume radius where $\bar{u}/\bar{u}_s = \exp(-1)$. The best fit of the present data in the self-preserving region yielded $U(0) = 4.3$ and $k_s^2 = 93$, with $l_s/(x - x_0) = 0.10$. The resulting correlation is seen to be a good representation of the measurements illustrated in Fig. 1.

Present measurements of mean streamwise velocities in the self-preserving region of turbulent plumes yield narrower profiles with larger values near the axis (when appropriately scaled) than

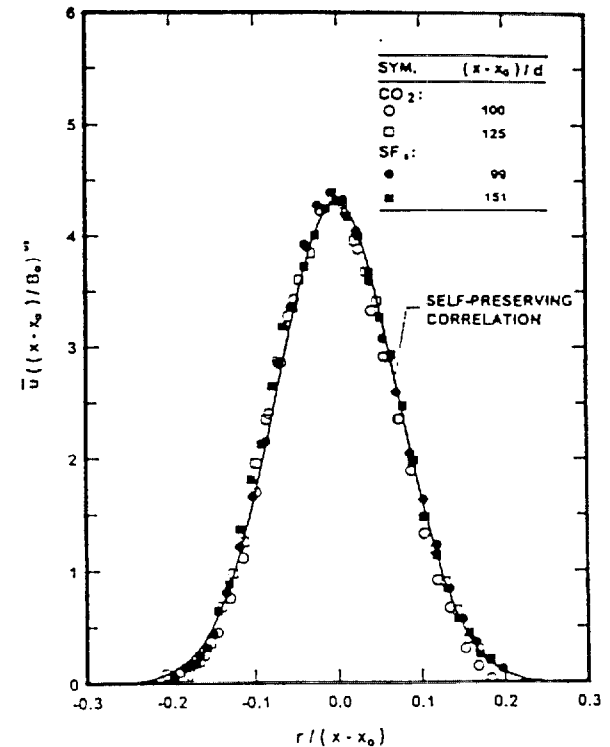


Fig. 1 Radial profiles of mean streamwise velocities in self-preserving buoyant turbulent plumes

earlier results obtained at smaller distances from the source. This behavior is quantified in Table 2, where the range of streamwise distances considered for measurements of radial profiles of self-preserving plume properties, and the corresponding reported values of k_0^2 , $U(0)$, and $l_0/(x - x_0)$, are summarized for representative past studies and associated earlier work from the same laboratories. Past measurements generally satisfy the criterion for buoyancy-dominated flow, i.e., $(x - x_0)/l_0 > 6$ (Papanicolaou and List, 1987, 1988). However, except for the present study, the measurements were obtained at values of $(x - x_0)/d$ that normally are not associated with self-preserving conditions for jetlike sources. Somewhat like the tendency for transitional plumes to have broader profiles than the self-preserving region, mentioned earlier, the values of k_0^2 tend to increase as the maximum streamwise position considered is increased, exhibiting an increase of 40 percent for the range of conditions given in Table 2. This yields a corresponding reduction of the characteristic plume radius of 40 percent, and an increase of $U(0)$ of 25 percent, when approaching self-preserving conditions over the range considered in Table 2.

Present measurements of radial profiles of mean radial velocities are illustrated in Fig. 2. The scaling parameters used in the figure for \bar{v} and radial distance provide universal plots within the self-preserving region as well as a check of the internal consistency of the present measurements of \bar{u} and \bar{v} . This behavior can be seen from conservation of mass in the self-preserving region where the variation of density is small, e.g.:

$$r\partial\bar{u}/\partial x + \partial r\bar{v}/\partial r = 0 \quad (13)$$

Integrating Eq. (13), noting that $r\bar{v} = 0$ at $r = 0$, then yields:

$$r\bar{v}/((x - x_0)\bar{u}_c) = \int_0^\eta ((x - x_0)/\bar{u}_c)(\partial\bar{u}/\partial x)\eta d\eta \quad (14)$$

where

$$\eta = r/(x - x_0) \quad (15)$$

The integral on the right-hand side of Eq. (14) can be evaluated for self-preserving conditions after substituting from Eqs. (8) and (11) for \bar{u} and \bar{u}_c . This yields:

$$r\bar{v}/((x - x_0)\bar{u}_c) = (5/6k_0^2)[(1 + 6k_0^2\eta^2/5) \times \exp(-k_0^2\eta^2) - 1] \quad (16)$$

which demonstrates the universality of the scaled value of $r\bar{v}$ as a function of η within the self-preserving region. Finally, adopting $k_0^2 = 93$ from present measurements (see Table 2) yields the plot based on the mean streamwise velocity measurements illustrated in Fig. 2.

The measurements of \bar{v} illustrated in Fig. 2 exhibit universal behavior for the two test plumes, as anticipated for the self-preserving region. Additionally, the measurements of \bar{v} also are consistent with present measurements of \bar{u} , based on good agreement with the correlation found from \bar{u} through the continuity equation. This check is important because \bar{v} is small, roughly an order

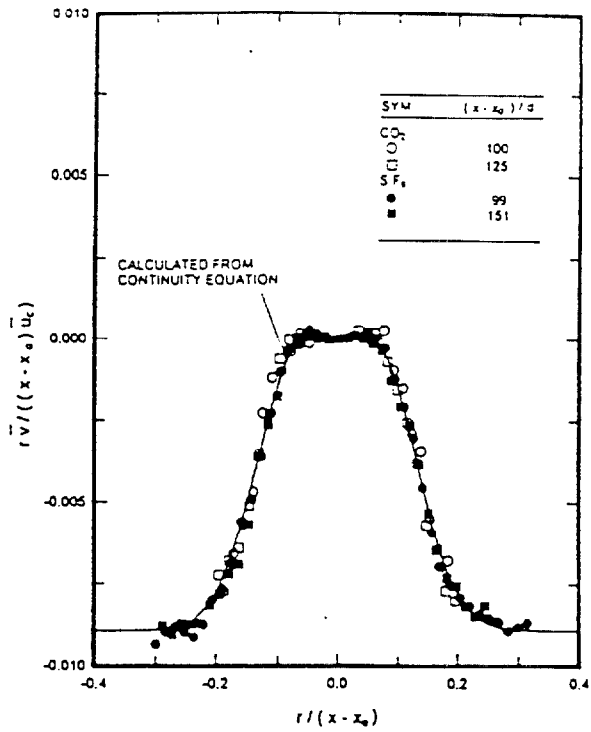


Fig. 2 Radial profiles of mean radial velocities in self-preserving buoyant turbulent plumes

of magnitude smaller than \bar{u}' , so that it is difficult to measure due to its rather low signal-to-noise ratios.

The asymptotic values of $r\bar{v}$ at large absolute values of η are proportional to the entrainment constant of the plumes, which is important for integral theories of plume scaling and as a measure of turbulent mixing rates (Morton, 1959; Morton et al., 1956). Entrainment behavior can be seen by integrating Eq. (13) to obtain an expression for the rate of change of the volumetric flow rate within the plumes at self-preserving conditions where the density of the flow is nearly constant:

$$d/dx \int_0^\infty r\bar{u} dr = dQ/dx = -(r\bar{v})_\infty \quad (17)$$

An estimate of $(r\bar{v})_\infty$ can be found from the measurements of mean streamwise velocities through Eq. (16), as follows:

$$-(r\bar{v})_\infty/((x - x_0)\bar{u}_c) = 5/(6k_0^2) \quad (18)$$

In view of the agreement between measurements of $r\bar{v}$ and Eq. (16), discussed earlier, Eq. (18) provides a reasonable estimate of entrainment properties. Then, noting that $k_0^2 = 93$, Eq. (18) yields $-(r\bar{v})_\infty/((x - x_0)\bar{u}_c) = 0.0090$.

Actual entrainment constants have values that depend on the characteristic radius and velocity used in their definition (Morton, 1959). For present purposes, it is convenient to use l_0 and \bar{u}_c as the radius and velocity scales so that the entrainment constant, E_0 , is defined as follows:

$$dQ/dx = E_0 l_0 \bar{u}_c \quad (19)$$

Then, an expression for E_0 can be found in terms of measurements of mean streamwise velocities from Eqs. (12), (17), (18) and (19), as follows:

$$E_0 = 5/(6k_0^2) \quad (20)$$

Table 2 Summary of self-preserving buoyant turbulent plume velocity properties*

Source	Medium	$(x - x_0)/d$	$(x - x_0)/l_0$	k_0^2	$U(0)/\bar{u}_c$	l_0/\bar{u}_c	l_0/d
Present study	gaseous	87-151	12-43	93	0.10	4.3	0.22
Papanicolaou and List (1988)	liquid	22-62	4-62	93	0.11	3.9	0.23
Shah and George (1992)	gaseous	10-25	6-13	56	0.13	3.4	0.32
George et al. (1977)	gaseous	8-16	6-12	35	0.14	3.4	0.24
Ogden et al. (1980)	liquid	6-16	3-13	51	0.14	3.4	0.117
Neelapatt and Murthy (1977)	gaseous	5-13	-	48	0.14	3.9	0.21

*Based on present plume data, universal entrainment constant E_0 of measurements obtained are for conditions where quasi self-preserving properties were found from measurements over the entire section of the plume. Entries are reported in terms of entrainment E_0 .
*Found from Eq. (20).

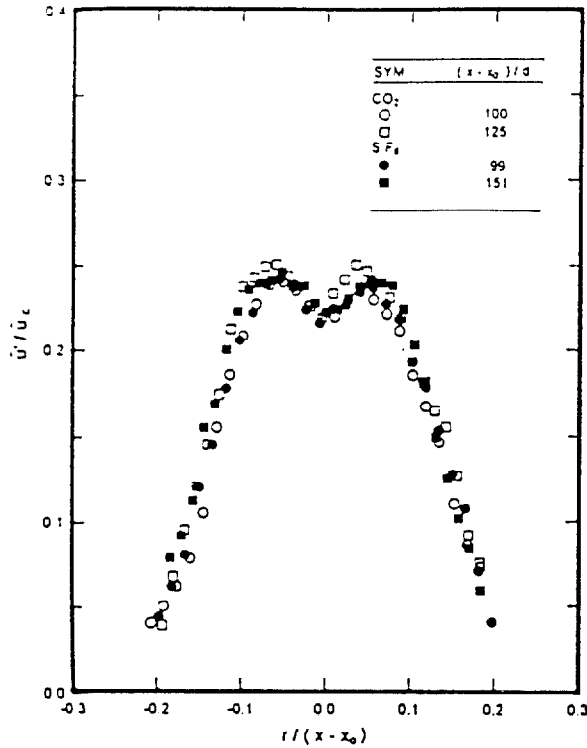


Fig. 3 Radial profiles of streamwise velocity fluctuations in self-preserving buoyant turbulent plumes

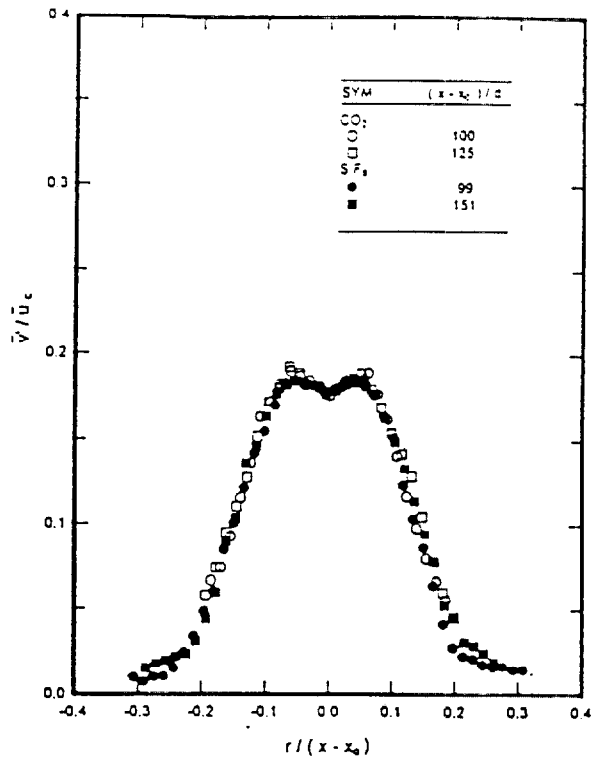


Fig. 4 Radial profiles of radial velocity fluctuations in self-preserving buoyant turbulent plumes

Values of E_1 found from Eq. (20) are summarized in Table 2 for various existing measurements. The main trend of the data is for E_1 to decrease as self-preserving conditions are approached at large distances from the source, with E_1 decreasing roughly 40 percent over the range of existing measurements.

Velocity Fluctuations. Radial profiles of streamwise, radial, and tangential velocity fluctuations for the self-preserving region of the two sources, $(x - x_0) / d \geq 87$ and $(x - x_0) / l_w \geq 12$, are illustrated in Figs. 3-5. It is seen that over the range of streamwise distances considered, the profiles are universal within experimental uncertainties. Results at smaller distances (not shown in Figs. 3-5), however, exhibited broader profiles, analogous to the other mean and fluctuating properties within the transitional region of buoyant turbulent plumes. The magnitude of streamwise turbulence intensities near the axis, however, actually decreases slightly during the latter stages of development of the transitional plumes. This behavior appears to be due to the increase of mean velocities near the axis (when appropriately scaled) as the self-preserving region of the flow is approached. Thus, present estimates of $(\overline{u' / \bar{u}}) = 0.22$ generally are lower than values in the range 0.25-0.32 observed earlier for transitional plumes, see Table 2.

The presence of the dip in streamwise velocity fluctuations near the axis for the self-preserving region, seen in Figs. 3-5, is similar to the behavior of nonbuoyant jets, see Papanicolaou and List (1988) and references cited therein, and is expected because turbulence production is reduced near the axis due to symmetry. In contrast, Dai et al. (1994) did not observe a corresponding dip near the axis for mixture fraction fluctuations, within self-preserving buoyant turbulent plumes, which they attribute to buoyancy/turbulence interactions because such dips are observed in nonbuoyant turbulent jets (Becker et al., 1967). Another unusual effect of buoyancy is that streamwise turbulence intensities near

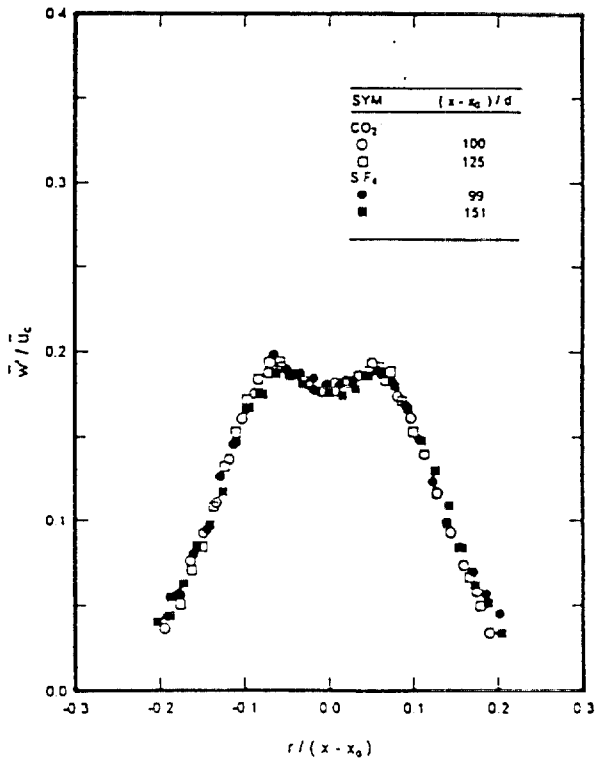


Fig. 5 Radial profiles of tangential velocity fluctuations in self-preserving buoyant turbulent plumes

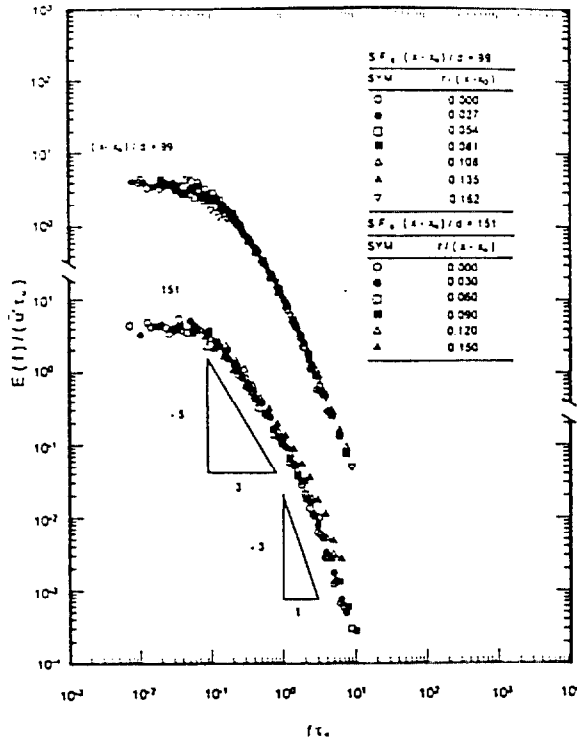


Fig. 6 Temporal power spectra of streamwise velocity fluctuations in the self-preserving portion of buoyant turbulent sulfur hexafluoride plumes

the axis of self-preserving plumes are slightly lower than for nonbuoyant jets, 0.22 in comparison to 0.25, see Papanicolaou and List (1988) for a discussion of existing turbulent jet data. Thus, buoyancy/turbulence interactions simultaneously act to reduce velocity fluctuation intensities, and to increase mixture fraction fluctuation intensities, near the axis of self-preserving turbulent plumes, in comparison to values found for nonbuoyant jets. Other properties of the velocity fluctuations in the self-preserving region of buoyant turbulent plumes are qualitatively similar to nonbuoyant turbulent jets (List, 1982). For example, $\bar{u}' \approx \bar{v}' \approx \bar{w}'$ throughout the self-preserving region, while the outer edge of the flow is nearly isotropic, e.g., $\bar{u}' \approx \bar{v}' \approx \bar{w}'$ for $r/(x-x_0) \geq 0.2$. In contrast, the flow exhibits greater anisotropy near the axis, e.g., $\bar{u}' \approx 1.25\bar{v}' \approx 1.25\bar{w}'$ for $r/(x-x_0) < 0.1$. Finally, the region of peak values of \bar{u}' , \bar{v}' and \bar{w}' is nearly the same, e.g., $r/(x-x_0)$ of roughly 0.05.

Some typical temporal power spectra of streamwise velocity fluctuations for the self-preserving region of the sulfur hexafluoride plumes are illustrated in Fig. 6. Results for the self-preserving region of the carbon dioxide plumes are similar. The spectra are relatively independent of radial position, when normalized in the manner of Fig. 6. The spectra initially decay according to the $-1/3$ power of frequency, analogous to the well-known inertial-convection region for scalar property and velocity fluctuations in nonbuoyant turbulence (Tennekes and Lumley, 1972). At higher frequencies, however, there is a prominent region where the spectra decay according to the -3 power of frequency, which has been observed before but only in buoyant turbulent flows (Dai et al., 1994; Mizushima et al., 1979; Papanicolaou and List, 1987, 1988). This region has been called the inertial-diffusive subrange, where the variation of the local rate of dissipation of velocity fluctuations in buoyant flows is due to buoyancy-generated inertial forces rather than viscous forces. This effect is plausible due to the progressive increase in the span of the inertial range

as $(x-x_0)/d$, or the plume Reynolds number, increases. For example, the intersections of the $-1/3$ and -3 subranges occur at higher values of $n\tau_w$, and $(x-x_0)/d$ increases; similar behavior has been observed for mixture fraction fluctuations in the self-preserving region of buoyant turbulent plumes (Dai et al., 1994). At higher frequencies, power spectral densities should become small as the Kolmogorov scale is approached. However, present measurements could not resolve this region due to seeding limitations, which introduced effects of step noise.

The measured values of the temporal integral scales are illustrated in Fig. 7 for the self-preserving region of the two plumes. Additionally, streamwise spatial integral scales have been found from the temporal integral scale data using Taylor's hypothesis, e.g., $\Lambda_{xx} = \bar{u}'\tau_w$, and are plotted in Fig. 7 as well. Self-preserving normalization has been used for both integral scales, similar to past treatment of integral scales relevant to mixture fraction fluctuations (Dai et al., 1994). Both integral scales approximate universal behavior for self-preserving conditions when plotted in the manner of Fig. 7. The spatial integral scale for streamwise velocity, Λ_{xx} , exhibits a slight reduction near the axis, which is not observed for spatial integral scales associated with mixture fraction fluctuations. The increase of τ_w near the edge of the flow is similar to the behavior of τ_T observed by Dai et al. (1994); this increase is caused by smaller mean velocities near the edge of the flow, combined with relatively uniform spatial integral scales, through Taylor's hypothesis.

Reynolds Stress. Present measurements of Reynolds stress for the self-preserving region of the two plumes are illustrated in Fig. 8. The measurements are seen to exhibit universal behavior throughout the self-preserving region, with $u'v' = 0$ at $r = 0$, and then increasing to a maximum value near $r/(x-x_0) = 0.05$ (in the absolute sense), before decreasing to zero once again at large r . Notably, the region of the maximum Reynolds stress in Fig. 8 roughly corresponds to the region of maximum velocity fluctuations in Figs. 3-5.

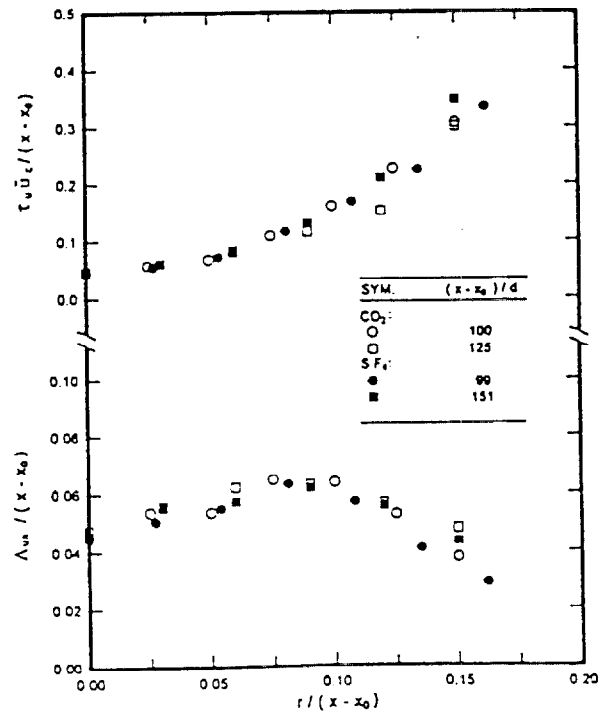


Fig. 7 Temporal and spatial integral scales of streamwise velocity fluctuations in self-preserving buoyant turbulent plumes

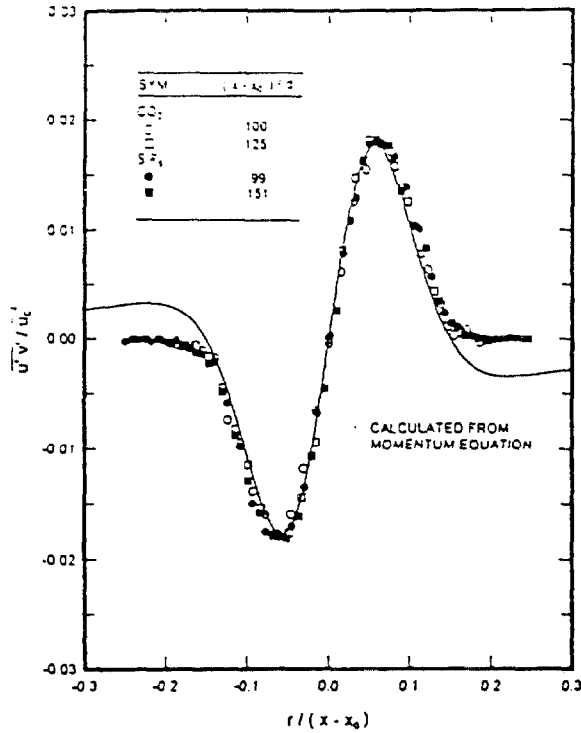


Fig. 8 Radial profiles of Reynolds stress in self-preserving buoyant turbulent plumes

The consistency of measured values of Reynolds stress with other measurements of mean and fluctuating quantities was evaluated, similar to the conservation of mass considerations for \bar{u} , discussed earlier. Imposing the approximations of a thin, boundary-layer-like plume flow, self-preserving conditions so that density variations are small, and neglecting viscous stresses in comparison to turbulent stresses, there results:

$$\bar{u} \partial \bar{u} / \partial x - \bar{v} \partial \bar{u} / \partial r = \partial / \partial x (\bar{v}'^2 - \bar{u}'^2) + g(1 - \rho_s / \rho_0) \bar{r} - \partial / \partial r (r \overline{u'v'}) / r \quad (21)$$

Then, integrating Eq. (21), assuming $(\bar{u}'^2 - \bar{v}'^2) / \bar{u}^2 \ll 1$, and using the present correlations for \bar{u} and \bar{v} and the correlation for \bar{r} from Dai et al. (1994), all for the self-preserving portion of the flow, yields the following expression for Reynolds stresses:

$$\overline{u'v'} / \bar{u}^2 = (F(0) / (2\eta k_j^2 U(0)^2)) (1 - \exp(-k_j^2 \eta^2)) + (\eta - 1 / (3\eta k_j^2)) \exp(-2k_j^2 \eta^2) - 1 / (3k_j^2 \eta^2) - \bar{u} \bar{v} / \bar{u}^2 \quad (22)$$

Equation (22) also is plotted in Fig. 8. In general, this relationship is in good agreement with the measurements, implying reasonably good internal consistency of the present data. The main discrepancies between Eq. (22) and present measurements of Reynolds stresses are observed near the edge of the flow. This difficulty is mainly thought to be due to errors in the fits of mean velocities and mixture fractions by Gaussian functions near the edge of the flow.

Conclusions

Velocity statistics were measured in round buoyant turbulent plumes in still and unstratified air, in order to supplement earlier measurements of mixture fraction statistics for these flows due to Dai et al. (1994). The test conditions involved buoyant jet

sources of carbon dioxide and sulfur hexafluoride to give ρ_s / ρ_0 of 1.51 and 5.06 and source Froude numbers of 7.80 and 3.75, respectively, with $(x - x_0) / d$ in the range 87–151 and $(x - x_0) / l_0$ in the range 12–43. The major conclusions of the study are as follows:

1 Present measurements yielded distributions of mean streamwise velocities in self-preserving plumes that were up to 40 percent narrower, with larger mean streamwise velocities near the axis (when appropriately scaled), and smaller entrainment rates, than earlier results in the literature. The reason for these differences is that the earlier measurements were limited to $(x - x_0) / d \leq 62$, which is not a sufficient distance from the source to observe self-preserving behavior. Notably, these observations confirm the earlier results of Dai et al. (1994) concerning the requirements for self-preserving buoyant turbulent plume behavior, based on measurements of mixture fraction statistics.

2 Radial profiles of velocity fluctuations in self-preserving buoyant turbulent plumes and nonbuoyant turbulent jets are similar: the streamwise component exhibits a dip near the axis with intensities at the axis of roughly 22 percent for buoyant turbulent plumes, and there is a tendency toward isotropic behavior near the edge of the flow. This behavior is in sharp contrast to mixture fraction statistics where mixture fraction fluctuations within buoyant turbulent plumes do not exhibit a dip near the axis, unlike nonbuoyant turbulent jets. Effects of buoyancy/turbulence interactions causing this contrasting behavior for velocity and mixture fraction statistics clearly merit further study.

3 The temporal power spectra of streamwise velocity and mixture fraction fluctuations are qualitatively similar: The low-frequency portions scale in a robust manner even in the transitional plume region, there is an inertial region where the spectra decay according to the $-3/2$ power of frequency, and there is an inertial-diffusive region at higher frequencies where the spectra decay according to the -3 power of frequency. The inertial-diffusive region has been observed by others for buoyant flows but is not observed in nonbuoyant flows; thus, the inertial-diffusive region is an interesting buoyancy/turbulence interaction that merits further study.

4 Past evaluations of turbulence models for buoyant turbulent flows, based on the assumption of self-preserving behavior for earlier measurements within buoyant turbulent plumes, should be reconsidered. In particular, present measurements suggest that such evaluations were compromised by effects of flow development because past measurements generally involved transitional plumes.

Acknowledgments

This research was supported by the United States Department of Commerce, National Institute of Standards and Technology, Grant No. 60NANBID1175, with H. R. Baum of the Building and Fire Research Laboratory serving as Scientific Officer.

References

Abraham, G., 1960, "Jet Diffusion in Liquid of Greater Density," *ASCE J. Hydr. Div.*, Vol. 86, pp. 1–13.
 Becker, H. A., Hotel, H. C., and Williams, G. C., 1967, "The Nozzle-Fluid Concentration Field of the Round, Turbulent, Free Jet," *J. Fluid Mech.*, Vol. 30, pp. 285–303.
 Chen, C. J., and Rodi, W., 1980, *Vertical Turbulent Buoyant Jets: A Review of Experimental Data*, Pergamon Press, Oxford, p. 16.
 Dai, Z., Tseng, L.-K., and Faeth, G. M., 1994, "Structure of Round, Fully Developed, Buoyant Turbulent Plumes," *ASME JOURNAL OF HEAT TRANSFER*, Vol. 116, pp. 409–417.
 George, W. K., Jr., Alpert, R. L., and Tamanini, F., 1977, "Turbulence Measurements in an Axisymmetric Buoyant Plume," *Int. J. Heat Mass Trans.*, Vol. 20, pp. 1145–1154.
 Hinze, J. O., 1975, *Turbulence*, 2nd ed., McGraw-Hill, New York, pp. 175–319.
 Katsivos, N. E., 1985, "Temperature Measurements in a Turbulent Round Plume," *Int. J. Heat Mass Trans.*, Vol. 28, pp. 771–777.
 Katsivos, N. E., and List, E. J., 1977, "Turbulent Buoyant Jets Part I: Integral Properties," *J. Fluid Mech.*, Vol. 81, pp. 25–44.

- Kounalakis, M. E., Sivachandran, Y. R., and Faeth, G. M., 1991, "Infrared Radiation Statistics of Nonluminous Turbulent Diffusion Flames," *ASME JOURNAL OF HEAT TRANSFER*, Vol. 113, pp. 437-445.
- Lau, M.-C., and Faeth, G. M., 1987, "A Combined Laser-Doppler Anemometer/Laser-Induced Fluorescence System for Turbulent Transport Measurements," *ASME JOURNAL OF HEAT TRANSFER*, Vol. 109, pp. 254-256.
- List, E. J., 1982, "Turbulent Jets and Plumes," *Ann. Rev. Fluid Mech.*, Vol. 14, pp. 189-212.
- Mizushima, T., Ogino, F., Veda, H., and Komori, S., 1979, "Application of Laser-Doppler Velocimetry to Turbulence Measurements in Non-isothermal Flow," *Proc. Roy. Soc. London*, Vol. A366, pp. 63-79.
- Morton, B. R., Taylor, G. I., and Turner, J. S., 1956, "Turbulent Gravitational Convection From Maintained and Instantaneous Sources," *Proc. Roy. Soc. London*, Vol. A234, pp. 1-23.
- Morton, B. R., 1959, "Forced Plumes," *J. Fluid Mech.*, Vol. 5, pp. 151-163.
- Nakagome, H., and Hirata, M., 1977, "The Structure of Turbulent Diffusion in an Axisymmetrical Thermal Plume," *Heat Transfer and Turbulent Buoyant Convection*, D. B. Spalding and N. Afgan, eds., McGraw-Hill, New York, pp. 367-372.
- Ogino, F., Takeuchi, H., Kudoh, I., and Mizushima, T., 1980, "Heated Jet Discharged Vertically in Ambients of Uniform and Linear Temperature Profiles," *Int. J. Heat Mass Trans.*, Vol. 23, pp. 1581-1588.
- Papanicolaou, P. N., and List, E. J., 1987, "Statistical and Spectral Properties of Tracer Concentration in Round Buoyant Jets," *Int. J. Heat Mass Trans.*, Vol. 30, pp. 2059-2071.
- Papanicolaou, P. N., and List, E. J., 1988, "Investigation of Round Vertical Turbulent Buoyant Jets," *J. Fluid Mech.*, Vol. 195, pp. 341-391.
- Papanicolaou, D., and List, E. J., 1989, "Large Scale Structure in the Far Field of Buoyant Jets," *J. Fluid Mech.*, Vol. 209, pp. 151-190.
- Peterson, J., and Bayazitoglu, Y., 1992, "Measurements of Velocity and Turbulence in Vertical Axisymmetric Isothermal and Buoyant Plumes," *ASME JOURNAL OF HEAT TRANSFER*, Vol. 114, pp. 135-142.
- Rouse, H., Yih, C. S., and Humphreys, H. W., 1952, "Gravitational Convection From a Boundary Source," *Tellus*, Vol. 4, pp. 201-210.
- Seban, R. A., and Behnia, M. M., 1976, "Turbulent Buoyant Jets in Unstratified Surroundings," *Int. J. Heat Mass Trans.*, Vol. 19, pp. 1197-1204.
- Shabbir, A., and George, W. K., 1992, "Experiments on a Round Turbulent Buoyant Plume," NASA Technical Memorandum 105955.
- Tennekes, H., and Lumley, J. L., 1972, *A First Course in Turbulence*, MIT Press, Cambridge, MA.
- Zimin, V. D., and Fnk, P. G., 1977, "Averaged Temperature Fields in Axisymmetrical Turbulent Streams Over Localized Heat Sources," *Izv. Akad. Nauk. SSSR, Mekhanika Zhidkosti Gazu*, Vol. 2, pp. 199-203.



The American Society of
Mechanical Engineers

ASME AT YOUR FINGERTIPS

At ASME Information Central, you are our top priority. We make every effort to answer your questions and expedite your orders. Our representatives are always ready to assist you with most any ASME product or service. And now, reaching us is easier than ever. . .

TELEPHONE

Toll Free in US & Canada
800-THE-ASME
(800-843-2763)

Toll Free in Mexico
95-800-843-2763

Universal
201-882-1167

FAX

201-882-1717
or 201-882-5155

E-MAIL

infocentral@asme.org

MAIL

ASME
22 Law Drive
P.O. Box 2900
Fairfield, New Jersey
07007-2900

Appendix C: Dai et al. (1995b)

Velocity/Mixture Fraction Statistics of Round, Self-Preserving, Buoyant Turbulent Plumes

Z. Dai

Graduate Student Research Assistant.

L. K. Tseng¹

Research Fellow.

G. M. Faeth

Professor,
Fellow ASME

Department of Aerospace Engineering,
The University of Michigan,
Ann Arbor, MI 48109-2118

An experimental study of the structure of round buoyant turbulent plumes was carried out, limited to conditions in the self-preserving portion of the flow. Plume conditions were simulated using dense gas sources (carbon dioxide and sulfur hexafluoride) in a still and unstratified air environment. Velocity/mixture-fraction statistics, and other higher-order turbulence quantities, were measured using laser velocimetry and laser-induced fluorescence. Similar to earlier observations of these plumes, self-preserving behavior of all properties was observed for the present test range, which involved streamwise distances of 87-151 source diameters and 12-43 Morton length scales from the source. Streamwise turbulent fluxes of mass and momentum exhibited countergradient diffusion near the edge of the flow, although the much more significant radial fluxes of these properties satisfied gradient diffusion in the normal manner. The turbulent Prandtl/Schmidt number, the ratio of time scales characterizing velocity and mixture fraction fluctuations and the coefficient of the radial gradient diffusion approximation for Reynolds stress, all exhibited significant variations across the flow rather than remaining constant as prescribed by simple turbulence models. Fourth moments of velocity and velocity/mixture fraction fluctuations generally satisfied the quasi-Gaussian approximation. Consideration of budgets of turbulence quantities provided information about kinetic energy and scalar variance dissipation rates, and also indicated that the source of large mixture fraction fluctuations near the axis of these flows involves interactions between large streamwise turbulent mass fluxes and the rapid decay of mean mixture fractions in the streamwise direction.

Introduction

The structure of round buoyant turbulent plumes in still and unstratified environments is a classical problem that has attracted significant attention in order to gain a better understanding of buoyancy/turbulence interactions; see Chen and Rodi (1980), Kotsovinos (1985), List (1982), Papanicolaou and List (1987, 1988) and references cited therein for summaries of past turbulent plume studies. In general, most investigations of this flow have emphasized the fully developed region where effects of the source have been lost and flow properties become self-preserving, in order to simplify both theoretical considerations and the interpretation of measurements (Morton, 1959; Morton et al., 1956; Rouse et al., 1952; Tennekes and Lumley, 1972). Motivated by these observations, measurements of mean and fluctuating velocities and scalar properties in self-preserving round buoyant turbulent plumes were recently completed in this laboratory (Dai et al., 1994, 1995). The objectives of the present investigation were to extend these measurements to consider additional turbulence properties within round self-preserving buoyant turbulent plumes—emphasizing combined velocity/mixture fraction statistics, higher-order correlations, budgets of turbulence properties and conservation checks, which should be helpful for developing and evaluating models of buoyant turbulent flows.

Buoyant jets were used as the source of the present round buoyant turbulent plumes, similar to most past studies of this

flow. Then, all scalar properties are conveniently represented as functions of the mixture fraction (which corresponds to the mass fraction of source material in a sample) called state relationships (Dai et al., 1994, 1995). Additionally, reaching self-preserving conditions for buoyant jet sources requires streamwise distances that are large in comparison to both the source diameter, d , as a measure of conditions where source disturbances have been lost, and the Morton length scale, l_M , as a measure of conditions where the buoyant features of the flow are dominant (Morton, 1959; List, 1982; Papanicolaou and List, 1988). When these requirements are satisfied, $f \ll 1$ so that the state relationship giving the density as a function of mixture fraction can be linearized as follows (Dai et al., 1994, 1995):

$$\rho = \rho_m + f\rho_s(1 - \rho_m/\rho_s), \quad f \ll 1 \quad (1)$$

Noting that the buoyancy flux of the plume, B_0 , is conserved, mean streamwise velocities and mixture fractions can be scaled as follows for self-preserving conditions (Dai et al., 1995; List, 1982):

$$\bar{u}((x - x_0)/B_0)^{1/3} = U(\eta) \quad (2)$$

$$f\alpha B_0^{-2/3}(x - x_0)^{2/3}|d(\ln \rho)/df|_{f=0} = F(\eta) \quad (3)$$

where from Eq. (1)

$$|d(\ln \rho)/df|_{f=0} = |\rho_s - \rho_m|/\rho_s \quad (4)$$

The functions $U(\eta)$ and $F(\eta)$ generally are approximated by Gaussian fits, as follows (Rouse et al., 1952; Papanicolaou and List, 1988; Mizushima et al., 1979; Ogino et al., 1980; Shabbir and George, 1992; George et al., 1977):

¹ Current address: School of Mechanical Engineering, Purdue University, West Lafayette, IN.

Contributed by the Heat Transfer Division for publication in the JOURNAL OF HEAT TRANSFER. Manuscript received by the Heat Transfer Division December 1994; revision received July 1995. Keywords: Natural Convection, Plumes, Turbulence. Associate Technical Editor: Y. Jaluria.

$$U(\eta) = U(0) \exp(-(k_u \eta)^2),$$

$$F(\eta) = F(0) \exp(-(k_f \eta)^2) \quad (5)$$

where

$$k_u = (x - x_0)/l_u, \quad k_f = (x - x_0)/l_f \quad (6)$$

and l_u and l_f are characteristic plume radii where $\bar{u}/\bar{u}_c = \bar{f}/\bar{f}_c = \exp(-1)$, respectively.

Following the classical experimental study of round buoyant turbulent plumes of Rouse et al. (1952), where source properties and thus estimates of $(x - x_0)/d$ and $(x - x_0)/l_M$ are difficult to define, attempts generally have been made to carry out measurements at increasing distances from the source in order to approach self-preserving conditions more closely; see Abraham (1960), Seban and Behnia (1976), Nagagome and Hirata (1977), Zimin and Frik (1977), Mizushima et al. (1979), Ogino et al. (1980), Shabbir and George (1992), Peterson and Bayazitoglu (1992), Papanicolaou and List (1987, 1988), Papantoniou and List (1989), and Dai et al. (1994, 1995). Except for the measurements of Papantoniou and List (1989) and Dai et al. (1994, 1995), to be discussed subsequently, however, these measurements were limited to $(x - x_0)/d \leq 62$, which seems rather small to achieve self-preserving behavior compared to nonbuoyant jets where recent work suggests that $(x - x_0)/d \geq 70$ is required to reach self-preserving behavior for both mean and fluctuating properties; see Panchapakesan and Lumley (1993a, b). Thus, not surprisingly, recent measurements of round buoyant turbulent plumes from Papantoniou and List (1989) and Dai et al. (1994, 1995) found that self-preserving behavior of mean and fluctuating velocities and mixture fractions only was achieved when $(x - x_0)/d$ and $(x - x_0)/l_M$ were greater than roughly 90 and 12, respectively. These results also showed that self-preserving round buoyant turbulent plumes were narrower, with larger values of mean velocities and both mean and fluctuating mixture fractions near the axis (when appropriately scaled), than earlier reported measurements of self-preserving properties made closer to the source. For example, values of characteristic plume radii were reduced up to 40 percent, and corresponding values of $U(0)$ and $F(0)$ were increased up to 40 percent, over the range of the experiments mentioned earlier (Dai et al., 1994, 1995). It seems likely that self-preserving behavior for other properties is only achieved at comparable conditions.

In view of the previous discussion, additional measurements within the self-preserving region of round buoyant turbulent plumes clearly are needed in order to supplement the results available from Papantoniou and List (1989) and Dai et al. (1994, 1995). Thus, the present objectives were to carry out a study along these lines, involving new measurements of velocity/mixture function statistics and other higher-order turbulence quantities, using the experimental conditions of Dai et al. (1994, 1995). These results were also exploited to complete conservation checks of the experiments of Dai et al. (1994, 1995), to compute budgets of turbulence quantities, and to begin assessment of contemporary models of buoyant turbulent flows. The test conditions of Dai et al. (1994, 1995) were considered, which involved round source flows of carbon dioxide and sulfur hexafluoride in still air at room temperature and atmospheric pressure. Thus, these conditions yield downward-flowing round buoyant turbulent plumes in still and unstratified environments, while providing a straightforward specification of plume buoyancy fluxes. Instrumentation involved laser velocimetry (LV) to measure velocities and laser-induced iodine fluorescence (LIF) to measure mixture fractions, similar to Dai et al. (1994, 1995).

Experimental Methods

Test Apparatus. Descriptions of the experimental apparatus, instrumentation, and test conditions will be brief; see Dai et al. (1994, 1995) for more details. The test plumes were observed in a screened enclosure that could be traversed to accommodate rigidly mounted instrumentation, which was mounted within an outer enclosure. The outer enclosure had plastic side walls with a screen across the top for air inflow in order to compensate for the removal of air entrained by the plume. The plume flow was removed through ducts located at the lower corners of the outer enclosure using a bypass/damper system to match plume entrainment rates. Effects of coflow and confinement on flow properties were evaluated and found to be negligible. All components that might contact iodine vapor were plastic, painted, or sealed in plastic wrap, in order to prevent corrosion.

The plume sources consisted of long rigid round plastic tubes that could be traversed in the vertical direction to accommodate measurements at various streamwise distances from the source. Gas flows to the sources were controlled and measured using

Nomenclature

a = acceleration of gravity	l_f, l_u = characteristic plume radii based on \bar{f} and \bar{u} , Eq. (6)	ν = molecular kinematic viscosity
B_0 = source buoyancy flux	l_M = Morton length scale = $M_0^{3/4}/B_0^{1/2}$	ν_t = effective turbulence kinematic viscosity
C_{r2} = turbulence modeling constant, Eq. (20)	M_0 = source-specific momentum flux	ρ = density
C_μ = turbulence modeling constant, Eq. (21)	P, P_k = mechanical production of k and g , Eqs. (15) and (19)	σ_T = effective turbulence Prandtl/Schmidt number
d = source diameter	r = radial distance	ϕ = generic variable
D, D_k = turbulent diffusion of k and g , Eqs. (13) and (18)	Re_0 = source Reynolds number = $u_0 d / \nu_0$	Subscripts
f = mixture fraction	T = pressure diffusion of k , Eq. (14)	c = centerline value
$F(\eta)$ = scaled radial distribution of \bar{f} , Eqs. (3) and (5)	u = streamwise velocity	o = initial value or virtual origin location
Fr_0 = source Froude number = $(4/\pi)^{1/4} l_M / d$	$U(\eta)$ = scaled radial distribution of \bar{u} , Eqs. (2) and (5)	∞ = ambient value
g = variance of mixture fraction fluctuations = \bar{f}'^2	v = radial velocity	Superscripts
G = buoyant production of k , Eq. (16)	w = tangential velocity	$(\bar{\quad})$ = time-averaged mean value
k = turbulence kinetic energy	x = streamwise distance	$(\overline{\quad})'$ = root-mean-squared fluctuating value
k_f, k_u = plume width coefficients based on \bar{f} and \bar{u} , Eq. (6)	ϵ, ϵ_k = rate of dissipation of k and g	
	η = dimensionless radial distance = $r/(x - x_0)$	

pressure regulators in conjunction with critical flow orifices. The source flows were seeded with iodine vapor for LIF measurements. The ambient air was seeded with oil drops (roughly 1 μm nominal diameter) for LV measurements using several multiple jet seeders that discharged above the screened top of the outer enclosure. Maximum mixture fractions in the self-preserving region were less than 6 percent; therefore, effects of concentration bias, because only the ambient air was seeded, were negligible.

Instrumentation. The combined LV/LIF measuring system was similar to the arrangement described by Lai and Faeth (1987). A dual-beam, frequency-shifted LV was used for velocity measurements. The arrangement was based on the 514.5 nm line of an argon-ion laser, and had a horizontal optical axis and a measuring volume diameter and length of 400 and 260 μm , respectively. Different orientations of the plane of the laser beams, the direction of the optical axis, and the direction of horizontal traverse of the plumes were used to resolve various correlations of velocity and mixture fraction fluctuations, as described by Lai and Faeth (1987). The detector output was processed using a burst-counter signal processor. The low-pass-filtered analog output of the signal processor was sampled at equal time intervals in order to avoid problems of velocity bias, while directional bias and ambiguity were controlled by frequency shifting. The processor output was sampled at rates more than twice the break frequency of the low-pass-filter in order to control alias signals. Seeding levels were controlled so that effects of step noise contributed less than 3 percent to determinations of velocity fluctuations (Dai et al., 1995). Experimental uncertainties (95 percent confidence) are estimated to be less than 5, 10, 15, and 20 percent, for first, second, third, and fourth-order moments of particular components of velocity fluctuations, respectively; uncertainties of corresponding moments involving several components of velocity fluctuations are generally larger, up to twice as large. These uncertainties were maintained up to $r/(x - x_o) = 0.15$ but increased at larger radial distances, roughly inversely proportional to \bar{u} .

The LIF signal was produced by the fluorescence of iodine in the 514.5 nm laser beams used for LV. The detector was positioned at right angles to the optical axis to yield a measuring volume diameter and length of 260 and 1000 μm , respectively. The LIF signal was separated from the light scattered at the laser line using a long-pass optical filter with a cut-off wavelength of 530 nm. The detector output was amplified and low-pass filtered to control alias signals using a sixth-order Chebychev filter having a break frequency of 500 Hz. The absorption and LIF signals were calibrated based on measurements across the source exit by mixing the source flow with air to simulate various mixture fractions. These calibrations showed that iodine seeding level fluctuations were less than 1 percent, that the LIF signal varied linearly with laser power and iodine concentration, and that reabsorption of scattered light was negligible. Differential diffusion effects between the source gas (carbon dioxide or sulfur hexafluoride) and iodine also are negligible, as discussed by Dai et al. (1994). Analysis of experimental uncertainties indicated values less than 5, 10, 15, and 20 percent for first, second, third, and fourth-order moments of mixture-fraction fluctuations, respectively. These uncertainties were maintained up to $r/(x - x_o) = 0.15$ but increased at larger radial distances, roughly inversely proportional to \bar{f} . As before, uncertainties of moments involving several components of velocity and mixture-fraction fluctuations are larger, up to 50 percent larger.

Test Conditions. The test conditions for the carbon dioxide and sulfur hexafluoride plumes are summarized in detail by Dai et al. (1994, 1995). Major parameters for the carbon dioxide and sulfur hexafluoride sources, respectively, are as follows: $d = 9.7$ and 6.4 mm, $\rho_o/\rho_\infty = 1.51$ and 5.06 , $\text{Re}_o = 2000$ and 4600 , $\text{Fr}_o = 7.80$ and 3.75 , and $l_w/d = 7.34$ and 3.53 . The virtual origins of the two flows were found by extrapolating

measurements of mean velocities and mixture fractions along the axis of the self-preserving region according to Eqs. (2) and (3); see Dai et al. (1994) for a plot of this extrapolation for mean mixture fractions; the resulting virtual origins of the two flows were relatively small, i.e., $x_o/d \leq 12.7$. Finally, measurements within the self-preserving regions of these plumes yielded flow width parameters, as follows: $k_u^2 = 93$, $k_f^2 = 125$, $l_w/(x - x_o) = 0.10$, and $l_f/(x - x_o) = 0.09$.

The present measurements and those of Dai et al. (1994, 1995) were used to complete conservation checks along the lines of Shabbir and Taulbee (1990). The results showed that the present measurements satisfied the governing equations within experimental uncertainties. In addition, buoyancy fluxes were conserved within 5 percent and the balance between the plume momentum and buoyancy terms in the integrated form of the governing equation for conservation of momentum was satisfied within an average of 18 percent, which is compatible with the experimental uncertainties of these properties.

Results and Discussion

Results will be presented by considering second, third, and fourth moments of fluctuating quantities, in turn, before concluding with a discussion of budgets of turbulence quantities. It should be noted at the outset that all properties measured during the present investigation exhibited self-preserving behavior over the test range, e.g., $87 \leq (x - x_o)/d \leq 151$ and $12 \leq (x - x_o)/l_w \leq 43$, which agrees with the earlier observations of Dai et al. (1994, 1995).

Second Moments. Mean quantities (e.g., \bar{f} , \bar{u} , and \bar{v}), some second moments of fluctuating quantities (e.g., $\overline{f'^2}$, $\overline{u'^2}$, $\overline{v'^2}$, $\overline{w'^2}$, and $\overline{u'v'}$) and associated quantities (e.g., probability density functions, spatial correlations, temporal power spectra, and temporal and spatial integral scales) can be found in Dai et al. (1994, 1995). Other similar parameters at this level (e.g., $\overline{w'v'}$, $\overline{w'u'}$, and $\overline{w'u'}$) are formally zero. Thus, the present measurements of second moments concentrated on combined mixture fraction/velocity correlations (e.g., the turbulent mass fluxes, $\overline{f'u'}$, $\overline{f'v'}$, and $\overline{f'w'}$, and the turbulent Prandtl/Schmidt number).

The present measurements of the turbulent mass fluxes, $\overline{f'u'}$, $\overline{f'v'}$, and $\overline{f'w'}$, are illustrated in Fig. 1. The tangential turbulent mass flux $\overline{f'w'}$ = 0, for an axisymmetric flow, which was adequately represented by present measurements. The radial turbulent mass flux, $\overline{f'v'}$, is the most important turbulent mass diffusion parameter in the present boundary-layer-like flow. Similar to $\overline{u'v'}$ discussed by Dai et al. (1995), $\overline{f'v'}$ = 0 at $r = 0$ due to symmetry, and then increases to a maximum near $r/(x - x_o) = 0.06$ (in the absolute sense) before decreasing to zero once again at large r . Finally, $\overline{f'u'}$ exhibits rather large values in the present flows, somewhat analogous to $\overline{u'^2}$ and $\overline{f'^2}$ discussed by Dai et al. (1994, 1995). In fact, the correlation coefficient $(\overline{f'u'}/(\overline{f'u'}))_c = 0.7$, which is unusually large. This behavior is caused by the intrinsic instability of plumes, where large values of f provide a corresponding potential to generate large values of u through effects of buoyancy (George et al., 1977). Another aspect of the large values of $\overline{f'u'}$ is that the turbulent mass flux contribution to the total buoyancy flux of the plume is appreciable (roughly 15 percent) and must be considered in conservation checks.

The consistency of present measured values of $\overline{f'v'}$ was evaluated similar to earlier considerations of \overline{v} and $\overline{u'v'}$ by Dai et al. (1995). Imposing the approximations of a boundary-layer-like flow, self-preserving conditions so that density variations are small, and neglecting molecular mass diffusion in comparison to turbulent mass diffusion, the governing equation for mean mixture fraction becomes:

$$\bar{u}\partial\bar{f}/\partial x + \bar{v}\partial\bar{f}/\partial r = -\partial/\partial x(\overline{f'u'}) - \partial/\partial r(\overline{r f'v'})/r \quad (7)$$

Then, integrating Eq. (7), both ignoring and considering the

streamwise turbulent mass flux, $\overline{f'u'}$, and using correlations of $\overline{u'v'}$ and \overline{f} in the self-preserving portion of the flow from Dai et al. (1994, 1995), yields the two predictions of $\overline{f'v'}$ illustrated in Fig. 1. Including $\overline{f'u'}$ in the integration does not have a large effect on predictions of $\overline{f'v'}$ because even though $\overline{f'u'}$ is large near the axis, $\overline{f'v'}$ is small in this region due to the requirements of symmetry. Thus, both predictions are in good agreement with the present measurements of $\overline{f'v'}$, which helps to confirm the internal consistency of the measurements.

The gradient diffusion approximation is commonly made for simplified models of turbulent mixing, which implies the following relationships for the radial and streamwise turbulent mass fluxes:

$$\overline{f'v'} = -(\nu_T/\sigma_T)\partial\overline{f}/\partial r, \quad \overline{f'u'} = -(\nu_T/\sigma_T)\partial\overline{f}/\partial x \quad (8)$$

This approach is generally acceptable for the radial direction, based on present measurements of $\overline{f'v'}$ illustrated in Fig. 1 and the correlation for \overline{f} given by Eqs. (3) and (5). Unfortunately, the approach yields estimates of countergradient diffusion in the streamwise direction, e.g., $\overline{f'u'} > 0$ from Fig. 1 but $\partial\overline{f}/\partial x \geq 0$ when $r/(x-x_0) \geq (\frac{1}{2})^{1/2}/k_r = 0.082$, which implies an unphysical negative value of ν_T near the edge of the flow as well as a clear absence of the isotropy of ν_T implied by Eq. (8). Analogous considerations for turbulent stresses, based on the measurements of Dai et al. (1995), again yield acceptable behavior for the radial direction; however, countergradient diffusion is encountered for the streamwise direction when $r/(x-x_0) \geq (\frac{1}{2})^{1/2}/k_r = 0.042$. Naturally, these countergradient diffusion effects in the streamwise direction are not very important for boundary layer flows like the present plumes, where streamwise turbulent transport is ignored in any event; nevertheless, this deficiency raises concerns about the use of simple gradient diffusion hypotheses for more complex buoyant turbulent flows of interest in practice.

Simple gradient diffusion hypotheses, with constant turbulent Prandtl/Schmidt numbers, are even problematical for transport

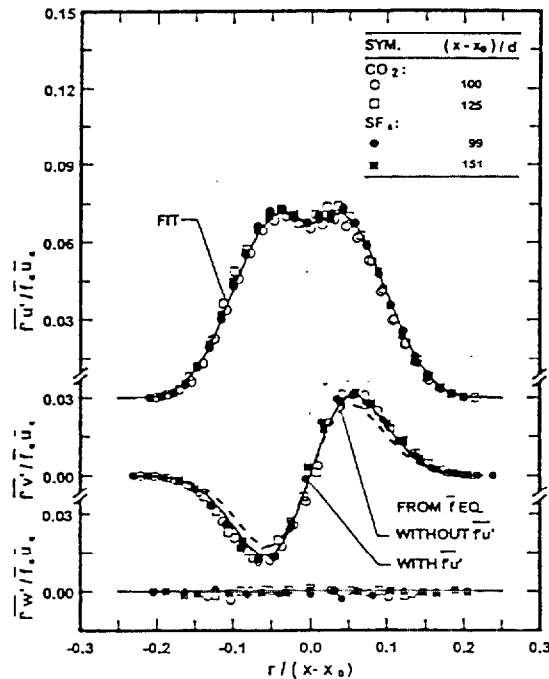


Fig. 1 Radial distributions of turbulent mass fluxes within round self-preserving buoyant turbulent plumes

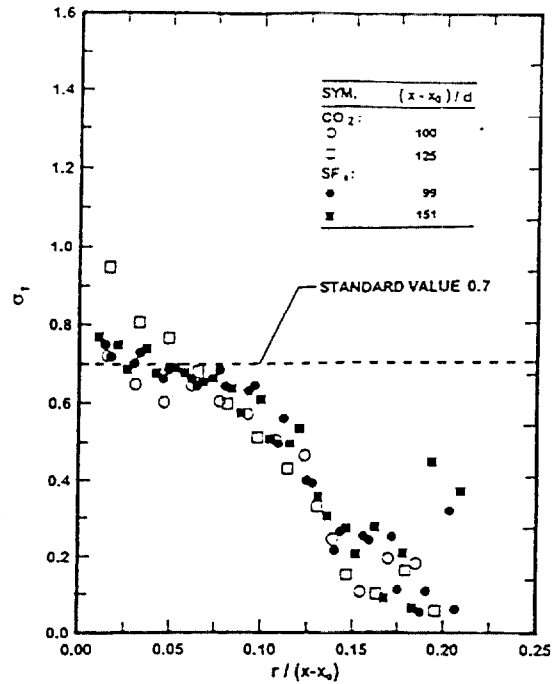


Fig. 2 Radial distribution of turbulent Prandtl/Schmidt numbers within round self-preserving buoyant turbulent plumes

in the radial direction within self-preserving buoyant turbulent plumes. For example, introducing the gradient diffusion hypothesis for the Reynolds stress, as follows:

$$\overline{u'v'} = -\nu_T \partial \overline{u} / \partial r \quad (9)$$

and eliminating ν_T between Eq. (9) and the expression for $\overline{f'v'}$ in Eq. (8), yields the following expression for the turbulent Prandtl/Schmidt number:

$$\sigma_T = (\overline{u'v'} / \overline{f'v'}) (\partial \overline{f} / \partial r) / (\partial \overline{u} / \partial r) \quad (10)$$

The available measurements of $\overline{u'v'}$, $\overline{f'v'}$, \overline{f} , and \overline{u} from Dai et al. (1994, 1995) and the present study were used to find σ_T as a function of the radial position in the self-preserving region of the flow as illustrated in Fig. 2. The measurements exhibit significant scatter, which is unavoidable because finding σ_T involves four measurements including two determinations of gradients. Keeping this limitation in mind, the results indicate crude self-preserving behavior for σ_T , with σ_T near 0.8 at $r = 0$ and then decreasing progressively with increasing radial distance toward $\sigma_T \approx 0.1$ near the edge of the flow (except for a few outlying points at the flow edge where present experimental uncertainties are large). Clearly, this behavior departs significantly from assumptions of $\sigma_T = 0.7$ or 0.9 across the width of the flow that are made in simple turbulence models; see Lockwood and Naguib (1975), Lumley (1978), Shabbir and Taulbee (1990), Taulbee (1992), and references cited therein. Thus, the difficulty with σ_T also suggests that higher-order turbulent closures are needed to treat flow development effects reliably in buoyant turbulent flows.

Third Moments. Gradients of third moments of velocity fluctuations determine the turbulent diffusion of turbulence kinetic energy and turbulent stresses, and are important for estimating the turbulence kinetic energy budget and developing higher-order models of turbulence (Malin and Younis, 1990; Panchapakesan and Lumley, 1993a, b; Shih et al., 1987). For the present flows, several of these correlations are zero due to

axial symmetry, e.g., $\overline{w'u'^2} = \overline{w'v'^2} = \overline{w'^3} = 0$; of these, the last was observed and was found to be properly equal to zero as a check of the measurements.

Measurements of all other third moments of velocity fluctuations— $\overline{u'^3}$, $\overline{v'^3}$, $\overline{u'v'^2}$, $\overline{u'v'u'^2}$, $\overline{v'w'^2}$, and $\overline{u'w'^2}$ —were completed and are illustrated in Fig. 3, after normalizing in a manner appropriate for round self-preserving buoyant turbulent plumes. As noted earlier, these correlations are self-preserving within experimental uncertainties, and have been approximated by local least-squares fits in preparation for the calculation of budgets to be discussed later. Panchapakesan and Lumley (1993a) report recent measurements of these moments, and discuss earlier measurements as well, for round nonbuoyant turbulent jets; they find maximum values of $\overline{u'^3}$ and $\overline{v'^3}$ at $\sim r/(x-x_0) \approx 0.1$ with a maximum value of $\overline{v'^3}/\overline{u'^2}$ are somewhat larger for nonbuoyant than buoyant turbulent flows, 0.0055 compared to 0.0040; this behavior corresponds to the somewhat larger second moments of velocity fluctuations for nonbuoyant than for buoyant flows observed by Dai et al. (1995). The other moments illustrated in Fig. 3 are qualitatively similar to the results measured by Panchapakesan and Lumley (1993a) for round nonbuoyant turbulent jets.

Gradients of third moments of combined velocity/mixture fraction fluctuations determine the turbulent diffusion of scalar variance and scalar fluxes, and hence are important for estimating the scalar variance budget and developing higher-order models of turbulence. Terms of this type also appear at lower order when the governing equations are formulated using mass-weighted (Favre) averages, as advocated by Bilger (1976) for flame environments. Several of these correlations are zero due to axial symmetry, e.g., $\overline{f'u'w'} = \overline{f'v'w'} = 0$; of these, the last was measured and found to be properly equal to zero as a check of the present measurements.

Measurements of the nonzero third moments of velocity/mixture fraction fluctuations— $\overline{f'u'^2}$, $\overline{f'v'^2}$, $\overline{f'w'^2}$, $\overline{f'u'v'}$, $\overline{f'^2u'}$, and $\overline{f'^2v'}$ —are illustrated in Fig. 4, after normalization

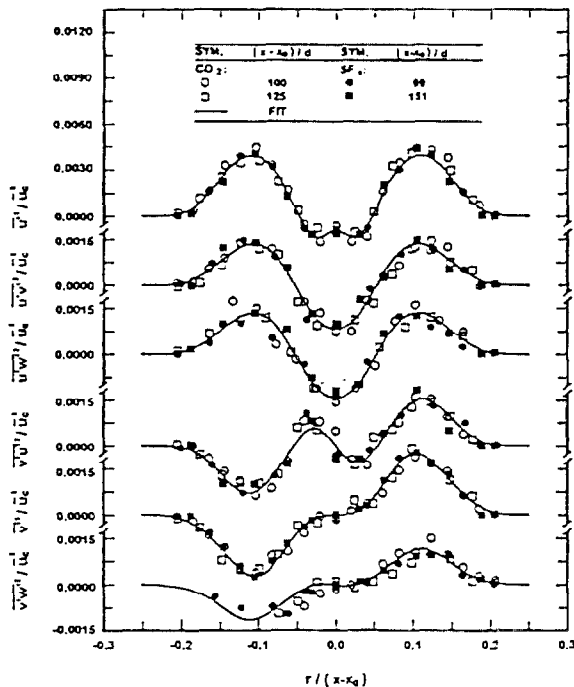


Fig. 3 Radial distribution of triple moments of velocity fluctuations within round self-preserving buoyant turbulent plumes

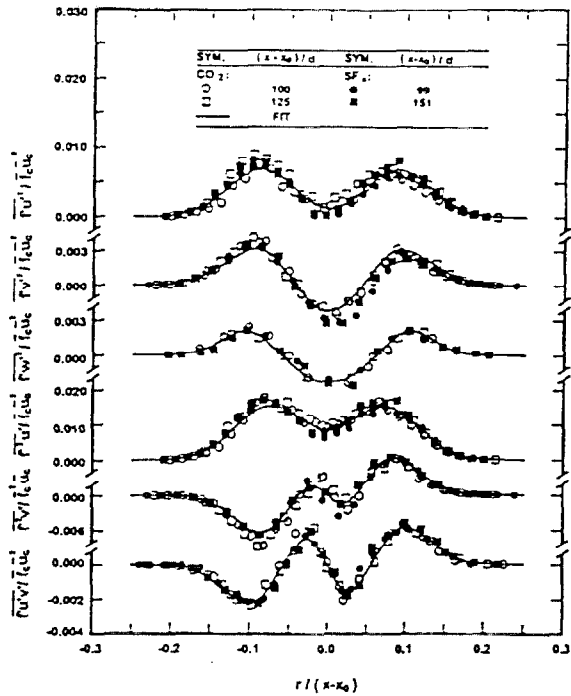


Fig. 4 Radial distribution of triple moments of velocity-mixture fraction fluctuations within round self-preserving buoyant turbulent plumes

in a manner appropriate for round self-preserving buoyant turbulent plumes. Similar to other correlations, these results exhibit self-preserving behavior and least-squares fits have been found for them for later use in computing budgets. Other measurements of these properties are rare; therefore, about all that can be said is that there are qualitative similarities between present measurements and those of Panchapakesan and Lumley (1993b) for a transitional buoyant plume.

Fourth Moments. The fourth moments of velocity and velocity/mixture fraction fluctuations are needed to find appropriate expressions for the diffusion terms of triple-moment models. One approach for modeling fourth moments is to use the quasi-Gaussian approximation where fourth moments are approximated by products of second moments, as follows (Panchapakesan and Lumley, 1993a):

$$\overline{\phi'_i \phi'_j \phi'_m \phi'_n} = \overline{(\phi'_i \phi'_j)} \overline{(\phi'_m \phi'_n)} + \overline{(\phi'_j \phi'_m)} \overline{(\phi'_i \phi'_n)} + \overline{(\phi'_i \phi'_m)} \overline{(\phi'_j \phi'_n)} \quad (11)$$

where ϕ'_i , etc., are generic vector or scalar fluctuating quantities. This approximation is exact if each of the fluctuating variables satisfies a Gaussian probability density function (PDF), e.g., $\overline{u'^4} = 3(\overline{u'^2})^2$, etc., implies a kurtosis of 3, which is correct for a Gaussian PDF of u' . In the present instance, velocity fluctuations mainly satisfy Gaussian PDFs, but modifications due to intermittency must be anticipated near the edge of the flow. In addition, the mixture fraction exhibits additional effects of intermittency because it has a finite range, $0 \leq f \leq 1$, and cannot fundamentally satisfy a Gaussian PDF, although past work suggests that a clipped-Gaussian PDF is a reasonably good approximation for its behavior (Dai et al., 1994). Thus, effects of intermittency, which penetrate clear to the axis for self-preserving round buoyant turbulent plumes (Dai et al., 1994) are an issue for present flows; therefore, efforts were made to evalu-

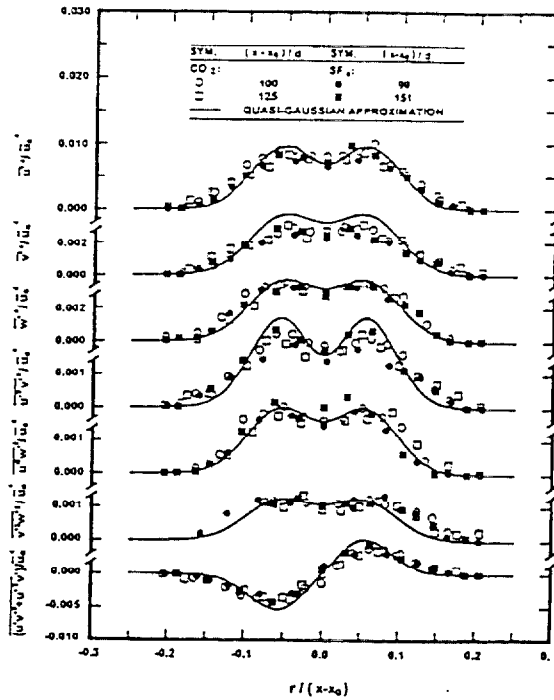


Fig. 5 Radial distribution of fourth moments of velocity fluctuations within round self-preserving buoyant turbulent plumes

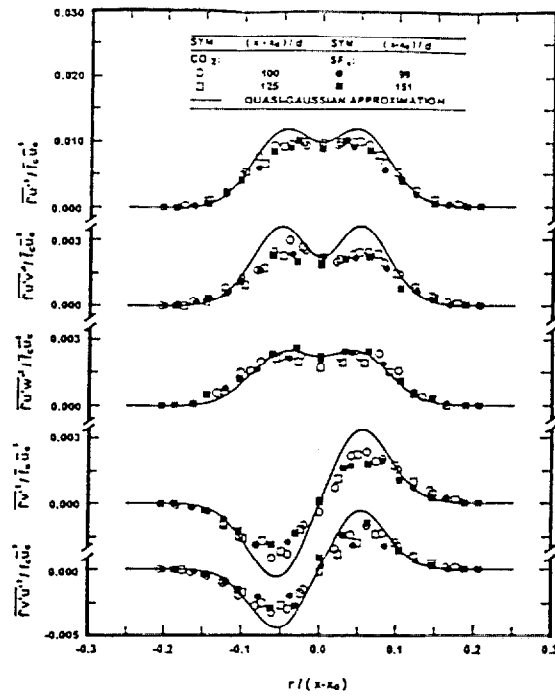


Fig. 6 Radial distribution of fourth moments of velocity-mixture fraction fluctuations involving first moments of mixture fraction fluctuations within round self-preserving buoyant turbulent plumes

ate the effectiveness of the Gaussian approximation for estimating the fourth moments of fluctuating quantities.

The fourth moments of velocity fluctuations considered during the present investigation, along with corresponding quasi-Gaussian approximations using the measurements of Dai et al. (1995) for second moments of velocity fluctuations, are illustrated in Fig. 5. Correlations considered include $\overline{u'^4}$, $\overline{v'^4}$, $\overline{w'^4}$, $\overline{u'^2v'^2}$, $\overline{u'^2w'^2}$, $\overline{v'^2w'^2}$, and the sum $(\overline{u'^2v'^2} + \overline{u'^2w'^2})$, which could not be separated using the present test and LV configuration. Typical of other properties, these correlations exhibit self-preserving behavior within experimental uncertainties. Similar to the observations of Panchapakesan and Lumley (1993a) for round nonbuoyant turbulent jets, the quasi-Gaussian approximation is reasonable even though present flows exhibit significant intermittency for $r/(x - x_0) > 0.1$. Corresponding to the somewhat lower second moments of velocity fluctuations seen for buoyant turbulent plumes in comparison to nonbuoyant turbulent jets, correlations like $\overline{u'^2w'^2}$ have somewhat lower maximum values in the present buoyant turbulent plumes than in the nonbuoyant turbulent jets observed by Panchapakesan and Lumley (1993a).

The fourth moments of combined velocity/mixture fraction fluctuations considered during the present investigation, along with corresponding quasi-Gaussian approximations using both present measurements and those of Dai et al. (1994, 1995) for second moments, are illustrated in Figs. 6 and 7. Correlations considered include the first moments of f' in Fig. 6 (e.g., $\overline{f'u'^3}$, $\overline{f'u'v'^2}$, $\overline{f'u'w'^2}$, $\overline{f'v'^3}$, and $\overline{f'v'u'^2}$), and the higher moments of f' in Fig. 7 (e.g., $\overline{f'^2u'^2}$, $\overline{f'v'^2}$, $\overline{f'w'^2}$, $\overline{f'^3u'}$, $\overline{f'v'}$, and $\overline{f'w'}$). These correlations also exhibit self-preserving behavior and are in reasonably good agreement with the quasi-Gaussian approximation, within experimental uncertainties, in spite of anticipated effects of intermittency for $r/(x - x_0) > 0.1$. Finally, several fourth-order moments that should be zero due to symmetry, e.g., $\overline{f'w'^3}$, $\overline{f'u'^2w'}$, $\overline{f'^2u'w'}$, and $\overline{f'^3w'}$ were measured, and were all properly

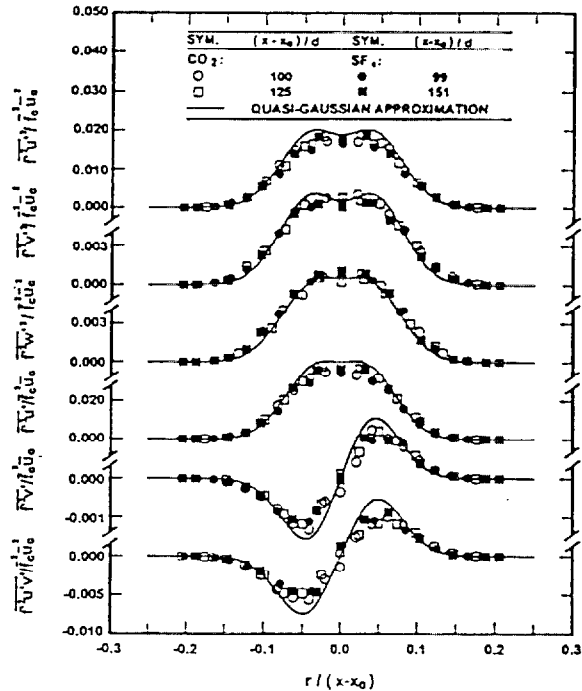


Fig. 7 Radial distribution of fourth moments of velocity and higher-order moments of mixture-fraction fluctuations within round self-preserving buoyant turbulent plumes

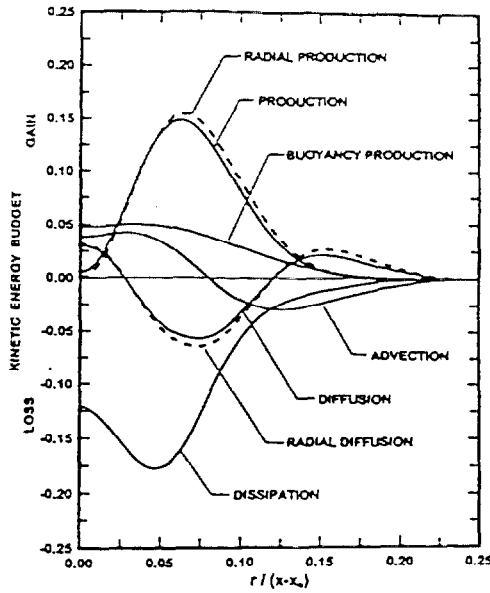


Fig. 8 Turbulence kinetic energy budget within round self-preserving buoyant turbulent plumes

found to be equal to zero within experimental uncertainties as a check of the measurements.

Budgets. Budgets of turbulence kinetic energy and scalar variance were considered in order to provide estimates of the rates of dissipation, which were not measured directly during the experiments, and to highlight the mechanisms of turbulent mixing in buoyant turbulent flows. Properties needed to compute budgets were found from Dai et al. (1994, 1995) and the present study. The procedure involved using the general expressions of Eqs. (2)–(6) for \bar{u} and \bar{f} , along with the local least-squares fits illustrated on the plots of other properties.

The governing equations for the turbulence kinetic energy, $k = (\bar{u}'^2 + \bar{v}'^2 + \bar{w}'^2)/2$, and the scalar variance, $g = \bar{f}'^2$, were found at the high Reynolds number limits appropriate for present experimental conditions where direct effects of molecular diffusion can be ignored. In order to simplify the following discussion, it was assumed that $\bar{v}'^2 = \bar{w}'^2$, which is a good approximation for the present flows based on the measurements of Dai et al. (1995). Under these approximations, the governing equation for turbulence kinetic energy can be written as follows (Panchapakesan and Lumley, 1993b):

$$\bar{u}\partial k/\partial x + \bar{v}\partial k/\partial r = D + T + P + G - \epsilon \quad (12)$$

where

$$D = -\partial/\partial x(\bar{u}'k) - \partial/\partial r(\bar{r}'k)/r \quad (13)$$

$$T = -\partial/\partial x(\bar{p}'u') - \partial/\partial r(\bar{r}'p'v')/r \quad (14)$$

$$P = -(\bar{u}'^2 - \bar{v}'^2)\partial\bar{u}/\partial x - \bar{u}'v'(\partial\bar{u}/\partial r + \partial\bar{u}/\partial x) \quad (15)$$

$$G = (1 - \rho_w/\rho_o)\bar{a}'\bar{f}'u' \quad (16)$$

The terms on the left-hand side (LHS) of Eq. (12) represent advection while the terms on the right-hand side (RHS) represent turbulent diffusion (diffusion), pressure diffusion, mechanical production (production), buoyancy production, and dissipation, respectively.

The present determinations of the terms in the equation of conservation of turbulence kinetic energy for the self-preserving region are plotted in Fig. 8. Each term in the plots has been made dimensionless by multiplying it by $(x - x_0)/\bar{u}_c^3$, which

is consistent with self-preserving scaling. In this case, the radial production, the total production (production), the buoyancy production, the advection, the total diffusion (diffusion), and the radial diffusion terms have been found directly from the measurements. In contrast, the sum of dissipation plus pressure diffusion (which is labeled dissipation in the figure) has been found from the budget as a balance. In the following, the pressure diffusion effect will be ignored and the sum will be treated as dissipation alone, similar to other treatments of turbulent flows having nearly constant density (Panchapakesan and Lumley, 1993a, b; Shih et al., 1987). The radial and total production terms, and the radial and total diffusion terms, are nearly the same as expected for a boundary layer flow. Near the axis, advection, radial diffusion, and buoyancy production are all roughly the same, and their sum is balanced by dissipation. The profiles of production, diffusion, and dissipation are qualitatively similar to the results reported by Panchapakesan and Lumley (1993a) for nonbuoyant turbulent jets; however, advection near the axis is much smaller for plumes than for jets (by a factor of 2–3), which is compensated by contributions from buoyancy production and diffusion for the plumes.

Under the same approximations as the k equation, the governing equations for the scalar variance can be written as follows (Panchapakesan and Lumley, 1993b):

$$\bar{u}\partial g/\partial x + \bar{v}\partial g/\partial r = D_s + P_s - 2\epsilon_s \quad (17)$$

where

$$D_s = -\partial/\partial x(\bar{u}'g) - \partial/\partial r(\bar{r}'g)/r \quad (18)$$

$$P_s = -2\bar{f}'u'\partial\bar{f}/\partial x - 2\bar{f}'v'\partial\bar{f}/\partial r \quad (19)$$

The term on the LHS of Eq. (17) is the advection while the terms on the RHS are the turbulent diffusion (diffusion), mechanical production (production), and dissipation, respectively.

The present determinations of the terms in the equation for scalar variance for the self-preserving region are plotted in Fig. 9. Each term in the plots has been made dimensionless by multiplying it by $(x - x_0)/(\bar{f}'^2\bar{u}_c)$, which is consistent with self-preserving scaling. In this case, the advection, the total production (production), the radial production, the total diffu-

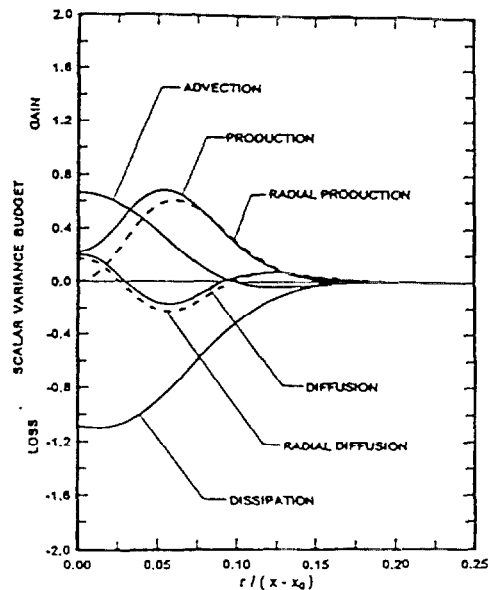


Fig. 9 Mixture fraction fluctuation budget within round self-preserving buoyant turbulent plumes

Table 1 Summary of turbulence model parameters for round self-preserving buoyant turbulent plumes

$r/(x-x_0)$	0.00	0.05	0.10	0.15	0.20
$C_{\epsilon 2}$	2.56	1.96	3.70	4.55	4.17
C_{μ}^b	0.10	0.11	0.043	0.031	0.040

^aRatio of characteristic velocity to mixture-fraction time scales, $C_{\epsilon 2} = \epsilon_f k/(\epsilon g)$.

^bTurbulence modeling constant, $C_{\mu} = \epsilon u^2 \overline{v'v'}/(k^2 \partial \bar{u}/\partial r)$.

sion (diffusion), and the radial diffusion have been found directly from the measurements. In contrast, the dissipation has been found from the budget as a balance. Radial and total diffusion are nearly the same, which is typical of a boundary-layer flow. In contrast, streamwise and radial production are only comparable near the edge of the flow, while streamwise production dominates near the axis, as discussed earlier, due to the large streamwise gradient of \bar{f} and large values of $\overline{f'u'}$ in this region. It is likely that this large level of streamwise production near the axis is responsible for the large values of scalar variance in this region; see Dai et al. (1994). Near the axis, advection (with smaller contributions from production and diffusion) is balanced by dissipation. Near the edge of the flow, however, advection becomes small and radial production balances diffusion. These trends are similar to the observations of Panchapakesan and Lumley (1993b) for a transitional buoyant turbulent jet, except that the present flows have larger contributions to advection, balanced by increased dissipation, near the axis.

Present estimates of ϵ and ϵ_f from Figs. 8 and 9 are helpful for studying approximations used in turbulence models. Two parameters of interest that will be considered are the ratio of the characteristic velocity to mixture-fraction time scales, $C_{\epsilon 2}$, and the constant in the gradient diffusion approximation for the Reynolds stress, C_{μ} . These two properties can be evaluated, as follows:

$$C_{\epsilon 2} = \epsilon_f k/(\epsilon g) \quad (20)$$

and

$$C_{\mu} = -\overline{u'v'}/(k^2 \partial \bar{u}/\partial r) \quad (21)$$

Continuing the approximation that the pressure diffusion terms can be ignored when evaluating ϵ , the present measurements and those of Dai et al. (1994, 1995) provide all the properties on the RHS of Eqs. (20) and (21), which allows $C_{\epsilon 2}$ and C_{μ} to be evaluated. The resulting measured values of $C_{\epsilon 2}$ and C_{μ} are summarized as a function of $r/(x-x_0)$ in Table 1. Analogous to the turbulent Prandtl/Schmidt number illustrated in Fig. 2, the values of $C_{\epsilon 2}$ and C_{μ} vary considerably as $r/(x-x_0)$ varies, possibly due to intermittency, rather than remaining constant in accord with the approximations of simple turbulence models. Near the axis, however, $C_{\epsilon 2}$ is in the range 1.96–2.56, which is comparable to the value of this constant used in simple turbulence models where $C_{\epsilon 2}$ is in the range 1.87–1.92; see Lockwood and Naguib (1975). Similarly, values of C_{μ} near the axis are 0.10–0.11, which also is comparable to the widely used value, $C_{\mu} = 0.09$; see Lockwood and Naguib (1975). In any event, these deficiencies of $C_{\epsilon 2}$ and C_{μ} in simple turbulence models support the need for higher-order closures to treat effects of flow development reliably within buoyant turbulent flows.

Conclusions

Velocity/mixture fraction statistics and other higher-order turbulence quantities were measured within self-preserving of round buoyant turbulent plumes in still and unstratified air, in order to supplement earlier measurements of mixture fraction and velocity statistics for these flows due to Dai et al. (1994,

1995). Test conditions involved buoyant jet sources of carbon dioxide and sulfur hexafluoride to give ρ_0/ρ_∞ of 1.51 and 5.06 and source Froude numbers of 7.80 and 3.75, respectively, with $(x-x_0)/d$ in the range 87–151 and $(x-x_0)/l_w$ in the range 12–43. The major conclusions of the study are as follows:

1 All moments observed during the present investigation, which extended up to fourth moments of combined velocity/mixture fraction fluctuations, exhibited self-preserving behavior within experimental uncertainties over the test range, similar to the earlier observations of Dai et al. (1994, 1995).

2 Streamwise turbulent fluxes of mass and momentum exhibited countergradient diffusion for $r/(x-x_0) \geq 0.082$ and 0.042, respectively, although the much more significant radial fluxes of these properties satisfied gradient diffusion in the normal manner for the present boundary layer flows. Nevertheless, even though the countergradient diffusion deficiency is not very important for self-preserving round turbulent plumes, the present observations raise concerns about the use of simple gradient diffusion hypotheses for more complex buoyant turbulent flows of interest in practice.

3 The turbulent Prandtl/Schmidt number, the ratio of characteristic velocity to mixture fraction time scales and the coefficient of the radial gradient diffusion approximation for Reynolds stress, all exhibited significant variations across the flow rather than remaining constant as prescribed by simple turbulence models. These variations tend to parallel the variation of intermittency so that the presence of nonturbulent fluid may be responsible for the behavior. These variations of flow properties also suggest that higher-order model closures are needed to treat effects of flow development reliably within buoyant turbulent flows.

4 Fourth moments of velocity and velocity/mixture fraction fluctuations generally satisfied the quasi-Gaussian approximation across the flow width. This behavior also has been observed by Panchapakesan and Lumley (1993a, b) for nonbuoyant and buoyant jets, but it still was surprising in view of potential effects of intermittency and the departure of the PDF of mixture fraction from Gaussian behavior near the edge of the flow.

5 Streamwise turbulent mass fluxes are quite large near the axis in buoyant turbulent plumes, where the corresponding correlation coefficients are roughly 0.7. This behavior, combined with the rapid decay of mean mixture fraction in the streamwise direction, is a strong source of production of scalar fluctuations, which probably is responsible for the large values of mixture fraction fluctuation intensities, roughly 0.45, observed near the axis of round self-preserving buoyant turbulent plumes.

Acknowledgments

This research was supported by the United States Department of Commerce, National Institute of Standards and Technology, Grant Nos. 60NANB1D1175 and 60NANB4D1696, with H. R. Baum and K. C. Smyth of the Building and Fire Research Laboratories serving as Scientific Officers.

References

- Abraham, G., 1960, "Jet Diffusion in Liquid of Greater Density," *ASCE J. Hyd. Div.*, Vol. 86, pp. 1–13.
- Bilger, R. W., 1976, "Turbulent Jet Diffusion Flames," *Prog. Energy Combust. Sci.*, Vol. 1, pp. 87–109.
- Chen, C. J., and Rodi, W., 1980, *Vertical Turbulent Buoyant Jets: A Review of Experimental Data*, Pergamon Press, Oxford, United Kingdom, p. 16.
- Dai, Z., Tseng, L.-K., and Faeth, G. M., 1994, "Structure of Round, Fully Developed, Buoyant Turbulent Plumes," *ASME JOURNAL OF HEAT TRANSFER*, Vol. 116, pp. 409–417.
- Dai, Z., Tseng, L.-K., and Faeth, G. M., 1995, "Velocity Statistics of Round, Fully Developed Buoyant Turbulent Plumes," *ASME JOURNAL OF HEAT TRANSFER*, Vol. 117, pp. 138–145.
- George, W. K., Jr., Alpert, R. L., and Tamanini, F., 1977, "Turbulence Measurements in an Axisymmetric Buoyant Plume," *Int. J. Heat Mass Trans.*, Vol. 20, pp. 1145–1154.

- Kotsovinos, N. E., 1985, "Temperature Measurements in a Turbulent Round Plume," *Int. J. Heat Mass Trans.*, Vol. 28, pp. 771-777.
- Lai, M.-C., and Faeth, G. M., 1987, "A Combined Laser-Doppler Anemometer/Laser-Induced Fluorescence System for Turbulent Transport Measurements," *ASME JOURNAL OF HEAT TRANSFER*, Vol. 109, pp. 254-256.
- List, E. J., 1982, "Turbulent Jets and Plumes," *Ann. Rev. Fluid Mech.*, Vol. 14, pp. 189-212.
- Lockwood, F. C., and Naguib, A. S., 1975, "The Prediction of Fluctuations in the Properties of Free, Round-Jet Turbulent Diffusion Flames," *Combust. Flame*, Vol. 24, pp. 109-124.
- Lumley, J. L., 1978, "Computational Modeling of Turbulent Flows," *Adv. Appl. Mech.*, Vol. 18, pp. 123-176.
- Malin, M. R., and Younis, B. A., 1990, "Calculation of Turbulent Buoyant Plumes With a Reynolds Stress and Heat Flux Transport Closure," *Int. J. Heat Mass Trans.*, Vol. 33, pp. 2247-2264.
- Mizushima, T., Ogino, F., Veda, H., and Komori, S., 1979, "Application of Laser-Doppler Velocimetry to Turbulence Measurements in Non-isothermal Flow," *Proc. Roy. Soc. London*, Vol. A366, pp. 63-79.
- Morton, B. R., Taylor, G. I., and Turner, J. S., 1956, "Turbulent Gravitational Convection From Maintained and Instantaneous Sources," *Proc. Roy. Soc. London*, Vol. A234, pp. 1-23.
- Morton, B. R., 1959, "Forced Plumes," *J. Fluid Mech.*, Vol. 5, pp. 151-163.
- Nakagome, H., and Hirata, M., 1977, "The Structure of Turbulent Diffusion in an Axi-Symmetrical Thermal Plume," *Heat Transfer and Turbulent Buoyant Convection*, D. B. Spalding and N. Afgan, eds., McGraw-Hill, New York, pp. 367-372.
- Ogino, F., Takeuchi, H., Kudo, I., and Mizushima, T., 1980, "Heated Jet Discharged Vertically in Ambients of Uniform and Linear Temperature Profiles," *Int. J. Heat Mass Trans.*, Vol. 23, pp. 1581-1583.
- Panchapakesan, N. R., and Lumley, J. L., 1993a, "Turbulence Measurements in Axisymmetric Jets of Air and Helium. Part 1. Air Jet," *J. Fluid Mech.*, Vol. 246, pp. 197-223.
- Panchapakesan, N. R., and Lumley, J. L., 1993b, "Turbulence Measurements in Axisymmetric Jets of Air and Helium. Part 2. Helium Jet," *J. Fluid Mech.*, Vol. 246, pp. 225-247.
- Papanicolaou, P. N., and List, E. J., 1987, "Statistical and Spectral Properties of Tracer Concentration in Round Buoyant Jets," *Int. J. Heat Mass Trans.*, Vol. 30, pp. 2059-2071.
- Papanicolaou, P. N., and List, E. J., 1988, "Investigation of Round Vertical Turbulent Buoyant Jets," *J. Fluid Mech.*, Vol. 195, pp. 341-391.
- Papantoniou, D., and List, E. J., 1989, "Large Scale Structure in the Far Field of Buoyant Jets," *J. Fluid Mech.*, Vol. 209, pp. 151-190.
- Peterson, J., and Bayazitoglu, Y., 1992, "Measurements of Velocity and Turbulence in Vertical Axisymmetric Isothermal and Buoyant Plumes," *ASME JOURNAL OF HEAT TRANSFER*, Vol. 114, pp. 135-142.
- Rouse, H., Yih, C. S., and Humphreys, H. W., 1952, "Gravitational Convection From a Boundary Source," *Tellus*, Vol. 4, pp. 201-210.
- Seban, R. A., and Behnia, M. M., 1976, "Turbulent Buoyant Jets in Unstratified Surroundings," *Int. J. Heat Mass Trans.*, Vol. 19, pp. 1197-1204.
- Shabbir, A., and Taulbee, D. B., 1990, "Evaluation of Turbulence Models for Predicting Buoyant Flows," *ASME JOURNAL OF HEAT TRANSFER*, Vol. 112, pp. 945-951.
- Shabbir, A., and George, W. K., 1992, "Experiments on a Round Turbulent Buoyant Plume," NASA Technical Memorandum 105955.
- Shih, T.-H., Lumley, J. L., and Janicka, J., 1987, "Second-Order Modeling of a Variable-Density Mixing Layer," *J. Fluid Mech.*, Vol. 180, pp. 93-116.
- Taulbee, D. B., 1992, "An Improved Algebraic Reynolds Stress Model and Corresponding Nonlinear Stress Model," *Phys. Fluids A*, Vol. 4, pp. 2555-2561.
- Tennekes, H., and Lumley, J. L., 1972, *A First Course in Turbulence*, MIT Press, Cambridge, MA.
- Zimin, V. D., and Frik, P. G., 1977, "Averaged Temperature Fields in Asymmetrical Turbulent Streams Over Localized Heat Sources," *Izv. Akad. Nauk SSSR, Mekhanika Zhidkosti Gaza*, Vol. 2, pp. 199-203.

Appendix D: Dai and Faeth (1996)

- Chung, B. T. F., and Zhang, B. X., 1991a, "Minimum Mass Longitudinal Fins With Radiation Interaction at the Base," *Journal of the Franklin Institute*, Vol. 323, pp. 143-161.
- Chung, B. T. F., and Zhang, B. X., 1991b, "Optimization of Radiating Fin Array Including Mutual Irradiations Between Radiator Elements," *ASME JOURNAL OF HEAT TRANSFER*, Vol. 113, pp. 314-322.
- Delves, L. M., and Mohamed, J. L., 1985, *Computational Methods for Integral Equations*, Cambridge University Press, Cambridge, United Kingdom.
- Gill, P. E., Murray, W., and Wright, M. H., 1981, *Practical Optimization*, Academic Press, Inc., London.
- Ozizik, M. N., 1973, *Radiative Transfer and Interactions With Conduction and Convection*, Wiley, New York.
- Schnurr, N. M., Shapiro, A. B., and Townsend, M. A., 1976, "Optimization of Radiating Fin Arrays With Respect to Weight," *ASME JOURNAL OF HEAT TRANSFER*, Vol. 98, pp. 643-648.
- Sparrow, E. M., Eckert, E. R. G., and Irvine, T. F., Jr., 1961, "The Effectiveness of Radiating Fins With Mutual Irradiation," *Journal of the Aerospace Sciences*, Vol. 28, pp. 763-772.
- Sparrow, E. M., and Eckert, E. R. G., 1962, "Radiant Interaction Between Fin and Base Surfaces," *ASME JOURNAL OF HEAT TRANSFER*, Vol. 84, pp. 12-13.
- Sparrow, E. M., and Cess, R. D., 1978, *Radiation Heat Transfer*, Augmented Edition, Hemisphere, Washington, DC.

Measurements of the Structure of Self-Preserving Round Buoyant Turbulent Plumes

Z. Dai¹ and G. M. Faeth¹

Nomenclature

- a = acceleration of gravity
 B_o = source buoyancy flux
 d = source diameter
 f = mixture fraction
 $F(r/(x-x_o))$ = scaled radial distribution of \bar{f} , Eq. (1)
 Fr_o = source Froude number = $(4/\pi)^{1/4} l_w/d$
 k_f, k_u = plume width coefficients based on \bar{f} and \bar{u}
 l_w = Morton length scale = $M_o^{3/4}/B_o^{1/2}$
 M_o = source specific momentum flux
 r = radial distance
 u = streamwise velocity
 $U(r/(x-x_o))$ = scaled radial distribution of \bar{u} , Eq. (2)
 x = streamwise distance
 ρ = density

Subscripts

- c = centerline value
 o = initial value or virtual origin location
 ∞ = ambient value

Superscripts

- $(\bar{\quad})$ = time-averaged mean value
 $(\overline{\quad})$ = root-mean-squared fluctuating value

Introduction

Round buoyant turbulent plumes in still and unstratified environments are classical flows that are important for evaluating concepts and models of buoyancy/turbulence interactions. Fully

developed buoyant turbulent plumes are of greatest interest because they have lost extraneous source disturbances and their structure is self-preserving, which simplifies both theory and the interpretation of measurements (Morton, 1959). These observations have prompted many studies of self-preserving buoyant turbulent plumes; see, for example, Dai et al. (1994, 1995a, b), Papanicolaou and List (1988), Papanitiou and List (1989), Shabbir and George (1992), and references cited therein. In contrast to most earlier studies, which were carried out nearer to the source, however, the recent measurements of Dai et al. (1994, 1995a, b) showed that self-preserving round buoyant turbulent plumes were narrower, and had larger mean mixture fractions and streamwise velocities near the axis, than previously thought. The objective of the present investigation was to extend earlier evaluations of these measurements, emphasizing potential problems due to flow confinement, to help insure that an artifact of the experiments was not responsible for these somewhat startling findings.

Consistent with most studies of round buoyant turbulent plumes, self-preserving plume properties will be defined for conditions where buoyant jets are used as plume sources and all scalar properties can be represented conveniently as functions of the mixture fraction. Reaching self-preserving conditions for buoyant jet sources requires that $(x-x_o)/d$ and $(x-x_o)/l_w \gg 1$, to insure that effects of both source disturbances and source momentum have been lost (Morton, 1959; List, 1982); then, self-preserving behavior implies that $f \ll 1$, that the buoyancy flux is conserved, and that \bar{f} and \bar{u} scale as follows:

$$\bar{f} A B_o^{-2/3} (x-x_o)^{2/3} |d(\ln \rho)/df|_{f=0} = F(r/(x-x_o)) \quad (1)$$

$$\bar{u} ((x-x_o)/B_o)^{1/3} = U(r/(x-x_o)) \quad (2)$$

where $F(r/(x-x_o))$ and $U(r/(x-x_o))$ are universal functions that generally are approximated by Gaussian fits; in addition, various other flow statistics can be represented as universal functions of $r/(x-x_o)$ after normalizing mixture fraction and velocity properties by \bar{f}_c and \bar{u}_c , respectively (Dai et al., 1994, 1995a, b).

The controversy concerning the properties of self-preserving round buoyant turbulent plumes involves both the conditions needed to observe them and their structure. In particular, most earlier measurements to establish the self-preserving structure of round buoyant turbulent plumes were limited to $(x-x_o)/d \leq 62$, which seems small for self-preserving behavior. For example, Panchapakesan and Lumley (1993) only observed self-preserving behavior for round nonbuoyant turbulent jets when $(x-x_o)/d \geq 70$, which is consistent with the observations of Dai et al. (1994, 1995a, b), that self-preserving behavior for round buoyant turbulent plumes required $(x-x_o)/d \geq 87$ and $(x-x_o)/l_w \geq 12$. In addition, Dai et al. (1994, 1995a) found that characteristic flow widths were up to 40 percent smaller, and $F(0)$ and $U(0)$ were up to 30 percent larger, than earlier results in the literature. Notably, this behavior is consistent with the development of plume structure toward self-preserving conditions for buoyant jet sources, where normalized flow widths progressively decrease, and $F(0)$ and $U(0)$ progressively increase, with increasing streamwise distance until the flow becomes self-preserving (Dai et al., 1994). Finally, the self-preserving plume properties of \bar{f} observed by Dai et al. (1994) were in good agreement with measurements of Papanitiou and List (1989), which were carried out at comparable distances from the source.

Dai et al. (1994, 1995a, b) completed several typical checks of their measurements, including evaluating the measurements using the governing equations for mean quantities, establishing that the measurements satisfied conservation of buoyancy fluxes, and showing that the measurements were relatively independent of the rate of removal of plume gases from the test enclosure. Nevertheless, observing narrower self-preserving plumes than numerous earlier studies raises new concerns about

¹Department of Aerospace Engineering, The University of Michigan, Ann Arbor, MI.

Contributed by the Heat Transfer Division of THE AMERICAN SOCIETY OF MECHANICAL ENGINEERS. Manuscript received by the Heat Transfer Division August 1995; revision received February 1996. Keywords: Natural Convection, Plumes, Turbulence. Associate Technical Editor: Y. Jaluria.

effects of removal rates of exhaust gases from the test enclosure because this flow places the plumes in a coflow, which would tend to make them narrower than truly unconfined self-preserving round buoyant turbulent plumes (see Shabbir and George (1992) for a detailed discussion of this and other potential error sources for measurements of buoyant turbulent plumes). Thus, in order to resolve these concerns about the measurements of Dai et al. (1994, 1995a, b), the objective of the present investigation was to quantify the effects of plume exhaust rates on their reported self-preserving distributions of \bar{f} , \bar{u} , \bar{f}' , and \bar{u}' .

Experimental Methods

Test Apparatus. Experimental methods were identical to those of Dai et al. (1994, 1995a, b) and will only be described briefly. Present considerations were limited to downward-flowing plumes from a source flow of sulfur hexafluoride in still air at atmospheric pressure and temperature, and involved laser-induced iodine fluorescence (LIF) to measure mixture fractions and laser velocimetry (LV) to measure streamwise velocities. The plumes were observed in a 3000 × 3000 × 3400 mm high plastic enclosure within a large high-bay test area, which had a screen across the top for air inflow, to compensate for the removal of air entrained by the plume. The plume flow was removed by 300-mm-dia ducts mounted on the floor at the four corners of the outer enclosure, with the exhaust flow controlled by a bypass/damper system. Probe measurements showed that exhaust flows through the four exhaust duct inlets were essentially the same, and provided measurements of exhaust flow rates (95 percent confidence) within 10 percent. The test plume was within a smaller enclosure (1100 × 1100 × 3200 mm high) with plastic screen walls; however, this enclosure had no effect on flow properties, i.e., measurements with and without these screens present were identical. The plume sources were mounted on the inner enclosure, which could be traversed to accommodate rigidly mounted instrumentation. The plume sources consisted of rigid plastic tubes with flow straighteners at the inlet and length-to-diameter ratios of 50:1. The source flows were seeded with iodine vapor for LIF measurements, while the ambient air was seeded with oil drops for LV measurements. Maximum mean mixture fractions in the self-preserving region were less than 6 percent; therefore, effects of concentration bias of LV measurements, because only the ambient air was seeded, were negligible.

Instrumentation. The LIF signal was produced by the fluorescence of iodine at the 514.5 nm line of an argon-ion laser, separating the LIF emission from light scattered at the laser line using a long-pass optical filter. The detector output was amplified and low-pass filtered to control alias signals to provide roughly four decades of power spectral densities in the present flow. Calibration showed that iodine seeding levels varied less than 1 percent, that the LIF signal varied linearly with laser power and iodine concentration, that reabsorption of the LIF emission was negligible, and that differential diffusion effects between the source gases and iodine were negligible (Dai et al., 1994). Finally, experimental uncertainties (95 percent confidence) were less than 5 and 10 percent for \bar{f} and \bar{f}' up to $r/(x - x_0) = 0.15$ but increased roughly inversely proportional to \bar{f} at larger radial distances.

A dual-beam, frequency-shifted LV was used for velocity measurements, based on the 514.5 nm line of an argon-ion laser. The detector output was processed using a burst-counter signal processor with the low-pass-filtered analog output of the signal processor sampled at equal times to avoid problems of velocity bias, while directional bias and ambiguity were controlled by frequency shifting. The processor output was sampled at rates more than twice the break frequency of the low-pass filter to control alias signals. Effects of step noise contributed less than 3 percent to the determination of velocity fluctuations, while the

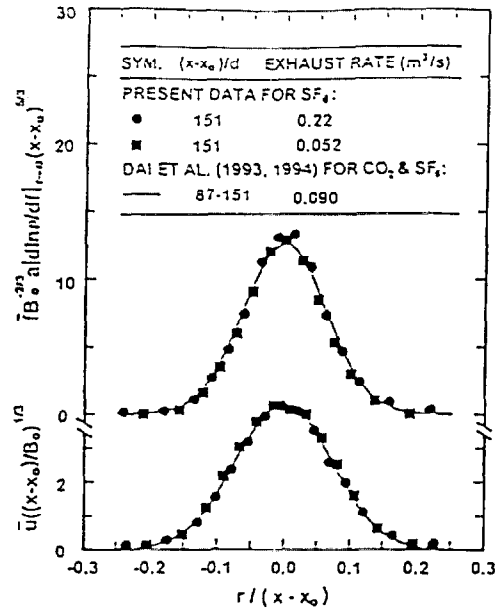


Fig. 1 Radial profiles of mean mixture fractions and streamwise velocities for self-preserving round buoyant turbulent plumes

measurements yielded roughly four decades of power spectral densities similar to the mixture fraction fluctuations (Dai et al., 1995a). Experimental uncertainties of \bar{u} and \bar{u}' were similar to \bar{f} and \bar{f}' .

Test Conditions. Major parameters of the present measurements of SF_6 plumes were as follows: $d = 6.4$ mm, $u_0 = 1890$ mm/s, $\rho_0/\rho_a = 5.06$, $Fr_0 = 3.75$, $l_0/d = 3.53$, and $x_0/d = 0.0$. The measuring station farthest from the source was at $(x - x_0)/d = 151$, while the edge of the plume is at roughly $r/(x - x_0) = 0.2$, which yields plume diameters and streamwise distances less than 360 and 900 mm. This implies that the maximum plume cross-sectional area is less than 1.2 percent of the enclosure cross-sectional area. Exhaust volume flow rates were roughly half, equal to, and twice the nominal flow rates used earlier, or 0.052, 0.090, and 0.22 m^3/s . Assuming uniform conditions over the cross section of the enclosure, these exhaust flows imply coflow velocities of roughly 6, 10, and 24 mm/s at the plane of the source exit, which are less than 1.3 percent of the source velocity.

Results and Discussion

Present measurements at the nominal exhaust flow rate agreed with Dai et al. (1994, 1995a, b) within experimental uncertainties; therefore, these results will be represented by their earlier correlations. Present measurements of \bar{f} and \bar{u} in the self-preserving region of buoyant turbulent plumes are plotted in Fig. 1 for the various flow rates according to the self-preserving scaling parameters of Eqs. (1) and (2). The present measurements were limited to $(x - x_0)/d = 151$ because this was the most critical condition with respect to potential coflow effects. The effect of varying plume exhaust rates, and thus coflow velocities, is seen to be negligible over the present range, with profiles of \bar{f} and \bar{u} for all coflow rates agreeing within experimental uncertainties. Thus, including the new measurements with the earlier results of Dai et al. (1994, 1995a, b) yields the same universal fitting parameters as before: $F(0) = 12.6$ and $k_f^2 = 125$, $U(0) = 4.3$ and $k_u^2 = 93$. The main effect of increased coflow velocities was evidence of a slight increase of streamwise velocity near the edge of the plume, which can be seen

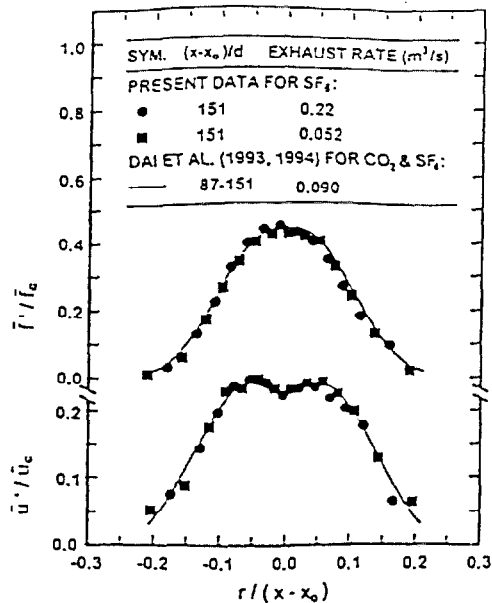


Fig. 2 Radial profiles of rms mixture fraction and streamwise velocity fluctuations for self-preserving round buoyant turbulent plumes

most clearly at the outmost points of \bar{u} at an exhaust flow rate of 0.22 m³/s.

Radial profiles of fluctuating mixture fractions and streamwise velocities are illustrated in Fig. 2 for the various exhaust flow rates. The values of f' and u' are plotted according to the self-preserving scaling observed by Dai et al. (1994, 1995a). Similar to the results for mean properties in Fig. 1, the fluctuating properties illustrated in Fig. 2 exhibit variations with exhaust rate within experimental uncertainties. Thus, present estimates of mixture fraction and streamwise velocity intensities at the axis are not changed significantly from the findings of Dai et al. (1994, 1995a), i.e., $(f'/f_c)_c = 0.45$ and $(u'/u_c)_c = 0.22$.

Taking the findings illustrated in Figs. 1 and 2 together, it appears that the measurements of flow properties within the self-preserving region of round buoyant turbulent plumes due to Dai et al. (1994, 1995a) were not affected by coflow caused by effects of confinement within their stated experimental uncertainties. Thus, the fact that the measured profiles of Dai et al. (1994, 1995a, b) are narrower, and have larger scaled mean values of mixture fractions and velocities near the axis, than previously thought, is due to additional flow development to reach truly self-preserving behavior compared to most earlier measurements, rather than due to an effect of coflow.

Acknowledgments

This research was sponsored by the United States Department of Commerce, National Institute of Standards and Technology, Grant Nos. 60NANB1D1175 and 60NANB4D1696, with H. R. Baum and K. C. Smyth of the Building and Fire Research Laboratories serving as Scientific Officers.

References

- Dai, Z., Tseng, L.-K., and Faeth, G. M., 1994, "Structure of Round, Fully Developed, Buoyant Turbulent Plumes," *ASME JOURNAL OF HEAT TRANSFER*, Vol. 116, pp. 409-417.
- Dai, Z., Tseng, L.-K., and Faeth, G. M., 1995a, "Velocity Statistics of Round, Fully Developed Buoyant Turbulent Plumes," *ASME JOURNAL OF HEAT TRANSFER*, Vol. 117, pp. 133-145.
- Dai, Z., Tseng, L.-K., and Faeth, G. M., 1995b, "Velocity/Mixture-Fraction Statistics of Round, Self-Preserving Buoyant Turbulent Plumes," *ASME JOURNAL OF HEAT TRANSFER*, Vol. 117, pp. 918-926.

- List, E. J., 1932, "Turbulent Jets and Plumes," *Ann. Rev. Fluid Mech.*, Vol. 14, pp. 139-212.
- Morton, B. R., 1959, "Forced Plumes," *J. Fluid Mech.*, Vol. 5, pp. 151-163.
- Panchapakesan, N. R., and Lumley, J. L., 1993, "Turbulence Measurements in Axisymmetric Jets of Air and Helium. Part. I. Air Jet," *J. Fluid Mech.*, Vol. 246, pp. 197-223.
- Papanicolaou, P. N., and List, E. J., 1953, "Investigation of Round Vertical Turbulent Buoyant Jets," *J. Fluid Mech.*, Vol. 193, pp. 241-291.
- Papanoniu, D., and List, E. J., 1989, "Large Scale Structure in the Far Field of Buoyant Jets," *J. Fluid Mech.*, Vol. 209, pp. 131-190.
- Rouse, H., Yih, C. S., and Humphreys, H. W., 1952, "Gravitational Convection From a Boundary Source," *Tellus*, Vol. 4, pp. 201-210.
- Shabbir, A., and George, W. K., 1992, "Experiments on a Round Turbulent Buoyant Plume," NASA Technical Memorandum 105953.

A Calculation and Experimental Verification of the Infrared Transmission Coefficient of Straight Cylindrical Metal Tubes

P. Cavaleiro Miranda¹

Introduction

An accurate figure for the infrared (IR) transmission coefficient of a stainless steel guide tube that transports ultra-cold neutrons (UCN) from a cryostat at 0.5 K to a room temperature apparatus is required in order to estimate the reduction in the heat load on the cryostat's UCN window achieved by cooling down the guide tube from 300 K to 77 K. The heat emitted by the cooled guide tube is negligible compared to the heat input from the room temperature apparatus, which behaves approximately like a blackbody at 300 K, and so the reduction in heat load is given by the transmission coefficient of the guide tube for 300 K blackbody radiation.

It was shown by Ohlmann et al. (1955) that the transmission of infrared (IR) radiation by cylindrical metal pipes decreases exponentially with length, for a monochromatic point source located on-axis and taking into account only rays making small grazing angles with the wall. In the case of an IR source covering the whole cross section of the tube and providing 2π steradians illumination a significant part of the emitted energy is carried by skew rays. As these rays undergo more reflections the attenuation will be significantly higher than that predicted by Ohlmann's formula.

Calculation of the IR Transmission Coefficient of a Straight Cylindrical Metal Pipe

In the case of 300 K blackbody radiation traveling in a vacuum and incident on stainless steel, the low-frequency limit expressions for the reflection coefficients apply. The coefficients for both polarizations, ρ_{\perp} and ρ_{\parallel} , depend essentially on the wavelength λ , the cosine of the angle of incidence Φ , and the DC electrical conductivity k , of the metal (e.g., Stratton, 1941). For one particular ray of unpolarized "light" traveling down the tube and making a total of N identical reflections, the fraction t of energy transmitted will be

¹ Institut Laue Langevin, 156X, 38042 Grenoble Cedex, France; present position and address: Assistant Professor, Departamento de Física, Faculdade de Ciências da Universidade de Lisboa, Campo Grande, 1700 Lisboa, Portugal.

Contributed by the Heat Transfer Division of THE AMERICAN SOCIETY OF MECHANICAL ENGINEERS. Manuscript received by the Heat Transfer Division November 1994; revision received October 1995. Keywords: Radiation, Associate Technical Editor: M. F. Modest.

Appendix E: Sangras et al. (1998a)

MIXING STRUCTURE OF PLANE SELF-PRESERVING BUOYANT TURBULENT PLUMES

R. Sangras,* Z. Dai† and G.M. Faeth**

Abstract

Measurements of the structure of plane buoyant turbulent plumes are described, emphasizing conditions in the fully-developed (self-preserving) portion of the flow. Plumes were simulated using helium/air sources in a still and unstratified air environment. Mean and fluctuating mixture fractions were measured using laser-induced iodine fluorescence. Present measurements extended farther from the source (up to 155 source widths) and had more accurate specifications of plume buoyancy fluxes than past measurements and yielded narrower plume widths and different scaled mean and fluctuating mixture fractions near the plane of symmetry than previously thought. Measurements of probability density functions, temporal power spectra and temporal integral scales of mixture fraction fluctuations are also reported.

Nomenclature

b	=	source width
B_o	=	source buoyancy flux
d	=	source diameter
$E_f(n)$	=	temporal power spectral density of f
f	=	mixture fraction
$F(y/(x-x_o))$	=	scaled cross stream distribution of \bar{f} in the self-preserving region
Fr_o	=	source Froude number, Eq. (2)
g	=	acceleration of gravity
k_r	=	plume width coefficient based on \bar{f} , Eq. (9)
k_u	=	plume width coefficient based on \bar{u}

Keywords: Natural Convection, Nonintrusive Diagnostics, Plumes, Turbulence

*Graduate Student Research Assistant

†Research Fellow

**Professor, Fellow ASME

ℓ_f	= characteristic plume half-width based on \bar{f} , Eq. (10)
ℓ_M	= Morton length scale, Eq. (10)
ℓ_u	= characteristic plume half-width based on \bar{u} , analogous to Eq. (10)
$\ell_{1/2}$	= characteristic plume halfwidth where $\bar{f} = \bar{f}/2$
n	= frequency
PDF(f)	= probability density function of mixture fraction
Re_c	= characteristic plume Reynolds number, Eq. (8)
Re_o	= source Reynolds number, $2\bar{u}_o b/\nu_o$
u	= streamwise velocity
$U(y/(x-x_o))$	= scaled cross stream distribution of \bar{u} in the self-preserving region
x	= streamwise distance
y	= cross stream distance
z	= distance along slot from its midplane location
Z	= slot length
ν	= kinematic viscosity
ρ	= density
τ_f	= temporal integral scale of mixture fraction fluctuations
Subscripts	
c	= centerline value
o	= initial value or virtual origin location
∞	= ambient value
Superscripts	
(\quad)	= time-averaged mean value
$(\quad)'$	= root-mean-squared fluctuating value

Introduction

The structure and mixing properties of buoyant turbulent plumes in still and unstratified air environments are important fundamental problems that have attracted significant attention since the classical study of Rouse et al. (1952). Recent work has highlighted the need for a better understanding of buoyant turbulent plumes, however, in order to address turbulence/radiation and turbulence/buoyancy interactions (Faeth et al.,

1989; Panchapakesan and Lumley, 1993). Thus, the overall objective of the present investigation was to extend recent measurements of round buoyant turbulent plumes (Dai and Faeth, 1996; Dai et al., 1994; 1995a,b) to consider plane buoyant turbulent plumes using similar methods. The fully-developed region, where effects of the source have been lost and the properties of the flow become self-preserving, was emphasized because these conditions simplify reporting and interpreting measurements (Tennekes and Lumley, 1972), even though few practical buoyant turbulent plumes ever reach the self-preserving region.

Self-preserving buoyant turbulent plumes are reached when streamwise distances from the plume source are large compared to the characteristic source size (typically the source width and diameter for plane and round plumes, respectively) as a measure of conditions where effects of source disturbances have been lost. Another requirement is that streamwise distances must be large compared to the Morton length scale, ℓ_M , as a measure of conditions where effects of source momentum have been lost and effects of buoyancy are dominant. The Morton length scale can be defined as follows for plane plumes having uniform source properties (List, 1982):

$$\ell_M/b = (\rho_o/\rho_\infty) u_o^2 / (bu_o g |\rho_o - \rho_\infty| / \rho_\infty)^{2/3} \quad (1)$$

In Eq. (1), an absolute value has been used for the density difference in order to account for both rising and falling plumes; this practice will be adopted for the remainder of the article. A related parameter used to define source properties is the source Froude number, Fr , defined as follows:

$$Fr^2 = \rho_o u_o^2 / (2bg |\rho_\infty - \rho_o|) \quad (2)$$

The final requirements for self-preserving flow are that $f \ll 1$, so that there is a linear relationship between mixture fraction and fluid density, and that the characteristic plume Reynolds number (Re_c , which will be defined later) is sufficiently large so that transport is

dominated by turbulent rather than molecular effects. Once the flow satisfies these criteria, both mean and fluctuating properties satisfy the relatively simple scaling relationships of self-preserving behavior (List, 1982; Rouse et al., 1952).

In view of the increased generality of the findings, past studies of plane buoyant turbulent plumes emphasized the properties of the self-preserving region of the flow. These studies included Rouse et al. (1952), Lee and Emmons (1961), Harris (1967), Anwar (1967), Kotsovinos (1977,1985) and Ramaprian and Chandrasekhara (1985,1989). The results of these studies are in reasonably good agreement; for example, appropriately scaled flow widths and mean mixture fractions near the plane of symmetry agree within 13%, which is comparable to anticipated experimental uncertainties. Whether these results actually represent self-preserving behavior still is questionable, however, because the measurements generally were limited to the region relatively close to the source $(x-x_0)/b \leq 60$ with values of $(x-x_0)/\ell_M$ as small as 2-3, aside from two exceptions to be discussed later. In contrast, Dai et al. (1994,1995a,b) and Dai and Faeth (1996), only observe self-preserving behavior for round buoyant turbulent plumes farther from the source, $(x-x_0)/d > 80$ and $(x-x_0)/\ell_M > 12$, and found that flow widths were significantly smaller than earlier observations that were limited to the near source region with $(x-x_0)/d \leq 60$ and $(x-x_0)/\ell_M$ as small as 5-6. Another limitation of past studies of plane buoyant turbulent plumes is that measurements of turbulence properties are very limited for all these flows, and are nonexistent for gaseous plumes typical of many practical applications.

In view of these observations, the objective of the present investigation was to complete measurements of the mean and fluctuating mixture fraction properties of plane buoyant turbulent gaseous plumes in still gases, emphasizing conditions within the self-preserving region where the specific features of the source have been lost. Mixture fraction properties that were considered included mean and fluctuating values, probability density

functions, temporal power spectra and temporal integral scales. The experiments consisted of helium/air source flows in still air at normal temperature and pressure, in order to provide a straightforward specification of the buoyancy flux within the test plumes. Measurements of mixture fraction properties were carried out using laser-induced iodine fluorescence (LIF).

Experimental Methods

Apparatus. A sketch of the experimental apparatus appears in Fig. 1. In order to minimize room disturbances, the plumes were observed within a double enclosure contained within a large high-bay test area. The outer enclosure ($3400 \times 2000 \times 3600$ mm high) had porous side walls (the walls parallel to the source) and a porous ceiling made of filter material (Americal Air Filter, filter media pads, 102 mm thick). The filter material prevented flapping of the plume due to room disturbances as well as leakage of background light into the test enclosure. At the same time, the filter material allowed free inflow of air entrained by the plumes which controlled entrained air coflow effects, and free exhaust of the plume itself from the test enclosure. Varying the thickness of the filter material (by a factor of two) had negligible effect on plume properties. After leaving the test enclosure, the plume gases were captured in an upper hood near the ceiling of the laboratory, and were subsequently exhausted by a variable-flow blower. The upper hood was separated from the ceiling area of the plume enclosure so that there was no feedback between blower flow rates and plume properties, i.e., varying blower flow rates also had negligible effect on plume properties.

The test plume was centered at the plane of symmetry of the smaller inner enclosure. The source slot (876 mm long \times 9.4 mm wide) was mounted at the center of the flat floor (876 mm long \times 1220 mm wide) of the inner enclosure. The floor/slot assembly

was mounted normal to end walls (1220 × 2440 mm high). The inner enclosure was completed by installing screen arrays (a pair of screens, 16 mesh × 0.28 mm wire diameter, separated by a distance of 38 mm) across the openings between the outer extremities of the two end walls. The use of screens to control room disturbances in this way was based on successful past use of similar methods by Gutmark and Wygnanski (1976) for plane free turbulent jets and Dai et al. (1994,1995a,b) and Dai and Faeth (1996) for round buoyant turbulent plumes. Other modifications of the inner enclosure were studied as follows: extended end walls, rounded contractions at the outer edge of the end walls and the floor to smooth the flow of entrained fluid, and various screen and honeycomb arrangements across the openings at the extremities of the end walls. None of these changes had an appreciable effect on plume properties, however, and they were eliminated in favor of the simplest effective approach for controlling room disturbances, as described earlier.

Optical access for measurements of plume properties was provided by fixed windows (914 mm wide × 203 mm high, mounted flush to the inner surfaces of the end walls), centered on the optical axis (nominally passing halfway between the end walls, roughly 2080 mm above the floor of the test enclosure). Various distances from the source were considered by mounting the source at different heights along the end walls. Horizontal traversing in the cross stream direction was provided by mounting the entire floor/wall assembly on linear bearings so that it could be moved by a stepping-motor-driven linear positioner (5 μm positioning accuracy) in order to accommodate rigidly-mounted instrumentation. Finally, various positions along the slot could be considered, to check for two-dimensionality, by shifting the floor/wall assembly along the linear bearing mount.

The gas supply system of the plume source involved mixing helium (commercial grade, 99.995 percent purity) and air (laboratory supply having a dewpoint less than 240 K). These flows were controlled by pressure regulators and metered using critical flow orifices in conjunction with absolute pressure gages (Heisse, Model CC, 0-2000 kPa range, 0.15 percent full-scale accuracy). The critical flow orifices were calibrated in turn by either wet test meters or a standard turbine flow meter (EG&G, Flow Technology, Model FT68AENA615A 1). After mixing, the source flows passed through beds of iodine flakes to provide iodine seeding for LIF measurements. The source flow then passed through four parallel lines having length-to-diameter ratios greater than 1200 to ensure uniform mixing. These flows subsequently entered the source manifold, passed through a bed of glass beads (0.5 mm bead diameter with bed dimensions of 876 mm long \times 32 mm wide \times 120 mm deep), a filter (3M, OCELLO, scouring pad, 876 mm long \times 32 mm wide \times 5 mm thick), and a contraction to a final slot width of 9.4 mm. All components in contact with the flow after seeding with iodine were either plastic or painted to avoid corrosion. The final plume flow in the exhaust blower was an exception because iodine concentrations at this point were less than 100 ppb and caused no corrosion problems.

Instrumentation. Mixture fractions were measured using laser-induced iodine fluorescence, similar to Dai et al. (1994). The LIF signal was produced by a focused argon-ion laser beam at 514.5 nm (measuring volume diameter at the e^{-2} points of 0.16 mm with a maximum optical power of roughly 1800 mW). This wavelength is absorbed by iodine and causes it to fluoresce at longer wavelengths in the visible. The laser beam was horizontal and directed normal to the plume source slot near its midpoint and roughly 2080 mm above the floor of the enclosure. The operation of the laser beam was monitored using two laser power meters that measured laser power before and after passing through the flow. Absorption of the laser beam was less than 1 percent and was even smaller for the

fluorescence emissions, thus, it was not necessary to correct the LIF signal for effects of absorption.

The fluorescence signals were observed at right angles to the laser beam using f5:1 collecting lenses having diameters of 100 mm. The LIF signal was separated from light scattered at the laser line using long-pass optical filters (cut off wavelength of 530 nm). The resulting signal was measured with a detector (Hamamatsu, Model R269) with the detector aperture selected to provide a measuring volume length of 2 mm. The detector outputs were amplified and then low-pass filtered using sixth-order Chebychev filters to control alias signals. The detector signals were sampled using an a/d converter and then transferred to a computer for processing and storage. The detector signals were also monitored using a digital oscilloscope.

The LIF signals were calibrated based on measurements at the source exit by mixing the source flow with air to vary the mixture fraction. These tests showed that fluctuations of iodine seeding levels were less than 1 percent. The LIF signal was not saturated for present conditions and varied linearly with laser power. The LIF signals also varied linearly with the mixture fraction. These calibrations were checked periodically by diverting a portion of the source flow through a plastic tube whose exit was mounted temporarily just below the measurement location. Final processing of the data accounted for both absorption of the laser beam by iodine vapor and laser power variations.

Differential diffusion between the source of buoyancy in the source gas (helium) and the iodine vapor can be a significant source of error for LIF measurements. Effects of differential diffusion were evaluated using the approach of Stårner and Bilger (1983), noting that the binary diffusivities of helium and iodine in air at normal temperature and pressure are 70 and 8 mm²/s (Bird et al., 1960). For conditions of present interest in the self-preserving region of the flows, local Reynolds numbers are reasonably large; ($Re > 3700$ in the self-preserving portions of the flow, as discussed later); therefore, maximum

errors of mean and fluctuating mixture fractions due to effects of differential diffusion were estimated to be less than 0.1 percent.

Experimental uncertainties (95 percent confidence) were found following Moffat (1982). Gradient broadening errors were small (less than 1 percent) at the locations where the measurements were made. Experimental uncertainties of source properties and distances from the source were also small (less than 1 percent). Signal sampling times were chosen to maintain experimental uncertainties near the plane of symmetry less than 6 and 10 percent for mean and fluctuating mixture fractions, respectively, with both properties being repeatable well within these ranges. Corresponding experimental uncertainties of other flow properties reported here are as follows: 6 percent for $F(y/(x-x_0))$, 12 percent for \bar{f}'/\bar{f}_c , 10 percent for PDF(f), 40 percent for the low frequency region of $E_f(n)/(\tau_f \bar{f}'^2)$ and 35 percent for $B_0^{1/3} \tau_f / (x - x_0)$. These uncertainties were maintained at these values up to half the maximum value of the parameter (excluding the spike region of the PDF) but increased at smaller values roughly inversely proportional to the value of the parameter.

Test Conditions. The test conditions are summarized in Table 1. Two source flows were considered, having initial density ratios, $\rho_0/\rho_\infty = 0.770$ and 0.500. Source Froude numbers were kept near current estimates of asymptotic plane plume Froude numbers in order to enhance the development of the flow toward self-preserving conditions (Grella and Faeth, 1975; Liburdy and Faeth, 1978). In view of the large source flow rates of line plumes from a source having dimensions of 9.4×876 mm, it was difficult to maintain a large source Reynolds number, Re_0 , at the same time. Thus, source Reynolds numbers were roughly equal to 800. The self-preserving regions were relatively far from the source, $(x-x_0)/b \geq 76$; therefore, locations of the virtual origins could not be distinguished from $x_0/b = 0$ within present experimental uncertainties.

Self-Preserving Scaling

The state relationship for density as a function of mixture fraction, assuming an ideal gas mixture, is as follows (Dai et al., 1994):

$$\rho = \rho_{\infty} / (1 - f(1 - \rho_{\infty} / \rho_0)) \quad (3)$$

Far from the source where the flow becomes self-preserving, Eq. (3) can be linearized as follows:

$$\rho = \rho_{\infty} + f\rho_{\infty} (1 - \rho_{\infty} / \rho_0), f \ll 1 \quad (4)$$

Present measurements consisted of mean and fluctuating mixture fraction properties at various streamwise positions. Mean mixture fractions were then scaled in terms of self-preserving variables as follows (List, 1982):

$$F(y/(x-x_0)) = \bar{f} g B_0^{-2/3} (x-x_0) |1 - \rho_{\infty} / \rho_0| \quad (5)$$

where $F(y/(x-x_0))$ represents an appropriately scaled cross stream profile function of mean mixture fraction, which becomes a universal function far from the source where Eq. (4) applies. The source buoyancy flux, B_0 , is a conserved scalar of the flow which can be written as follows for plane plumes having uniform source properties (List, 1982):

$$B_0 = bu_0 g |\rho_0 - \rho_{\infty}| / \rho_{\infty} \quad (6)$$

The self-preserving relationship for streamwise mean velocity was not studied during the present investigation but velocity properties are useful to help define the turbulence properties of the plume. Thus, it should be noted that mean streamwise velocities within self-preserving plane buoyant turbulent plumes can be scaled as follows (List, 1982):

$$U(y/(x-x_0)) = \bar{u} / B_0^{1/3} \quad (7)$$

where $U(y/(x-x_0))$ is an appropriately-scaled cross stream profile function. The corresponding characteristic plume Reynolds number can be written as follows for self-preserving conditions:

$$Re_c = \bar{u}_c \ell_u / \nu_\infty = U(0) B_0^{1/3} (x-x_0) / (k_u \nu_\infty) \quad (8)$$

where for present purposes, values of k_u and $U(0)$ were taken from Rouse et al. (1952).

Results and Discussion

Mean Mixture Fractions. Distributions of mean mixture fractions in the self-preserving region of the flow will be considered first. Present measurements of cross stream distributions of mean mixture fractions for the two sources are illustrated in Fig. 2. The scaling parameters of Eq. (5) have been used when plotting the figure so that the ordinate of the plot is equal to $F(y/(x-x_0))$. The results are plotted for $z/Z = 0$ and $1/4$ in order to evaluate the two dimensionality of the flow; it is evident that there is little variation of flow properties with position along the source (in the z direction) confirming that flow properties are reasonably two dimensional. Present measurements also yield the universal distributions within experiment uncertainties that are required for self-preserving flow, for $76 \leq (x-x_0)/b \leq 155$ and $9 \leq (x-x_0)/\ell_M \leq 21$ with flow aspect ratios $Z/(2\ell_p) \geq 2.6$. Measurements nearer to the source yielded broader distributions of scaled mean mixture fractions as will be discussed subsequently. Measurements were not undertaken farther from the source in order to avoid flow aspect ratios near unity that are affected by the presence of the end walls. Present conditions correspond to $3700 \leq Re_c \leq 7500$, which are reasonably large for unconfined turbulent flows; for example, the companion study of self-preserving round buoyant turbulent plumes due to Dai et al. (1994, 1995a,b) achieved $2500 \leq Re_c \leq 4200$.

Measurements of mean mixture fractions due to Rouse et al. (1952), Kotsovinos (1977) and Ramaprian and Chandrasekhara (1989) are also plotted in Fig. 2, for

comparison with the present measurements (results from other past studies have not been plotted in order to avoid cluttering the figure but will be considered later). These distributions are seen to be significantly broader (up to 30 percent broader at the e^{-1} points of the distributions) and significantly larger near the plane of symmetry (up to 30 percent larger), than the present measurements. Reasons for these differences between past and present measurements will be discussed next, considering scaled widths and magnitudes of scaled mean mixture fraction distributions, in turn.

The larger scaled widths of the mean mixture fraction distributions of the earlier studies plotted in Fig. 2 than the present study are typical of conditions in the developing plume region before self-preserving behavior is achieved. As discussed earlier, this behavior is expected because the results of earlier studies involved *averages* of measurements for $6 \leq (x-x_0)/b \leq 60$ (possibly except for the classical findings of Rouse et al. (1952) where the range of the measurements in terms of $(x-x_0)/b$ cannot be specified because the sources used were a linear array of combusting jets) whereas Dai et al. (1994) only observed self-preserving behavior in round buoyant turbulent plumes farther from the source at $(x-x_0)/d > 80$. Corresponding flow development behavior for plane buoyant turbulent plumes can be quantified from the results given in Table 2. In this table, characteristic plume half widths, $\ell_{1/2}/(x-x_0)$, are summarized as a function of scaled distance from the source, $(x-x_0)/b$, for the measurements of Kotsovinos (1977), Ramaprian and Chandrasekhara (1989) and the present investigation. Present scaled flow widths are similar to the other studies near the source, in spite of significant differences in source properties, and characteristic plume half widths tend to decrease with increasing distance from the source for all three studies. Present measurements, however, extend farther from the source with half widths eventually reaching smaller asymptotic values than the rest. In fact, $\ell_{1/2}/(x-x_0) = 0.08$ for $50 \leq (x-x_0)/b \leq 155$ for the present measurements providing rather strong evidence for the invariance of this property with streamwise distance. As

noted in the table, however, self-preserving behavior is deferred until $(x-x_0)/b \geq 76$ for present test conditions because the distributions of mixture fraction fluctuations was still developing in the region $50 \leq (x-x_0)/b \leq 76$. Considering all this evidence, it seems reasonable to conclude that flow widths observed during the earlier studies plotted in Fig. 2 are larger than observed during the present study because they were not obtained far enough from the source to achieve fully self-preserving behavior.

The second issue concerning the mean mixture fraction distributions plotted in Fig. 2 is that present scaled values of mixture fractions are generally smaller than the rest. It is felt that these differences are caused by problems of finding B_0 during the earlier studies, which all involved thermal plumes. In particular, B_0 was accurately prescribed by the gas mixture at the source exit for the present study but had to be obtained by measurements of distributions of plume velocity and temperature properties for the other studies due to the difficulties of determining energy losses from the thermal plumes near the source. Measuring B_0 from property distributions in plumes involves considerable uncertainties compared to the present approach, particularly because a significant portion of B_0 is transported by the streamwise turbulent flux of species or energy (for composition and thermal plumes, respectively) which is difficult to measure accurately, e.g., Dai et al. (1995b) and George et al. (1977) find that the streamwise turbulent flux contributes 15-16 percent of B_0 for round buoyant turbulent plumes with similar levels anticipated for plane buoyant turbulent plumes. Thus, it is not surprising that the measured scaled values of mean mixture fractions due to Rouse et al. (1952), where B_0 is probably underestimated because the turbulent contribution to it was not measured and had to be ignored, are generally larger than the present measurements. In contrast, Ramaprian and Chandrasekhara (1989) and Kotsovinos (1977) report turbulence contributions to B_0 of 6 and 38 percent, respectively, which differ considerably from each other and from the findings for round buoyant turbulent plumes. These differences clearly demonstrate the

problems of accurately finding the turbulent flux of B_o , and thus the correct value of B_o needed to scale self-preserving flow properties, uncertainties of the determination of the mean flow contribution to B_o from distributions of mean properties aside. Taken together, these observations provide a reasonable explanation why present measurements of scaled mean mixture fractions in Fig.2 are smaller than the rest.

Additional comparisons between present and earlier measurements will involve properties found from fits of the scaled mean mixture fraction distributions. Within the self-preserving region, present cross stream distributions of mean mixture fractions in Fig. 2 are reasonably approximated by a Gaussian fit, similar to the results of Rouse et al. (1952), Kotsovinos (1977) and Ramaprian and Chandrasekhara (1989) also shown on the plot. This type of correlation can be expressed as follows:

$$F(y/(x-x_o)) = F(0)\exp\{-k_f^2(y/(x-x_o))^2\} \quad (9)$$

where

$$k_f = (x-x_o)/\ell_f \quad (10)$$

Thus, ℓ_f represents the characteristic plume radius where $\bar{f}/\bar{f}_c = e^{-1}$. The best fit of the present data in the self-preserving region yielded $F(0) = 2.10$, $k_f^2 = 70$ and, thus, $\ell_f/(x-x_o) = 0.120$. These parameters yielded the correlation of present observations illustrated in Fig. 2, which is seen to be a good representation of the measurements.

The present values of normalized streamwise distance required to reach self-preserving conditions within plane buoyant turbulent plumes are similar to the observations of Dai et al. (1994,1995a,b) and Dai and Faeth (1996) for round buoyant turbulent plumes; however, they are generally larger than streamwise distances reached during past measurements of the self-preserving properties of plane buoyant turbulent plumes using a variety of sources. This behavior is quantified in Table 3, where the aspect ratio of the slot, Z/b , the range of streamwise distances, $(x-x_o)/b$, the smallest flow aspect ratio,

$(Z/(2\ell_f))_{\min}$, the streamwise distance in terms of the Morton length scale, $(x-x_0)/\ell_M$, and the corresponding reported values of k_f^2 , $\ell_f/(x-x_0)$ and $F(0)$ are summarized to the extent that they are known for the studies of Rouse et al. (1952), Lee and Emmons (1961), Harris (1967), Anwar (1968) and Kotsovinos (1977), Ramaprian and Chandrasekhara (1989) and the present investigation. The data summary of Table 3 shows that the most recent measurements of Ramaprian and Chandrasekhara (1989), Kotsovinos (1977), Anwar (1968) and Harris (1967) all involve relatively small values of $(x-x_0)/b$, and in some cases small $(x-x_0)/\ell_M$ and aspect ratios as well, so that broader flows in these instances, typical of flows developing toward self-preserving conditions, are not unexpected, as already discussed. The earlier studies of Lee and Emmons (1961) and to some extent Harris (1967), and Anwar (1968), however, were obtained at reasonably large distances from the source where self-preserving behavior should have been approached. Thus, in these cases, broader distributions of \bar{f} probably resulted from plume disturbances, that invariably increase plume widths and are difficult to avoid far from the source for plane plumes due to their large source flows and extensive flow fields. The results of Rouse et al. (1952), where streamwise distances in terms of source widths and Morton length scales cannot be specified, may also be broad for similar reasons. Taken together, the studies summarized in Table 3 exhibit flow widths (based on ℓ_f at conditions where $\bar{f}/\bar{f}_c = e^{-1}$) up to 36 percent larger, and scaled mean mixture fractions near the plane of symmetry up to 24 percent larger, than the present measurements. Such differences can have a significant impact on evaluation of turbulence models of buoyant turbulent plumes (Dai et al. (1994,1995a,b) as well as on the interpretation of the stabilizing effects of surfaces on the mixing properties of buoyant turbulent wall plumes (Grella and Faeth, 1975; Liburdy and Faeth, 1978; Liburdy et al., 1979; Lai et al., 1986; Lai and Faeth, 1987a).

Mixture Fraction Fluctuations. Measurements of cross stream distributions of rms mixture fraction fluctuations are plotted in Fig. 3. These results are plotted as \bar{f}'/\bar{f}_c as a

function of $y/(x-x_0)$, which corresponds to self-preserving scaling for buoyant turbulent plumes (Dai et al., 1994, 1995a,b). In addition to present measurements, for the same conditions as the results for \bar{f} in Fig. 2, the measurements of Kotsovinos (1977) and Ramaprian and Chandrasekhara (1989) are also shown in this plot. The distributions of Kotsovinos (1977) and Ramaprian and Chandrasekhara (1989) are rather broad and exhibit a dip near the plane of symmetry much like the behavior of round buoyant turbulent plumes near the source (Dai et al., 1994) and the behavior of nonbuoyant round jets (Becker et al., 1967; Papanicolaou and List, 1987, 1988). Present results generally reach a maximum near the plane of symmetry, with no dip, which is similar to the behavior observed by Dai et al. (1994) for self-preserving round buoyant turbulent plumes. The differences between present findings concerning mixture fraction fluctuations and earlier results nearer to the source are not surprising because self-preserving behavior for turbulence properties generally requires self-preserving behavior for mean properties (Tennekes and Lumley, 1972). Present measurements within the self-preserving region can be correlated reasonably well by the following expression which is also illustrated in Fig. 3:

$$\bar{f}'/\bar{f}_c = 0.47 \exp\{-25(y/(x-x_0))^{2.5}\} \quad (11)$$

The values of $(\bar{f}'/\bar{f})_c$ for Kotsovinos (1977), Ramaprian and Chandrasekhara (1985, 1989) and the present study, which are the only values available, are summarized in Table 3. The present value of 47 percent is significantly larger than the results of the other two studies, 42 percent, probably due to effects of flow development from relatively nonturbulent sources for the earlier studies. Present turbulence intensities of mixture fraction fluctuations near the plane of symmetry are also slightly larger than the value of 45 percent observed by Dai et al. (1994) at the axis of self-preserving round buoyant turbulent plumes but this difference is comparable to experimental uncertainties.

The absence of the dip near the center of mixture fraction fluctuation distributions for plane and round buoyant turbulent plumes is an interesting feature of free buoyant

turbulent flows. In contrast, round and plane nonbuoyant turbulent jets have reduced mixture fraction fluctuations near the axis and plane of symmetry because turbulence production is small in this region because the mean mixture fraction gradient is smaller due to symmetry requirements (Becker et al., 1967; Papanicolaou and List, 1987,1988). In spite of symmetry, however, effects of buoyancy provide a mechanism of turbulence production near the axis and plane of symmetry of round and plane plumes due to buoyant instability in the streamwise direction, i.e., the density always approaches the ambient density in the streamwise direction. As discussed by Dai et al. (1994), for round buoyant turbulent plumes, this instability is also responsible for larger mixture fraction fluctuations near the axis and plane of symmetry of round and plane plumes compared to nonbuoyant jets. Thus, the contribution of buoyancy to turbulence is appreciable in both round and plane buoyant turbulent plumes.

Probability Density Functions. Mixture fractions are limited to the finite range, 0-1, and cannot exhibit the simple Gaussian behavior typical of velocity probability density functions in turbulent flows. Representative plots of the PDF(f) of the present self-preserving plane buoyant turbulent plumes are illustrated in Fig. 4. These results are for the case 1 source at various cross stream distances and $x/b = 110$. The measurements are compared with predictions of the clipped-Gaussian and beta function distributions which are frequently used to represent PDF(f) for modeling purposes (Lockwood and Naguib, 1975). Both these distributions are defined by two moments, \bar{f} and \bar{f}'^2 ; therefore, the predicted distributions are based on the measured values of these moments at each condition considered.

The measured PDF(f) illustrated in Fig. 4 are similar to earlier measurements in flames, round plumes and jets (Kounalakis et al., 1991; Papanicolaou and List, 1987,1988; Dai et al., 1994; Becker et al., 1967). At the axis, the PDF(f) is nearly Gaussian, although the distribution is truncated while having a finite value at $f=0$ indicating the presence of

conditions where unmixed ambient fluid reaches the plane of symmetry. Finite values of $PDF(0)$ near the axis or plane of symmetry are typical of self-preserving buoyant turbulent plumes but this behavior for nonbuoyant turbulent mixing processes is much less prominent than the results illustrated in Fig. 4 (Dai et al., 1994). The value of $PDF(0)$ increases in magnitude with increasing cross stream distance and becomes spike-like and eventually dominates the mixture fraction distribution as the edge of the flow is approached where the observation point is mainly in ambient fluid. Similar to past observations of the $PDF(f)$ in self-preserving round buoyant turbulent plumes due to Dai et al. (1994), both the clipped-Gaussian and beta function PDF's provide reasonably good fits of the measurements. The beta function distribution probably will be preferred for most practical calculations of scalar plume properties, however, because it is easier to use than the clipped-Gaussian function (Lockwood and Naguib, 1975).

Temporal Power Spectral Densities. Temporal power spectral densities are of interest to illustrate the signal-to-noise ratios of the present mixture fraction measurements, to study aspects of buoyancy/turbulence interactions, and to provide information needed to understand the temporal properties of radiation fluctuations in buoyant turbulent plumes. Some typical measurements of temporal power spectra for the present self-preserving plane buoyant turbulent plumes are illustrated in Fig. 5. These results are for the case 1 plume with $76 \leq (x-x_0)/b \leq 155$, considering cross stream positions over the full width of the flow at each streamwise position. The measurements are normalized by local turbulence properties, τ_f and \bar{f}' , in the usual manner as described by Hinze (1975). The present spectra are qualitatively similar to earlier results for round plumes reported by Dai et al. (1994) and Papanicolaou and List (1987,1988). The normalized spectra are relatively independent of cross stream position at each streamwise location when scaled in the manner of Fig. 5, which provides a convenient summary of the data. Similarly, the low-frequency

portion of the spectra are relatively independent of streamwise position when normalized in the manner of Fig. 5.

The spectra illustrated in Fig 5 initially decay according to the $-5/3$ power of frequency; this behavior is typical of the inertial region of the turbulence spectrum of velocity fluctuations which has been called the inertial-convective region for scalar property fluctuations where effects of molecular diffusion are small (Tennekes and Lumley, 1972). This is followed by a prominent region where the spectrum decays roughly according to the -3 power of frequency, which has been termed the inertial-diffusive subrange by Papanicolaou and List (1987). This region is not observed in nonbuoyant flows and is thought to be caused by variations of the local rate of dissipation of mixture fraction fluctuations due to buoyancy-generated inertial forces. Thus, the -3 decay region of the temporal spectra merits additional study as an important buoyancy/turbulence interaction. The mixture fraction microscale, where temporal power spectral densities rapidly become small, should be observed at larger frequencies than the -3 decay region. Unfortunately, present measurements did not have the spatial and temporal resolution needed for observations at these conditions. Present measurements were able to resolve nearly five decades of the temporal power spectra, however, which provides the good signal-to-noise ratios needed to resolve mixture fraction fluctuations with the experimental uncertainties mentioned earlier.

Temporal Integral Scales. The properties of the temporal power spectra are completed by the temporal integral scales. Present measurements of the temporal integral scales are plotted as a function of cross stream distance in Fig. 6. The measurements are limited to the self-preserving region, $76 \leq (x-x_0)/b \leq 155$, for the case 1 source; however, effects of streamwise distance are relatively small when plotted in the manner of Fig. 6.

The temporal integral scales in Fig. 6 have been plotted by combining Taylor's hypothesis and the requirements of a self-preserving streamwise velocity field for plane buoyant turbulent jets. This implies that $\tau_f \bar{u} / \ell_u$ should be a universal function of $y/(x-x_0)$ within the self-preserving region of the flow, yielding the normalized variables of Fig. 6 after adopting the self-preserving velocity scale for plane buoyant turbulent plumes from Eq. (6). This approach provides a somewhat scattered but reasonable correlation of τ_f for self-preserving plane plumes, similar to earlier findings for self-preserving round turbulent plumes (Dai et al., 1994). The similarities of the behavior of τ_f for round and plane buoyant turbulent plumes suggest that streamwise spatial integral scales of mixture fraction fluctuations are relatively constant over the flow cross section for the present plane buoyant turbulent plumes. Then the increase of τ_f as the edge of the flow is approached results from the reduced values of \bar{u} in this region through Taylor's hypothesis. Measurements of the velocity properties of the present plumes are needed, however, in order to properly establish the behavior of spatial integral scales for these flows.

Conclusions

Mixture fraction statistics were measured in plane buoyant turbulent plumes in still air, emphasizing fully-developed (self-preserving) conditions where effects of source disturbances are lost and flow properties scale in a relatively simple manner. The test conditions consisted of buoyant jet sources of helium and air to give ρ_0/ρ_∞ of 0.500 and 0.770 and source Froude numbers of 3.39 and 3.78, respectively, with $(x-x_0)/b$ in the range 76-155 and $(x-x_0)/\ell_M$ in the range 9-21. The major conclusions of the study are as follows:

1. The present measurements yielded distributions of mean mixture fractions that were self-preserving for $(x-x_0)/b \geq 76$. In this region, distributions of mean mixture

fractions were up to 36 percent narrower, with scaled values at the plane of symmetry up to 24 percent smaller, than earlier results using buoyant jet sources in the literature. The earlier measurements generally were obtained for $(x-x_0)/b \leq 60$ which does not appear to be sufficiently far from the source to reach self-preserving conditions for the conditions of the earlier measurements, while also involving problems of accurately determining the value of the buoyancy flux needed to scale self-preserving properties, in some instances.

2. Cross stream distributions of mixture fraction fluctuations in the self-preserving region of plane buoyant turbulent plumes do not exhibit reduced values near the plane of symmetry, similar to plane nonbuoyant jets. Instead, effects of buoyancy cause mixture fraction fluctuations to reach a maximum at the plane of symmetry, to yield intensities of roughly 47 percent. These values are comparable to results observed in the self-preserving round buoyant turbulent plumes, 45 percent, and provide strong evidence of significant effects of buoyancy/turbulence interactions in both of these flows.
3. The probability density functions of mixture fractions in self-preserving plane buoyant turbulent plumes can be approximated reasonably well by either clipped-Gaussian and beta function distributions, and exhibit finite levels of intermittency at the plane of symmetry, similar to self-preserving round buoyant turbulent plumes.
4. The low frequency portion of the temporal spectra of mixture fraction fluctuations scale in a relatively universal manner. The spectra exhibit the well known $-5/3$ power inertial decay region but this is followed by a prominent -3 power inertial-diffusive decay region. These properties are very similar to observations in self-preserving round buoyant turbulent plumes. The -3 power inertial-diffusive region has been observed by others in buoyant turbulent flows but is not observed

in nonbuoyant turbulent flows; therefore, this spectral region represents an interesting buoyancy/turbulence interaction that merits further study.

5. Temporal integral scales could be correlated in a relatively universal manner in terms of self-preserving parameters. The temporal integral scales were smallest at the plane of symmetry. This behavior follows (based on similar behavior for round buoyant turbulent plumes) according to Taylor's hypothesis, noting that mean streamwise velocities reach a maximum at the plane of symmetry.

Acknowledgments

This research was supported by the United States Department of Commerce, National Institute of Standards and Technology, Grant No. 60NANB4D1696, with H. R. Baum of the Building and Fire Research Laboratory serving as Scientific Officer.

References

- Anwar, H.O., 1969, "Experiment on an Effluent Discharging from a Slot into Stationary or Slow Moving Fluid of Greater Density," J. Hydr. Res., Vol. 7, pp. 411-430.
- Becker, H.A., Hottel, H.C., and Williams, G.C., 1967, "The Nozzle-Fluid Concentration Field of the Round, Turbulent, Free Jet," J. Fluid Mech., Vol. 30, pp. 285-303.
- Bird, R.B., Stewart, W.E., and Lightfoot, E.N., 1960, *Transport Phenomena*, John Wiley & Sons, Inc., New York, pp. 502-513.
- Dai, Z., and Faeth, G.M., 1996, "Measurements of the Structure of Self-Preserving Round Buoyant Turbulent Plumes." J. Heat Trans., Vol. 118, pp. 493-495.
- Dai, Z., Tseng, L.-K., and Faeth, G.M., 1994, "Structure of Round, Fully-Developed, Buoyant Turbulent Plumes," J. Heat Trans., Vol. 116, pp. 409-417.

Dai, Z., Tseng, L.-K., and Faeth, G.M., 1995a, "Velocity Statistics of Round, Fully-Developed Buoyant Turbulent Plumes," J. Heat Trans., Vol. 117, pp. 138-145.

Dai, Z., Tseng, L.-K., and Faeth, G.M., 1995b, "Velocity/Mixture-Fraction Statistics of Round, Self-Preserving Buoyant Turbulent Plumes," J. Heat Trans., Vol. 117, pp. 918-926.

Faeth, G.M., Gore, J.P., Chuech, S.G., and Jeng, S.-M., 1989, "Radiation from Turbulent Diffusion Flames," *Annual Review of Numerical Fluid Mechanics and Heat Transfer*, Vol. 2, Hemisphere Publishing Corp., Washington, pp. 1-38.

George, W.K., Jr., Alpert, R.L., and Tamanini, F., 1977, "Turbulence Measurements in an Axisymmetric Buoyant Plume," Int. J. Heat Mass Transfer, Vol. 20, pp. 1145-1154.

Grella, J.J., and Faeth, G.M., 1975, "Measurements in a Two-Dimensional Thermal Plume Along a Vertical Adiabatic Wall," J. Fluid Mech., Vol. 71, pp. 701-710.

Gutmark, E., and Wygnanski, I., 1976, "The Plane Turbulent Jet," J. Fluid Mech., Vol. 73, pp. 465-495.

Harris, P.R., 1967, "The Densimetric Flows Caused by the Discharge of Heated Two-Dimensional Jets Beneath a Free Surface," Ph.D. Thesis, University of Bristol, Bristol, UK.

Hinze, J. O., 1975, *Turbulence*, 2nd ed., McGraw-Hill, New York, pp. 175-319.

Kotsovinos, N.E., 1977, "Plane Turbulent Buoyant Jets. Part 2. Turbulence Structure," J. Fluid Mech., Vol. 81, pp. 45-62.

Kotsovinos, N.E., 1985, "Temperature Measurements in a Turbulent Round Plume," Int. J. Heat Mass Trans., Vol. 28, pp. 771-777.

Kounalakis, M.E., Sivathanu, Y.R., and Faeth, G.M., 1991, "Infrared Radiation Statistics of Nonluminous Turbulent Diffusion Flames," J. Heat Trans., Vol. 113, pp. 437-445.

Lai, M.-C., and Faeth, G.M., 1987a, "Turbulence Structure of Vertical Adiabatic Wall Plumes," J. Heat Trans., Vol. 109, pp. 663-670.

Lai, M.-C., and Faeth, G.M., 1987b, "A Combined Laser-Doppler Anemometer/Laser-Induced Fluorescence System for Turbulent Transport Measurements," J. Heat Trans. Vol. 109, pp. 254-256.

Lai, M.-C., Jeng, S.-M., and Faeth, G.M., 1986, "Structure of Turbulent Adiabatic Wall Plumes," J. Heat Trans., Vol. 108, pp. 827-834.

Lee, S.L., and Emmons, H.W., 1961, "A Study of Natural Convection Above a Line Fire," J. Fluid Mech., Vol. 11, pp. 353-368.

Liburdy, J.A., and Faeth, G.M., 1978, "Heat Transfer and Mean Structure of a Turbulent Thermal Plume Along Vertical Isothermal Walls," J. Heat Trans., Vol. 100, pp. 177-183.

Liburdy, J.A., Groff, E.G., and Faeth, G.M., 1979, "Structure of a Turbulent Thermal Plume Rising Along an Isothermal Wall," J. Heat Trans., Vol. 101, pp. 299-355.

List, E.J., 1982, "Turbulent Jets and Plumes," Ann. Rev. Fluid Mech., Vol. 14, pp. 189-212.

Lockwood, F.C., and Naguib, A.S., 1975, "The Prediction of Fluctuations in the Properties of Free, Round-Jet Turbulent Diffusion Flames," Combust. Flame, Vol. 24, pp. 109-124.

Moffat, R.J., 1982, "Contribution to the Theory of Single-Sample Uncertainty Analysis," J. Fluids Engr., Vol. 104, pp. 250-258.

Panchapakesan, N.R., and Lumley, J.L., 1993, "Turbulence Measurements in Axisymmetric Jets of Air and Helium. Part 2. Helium Jet," J. Fluid Mech., Vol. 246, pp. 225-247.

Papanicolaou, P.N., and List, E.J., 1987, "Statistical and Spectral Properties of Tracer Concentration in Round Buoyant Jets," Int. J. Heat Mass Trans., Vol. 30, pp. 2059-2071.

Papanicolaou, P.N., and List, E.J., 1988, "Investigation of Round Vertical Turbulent Buoyant Jets," J. Fluid Mech., Vol. 195, pp. 341-391.

Ramaprian, B.R., and Chandrasekhara, M.S., 1985, "LDA Measurements in Plane Turbulent Jets," J. Fluids Engr., Vol. 107, pp. 264-271.

Ramaprian, B.R., and Chandrasekhara, M.S., 1989, "Measurements in Vertical Plane Turbulent Plumes," J. Fluids Engr., Vol. 111, pp. 69-77.

Rouse, H., Yih, C.S., and Humphreys, H.W., 1952, "Gravitational Convection from a Boundary Source," Tellus, Vol. 4, pp. 201-210.

Stårner, S. H., and Bilger, R W., 1983, "Differential Diffusion Effects on Measurements in Turbulent Diffusion Flames by the Mie Scattering Technique," Prog. Astro. and Aero., Vol. 88, pp. 81-104.

Tennekes, H., and Lumley, J.L., 1972, *A First Course in Turbulence*, MIT Press, Cambridge, Massachusetts, pp. 113-124.

Table 1. Summary of plane buoyant turbulent plume test conditions^a

Source Properties	Case 1	Case 2
Helium concentration (percent by volume)	26.7	58.1
Density (kg/m ³)	0.894	0.581
Kinematic viscosity (mm ² /s)	21.5	34.7
Average velocity (mm/s)	887	1455
Buoyancy flux, B _o (m ³ /s ³)	0.0188	0.0670
Density ratio, ρ_o/ρ_∞	0.770	0.500
Reynolds number, Re _o	780	790
Froude number, Fr _o	3.78	3.39
Morton length scale, ℓ_M/b	8.6	6.4

^aHelium/air source flow directed vertically upward in still air with an ambient pressure of 99 ± 0.5 kPa and temperature of 297 ± 0.5 K. Pure gas properties as follows: air density of 1.161 kg/m³, air kinematic viscosity of 15.9 mm²/s, helium density of 0.163 kg/m³ and helium kinematic viscosity of 122.5 mm²/s. Source slot width and length of 9.4 and 876 mm. Virtual origin based on \bar{f} of $x_o/b = 0$ determined from present measurements in the range $(x-x_o)/b = 76-155$ and $(x-x_o)/\ell_M = 9-21$.

Table 2. Development of plane buoyant turbulent plumes^a

Source	$(x - x_0)/b$	$\ell_{1/2}/(x - x_0)$
Present (developing region)	13	0.15
	50 ^b	0.08
Present (self-preserving region)	76-155	0.08
Ramaprian and Chandrasekhara (1989)	20	0.14
	50	0.13
	60	0.13
Kotsovinos (1977)	14	0.15
	36	0.13

^aPlane buoyant turbulent plumes in still and unstratified environments. Entries are ordered chronologically.

^bNot judged to be in self-preserving region because mixture fraction fluctuation intensity at the plane of symmetry was not equal to the self-preserving value of 47 percent.

Table 3. Summary of self-preserving properties of plane buoyant turbulent plumes^a

Source	Medium	Z/b	(x-x ₀)/b	(Z/(2ℓ _f)) _{min}	(x-x ₀)/ℓ _M	k _f ²	ℓ _f /(x-x ₀)	F(0)	(\bar{f}'/\bar{f}) _c
Present	gas	93	76-155	2.6	9-21	70	0.120	2.10	0.47
Ramaprian and Chandra- sekhar (1989)	liquid	50	20-60	2.6	3-15	39	0.160	2.56	0.42
Kotsovinos (1977)	liquid	13	6-30	1.0	2-122	47	0.146	2.38	0.42
Anwar (1969)	liquid	60	50	3.9	---	41	0.156	2.57	---
Harris (1967)	liquid	---	70	---	---	38	0.163	2.30	---
Lee and Emmons (1961)	gas	138	140	---	---	---	0.156	---	---
Rouse et al. (1952) ^b	gas	---	---	---	---	41	0.156	2.60	---

^aPlane buoyant turbulent plumes in still and unstratified environments. Range of streamwise distances are for conditions where quoted self-preserving properties were found from measurements over the cross section of the plumes. The entries are ordered chronologically.

^bSource was a linear array of combusting round jets so that slot properties cannot be defined.

List of Figures

- Fig. 1 Cross-sectional sketch of the plane buoyant turbulent plume apparatus.
- Fig. 2 Cross stream distributions of mean mixture fractions in plane self-preserving buoyant turbulent plumes. Measurements of Rouse et al. (1952), Kotsovinos (1977), Ramaprian and Chandrasekhara (1989) and the present investigation.
- Fig. 3 Cross stream distributions of rms mixture fraction fluctuations in plane self-preserving buoyant turbulent plumes. Measurements of Kotsovinos (1977), Ramaprian and Chandrasekhara (1989) and the present investigation.
- Fig. 4 Typical probability density functions in plane self-preserving buoyant turbulent plumes: Case 1 flow at $(x-x_0)/b = 110$.
- Fig. 5 Typical temporal power spectral densities of mixture fraction fluctuations in plane self-preserving buoyant turbulent plumes : Case 1 flow at $(x-x_0)/b = 76, 110$ and 155 .
- Fig. 6 Cross stream distributions of temporal integral scales of mixture fraction fluctuations in plane self-preserving buoyant turbulent plumes.

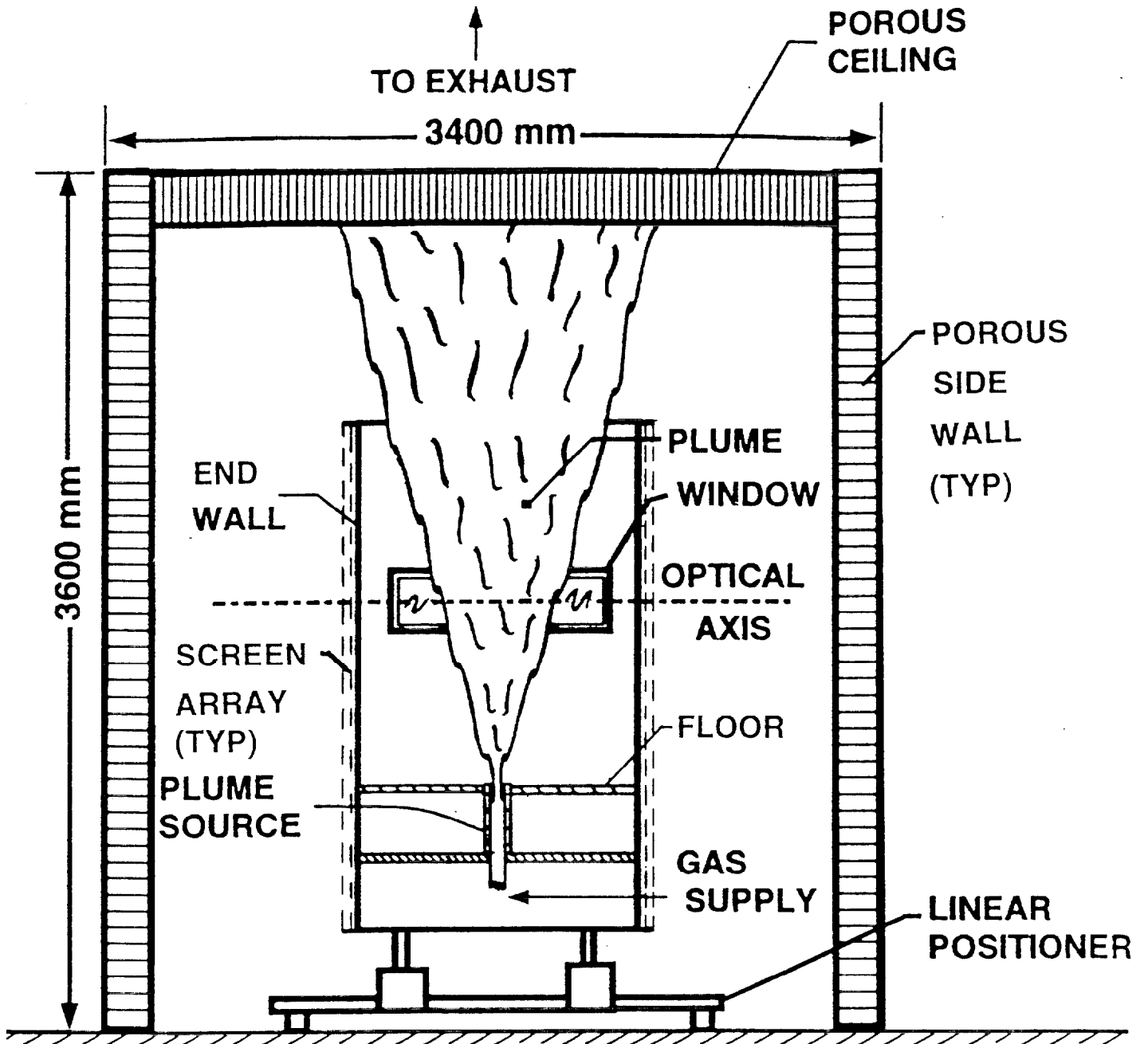


Fig. 1

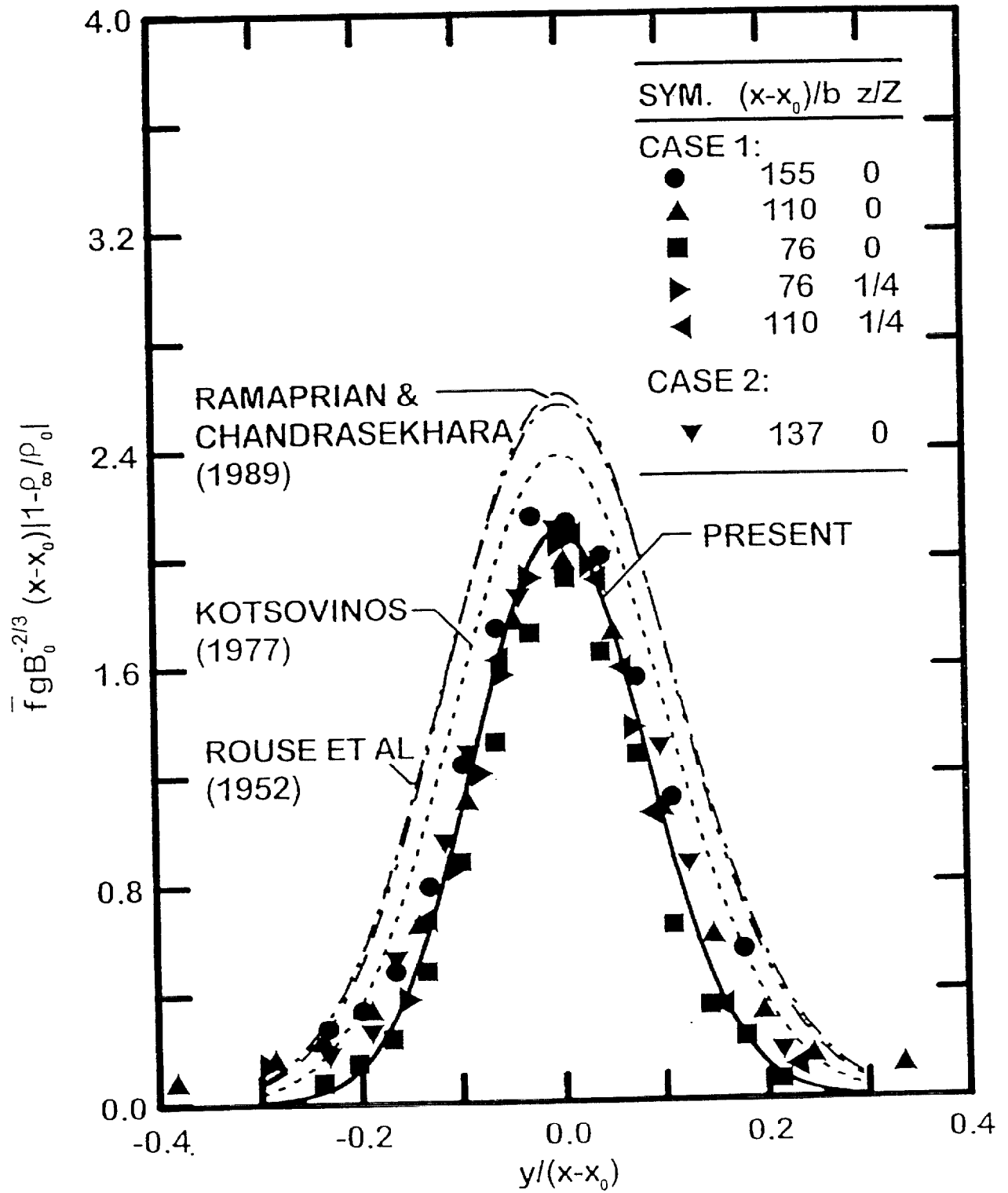


Fig. 2

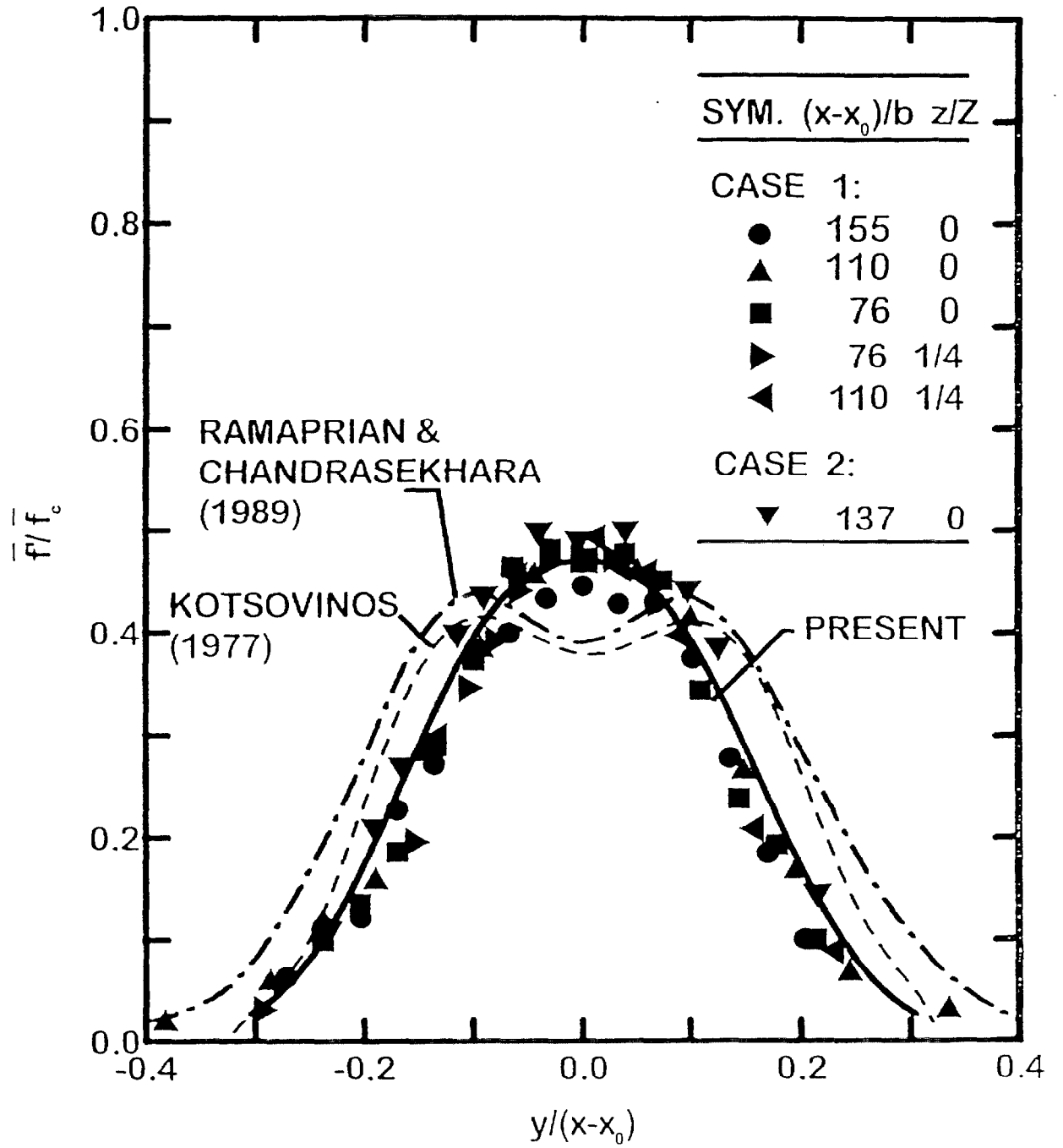


Fig. 3

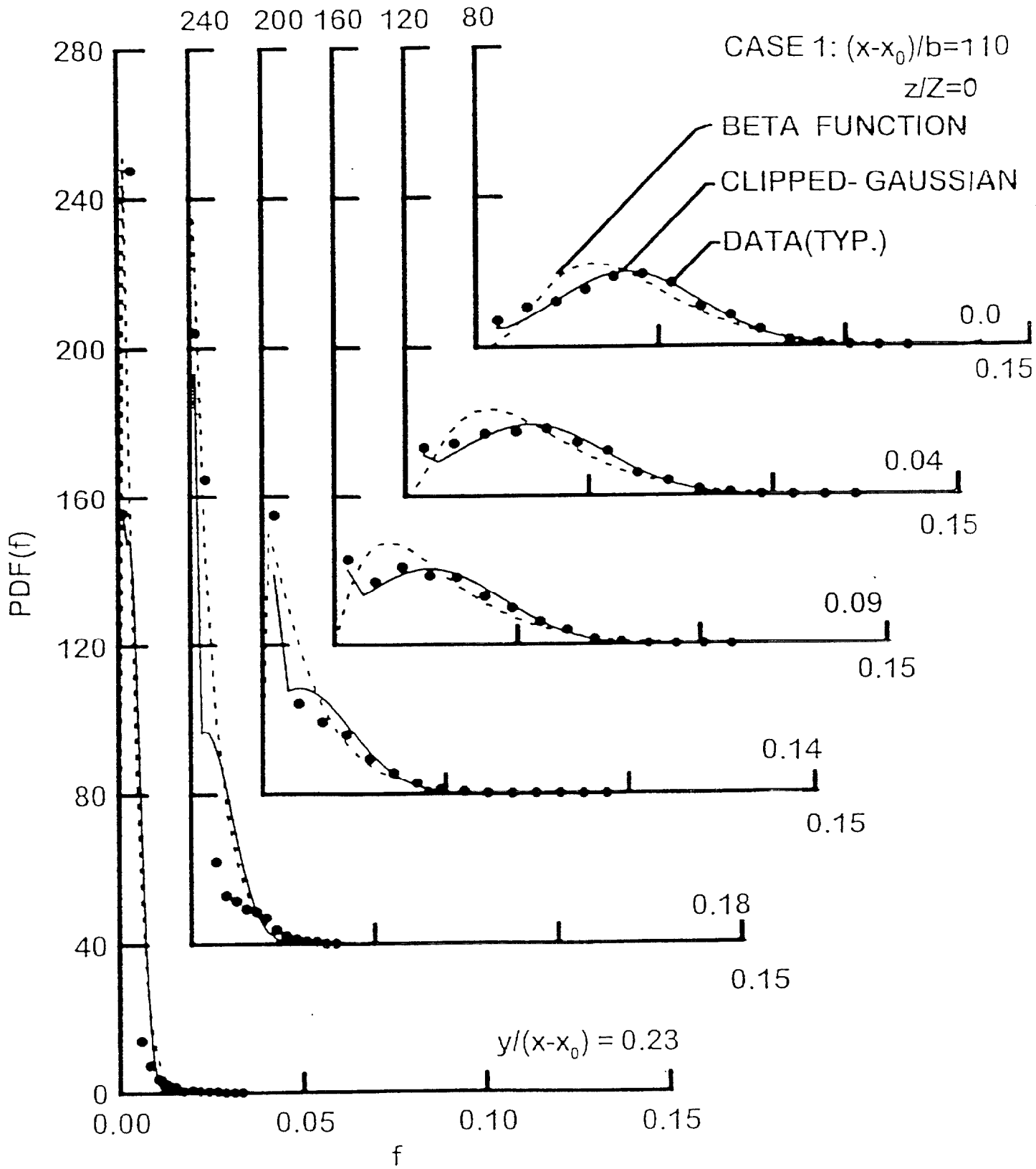


Fig.4

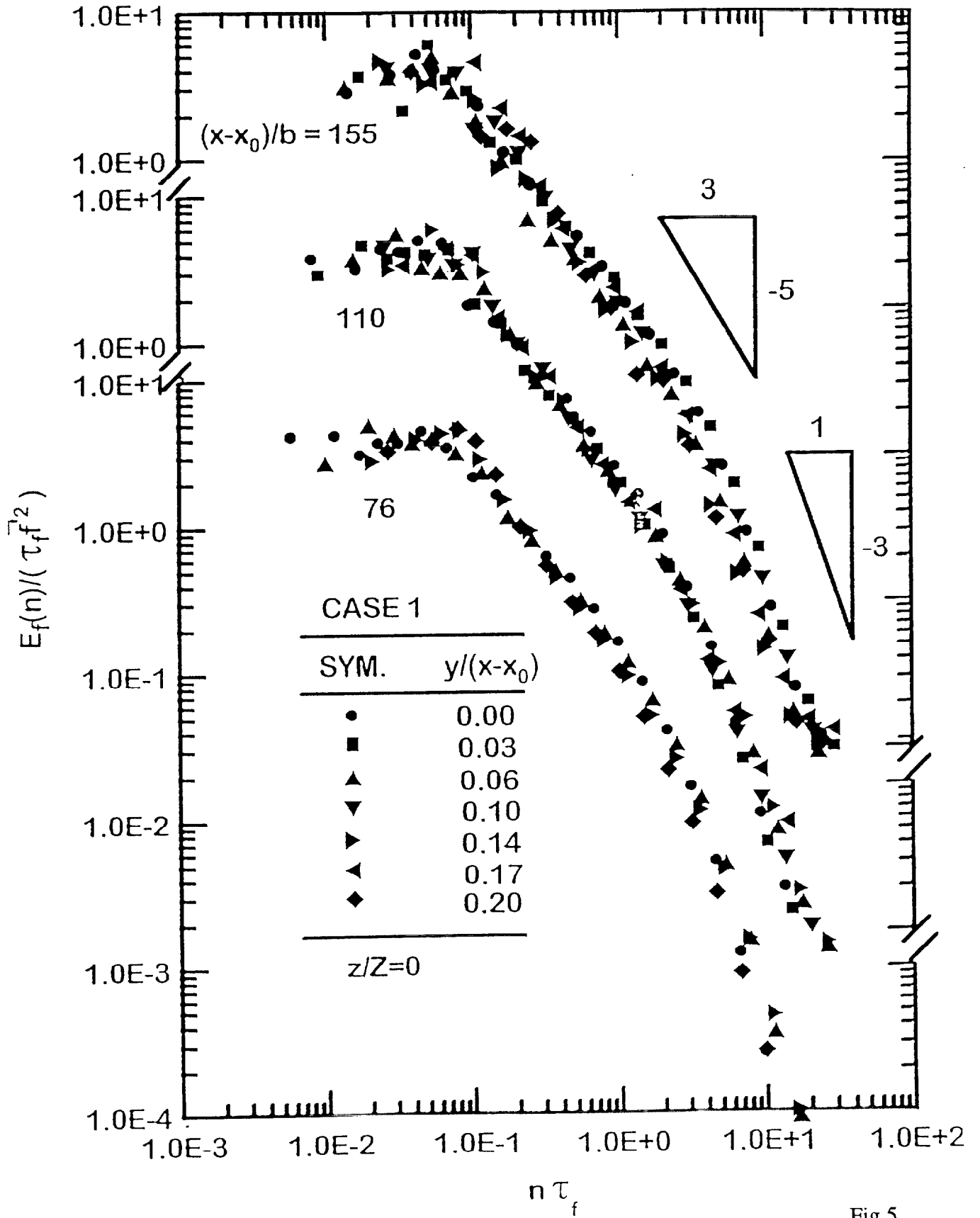


Fig.5

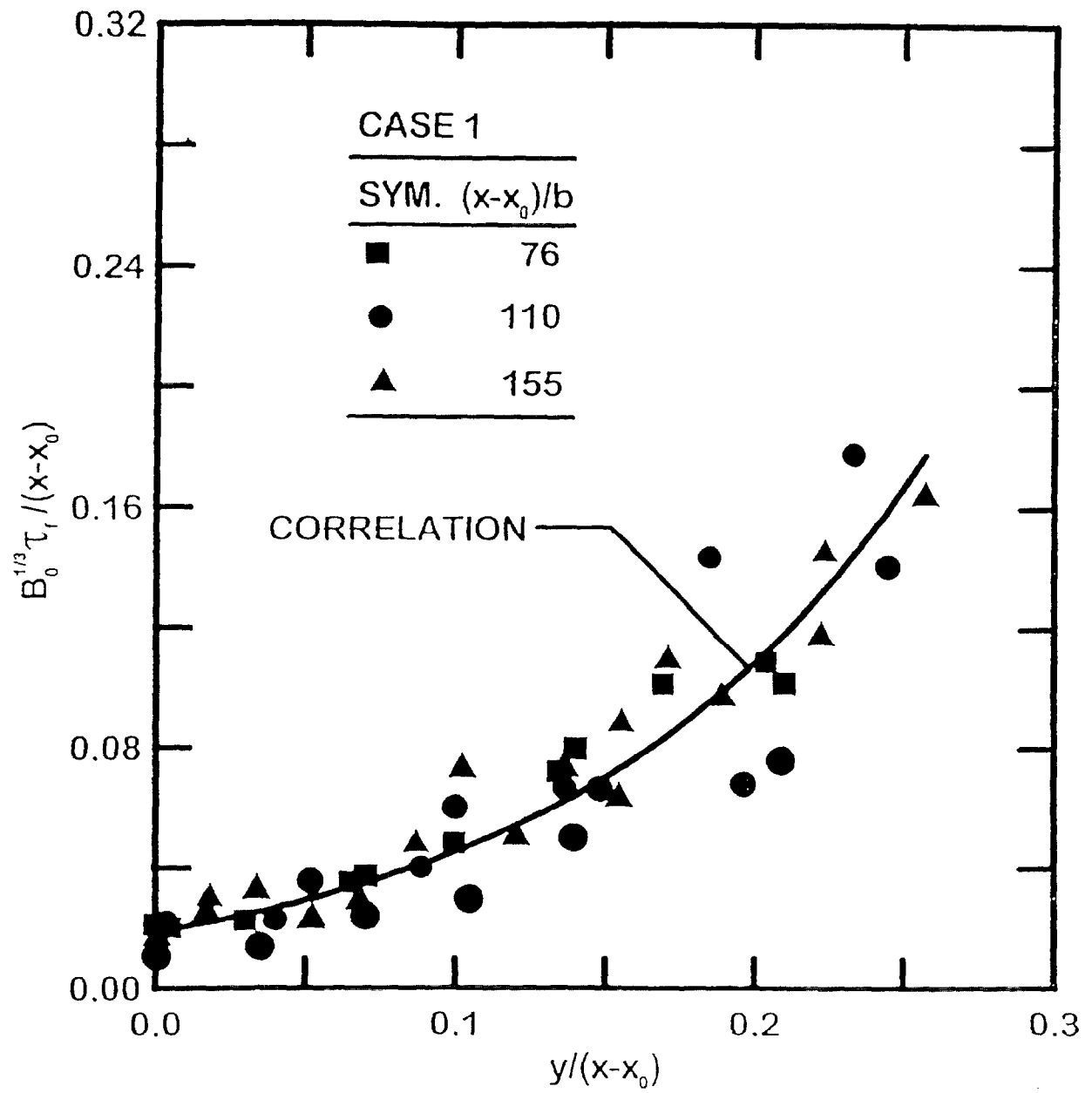


Fig.6

Appendix F: Sangras et al. (1998b)

MIXTURE FRACTION STATISTICS OF PLANE SELF-PRESERVING BUOYANT TURBULENT ADIABATIC WALL PLUMES

R. Sangras,^{*} Z. Dai[†] and G.M. Faeth^{**}
 Department of Aerospace Engineering
 The University of Michigan
 Ann Arbor, Michigan 48109-2140, U.S.A.

Abstract

Measurements of the mixture fraction properties of plane buoyant turbulent adiabatic wall plumes (adiabatic wall plumes) are described, emphasizing conditions far from the source where self-preserving behavior is approximated. The experiments involved helium/air mixtures rising along a smooth, plane and vertical wall. Mean and fluctuating mixture fractions were measured using laser-induced iodine fluorescence. Self-preserving behavior was observed 92-155 source widths above the source, yielding smaller normalized plume widths and near-wall mean mixture fractions than earlier measurements. Self-preserving adiabatic wall plumes mix slower than comparable free line plumes (which have 58 percent larger normalized widths) because the wall prevents mixing on one side and inhibits large-scale turbulent motion. Measurements of probability density functions, temporal power spectra and temporal integral scales of mixture fraction fluctuations are also reported.

Nomenclature

b	=	source width
B_o	=	source buoyancy flux
d	=	source diameter
$E_f(n)$	=	temporal power spectral density of f
f	=	mixture fraction

Keywords: Natural Convection, Nonintrusive Diagnostics, Plumes, Turbulence

^{*}Graduate Student Research Assistant.

[†]Research Fellow.

^{**}Professor, Fellow ASME.

$F(y/(x-x_0))$	=	normalized self-preserving cross stream distribution of \bar{f}
$F'(y/(x-x_0))$	=	normalized self-preserving cross-stream distributions of \bar{f}'
Fr_0	=	source Froude number, Eq. (2)
g	=	acceleration of gravity
ℓ_f	=	characteristic plume width based on \bar{f} , Eq. (5)
ℓ_M	=	Morton length scale, Eq. (1)
ℓ_u	=	characteristic plume width based on \bar{u} , Eq. (8)
n	=	frequency
PDF(f)	=	probability density function of mixture fraction
Re_c	=	characteristic plume Reynolds number, Eq. (9)
Re_0	=	source Reynolds number, $2\bar{u}_0 b/\nu_0$
u	=	streamwise velocity
$U(y/(x-x_0))$	=	normalized self-preserving cross stream distribution of \bar{u}
x	=	streamwise distance
y	=	cross stream distance
z	=	distance along source from its midplane location
Z	=	source length
ν	=	kinematic viscosity
ρ	=	density
τ_f	=	temporal integral scale of mixture fraction fluctuations
Subscripts		
max	=	condition where the property reaches a maximum value
o	=	initial value or virtual origin location
∞	=	ambient value
Superscripts		
(\quad)	=	time-averaged mean value
$(\quad)'$	=	root-mean-squared fluctuating value

Introduction

Plane turbulent wall plumes are caused by line sources of buoyancy along the base of flat walls. These flows are of interest because they are a classical buoyant turbulent flow

with numerous applications for confined natural convection processes and unwanted fires. Thus, the objective of the present investigation was to extend recent measurements of turbulent round and free line plumes (Dai and Faeth, 1996; Dai et al., 1994, 1995a,b; Sangras et al., 1998) to consider plane turbulent wall plumes using similar methods. Present observations were limited to turbulent wall plumes along smooth plane vertical surfaces for conditions where the streamwise buoyancy flux is conserved, which implies flow along an adiabatic wall for a thermal plume.

Present measurements emphasize fully-developed conditions far from the source where effects of source disturbances and momentum have been lost. Free line plumes become self-preserving at these conditions which simplifies reporting and interpreting measurements (Tennekes and Lumley, 1972). Adiabatic wall plumes never formally approach self-preserving behavior, however, because the streamwise growth rates of the near-wall boundary layer and the outer plume-like region are not the same. Nevertheless, the outer plume-like region grows more rapidly than the near-wall boundary layer and eventually dominates wall plumes far from the source, where wall plumes approximate self-preserving behavior with scaling similar to free line plumes (Grella and Faeth, 1975; Liburdy and Faeth, 1978). Thus, self-preserving behavior of adiabatic wall plumes was sought in this approximate sense during the present investigation.

Ellison and Turner (1959) and Turner (1973) describe some of the earliest studies of wall plumes, considering adiabatic wall plumes involving saline solutions in still water. The entrainment rates that they observed for wall plumes were much smaller than those observed for turbulent free line plumes by Rouse et al. (1952) and Lee and Emmons (1961). This behavior was attributed to both the wall preventing mixing on one side and inhibiting cross stream turbulent motion needed for effective mixing.

Grella and Faeth (1975) report hot-wire probe measurements of velocities and temperatures in weakly-buoyant turbulent adiabatic wall plumes along smooth vertical surfaces. A linear array of small flames was used for the buoyant source; therefore, source dimensions are hard to define and plume buoyancy fluxes are difficult to quantify due to near-source heat losses. The measurements suggest that approximate self-preserving behavior was approached but could not be achieved due to the limited dynamic range of hot-wire probes. Ljuboja and Rodi (1981) subsequently predicted the properties of these flows using a turbulence model that included effects of buoyancy/turbulence interactions. The agreement between predictions and measurements was reasonably good for conditions farthest from the source which best approached approximate self-preserving behavior.

Lai et al. (1986) and Lai and Faeth (1987) reported laser velocimetry (LV) and laser-induced fluorescence (LIF) measurements of mean and fluctuating concentrations in weakly-buoyant adiabatic wall plumes. Gas mixtures leaving a slot provided the buoyancy source so that source dimensions and buoyancy fluxes were well defined. These measurements were used to evaluate predictions based on simplified mixing length and turbulence models, finding good predictions of mean properties but considerable deficiencies for predictions of turbulence properties. These measurements were limited to flow development at near-source conditions, $0 \leq (x-x_0)/b \leq 37.5$, so that self-preserving behavior was not achieved. This behavior is consistent with recent measurements of turbulent free line plumes where self-preserving behavior was only observed for $(x-x_0)/b > 76$ (Sangras et al., 1998).

In addition to large values of $(x-x_0)/b$ to avoid effects of source disturbances, approximate self-preserving behavior also requires large values of $(x-x_0)/\ell_M$ to avoid effects of source momentum (Turner, 1973). Noting that plume behavior dominates

adiabatic wall plumes at self-preserving conditions, ℓ_M can be defined by analogy to free line plumes having uniform source properties, as follows (List, 1982):

$$\ell_M/b = (\rho_o/\rho_\infty) u_o^2 / (bu_o g |\rho_o - \rho_\infty|/\rho_\infty)^{2/3} \quad (1)$$

where the absolute value of the initial density difference is used to account for both rising and falling plumes. A related parameter used to characterize source momentum properties is the source Froude number, Fr , defined for adiabatic wall plumes by analogy to free line plumes, as follows:

$$Fr^2 = \rho_o u_o^2 / (2bg|\rho_\infty - \rho_o|) \quad (2)$$

Using these parameters, the measurements of Lai et al. (1986) and Lai and Faeth (1987) were limited to $(x-x_o)/\ell_M \leq 5$ which is small compared to the values on the order of 10 required for buoyancy-dominated self-preserving behavior for free line plumes (Sangras et al., 1998).

In view of these observations, the objective of the present investigation was to measure the mean and fluctuating scalar properties of adiabatic wall plumes, emphasizing conditions within the approximate self-preserving region far from the source. The experiments consisted of helium/air source flows, along a smooth plane and vertical wall in still air at standard temperature and pressure, which provides straightforward specifications of source dimensions and plume buoyancy fluxes. Scalar properties were characterized by mixture fractions, defined as the mass fraction of source gas in a sample (Sangras et al., 1998). Measurements of mixture fractions were carried out using iodine vapor LIF in order to provide the dynamic range needed to reach approximate self-preserving conditions.

Experimental Methods

Apparatus. Experimental methods were similar to the free line plume study of Sangras et al. (1998). The plumes were observed in an enclosure (3400 × 2000 × 3600 mm high) that had porous side walls (parallel to the source) and a porous ceiling made of filter material. This approach controlled room disturbances and ambient light leakage into the test enclosure while allowing free inflow of entrained air and free exhaust of the plume. The source slot (876 mm long × 9.4 mm wide) was mounted flush to a flat floor (876 mm long × 610 mm wide) with the vertical wall mounted adjacent to one edge of the slot. The floor/slot/wall assembly was mounted in turn normal to end walls (2440 mm high × 610 mm wide). A screen array (2 screens, 16 mesh × 0.20 mm wire diameter, separated by a distance of 38 mm) was installed across the outer edge of the end walls (facing the vertical wall) to further control room disturbances, following Gutmark and Wagnanski (1976), Sangras et al. (1998) and references cited therein. The entire floor/slot/wall assembly was traversed to accommodate rigid optical instruments in the same manner as Sangras et al. (1998)

Gas supplies to the source were metered and measured using critical flow orifices in conjunction with pressure regulators. These flow rates were calibrated using either wet test or turbine flow meters. After mixing, the source flows passed through beds of iodine flakes and feed lines having length-to-diameter ratios of 1200 to ensure uniformly seeded mixtures. Uniform source flow properties were provided by a bed of beads, a filter and a 3.4:1 contraction at the slot exit.

Instrumentation. The LIF signal was produced by an argon-ion laser operating at 514.5 nm (measuring volume diameter at e^{-2} points of 0.16 mm with a maximum optical

power of 1800 mW). The laser beam was horizontal and directed normal to the wall. The beam passed through an opening in the wall and was captured by a horn trap. Laser power was monitored to correct for power fluctuations. Absorption of the laser beam in the flow was less than one percent, and was even smaller for fluorescence emissions, so that it was not necessary to account for effects of absorption when data was processed.

LIF observations were made through windows (457 mm wide \times 203 mm high) mounted flush to the inner surface of the end walls and centered on the laser beam height. Collecting optics were f5.1 with a diameter of 100 mm. The LIF signal was separated from light scattered at the laser line using long-pass optical filters having a cutoff wavelength of 530 nm. The detector aperture provided a measuring volume length of 2 mm. Signal detection, processing and calibration were the same as Sangras et al. (1998).

Effects of differential diffusion of helium and iodine vapor were small, less than 0.1 percent, based on binary diffusivity estimates from Bird et al. (1960) and the analysis of Stårner and Bilger (1983). Gradient broadening errors were also small, less than one percent. Experimental uncertainties (95 percent confidence) were found following Moffat (1982) as discussed by Sangras et al. (1998), yielding maximum experimental uncertainties of the flow properties, as follows: 6 percent for $F(y/(x-x_0))$, 10 percent for $F'(y/(x-x_0))$, 10 percent for PDF(f), 40 percent for the low frequency region of $E_f(n)/(\tau_f \bar{f}'^2)$ and 35 percent for $B_0^{1/3} \tau_f/(x-x_0)$. These uncertainties were maintained up to half the maximum value of each measured parameter (excluding the spike region of the PDF) but increased at smaller values roughly inversely proportional to the value of the parameter.

Test Conditions. The test conditions are summarized in Table 1. Two source flows were considered in order to test scaling of source properties in the region of self-preserving behavior. Approximate self-preserving behavior for adiabatic wall plumes

plumes was only observed relatively far from the source $(x-x_0)/b \geq 92$; therefore, the locations of virtual origin could not be distinguished from $x_0/b = 0$ within present experimental uncertainties.

Self-Preserving Scaling

The state relationship for density as a function of mixture fraction, assuming an ideal gas mixture, can be found in Dai et al. (1994). Far from the source where the flow becomes self-preserving, this expression can be approximated as follows:

$$\rho = \rho_\infty + f\rho_\infty (1 - \rho_\infty/\rho_0), f \ll 1 \quad (3)$$

Assuming approximate self-preserving behavior for adiabatic wall plumes, in the sense discussed earlier, mean and fluctuating mixture fractions can be scaled in terms of self-preserving variables, as follows (List, 1982):

$$F(y/(x-x_0)) \text{ or } F'(y/(x-x_0)) = (\bar{f} \text{ or } \bar{f}') g B_0^{-2/3} (x-x_0) |1 - \rho_\infty/\rho_0| \quad (4)$$

where $F(y/(x-x_0))$ and $F'(y/(x-x_0))$ are appropriately scaled cross stream profile functions of mean and fluctuating mixture fractions, which approximate universal functions far from the source where Eq. (3) applies. A characteristic plume width, ℓ_f , based on \bar{f} is also defined, similar to turbulent free line plumes, as follows (Dai et al., 1994):

$$F(\ell_f/(x-x_0))/F(0) = e^{-1} \quad (5)$$

For plane turbulent adiabatic wall plumes, F decreases monotonically as y increases and there is only one location where Eq. (5) is satisfied. The source buoyancy flux, B_0 , is a conserved scalar of the flow which can be found as follows for plane plumes having uniform source properties (List, 1982):

$$B_0 = bu_0 g |\rho_0 - \rho_\infty| / \rho_\infty \quad (6)$$

The corresponding approximate self-preserving relationship for mean streamwise velocities was not studied here but these properties are useful for defining the turbulence properties of the wall plumes. Thus, mean streamwise velocities within approximate self-preserving turbulent adiabatic wall plumes can be scaled in terms of self-preserving variables, as follows (List, 1982):

$$U(y/(x-x_0)) = \bar{u} B_0^{1/3} \quad (7)$$

where $U(y/(x-x_0))$ is an appropriately scaled cross stream profile function. A characteristic plume width based on \bar{u} , ℓ_u , is also defined, similar to turbulent free line plumes, as follows (Dai et al., 1995a):

$$U(\ell_u/(x-x_0))/U_{\max} = e^{-1} \quad (8)$$

where ℓ_u is the largest value of cross stream distance where Eq. (8) is satisfied, noting that U is a double-valued function of y . The corresponding characteristic plume Reynolds number can be written as follows for approximate self-preserving conditions (Sangras et al., 1998):

$$Re_c = \bar{u}_{\max} \ell_u / \nu_{\infty} = U_{\max} B_0^{1/3} \ell_u / \nu_{\infty} \quad (9)$$

For present purposes, values of U_{\max} and ℓ_u were taken as averages of the measurements farthest from the source reported by Grella and Faeth (1975).

Results and Discussion

Mean Mixture Fractions. Distributions of mean mixture fractions in the approximate self-preserving region of the flow will be considered first. Present measurements of cross stream distributions of mean mixture fractions for the two sources are illustrated in Fig. 1. The scaling parameters of Eq. (4) have been used when plotting the figure so that the value of the ordinate is $F(y/(x-x_0))$. Result for $z/Z = 0$ and $1/4$ (where z is measured from a position halfway between the end walls), are in good agreement with each other which

confirms the two-dimensionality of the flow. The present measurements also yield universal distributions within experimental uncertainties for $92 \leq (x-x_0)/b \leq 155$ and $12 \leq (x-x_0)/\ell_M \leq 21$ with flow aspect ratios of $Z/\ell_f \geq 7.9$, as required for self-preserving flow. Present conditions within the self-preserving region of the flow correspond to $3800 \leq Re_c \leq 6700$ which is comparable to conditions within the self-preserving region of round and plane free turbulent plumes of $2500 \leq Re_c \leq 7500$ observed by Dai et al. (1994,1995a,b) and Sangras et al. (1998). These are reasonably large values of characteristic Reynolds numbers for turbulent plume-like flows. For example, this range is comparable to the largest values of Re_c where measurements of turbulent wake properties have been reported, while turbulent wakes exhibit self-preserving turbulence properties at values of Re_c as small as 70 (Wu and Faeth, 1993).

Measurements of F for a variety of plane turbulent plumes have been plotted in Fig. 1 for comparison with the present measurements, as follows: results for adiabatic wall plumes from Grella and Faeth (1975) and Lai and Faeth (1987), results for isothermal wall plumes from Liburdy and Faeth (1978) and results for free line plumes from Sangras et al. (1998). The measurements of Grella and Faeth (1975), Lai and Faeth (1987) and Liburdy and Faeth (1978) all exhibit streamwise variations of mean mixture fractions scaled for approximate self-preserving behavior; thus, the distributions plotted in Fig. 1 for these measurements are for conditions farthest from the source. The remaining results from Sangras et al. (1998) and the present study represent scaled mean mixture fractions averaged over the self-preserving portions of the plumes.

Considering the three adiabatic wall plume results in Fig. 2, it is evident that the measurements of Lai and Faeth (1987) are considerably broader than present results (22 percent broader at the e^{-1} points of the distributions) and that the values of F for both Grella

and Faeth (1975), and Lai and Faeth (1987) are considerably larger than the present results near the wall (up to 31 percent larger). The larger scaled widths of the mean mixture fraction distributions of the earlier adiabatic wall plumes are typical of conditions in the developing plume region before self-preserving behavior is achieved. Developing flow was especially evident for the measurements of Lai and Faeth (1987) which were limited to $(x-x_0)/b \leq 37.5$ while self-preserving behavior was only observed much farther from the source $(x-x_0)/b \geq 92$, during the present investigation. This behavior is illustrated by the values of $\ell_f/(x-x_0)$ summarized in Table 2 for the measurements of Lai et al. (1986) and the present investigation. The progressive reduction of $\ell_f/(x-x_0)$ with increasing distance from the source, tending toward the value observed during the present investigation, is quite evident. The corresponding streamwise locations of the measurements of Grella and Faeth (1975) cannot be stated in terms of $(x-x_0)/b$ because their source dimensions are not well defined; nevertheless, it is encouraging that the characteristic width of these measurements at the largest distance from the source is in good agreement with the present measurements.

Differences between the magnitudes of the scaled mean mixture fraction measurements of Grella and Faeth (1975) and the present investigation can be attributed to problems of specifying the buoyancy flux, B_0 , for the measurements of Grella and Faeth (1975). In particular, B_0 was accurately prescribed by the gas mixture at the source exit for the present study but B_0 had to be obtained from measurements of plume velocity and temperature properties for the study of Grella and Faeth (1975) due to the difficulties of determining energy losses from thermal plumes near the source. This approach introduces significant uncertainties in B_0 , particularly because a significant portion of B_0 is transported by streamwise turbulent motion, e.g., Dai et al. (1995b) and George et al. (1977) find that streamwise turbulent transport contributes 15-16 percent of B_0 for round buoyant turbulent plumes with similar levels anticipated for plane turbulent plumes. The streamwise transport contribution to B_0 was not measured by Grella and Faeth (1975) and had to be ignored so

that the corresponding underestimation of B_0 tends to increase values of F compared to present results as seen in Fig. 1.

The comparison between the distributions of F for adiabatic wall plumes and free line plumes, plotted in Fig. 1, is also of interest. Both sets of results represent self-preserving behavior and have the same buoyancy flux. Comparing the two flows, it is evident that the adiabatic wall plumes spread much slower than the free line plumes. For example, the characteristic widths, ℓ_p , are 58 percent larger for the free line plumes than the adiabatic wall plumes whereas the maximum scaled mean mixture fraction, $F(0)$, is 2.7 times larger for adiabatic wall plumes than for the free line plumes. This behavior has unfortunate implications for the environment of unwanted fires within structures where the reduced mixing rates of fire plumes along surfaces allow heated regions to extend much farther from the source than would be the case for unconfined fires; this behavior tends to enhance fire spread rates. These effects also tend to reduce dilution rates of pollutants and other hazardous substances within buoyant flows along surfaces compared to unconfined buoyant flows.

Reduced rates of mixing of adiabatic wall plumes compared to free line plumes can be attributed to reduced access to the ambient environment, the direct effects of wall friction and inhibition of turbulent mixing by the presence of the wall. The reduced access to the ambient environment comes about because adiabatic wall plumes can only mix on one side while free line plumes can mix on both sides. This effect might be expected to increase the maximum scaled mean mixture fraction, $F(0)$, by a factor of 2; instead, $F(0)$ increases even more, by a factor of 2.7, which suggests that other effects are influencing mixing rates as well. The direct effect of wall friction, however, does not explain any significant tendency to retard mixing rates for adiabatic wall plumes. For example, earlier studies of adiabatic wall plumes show the direct effects of wall friction on plume structure are small because the

wall boundary layer is much thinner than the outer plume-like region as self-preserving conditions are approached (Grella and Faeth, 1975; Lai et al., 1986; Lai and Faeth, 1987). Thus, the presence of the wall must reduce mixing in its own right, probably by inhibiting cross stream turbulent motion at the largest scales that significantly contribute to the mixing of free line plumes.

Results for isothermal wall plumes due to Liburdy and Faeth (1978) plotted in Fig. 1 also support the idea that the main functions of the wall are to limit mixing to just one side of the plume and to inhibit turbulent motion at the largest scales which tends to reduce mixing rates. In particular, Liburdy and Faeth (1978) find little effect of direct transport to the wall on reducing values of F as self-preserving conditions are approached (although wall heat losses near the source are very important for these thermal plumes). On the other hand, wall heat losses shift the maximum value of F away from the wall, tending to increase the thickness of the flow. This increased thickness accommodates larger scales of turbulence which increases mixing rates as evidenced by the smaller F_{\max} for isothermal wall plumes than for adiabatic wall plumes.

The differences between the various flows plotted in Fig. 1 are quantified in Table 3, where the aspect ratio of the slot, Z/b , the range of streamwise distances studied $(x-x_0)/b$, the smallest flow aspect ratios, $(Z/\ell)_{\min}$, the streamwise distance in terms of Morton length scale, $(x-x_0)/\ell_M$, and the corresponding values of $\ell/(x-x_0)$, F_{\max} and $\bar{f}'_{\max}/\bar{f}_{\max}$ are summarized to the extent they are known for adiabatic wall plumes, isothermal wall plumes and free line plumes. Earlier results for wall plumes exhibit some evolution of F with distance from the source over the range of the measurements; therefore, only findings farthest from the source are shown in the table in these cases. The measurements of Grella and Faeth (1975), Liburdy and Faeth (1978) and Liburdy et al. (1979) employed linear arrays of small flames as thermal sources for the plumes so that source dimensions cannot

be prescribed for these results. Variations of flow widths and values of F between the various flows have already been discussed in connection with Fig. 1; the properties of mixture fraction fluctuations will be taken up next.

Mixture Fraction Fluctuations. Measurements of cross stream distributions of mixture fraction fluctuations are plotted in Fig. 2. In addition to the present measurements for the same conditions as \bar{f} in Fig. 1, other measurements have been plotted in the figure, as follows: adiabatic wall plumes from Lai and Faeth (1987), isothermal wall plumes from Liburdy and Faeth (1978) and free line plumes from Sangras et al. (1998). As before, the measurements of Lai and Faeth (1987) and Liburdy and Faeth (1978) do not extend to fully self-preserving conditions so that only their results farthest from the source are shown. The remaining results from Sangras et al. (1998) and the present study represent scaled mixture fraction fluctuations in the self-preserving portions of the flow.

Present measurements of F' exhibit self-preserving behavior within experimental uncertainties over the test range. F' becomes small as the wall and the free stream are approached and reaches a maximum near $y/(x-x_0) = 0.02$. The values of \bar{f}' are actually larger for adiabatic wall plumes near this maximum than the values observed in free line plumes at similar conditions because the values of \bar{f} in this region are larger for adiabatic wall plumes than for free line plumes. The values of mixture fraction fluctuation intensities near the maximum \bar{f} condition, however, are actually smaller for adiabatic wall plumes than for free line plumes, e.g., 37 percent as opposed to 47 percent, see Table 3, which is consistent with the wall stabilizing turbulent motion. The adiabatic wall plume results of Lai and Faeth (1987) are similar to present results in terms of magnitudes, e.g., the values of $\bar{f}'_{\max}/\bar{f}_{\max}$ for the two studies are 34 and 37 percent, respectively. The distribution of F' is considerably broader for the measurements of Lai and Faeth (1987) than the present study,

however, which follows because self-preserving conditions were not reached, as noted earlier. The measurements of Liburdy et al. (1979) for isothermal wall plumes are considerably smaller than the other wall plumes for reasons that have yet to be explained; values of $\bar{f}'_{\max}/\bar{f}_{\max}$ for this flow are also lower than for all the other plumes, e.g., 25 percent, see Table 3.

Probability Density Functions. The measured PDF(f) are illustrated in Fig. 3 for self-preserving adiabatic wall plumes. These results are for the case 1 source at various cross stream distances and $(x-x_0)/b = 110$ but results at other self-preserving conditions were similar. The measurements are compared with predictions of clipped-Gaussian and beta function distributions which frequently are used to represent PDF(f) for modeling purposes (Lockwood and Naguib, 1975). These distributions are prescribed by the values of \bar{f} and \bar{f}' at each position.

The PDF(f) illustrated in Fig. 3 exhibit progressively increasing spikes at $f=0$ as $y/(x-x_0)$ increases, representative of increasing time periods spent in ambient fluid as the outer edge of the flow is approached. Both distributions provide a reasonably good representation of the measured PDF's. All these properties are similar to earlier findings for free line plumes (Sangras et al., 1998).

Temporal Power Spectral Densities. Typical temporal power spectra are illustrated in Fig. 4 for self-preserving adiabatic wall plumes. These results are for $92 \leq (x-x_0)/b \leq 155$ with the case 1 plume but results for other self-preserving conditions are similar. These measurements are normalized by local turbulence properties as described by Hinze (1975). These spectra are qualitatively similar to earlier results for round plumes reported by Dai et al. (1994) and for free line plumes reported by Sangras et al. (1998). The normalized

spectra are relatively independent of cross stream position at each streamwise location. The spectra exhibit a prominent $-5/3$ power decay in an inertial-convective subrange for scalar property fluctuations where effects of molecular diffusion are small (Tennekes and Lumley, 1972) followed by a prominent -3 power decay in an inertial-diffusion subrange for scalar property fluctuations where effects of molecular diffusion are significant (Papanicolaou and List, 1987). The latter region is not observed in nonbuoyant flows and represents an important buoyancy/turbulence interaction.

The properties of the temporal power spectra are completed by temporal integral scales, which are plotted as a function of cross stream distance in Fig. 5. These measurements are limited to the case 1 source for $92 \leq (x-x_0)/b \leq 155$, however, results at other self-preserving conditions are similar. The correlation for the temporal integral scales of self-preserving free line plumes from Sangras et al. (1998) is also shown in the plot for comparison with the present results. The present results provide a scattered correlation when plotted in the manner of Fig. 5; nevertheless, these results agree with the free line plume results within experimental uncertainties in spite of increased width of free line plumes. The shape of the plot generally agrees with expectations for temporal integral scales based on Taylor's hypothesis, as discussed by Sangras et al. (1998).

Conclusions

Mixture fraction statistics were measured in plane turbulent adiabatic wall plumes rising along flat smooth vertical walls in still air. Conditions far from the source were emphasized where effects of source disturbances are lost and the outer plume-like region of the flow approximates self-preserving behavior with scaling similar to self-preserving free line plumes. The test conditions consisted of buoyant jet sources of helium and air to obtain the source properties summarized in Table 1 with measurements involving $(x-x_0)/b$ in the

range 92-155 and $(x-x_0)/\ell_M$ in the range 12-21. The major conclusions of the study are as follows:

1. The present measurements yielded distributions of mean mixture fractions that approximated self-preserving behavior in the outer plume-like region of the flow for $(x-x_0)/b \geq 92$. In this region distributions of mean mixture fractions were up to 22 percent narrower, with scaled values at the wall up to 31 percent smaller than earlier results using buoyant jet sources in the literature. These differences were caused by past difficulties in achieving adequate distances from the source to reach self-preserving conditions and accurately determining the value of the buoyancy flux needed to scale self-preserving properties during the earlier studies.
2. Self-preserving turbulent adiabatic wall plumes mix much slower than comparable free line plumes with characteristic plume widths 58 percent larger and scaled maximum mean mixture fractions 2.7 times smaller for free line plumes than for comparable adiabatic wall plumes mainly because the wall limits mixing to one side of the flow and inhibits large-scale turbulent motion that is mainly responsible for mixing.
3. Cross stream distributions of mixture fraction fluctuations exhibit reduced values near the wall as expected. The stabilizing effect of the wall also reduces maximum mean mixture fraction fluctuation intensities in the self-preserving plane turbulent adiabatic wall plumes compared to corresponding turbulent free line plumes, e.g., the maximum intensities for the two flows are 37 and 47 percent, respectively.

4. The probability density functions of mixture fractions in self-preserving adiabatic wall plumes are approximated reasonably well by either clipped Gaussian or beta function distributions similar to corresponding free line plumes.
5. The low frequency portion of the spectra of mixture fraction fluctuations scale in a relatively universal manner while the spectra exhibit $-5/3$ power inertial-convective and -3 power inertial-diffusive decay regions. This behavior is typical of other turbulent plumes with the prominent -3 power inertial-diffusive decay region being a characteristic of buoyant flows that is not seen in nonbuoyant flows.
6. Temporal integral scales could be correlated in a relatively universal manner in terms of self-preserving parameters, with results for adiabatic wall plumes in qualitative agreement with the behavior of corresponding free line plumes.

Acknowledgments

This research was supported by the United States Department of Commerce, National Institute of Standards and Technology, Grant No. 60NANB4D1696, with H. R. Baum of the Building and Fire Research Laboratory serving as Scientific Officer.

References

- Bird, R.B., Stewart, W.E., and Lightfoot, E.N., 1960, *Transport Phenomena*, John Wiley & Sons, Inc., New York, pp. 502-513.
- Dai, Z., and Faeth, G.M., 1996, "Measurements of the Structure of Self-Preserving Round Buoyant Turbulent Plumes," *J. Heat Trans.*, Vol. 118, pp. 493-495.
- Dai, Z., Tseng, L.-K., and Faeth, G.M., 1994, "Structure of Round, Fully-Developed, Buoyant Turbulent Plumes," *J. Heat Trans.*, Vol. 116, pp. 409-417.

- Dai, Z., Tseng, L.-K., and Faeth, G.M., 1995a, "Velocity Statistics of Round, Fully-Developed Buoyant Turbulent Plumes," J. Heat Trans., Vol. 117, pp. 138-145.
- Dai, Z., Tseng, L.-K., and Faeth, G.M., 1995b, "Velocity/Mixture-Fraction Statistics of Round, Self-Preserving Buoyant Turbulent Plumes," J. Heat Trans., Vol. 117, pp. 918-926.
- Ellison, T.H., and Turner, J.S., 1959, "Turbulent Entrainment in Stratified Flows," J. Fluid Mech., Vol. 6, pp. 423-448.
- George, W.K., Jr., Alpert, R.L., and Tamanini, F., 1977, "Turbulence Measurements in an Axisymmetric Buoyant Plume," Int. J. Heat Mass Transfer, Vol. 20, pp. 1145-1154.
- Grella, J.J., and Faeth, G.M., 1975, "Measurements in a Two-Dimensional Thermal Plume Along a Vertical Adiabatic Wall," J. Fluid Mech., Vol. 71, pp. 701-710.
- Gutmark, E., and Wygnanski, I., 1976, "The Plane Turbulent Jet," J. Fluid Mech., Vol. 73, pp. 465-495.
- Hinze, J. O., 1975, *Turbulence*, 2nd ed., McGraw-Hill, New York, pp. 175-319.
- Lai, M.-C., and Faeth, G.M., 1987, "Turbulence Structure of Vertical Adiabatic Wall Plumes," J. Heat Trans., Vol. 109, pp. 663-670.
- Lai, M.-C., Jeng, S.-M., and Faeth, G.M., 1986, "Structure of Turbulent Adiabatic Wall Plumes," J. Heat Trans., Vol. 108, pp. 827-834.
- Lee, S.L., and Emmons, H.W., 1961, "A Study of Natural Convection Above a Line Fire," J. Fluid Mech., Vol. 11, pp. 353-368.
- Liburdy, J.A., and Faeth, G.M., 1978, "Heat Transfer and Mean Structure of a Turbulent Thermal Plume Along Vertical Isothermal Walls," J. Heat Trans., Vol. 100, pp. 177-183.

Liburdy, J.A., Groff, E.G., and Faeth, G.M., 1979, "Structure of a Turbulent Thermal Plume Rising Along an Isothermal Wall," J. Heat Trans., Vol. 101, pp. 299-355.

List, E.J., 1982, "Turbulent Jets and Plumes," Ann. Rev. Fluid Mech., Vol. 14, pp. 189-212.

Ljuboja, M., and Rodi, W., 1981, "Prediction of Horizontal and Vertical Turbulent Buoyant Wall Jets," J. Heat Trans., Vol. 103, pp. 343-349.

Lockwood, F.C., and Naguib, A.S., 1975, "The Prediction of Fluctuations in the Properties of Free, Round-Jet Turbulent Diffusion Flames," Combust. Flame, Vol. 24, pp. 109-124.

Moffat, R.J., 1982, "Contribution to the Theory of Single-Sample Uncertainty Analysis," J. Fluids Engr., Vol. 104, pp. 250-258.

Papanicolaou, P.N., and List, E.J., 1987, "Statistical and Spectral Properties of Tracer Concentration in Round Buoyant Jets," Int. J. Heat Mass Trans., Vol. 30, pp. 2059-2071.

Rouse, H., Yih, C.S., and Humphreys, H.W., 1952, "Gravitational Convection from a Boundary Source," Tellus, Vol. 4, pp. 201-210.

Sangras, R., Dai, Z., and Faeth, G.M., "Mixing Structure of Plane Self-Preserving Buoyant Turbulent Plumes," J. Heat Transfer, in press.

Stårner, S. H., and Bilger, R W., 1983, "Differential Diffusion Effects on Measurements in Turbulent Diffusion Flames by the Mie Scattering Technique," Prog. Astro. and Aero., Vol. 88, pp. 81-104.

Tennekes, H., and Lumley, J.L., 1972, *A First Course in Turbulence*, MIT Press, Cambridge, Massachusetts, pp. 113-124.

Turner, J.S., 1973, *Buoyancy Effects in Fluids*, Cambridge University Press, Cambridge, pp. 165ff.

Wu, J.-S., and Faeth, G.M., 1993, "Sphere Wakes in Still Surroundings at Intermediate Reynolds Numbers," AIAA J., Vol. 31, pp. 1448-1455.

Table 1. Summary of plane buoyant turbulent adiabatic wall plume test conditions^a

Source Properties	Case 1	Case 2
Helium concentration (percent by volume)	29.0	52.3
Density (kg/m ³)	0.871	0.639
Kinematic viscosity (mm ² /s)	22.1	31.3
Average velocity (mm/s)	868	1240
Buoyancy flux, B ₀ (m ³ /s ³)	0.0200	0.0514
Density ratio, ρ_0/ρ_∞	0.750	0.550
Reynolds number, Re ₀	740	745
Froude number, Fr ₀	3.50	3.20
Morton length scale, ℓ_M/b	7.7	6.1

^aHelium/air sources directed vertically upward at the base of a vertical smooth plane wall in still air with an ambient pressure of 99 ± 0.5 kPa and temperature of 297 ± 0.5 K. Pure gas properties as follows: air density of 1.161 kg/m³, air kinematic viscosity of 15.9 mm²/s, helium density of 0.163 kg/m³ and helium kinematic viscosity of 122.5 mm²/s. Source slot width and length of 9.4 and 876 mm. Virtual origin based on \bar{f} of $x_0/b = 0$ determined from present measurements in the range $(x-x_0)/b = 92-155$ and $(x-x_0)/\ell_M = 12-21$.

Table 2. Development of plane turbulent adiabatic wall plumes^a

Source	$(x - x_0)/b$	$\ell_r/(x-x_0)$
Lai et al. (1986)	10.0	0.173
	20.0	0.118
	37.5	0.093
Present (self-preserving region)	92-155	0.076

^aPlane turbulent adiabatic wall plumes in still and unstratified environments.

Table 3. Summary of self-preserving properties of plane buoyant turbulent plumes^a

Source	Plume Type	Z/b	(x-x ₀)/b	(Z/ℓ _f) _{min}	(x-x ₀)/ℓ _M	ℓ _f /(x-x ₀)	F _{max}	$\bar{f}'_{\max}/\bar{f}_{\max}$
Present	Adiabatic Wall	93	92-155	7.9	12-21	0.076	5.71	0.37
Lai et al. (1986) ^b	Adiabatic Wall	38	10-38	10.8	1-5	0.093	6.80	0.34
Grella & Faeth (1973) ^{b,c}	Adiabatic Wall	--	--	13.0	--	0.077	7.50	--
Liburdy & Faeth (1978) and Liburdy et al. (1979) ^{b,c}	Isothermal Wall	--	--	5.9	--	0.112	5.20	0.25
Sangras et al. (1998)	Free Line	93	76-155	2.6 ^d	9-21	0.120	2.10	0.47

^aPlane buoyant turbulent plumes in still and unstratified environments. Wall plumes are along vertical smooth surfaces. Range of streamwise distances are for conditions where measurements were made over the cross section of the plumes. Adiabatic wall plume entries are ordered chronologically.

^bThese flows were evolving over the range of the measurements so that the values of $\ell_f/(x-x_0)$, F_{\max} and $\bar{f}'_{\max}/\bar{f}_{\max}$ pertain to results obtained farthest from the source.

^cSource was a linear array of round jets so that slot properties cannot be defined.

^dThis value is $(Z/(2\ell_f))_{\min}$ which is the full characteristic width of the flow, similar to the other entries in this column.

List of Figures

- Fig. 1 Cross stream distributions of mean mixture fractions in plane buoyant turbulent plumes. Measurements of Grella and Faeth (1975), Lai and Faeth (1987) and the present investigation for adiabatic wall plumes; measurements of Liburdy and Faeth (1978) for isothermal wall plumes; and measurements of Sangras et al. (1998) for free line plumes. Results from Grella and Faeth (1975), Liburdy and Faeth (1978), and Lai and Faeth (1987) are for their largest distances from the source.
- Fig. 2 Cross stream distributions of rms mixture fraction fluctuations in plane buoyant turbulent plumes. Measurements of Lai and Faeth (1987) and the present investigation for adiabatic wall plumes; measurements of Liburdy and Faeth (1978) for isothermal wall plumes; and measurements of Sangras et al. (1998) for free line plumes. Results from Liburdy and Faeth (1978) and Lai and Faeth (1987) are for their largest distances from the source.
- Fig. 3 Typical probability density functions in plane self-preserving buoyant turbulent adiabatic wall plumes: Case 1 flow at $(x-x_0)/b = 110$.
- Fig. 4 Typical temporal power spectral densities of mixture fraction fluctuations in plane self-preserving buoyant turbulent adiabatic wall plumes : Case 1 flow at $(x-x_0)/b = 92, 110$ and 155 .
- Fig. 5 Radial distributions of temporal integral scales of mixture fraction fluctuations in plane self-preserving buoyant turbulent plumes. Measurements of the present investigation for adiabatic wall plumes; measurements of Sangras et al. (1998) for free line plumes.

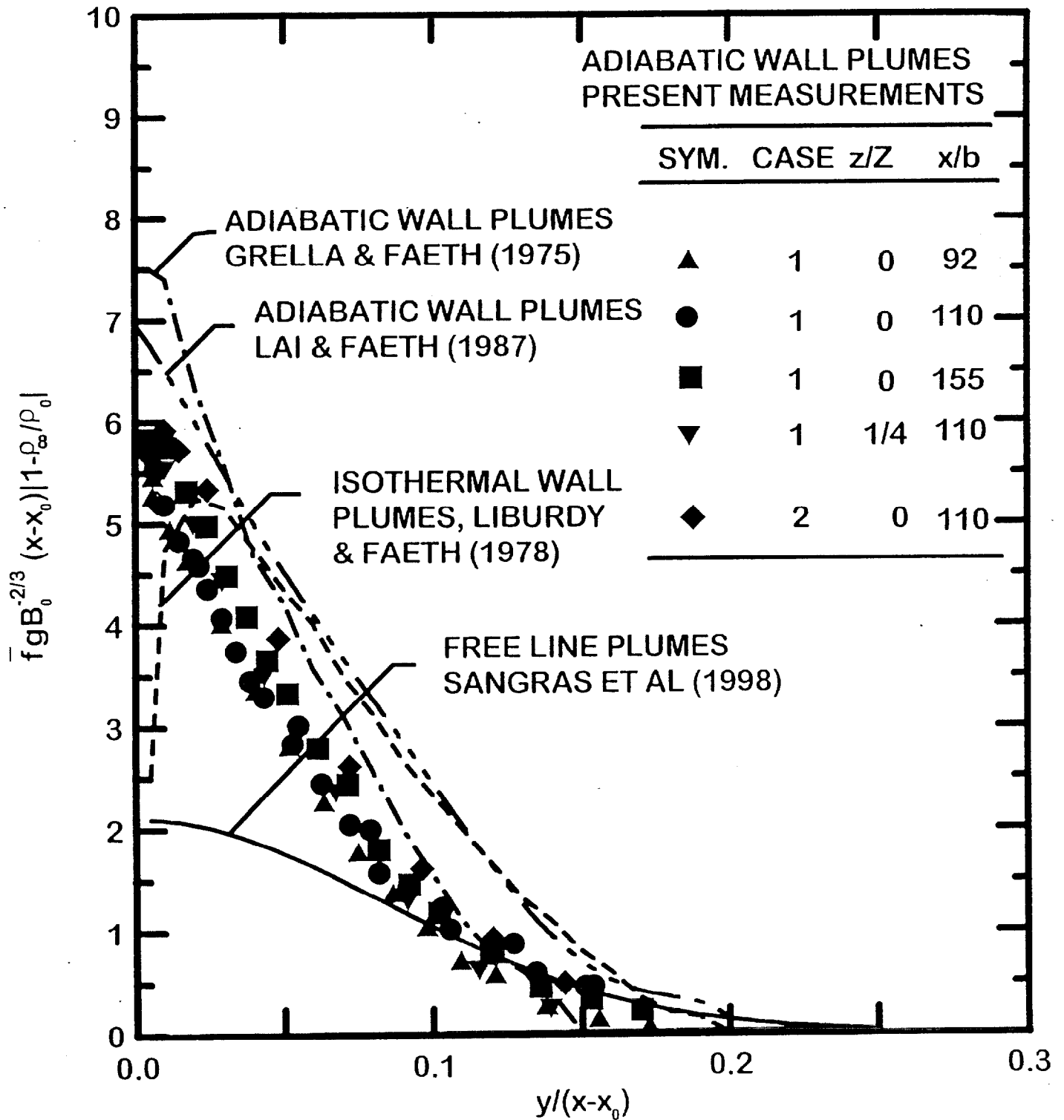


Fig. 1

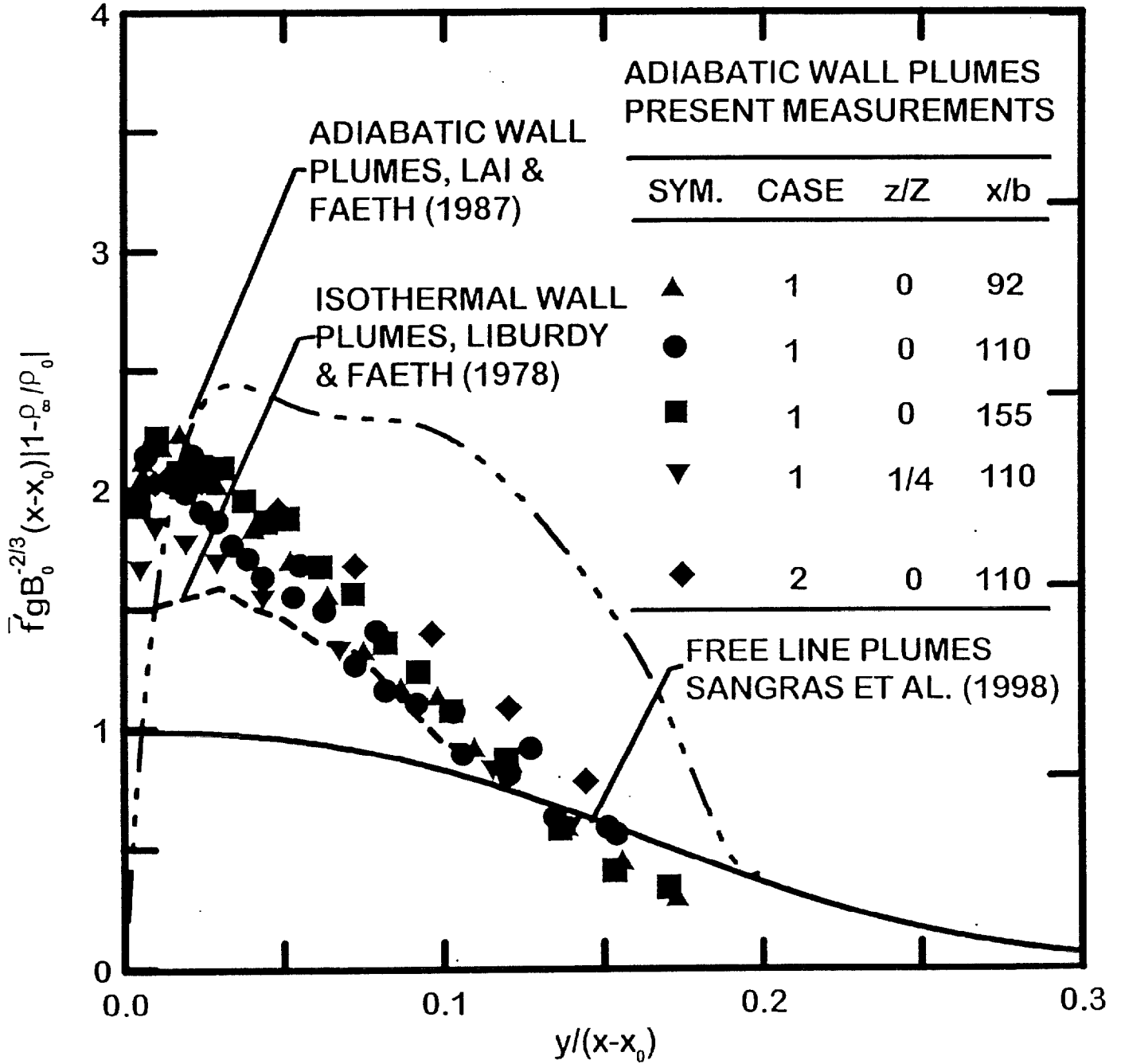


Fig. 2

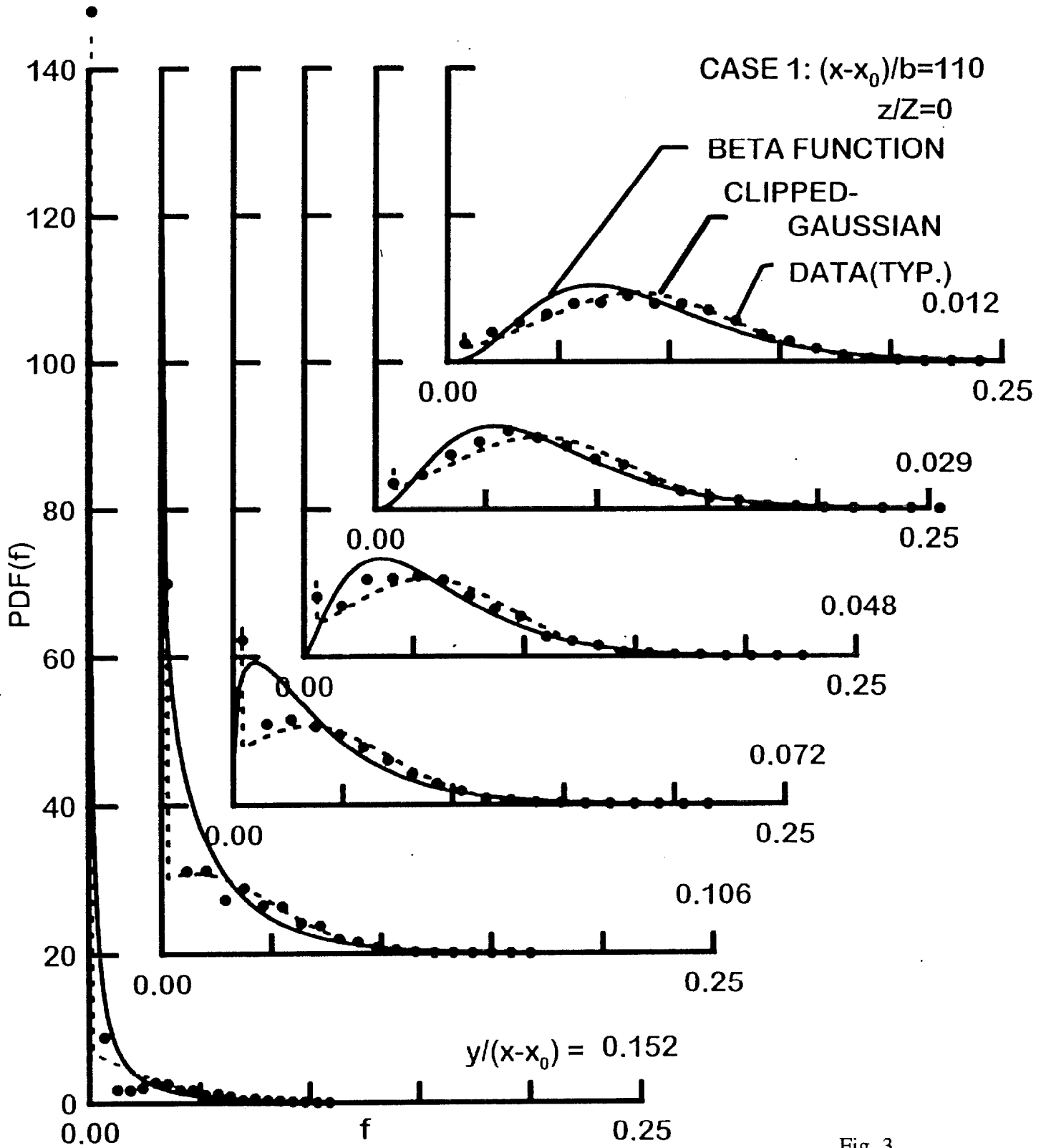


Fig. 3

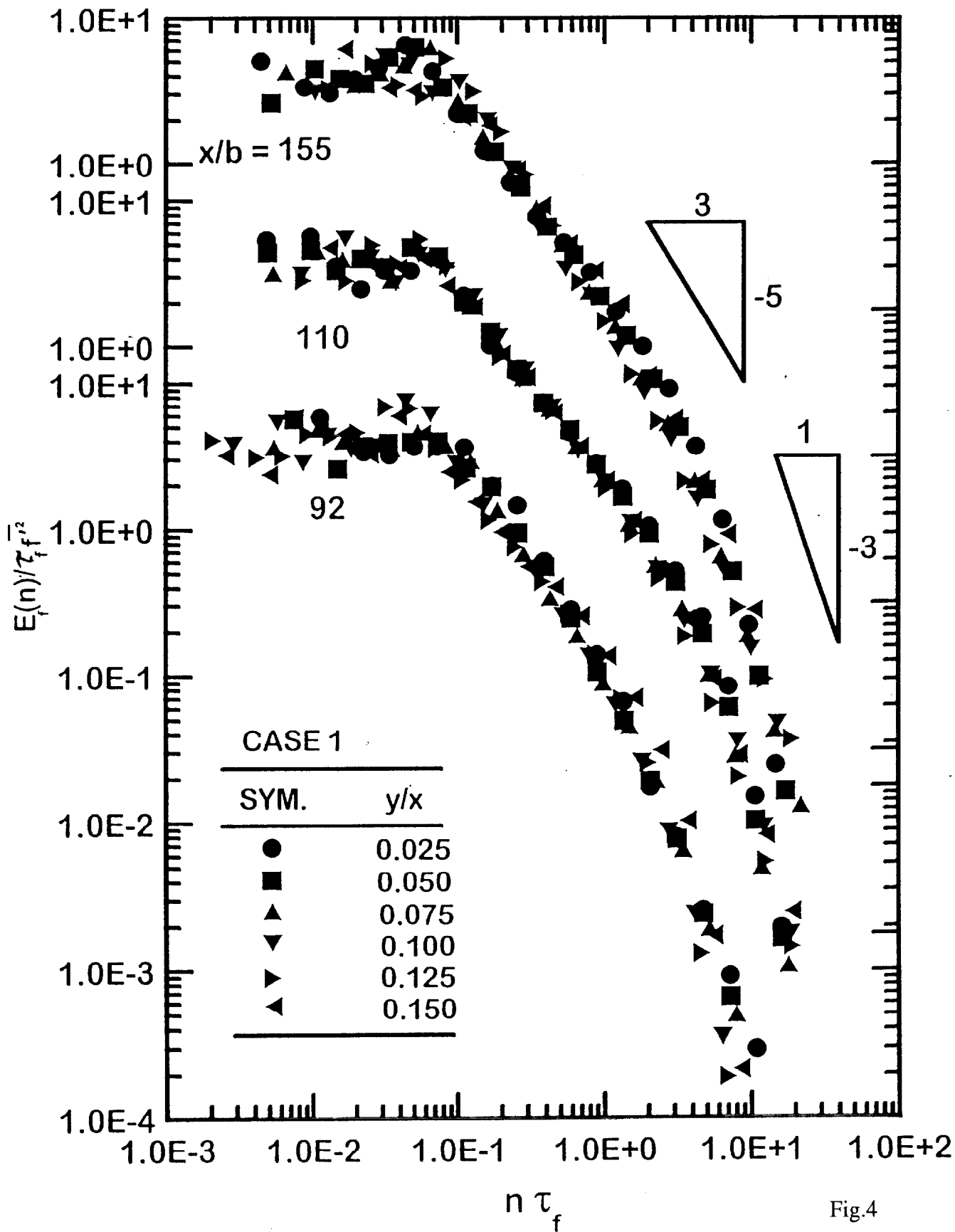


Fig.4

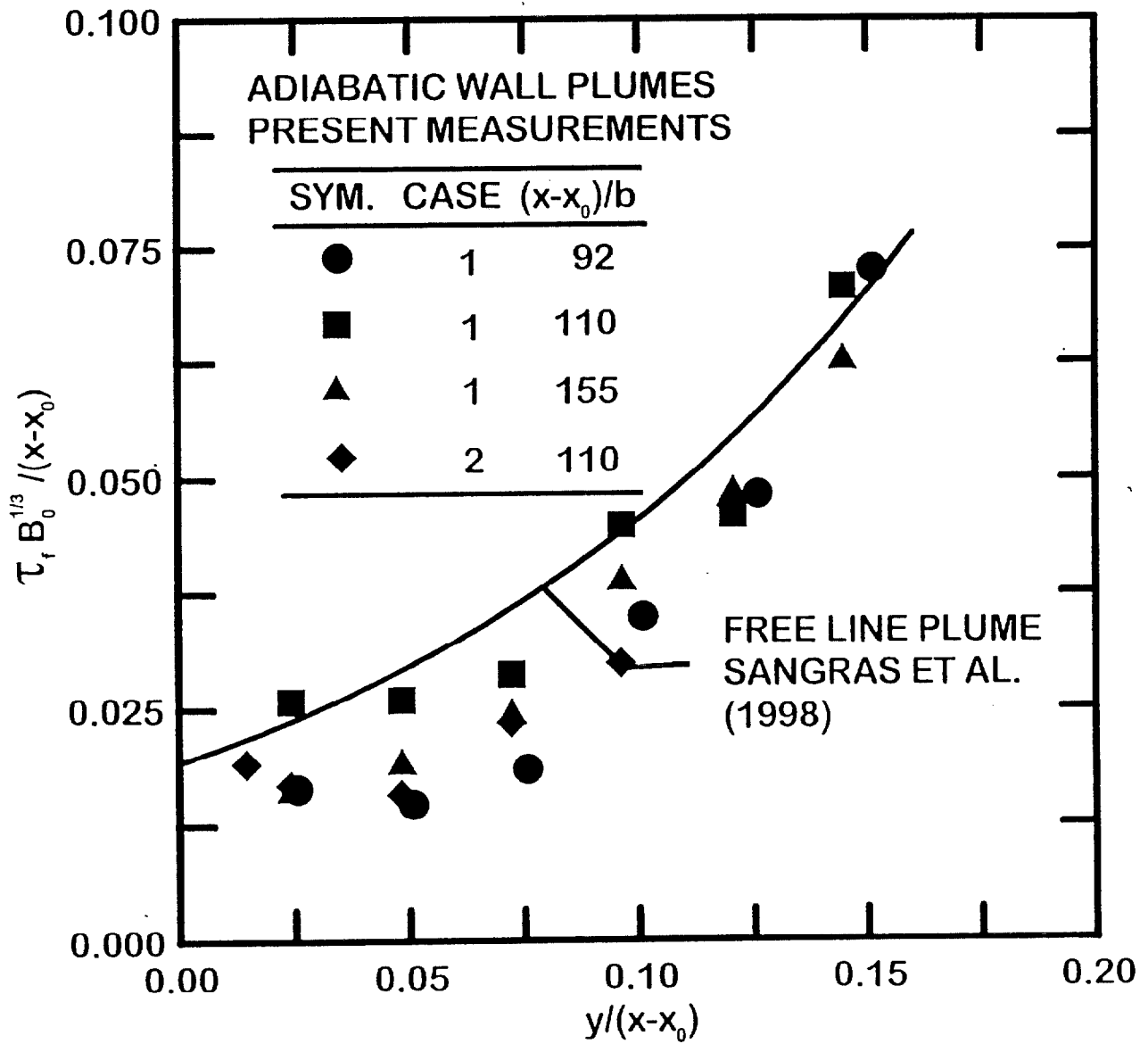


Fig.5

NIST-114 (REV. 11-94) ADMAN 4.09	U.S. DEPARTMENT OF COMMERCE NATIONAL INSTITUTE OF STANDARDS AND TECHNOLOGY		(ERB USE ONLY)	
			ERB CONTROL NUMBER	DIVISION
			PUBLICATION REPORT NUMBER	CATEGORY CODE
			NIST GCR 99-770	
MANUSCRIPT REVIEW AND APPROVAL			PUBLICATION DATE	NUMBER PRINTED PAGES
			March 1999	
INSTRUCTIONS: ATTACH ORIGINAL OF THIS FORM TO ONE (1) COPY OF MANUSCRIPT AND SEND TO THE SECRETARY, APPROPRIATE EDITORIAL REVIEW BOARD.				

TITLE AND SUBTITLE (CITE IN FULL) Mixing and Radiation Properties of Buoyant Luminous Flame Environments: I. Self-Preserving Plumes	
CONTRACT OR GRANT NUMBER 60NANB4D1696	TYPE OF REPORT AND/OR PERIOD COVERED Final Report
AUTHOR(S) (LAST NAME, FIRST INITIAL, SECOND INITIAL) Z. Dai, R. Sangras, L.-K. Tseng and G.M. Faeth	PERFORMING ORGANIZATION (CHECK (X) ONE BLOCK) <input checked="" type="checkbox"/> NIST/GAITHERSBURG <input type="checkbox"/> NIST/BOULDER <input type="checkbox"/> JILA/BOULDER

LABORATORY AND DIVISION NAMES (FIRST NIST AUTHOR ONLY) Building and Fire Research Laboratory, Fire Safety Engineering Division
SPONSORING ORGANIZATION NAME AND COMPLETE ADDRESS (STREET, CITY, STATE, ZIP) U.S. Department of Commerce National Institute of Standards and Technology Gaithersburg, MD 20899

PROPOSED FOR NIST PUBLICATION		
<input type="checkbox"/> JOURNAL OF RESEARCH (NIST JRES) <input type="checkbox"/> J. PHYS. & CHEM. REF. DATA (JPCRD) <input type="checkbox"/> HANDBOOK (NIST HB) <input type="checkbox"/> SPECIAL PUBLICATION (NIST SP) <input type="checkbox"/> TECHNICAL NOTE (NIST TN)	<input type="checkbox"/> MONOGRAPH (NIST MN) <input type="checkbox"/> NATL. STD. REF. DATA SERIES (NIST NSRDS) <input type="checkbox"/> FEDERAL INF. PROCESS. STDS. (NIST FIPS) <input type="checkbox"/> LIST OF PUBLICATIONS (NIST LP) <input type="checkbox"/> NIST INTERAGENCY/INTERNAL REPORT (NISTIR)	<input type="checkbox"/> LETTER CIRCULAR <input type="checkbox"/> BUILDING SCIENCE SERIES <input type="checkbox"/> PRODUCT STANDARDS <input checked="" type="checkbox"/> OTHER NIST GCR

PROPOSED FOR NON-NIST PUBLICATION (CITE FULLY)	<input checked="" type="checkbox"/> U.S. <input type="checkbox"/> FOREIGN	PUBLISHING MEDIUM <input type="checkbox"/> PAPER <input type="checkbox"/> CD-ROM <input type="checkbox"/> DISKETTE (SPECIFY) _____ <input type="checkbox"/> OTHER (SPECIFY) _____
--	---	--

SUPPLEMENTARY NOTES

ABSTRACT (A 2000-CHARACTER OR LESS FACTUAL SUMMARY OF MOST SIGNIFICANT INFORMATION. IF DOCUMENT INCLUDES A SIGNIFICANT BIBLIOGRAPHY OR LITERATURE SURVEY, CITE IT HERE. SPELL OUT ACRONYMS ON FIRST REFERENCE.) (CONTINUE ON SEPARATE PAGE, IF NECESSARY.) An investigation of the structure and mixing properties of buoyant turbulent plumes is described, motivated by the need to resolve effects of buoyancy/turbulence interactions and to provide data required to benchmark models of buoyant turbulent flows for fire environments. The flows considered included round free plumes, plane free plumes and plane adiabatic wall plumes in an attempt to consider various buoyant flow types representative of the environment of unwanted fires. Measurements included laser-induced fluorescence (LIF) to find mixture fraction statistics, laser velocimetry (LV) to find velocity statistics and combined LIF/LV to find combined mixture-fraction/velocity statistics. Present measurements emphasized self-preserving conditions far from the source where effects of source disturbances and momentum have been lost. The results show that earlier measurements in the literature were not carried out far enough from the source to provide self-preserving properties and that actual self-preserving plumes are narrower with larger maximum scaled mean mixture fractions and velocities than previously thought.
--

KEY WORDS (MAXIMUM OF 9; 28 CHARACTERS AND SPACES EACH; SEPARATE WITH SEMICOLONS; ALPHABETIC ORDER; CAPITALIZE ONLY PROPER NAMES) fire research; flame research; flame structure; optical properties; refractive index; soot; soot aggregates
--

AVAILABILITY <input checked="" type="checkbox"/> UNLIMITED <input type="checkbox"/> FOR OFFICIAL DISTRIBUTION - DO NOT RELEASE TO NTIS <input type="checkbox"/> ORDER FROM SUPERINTENDENT OF DOCUMENTS, U.S. GPO, WASHINGTON, DC 20402 <input checked="" type="checkbox"/> ORDER FROM NTIS, SPRINGFIELD, VA 22161	NOTE TO AUTHOR(S): IF YOU DO NOT WISH THIS MANUSCRIPT ANNOUNCED BEFORE PUBLICATION, PLEASE CHECK HERE.
--	--